DOE/PC/50035-T1
(DE84008799)

Energy

FOSSIL

CENTRIFUGAL SLURRY PUMP WEAR AND HYDRAULIC STUDIES

Phase II Report: Experimental Studies

By
D. Mistry
P. Cooper
C. Biswas
D. Sloteman
A. Onuschak

January 1983
Date Published

Work Performed Under Contract No. AC22-82PC50035

Ingersoll-Rand Research, Inc.
Princeton, New Jersey

Technical Information Center
Office of Scientific and Technical Information
United States Department of Energy

DISCLAIMER

DISCLAIMER

This report has been reproduced directly from the best available copy.

Available from the National Technical Information Service, U. S. Department of Commerce, Springfield, Virginia 22161.

Price: Printed Copy A12
Microfiche A01

Codes are used for pricing all publications. The code is determined by the number of pages in the publication. Information pertaining to the pricing codes can be found in the current issues of the following publications, which are generally available in most libraries: *Energy Research Abstracts (ERA); Government Reports Announcements* and Index (*GRA* and I); *Scientific and Technical Abstract Reports (STAR);* and publication NTIS-PR-360 available from NTIS at the above address.

DOE/PC/50035-T1
(DE84008799)
Distribution Category UC-90b

CENTRIFUGAL SLURRY PUMP WEAR AND HYDRAULIC STUDIES

PHASE II REPORT
EXPERIMENTAL STUDIES

By

D. Mistry, P. Cooper

C. Biswas, D. Sloteman, A. Onuschak

Ingersoll-Rand Research, Inc.

P.O. Box 301, Princeton, New Jersey

Date Published: January 1983

PREPARED FOR THE UNITED STATES

DEPARTMENT OF ENERGY

Under Contract Number DE-AC22-82PC50035

ABSTRACT

This report describes the work performed by Ingersoll-Rand Research, Inc., under Phase II, Experimental Studies for the contract entitled, "Centrifugal Slurry Pump Wear and Hydraulic Studies". This work was carried out for the U.S. Department of Energy under Contract No. DE-AC-82PC50035.

The basic development approach pursued during this phase is presented, followed by a discussion on wear relationships. The analysis, which resulted in the development of a mathematical wear model relating pump life to some of the key design and operating parameters, is presented. The results, observations, and conclusions of the experimental investigation on small scale pumps that led to the selected design features for the prototype pump are discussed.

The material investigation was performed at IRRI, ORNL and Battelle. The rationale for selecting the materials for testing, the test methods and apparatus used, and the results obtained are presented followed by a discussion on materials for a prototype pump. In addition, the prototype pump test facility description, as well as the related design and equipment details, are presented.

CONCLUSIONS AND RECOMMENDATIONS

The Phase-II "Experimental Studies" is complete and the following main conclusions and recommendations are made:

1. Based on the analytical and experimental investigation, a specific speed of 700 to 1000 offers a good compromise for the commercial scale coal liquefaction pump. A conservative specific speed of 700 is selected for the prototype pump.

2. The effect of the pump design and operating parameters and their relationship to wear in the pump were experimentally investigated in detail. The key areas of investigation were collector configuration including cutwater, pumpout vanes, impeller front leakage path, blade shape and shroud configuration at outside diameter. Operation at pilot plants indicated accelerated wear and high loss of material at the volute cutwater. Therefore, considerable effort was directed to improve and optimize this area, and successful design was achieved. Several impeller blading concepts were evaluated and optimum shape was developed. The impeller front leakage path configuration and pumpout vane were investigated adequately and sufficient design information was generated for a 700 specific speed pump. It is recommended that the prototype pump based on the information generated during this phase should be designed, fabricated, and test evaluated during the Phase III. It is also recommended that for the design of higher specific speed pump (above 700), the impeller inlet area (blade, leading edge, etc.) should be investigated

and further improvement and optimization should be carried out in the areas mentioned above.

3. The mathematical wear model relating pump life to some of the key design and operating parameters developed during this phase should be used as a guide to improve the pump scaling, design and performance. It is recommended that systematic experimental investigation be carried out to verify and improve the proposed analysis.

4. The corrosion of HC 250 material in coal liquefaction plant is insignificant. Erosive wear is the dominant factor for the life of pump internal components. Surface boronized HC 250 is ranked first amongst the seven materials evaluated during this phase. It is recommended that boronized HC 250 material be further evaluated in a prototype pump. Further, it is recommended that thermal shock and impact strength tests be carried out on promising pump materials to establish their capability and limitations.

5. Viscosity appears to have no influence on the wear locations in the pump, however, the wear pattern and wear rate changes somewhat with the viscosity. This observation is based on sand/water slurry where the density difference between solid and liquid is high. It is recommended that testing be carried out with coal-oil mixture where the density difference is low.

TABLE OF CONTENTS

TABLE OF CONTENTS

LIST OF FIGURES

LIST OF FIGURES

LIST OF FIGURES

LIST OF TABLES

1.0 OBJECTIVES AND SCOPE OF WORK

The overall objective of the program is to provide a technical data base on material wear and hydraulics for centrifugal pumps in coal liquefaction plant services. The development program is composed of three phases.

The objective of Phase I, Pilot-Plant Experience and Literature Search, is (1) to visit pilot plants and report their experience and (2) to summarize materials wear data and the effect of hydraulic parameters on wear patterns.

The objectives of Phase II, Experimental Studies, are as follows:

(1) To perform laboratory erosion tests for selected materials. The tests are to determine the effect of various parameters such as slurry type and temperature, solid particle characteristics, and properties of the materials of construction.

(2) To conduct tests to determine the effect and nature of corrosion.

(3) To perform hydraulic studies on the effect of various design and operating parameters such as cutwater and suction geometry, impeller vane shape, number of vanes, pumpout vanes, and specific speed.

Test facilities will be developed as required. The data generated during this phase will be analyzed and

used to improve the centrifugal pump design for coal liquefaction services.

Phase III, Prototype Pump for Pilot-Plant Evaluation, consists of the detailed design, construction and testing of an ideal pump derived from the information obtained in Phase II. Two pumps will be fabricated and tested in the laboratory followed by field evaluation at a DOE designated test site. Technical support in related areas will be provided during this phase.

2.0 SUMMARY OF PROGRESS

This report documents the work performed under Phase II - Experimental Studies for the centrifugal slurry pump development program. In this phase, studies were carried out in the areas of hydraulics and materials.

The successful development effort during this phase will permit the design of a 300 gpm, 300' head prototype pump in Phase III, featuring improved hydraulics and materials, for coal liquefication pilot plant use. In addition, a test facility has been developed in which to evaluate the prototype pump at full flow and pressure with a sand slurry.

The hydraulics investigation was initiated with an analysis of the areas where significant wear is observed in the pump and a review of the state-of-art wear model which relates some hydraulics parameters to wear in pump. The analysis was advanced to include the effect of some key design and operating parameters (solid particle size, specific speed, cutwater, impeller diameter) or pump life. This mathematical wear model requires reliable experimental data for verification.

The major effort in the hydraulic studies included the development of the small scale pump test facility, the design of the small pump hardware, followed by its test evaluation. Various pump hydraulic design parameters such as impeller blade shape, cut water design, pumpout vane, collector configuration, impeller front leakage path and outside diameter shroud configuration were screened and evaluated. In

addition, the effect of viscosity on performance was studied. The pump performance, with respect to head vs. flow, power, etc., was monitored and wear patterns were studied periodically during the testing leading to the desired prototype pump features discussed in Section 3.2.5.

The material studies included a review of available alloys, ceramics, coating and weld overlay. Several materials (about seven) were selected for test evaluation. The evaluation consisted of erosion testing at IRRI, corrosion testing at ORNL and hot coal-oil erosion-corrosion testing at Battelle. The IRRI erosion testing was performed with a jet-impingement nozzle tester using an aggressive sand/water slurry. The effects of impingement angles, jet velocity, and slurry viscosity were examined. The ORNL corrosion testing was performed using hot process solvent. The Battelle erosion-corrosion testing was performed with a jet-impingement nozzle tester using hot coal-oil slurry at two jet velocities. The results of all of these tests were analyzed in detail and compared to arrive at a ranking of all test materials. Based on this study the materials for the prototype pumps were selected and are discussed in Section 3.3.9.

In order to permit the evaluation of the prototype pump during the next phase a test facility was designed. The equipment was procured and the test loop has been erected. The test facility is capable of evaluating two full size (300 gpm, 300 ft. head) prototype pumps in series for the determination of performance and wear characteristics. The facility. which utilizes a 200 HP pump motor driver, is de-

signed to handle a sand slurry concentration up to 40% by weight. This facility will be capable of 24 hour, unattended operation.

3.0 DETAILED DESCRIPTION OF TECHNICAL PROGRESS

3.1 TECHNICAL APPROACH

The basic development approach consisted of several independent tasks which can lead to improved pump design and service life. The development was carried out primarily in the two most important areas: pump hydraulics and material for wear components.

The hydraulics investigation was initiated by reviewing the locations where significant wear is observed in the pump. Some of the key locations are cutwater, suction pipe and plate, and impeller blade leading and training edges. The state-of-art understanding of how various hydraulics parameters affect wear in the pump and the wear model was reviewed. Analysis was performed to develop a mathematical wear model relating pump life to some of the key design and operating parameters such as solid particle size, specific speed, cutwater and impeller diameters.

Experimental investigations included modifying an existing slurry test facility to accommodate comparative screening tests of two small scale pumps. These small scale pumps were designed, fabricated and tested to evaluate various impeller blade shapes, cutwater diameter, pump out vanes, inlet area, effect of viscosity, etc.. Wear patterns and performance were studied and evaluated in detail. leading to design improvements in several areas.

The materials investigation consisted of reviewing all the available materials for fabricating impeller, volute liner, and suction plate. Several materials

were selected for test evaluation. A minimum of one material from each of the following categories was selected for experimental investigation: alloys, weld overlays, surface alloying and ceramics. The investigation consisted of jet-impingement nozzle testing to determine erosion resistance of these materials with aggressive sand/water slurry and a sand/water slurry containing two percent by weight of sodium carboxy methyl-cellulose (high viscosity slurry) - both at room temperature. These materials were also evaluated for corrosion. Further, nozzle tests were carried out to examine erosion corrosion properties with hot coal-oil synfuel slurry. The information from these tests were analyzed and the results are discussed in Section 3.3.

In addition to investigating existing alloys for the pump material, attempts were made to develop new alloys which will have better erosion resistance properties.

A test facility is being developed to evaluate a pilot-scale/prototype pump. The design, procurement, installation activities and testing procedure are discussed in Section 3.4.

3.2 HYDRAULIC INVESTIGATION

3.2.1 WEAR RELATIONSHIPS

3.2.1.1 Current Wear Experience

One of the objectives of this program is to study wear in centrifugal pumps used in synfuel slurries and to improve and predict the life of both pilot-plant and full-scale plant pumps. At present, limited data exist. The life of the pilot-plant pumps surveyed is about one year or less, excluding seal failures and other minor problems unrelated to wear by hydraulic action in the flow passages of these machines.

Experience with wear in slurry pumps that have been employed in more traditional solids-handling applications is only of qualitative use; because the carrier fluid is usually water, and the usually denser solids readily move perpendicularly to the main flow direction under the influence of body forces initiated by turning of the fluid. This kind of motion and the attendant wear relationships would appear to be untypical of the more viscous synfuel slurries. Nevertheless, such experience is useful in delineating the specific locations in the pump where we can expect to see wear due to the action of synfuel slurries. For example, tabulations of pump life for various concentrations of phosphate slurries exist (1) - see Appendix A for the references. Furthermore, a comprehensive discussion of all aspects of wear and design of traditional slurry pumps was given by Wilson (2). Vocadlo (3) states in connection with his exposition of a performance model that the cross-streamline motion of solid particles

is sufficiently turbulent to justify the use of a constant drag coefficient for such motion. The value of the drag coefficient under these circumstances is low and therefore permits more particles to wear loaded hydraulic surfaces. Further, such behavior has different consequences with respect to speed, scale-up, head, and particle size effects on pump wear than if the cross-streamline motion of particles were laminar.

A recent study of wear rates by Tuzson for particle sizes of 0.1 mm (100 μm or 150 mesh) indicates that the cross-streamline particle drag is laminar (4), and this will be especially so in synfuel slurries with carrier kinematic viscosities from 10 to 1000 centistokes. To draw useful conclusions about wear, it is necessary to use the appropriate particle-motion model. It is also shown that the dominant wear phenomenon is scouring or sliding by particles on surfaces rather than impingement-type wear.

Zarzycki (5) and Bak (6) conducted wear tests on different types of impellers. Both reported slightly higher wear rates for a conventionally bladed design than for an unchokable channel type. Wiedenroth's visual studies (7) from his lacquer wear tests showed wear only on the suction side of the impeller blades when pumping sand but extending to the pressure side with fine gravel. Wear at the outlet tips increased with flow. Herbish's report (8) on dredge pump design mentions that the least wear occurred for a blade outlet angle of 22.5 degrees. Over the range of 22.5 degrees to 335 degrees the exit angle of the solid particles then corresponded closely to the blade angle.

Welte (9) while discussing wear patterns in dredge pumps states that wear is greatest at the impeller blade inlet and outlet edges and on the outer shroud walls on the suction side. Casing wear is usually greatest near the cutwater. Generally similar tendencies are noted by other authors (5, 6, 7, 10, and 11). Both Welte (9) and Ernst (12) show dredge pump design having a relatively small volute side clearance. However, Bergeron (11) in discussing the effects of primary and secondary flow patterns on pump wear recommends a large side clearance except where scraper vanes are used as well as shrouded impellers and large radii of curvature of the blades.

Regarding the less conventional pump types, Warman (13) compares casing wear patterns using the conventional and his own design and claims that wear is reduced with the latter's special impeller shape. Reference 14 also mentions this aspect. Wear is also stated to be less in the "TURO" design than in the conventional (14) but the only comparison reported involves a different pump material for each type.

Expressions for predicting pump life are given in References 6, 10, and 11. Bak (6) gives a formula:

$$\text{Life in hours, } T = A \frac{k\,Q^{n}}{H^{3/2} W_s X}$$

where A = constant factor (based on some known life figure); Q = solids concentration in mixture (pct); n = an exponent; k = impeller shape factor (1.0 for multibladed impellers and 1.4 for channel impellers); H = total head per stage, W_s = coefficient of

abrasive wear for impeller material = (volumetric wear of test material), and X = coefficient of abrasiveness of solids. Bergeron (11) also develops expressions for determining service lives of geometrically similar pumps of different size in terms of head and flow variations. Vasiliev (10) analyzes the statistical probability of a pump achieving a certain duration of trouble-free service defined by a specified maximum wear based on erosion tests.

It is questionable whether these complex theories can be used to predict pump life with any certainty -- most involve empirical constants and other parameters difficult to determine for an actual pump. In fact, Bergeron indicates that some of the assumptions made may be questionable. However, such theories are of some value in predicting likely trends of wear rates when only one or two of the relevant factors are altered.

3.2.1.2 Wear Locations and Phenomena

Good hydraulic design, particularly that which avoids rapid changes in flow directions, decreases wear. Slurry pump design has progressed in some instances to the point that a high degree of wear resistance has resulted. This has been accomplished through proper shaping of the hydraulic passages and adjacent flow elements over many year of development. Figure 1 shows a typical cross-section of such a pump and is referred to throughout the discussion of this section. A slurry pump experiences critical wear in the following areas:

a) Suction Pipe - Interaction of pump impeller

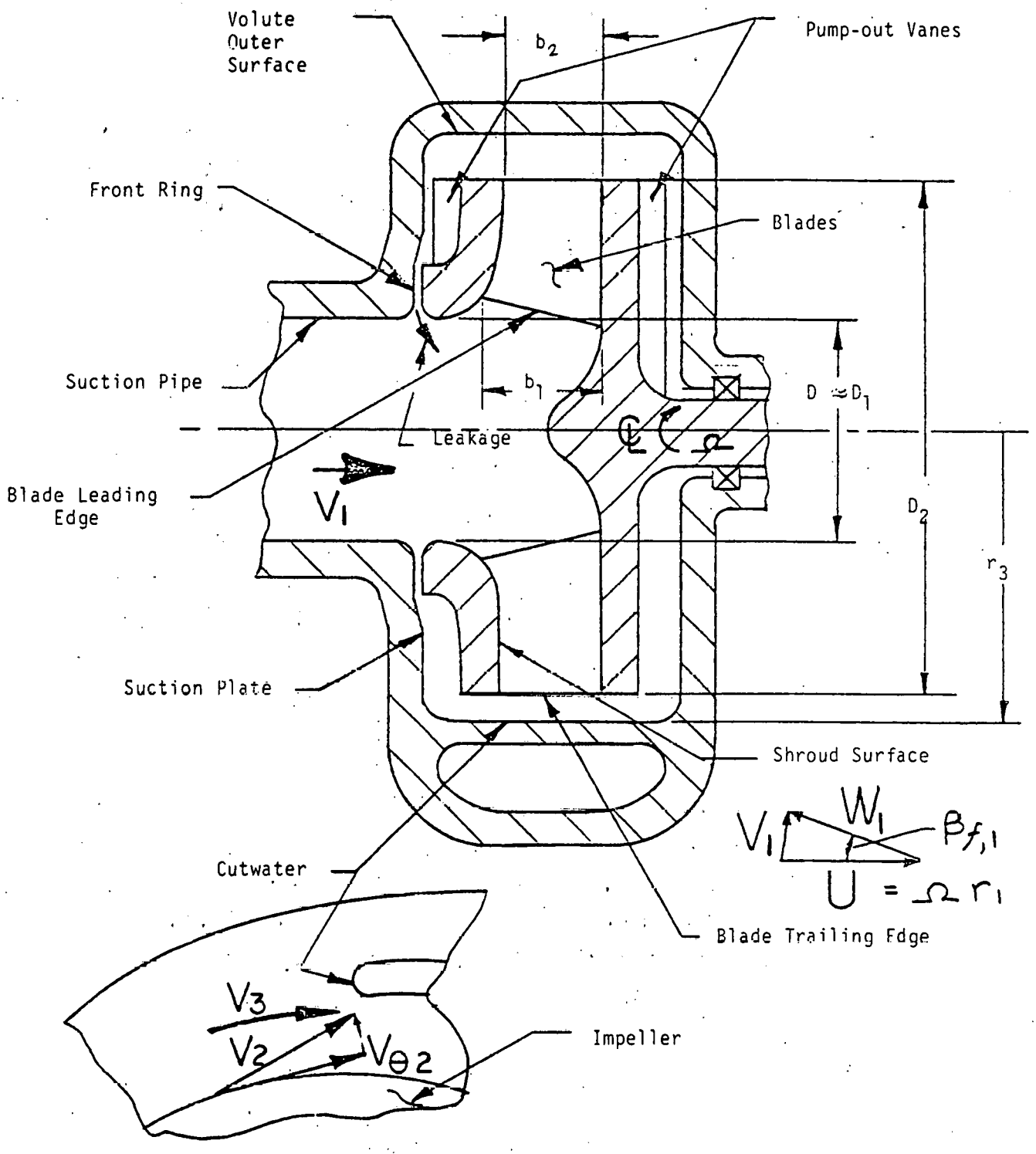

Figure 1: Typical Cross-section of Slurry Pump

front ring leakage with the incoming flow (or with backflow that can occur from the impeller eye at substantially lower-than normal flow rates), causes toroidal vortices whose solid particles can cut deep rings into the suction pipe and impeller eye I.D.

b) Impeller Blade Leading Edges - At the impeller inlet (Station 1), a high relative velocity W_1 seen by the blade can lead to many types of blade wear. Especially typical are horseshoe vortex gouges in the hub and shroud surfaces at the points where the blade leading edge intersects them.

c) Impeller Blade Surfaces - The blade surfaces can develop holes -- apparently originating on the driving face or pressure side. Scalloping (transverse to the flow), sometimes appears on the suction side or trailing faces -- probably due to secondary flows or transverse vortices in the boundary layer. Blade thicknesses of about 4 percent of impeller outside diameter, i.e., about twice the blade thickness of conventional clear water pumps, lengthen pump life.

d) Impeller Blade Trailing Edges - The blade land formed by the outside diameter machining of the impeller can develop circumferential grooves near the hub and shroud walls -- possibly from the interaction of emerging boundary layer flow with the adjacent fluid at the O.D.

e) Cutwater - Wear here is similar to that described for impeller blade leading edges and is the consequence of a high, largely circumferential approach velocity V_3 of the fluid emerging from the impeller. A large value of cutwater radius r_3 in

comparison to r_2 -- say $r_3/r_2 = 1.3$ or greater -- leads to lower values of approach velocity V_3 because the fluid tends to maintain constant angular momentum in flowing from impeller to cutwater.

f) Volute Outer Surface and Sidewalls - The volute liner experiences material removal by the action of particles moving at the scouring velocity -- about equal to V_3. Scaloping transverse to the flow direction sometimes can be seen on these surfaces -- again, probably the result of secondary flow in the volute cross sections or transverse vortices in the boundary layer.

g) Suction Plate - Slurry that leaks from impeller outside diameter through the front impeller ring acquires a very high circumferential velocity component because the angular momentum of the fluid tends to be conserved as it flows radially inward. With this velocity being at the outside diameter about half of impeller tip speed Ωr_2, it is easy to see that the suction plate can experience the highest velocities in the pump. Spirally-oriented gouging often appears on the suction plate, and the radially-oriented front ring clearance can wear rapidly. This, however, is less objectionable than the Taylor-Vortex-related circumferential grooving that would occur on the axially-oriented front ring clearance of conventional clear water pumps.

h) Pump-out Vanes - These are sometimes used to limit the circumferential velocity component adjacent to the impeller, to reduce leakage and related ring wear, and to provide axial thrust control. However, these vanes can cause objectionable wear on adjacent portions of the hub and shroud. Pump-out vanes on

the hub-side of the impeller help to protect the pump against seal failure.

It has been observed that the wide profile of the slurry pump impeller shown in Figure 4 leads to separation of the flow within the impeller, especially when combined with conventional blade shapes that yield large decelerations of the relative velocity W within the impeller passages. The resulting churning of the flow may be thought of as producing unwanted wear (15). However, with width b_2 being so large (namely, that resulting from radially parallel hub and shroud surfaces) -- a) there is more blade surface area to "spread" the particle abrasion load and b) the resulting separated, mixing flow may greatly decrease the otherwise thick particle layer which Tuzson shows to be highly damaging (4).

3.2.1.3 Wear Model

Evaluation of each wear phenomenon occuring in a slurry pump would be necessary to determine the life of the associated part of the machine. Without attempting to do this, however, some observation can be made about general trends that are evidenced for a given pump geometry by applying a fundamental model for wear by synfuel slurries. First the life of a critical component of thickness t is stated as follows:

$$\text{Life} = \frac{t}{e} \qquad (1)$$

where e is the local rate of increase of wear depth in the affected zone of the surface. Tuzson states that

$$e = \frac{\text{Erosive Power/Area of Surface}}{\text{Erosion Energy/Volume of Surface}} = \frac{P}{E_{sp}} \qquad (2)$$

where E_{sp} is also known as the specific energy of the surface and is equal to about twice the hardness p in kgf/mm^2. For example, p = 200 for cold-rolled, low-carbon steel and 650 for hardened 28-chrome iron. (16) All particles in Tuzson's apparatus joined an abrading layer and led to the followind development of Equation (2):

$$e = \frac{(\rho_s - \rho_f) C_v Q \Omega^2 r / b}{E_{sp}} \qquad (3)$$

where the Coriolis force that moved the particles toward his rotating paddle or blade of width b (cf. Figure 1) is related to $\Omega^2 r$ or the "g"-field of the flow. Here, ρ_s and ρ_f are the particle and carrier liquid densities, respectively. C_v is the concentration by volume and Q is the total slurry volume flow rate.

In an actual pump, the "g"-field is also properly represented by $\Omega^2 r$, and it consists of forces arising from centrifugal, Coriolis and streamline curvature effects -- the latter effect being the only one in the stationary passages. But, in a pump, not all the

particles reach the pressure side of the flow passage. In fact, some are even thrown out in other directions by centrifugal force.

Thus, a pump erosion model would properly take into account the ability of particles to cross streamlines at a velocity $W_\perp$ (or $V_\perp$ in stationary components), so that it is proposed that Tuzson's model be modified as follows:

$$e = k_g' \times \frac{(\rho_s - \rho_f) C_v \Omega^3 r_2^3}{E_{sp}} \left(\frac{W_\perp}{\Omega r_2}\right) \qquad (4)$$

where $k_g' \Omega r_2^2 = \left(\frac{Q}{\Omega r_2^3} \times \frac{1}{b_2/r_2}\right) \Omega r_2^2 \qquad (5)$

and k_g' is a constant of the geometry at a given flow condition, (which is what we are examining).
Experience indicates that the geometry or angularity of the solid particles influences wear rate. Therefore we will examine the same pump and the same particle geometry and include the latter also in the constant k_g'. Here, solution of the equation of motion for particle drag at velocity $W_\perp$ normal to a stremaline yields the following for a carrier fluid of kinematic viscosity ν_f and a particle of size d_p:

$$\frac{W_\perp}{\Omega r_2} = \frac{4}{3} \times \frac{d_p^2 \Omega}{\nu_f} \left(\frac{\rho_s}{\rho_f} - 1\right) \underbrace{\left(\frac{W^2}{\Omega^2 r_2^2 \frac{R}{r_2}} + \frac{r}{r_2}\cos\beta - \frac{2W}{\Omega r_2}\right)}_{\text{"G"}} \qquad (6)$$

where R is the radius of curvature of the streamline in the relative system (or in the absolute system for stationary components, where $W_\perp$ is replaced by $V_\perp$ and the other two "G" terms are zero), and β is the acute angle between the relative streamline and the tangential direction. In formulating Equation (6),

the laminar drag coefficient C_D for spheres was assumed to hold; namely,

$$C_D = \frac{24}{R_{e,\perp}} = \frac{24}{W_\perp d_p / \nu_f} \tag{7}$$

which is valid so long as the cross-streamline Reynolds number $R_{e,\perp}$ is less than 5. (16). As noted earlier, the constant includes the particle geometry and therefore the alteration required to C_D for particle angularity.

Combining Equations (1), (4), and (6), we obtain an Equation for pump life, assuming that t/r_2 is constant (= given geometry):

$$\text{Life} = k_g \frac{p \cdot \nu_f}{\rho_f \left(\frac{\rho_s}{\rho_f} - 1\right)^2 C_v g H \Omega^2 d_p^2} \tag{8}$$

where pump head $H \propto \Omega^2 r_2^2$ and where the concentration by volume C_v is found from that by weight, C_w as follows:

$$C_v = C_w \times \frac{\rho_f}{\rho_s - C_w(\rho_s - \rho_f)} \tag{9}$$

and other constants have been abosrbed into geometrical constant k_g.

Determining k_g from one of the two 3560 rpm pilot plant pumps for which we have approximate data, Equation (8) produces the curves of Figure 2, which shows the final form of the equation, employing the

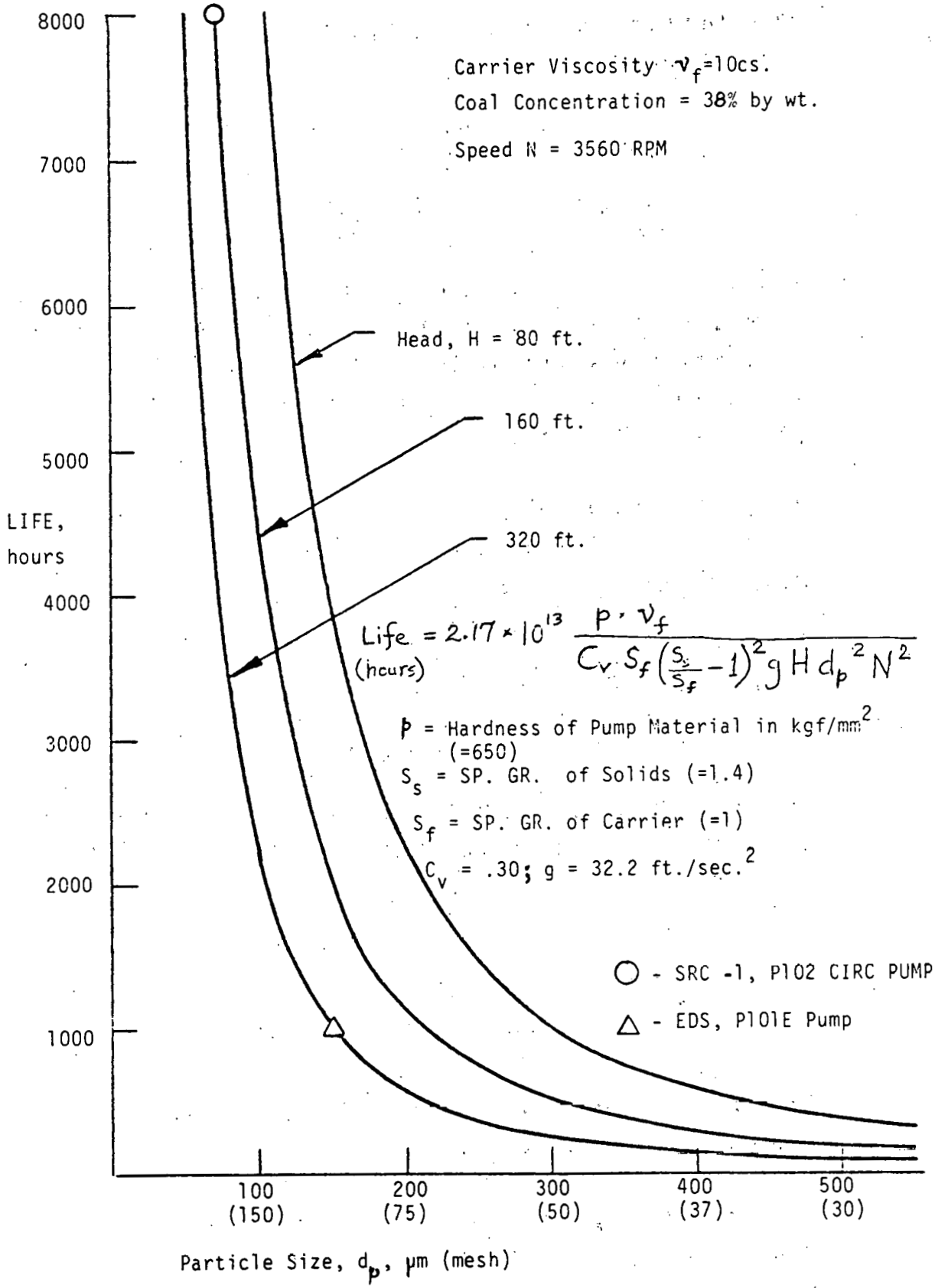

Figure 2: Approximate Life Relationship for Pilot Plant Pumps

units noted in the figure. The other pump fits this correlation. Approximately similar "front-end" slurries and similar abrading characteristics of the solids contained in them were involved in both cases. Both pumps were only partial departures from convential clear water designs from a hydraulic standpoint, but hard materials were employed in their construction. Specific speeds at the operating points were similar ($N_s \approx 900$), and speeds were high - - both ran at 3560 rpm.

Equation (8) and Figure 2 do not explicitly show that wear is proportional to the cube of fluid velocity or to $(\Omega r_2)^3$ as is often stated (17). However, from Equation (1) and the fact that t/r_2 was assumed constant in Equation (8), it is seen that the wear depth rate is given by

$$e = \frac{f_f \left(\frac{\rho_s}{\rho_f} - 1\right)^2 C_v g H \Omega^2 r_2 d_p^2}{k_g p V_f} \qquad (10)$$

With the pump head $H \propto \Omega^2 r_2^2$ and the fact that velocities in the pump are proportional to tip speed Ωr_2, we see now that

$$e \propto \Omega \cdot (\Omega r_2)^3$$

that is, the wear depth rate varies as the cube of velocity (or the 3/2 - power of pump head H) and directly with the pump rotative speed.

Included in the factor k_g is the abrasivity of the particles; i.e., k_g will be smaller for more highly abrasive slurries than the front-end synfuel slurry of Figure 2. For example, k_g may be inversely

preportional to particle abrasivity or knoop hardness. This does not necessarily mean that a bottoms slurry with, say, ash at C_v = 0.1 (10% concentration by volume) would reduce pump life below that of a similar pump in C_v = 0.3 front-end slurry -because (see equation 8) viscosity of the carrier is at least an order of magnitude greater in bottoms slurry, and the concentration there is lower than in front-end slurry.

To be put forward with confidence, however; this wear model, while yielding expected trends, requires more corroborating data than are currently available from pilot plant experience.

3.2.1.4 Specific Speed

If the speed of the pumps of Figure 2 had been more like that of most of the other pilot plant pumps, i.e., generally half of the 3560 rpm figure shown, the wear life would have been about four times greater than illustrated there. Thus, a designer needs criteria for choosing speed, based on life requirements.

A properly designed slurry pump will have critical velocities that essentially equalize the wear rates on various parts. This leads to a pump geometry that is characteristic of a particular value of specific speed N_s, where

$$N_s = \frac{N(\text{rpm})\ \sqrt{Q(\text{gpm})}}{[H(\text{ft.})]^{3/4}}$$

thereby dictating a speed N for a given head H and

volume flow rate Q.

The major geometrical influence leading to a value of specific speed arises from attempting to equalize the impeller inlet relative velocity W and the cutwater approach velocity V_3 (Figure 1). Except possibly for the front shroud leakage velocities in certain cases, these are the highest velocities that directly impinge on known high-wear locations of slurry pumps. This is explained as follows. Noting that for no prewhirl,

$$W_1 = \sqrt{V_1^2 + (\Omega r_1)^2} = \Omega r_1 \sqrt{\phi_e^2 + 1} \qquad (13)$$

and

$$V_3 = V_{\theta,2} \cdot \frac{r_2}{r_3} k_{2-3} \qquad (14)$$

where k_{2-3} (<1) is a factor that represents the reduction (due to sidewall friction) of V_3 below the value it would have it angular momentum were constant from impeller O.D. to cutwater. The flow coefficient $\phi_e = \frac{V_1}{\Omega r_1} \approx 0.4$; and k_{2-3} is 0.8 to 0.9 for $r = 1.3r$, as is often found in slurry pumps. The circumferential velocity component $V_\theta \left(= \psi/\eta_{hy}\right) \cdot \Omega r_2$, where η_{hy} is the hydraulic efficiency. The head coefficient $\psi = gH/\Omega^2 r_2^2$ is essentially equal to 0.5.

Requiring the velocities W_1 and V_3 to equal one another leads to the following requirement for specific speed:

$$\Omega_s = \psi^{-3/4}\left[\frac{k_{2-3}/\left(\frac{r_3}{r_2}\right)}{\eta_{hy}}\right]^{3/2}\frac{\sqrt{\pi\phi}}{(\phi_e^2+1)^{3/4}} \qquad (15)$$

where Ω_s is the (universal) unitless specific speed ($N_s/2733$):

$$\Omega_s = \Omega\sqrt{Q}/(gH)^{3/4} \qquad (16)$$

For $\psi = \frac{1}{2}$, $\eta_{hy} = \frac{3}{4}$, $k_{2-3} = 0.85$, $\phi_e = 0.4$ and $r_2/r_3 = 1.3$,

Equation (15) yields

$$N_s = 1327 \quad \text{and} \quad \Omega_s = 0.4854$$

Because of its predominant and direct effect on the critical approach velocities W_1 and V_3, the radius ratio r_3/r_2 has the primary effect on the geometrical constant k_g of the life equation (8). Conservatively, k_g is proportional to $(V_2/V_3)^2$ where, by definition

$$V_3/V_2 = k_{2-3}/\left(\frac{r_3}{r_2}\right) \qquad (17)$$

Wall drag studies suggest that

$$k_{2-3} \overset{\propto}{\approx} \sqrt{\frac{1}{r_3/r_2}}$$

so that the velocity reduction to the cutwater is represented by

$$k_{2-3} \Big/ \frac{r_3}{r_2} = \left[k_{2-3} \Big/ \left(\frac{r_3}{r_2} \right) \right]_o \times \left[\frac{(r_3/r_2)_o}{(r_3/r_2)} \right]^{1.1} \qquad (19)$$

where subscript o denotes base values (k_{2-3} = 0.85 and $(r_2/r_3)_o$ = 1.3). Thus from Equations (17) and (19) and $k_g \propto (V_2/V_3)^2$, we get the effect on the life factor of cutwater radius; namely,

$$k_g = k_{g,o} \left[\frac{r_3/r_2}{(r_3/r_2)_o} \right]^3 \qquad (20)$$

Assuming that the wear model of the preceeding section applies, Equation (8) becomes, (using Equation 16), the following:

$$Life = (k_g)_o \left[\frac{r_3/r_2}{(r_3/r_2)_o} \right]^3 \frac{p V_f Q}{C_v (gH)^{5/2} \Omega_s^2 d_p^2 \rho_f \left(\frac{\rho_s}{\rho_f} - 1 \right)^2} \qquad (21)$$

Now with Equation (19), the specific speed Ω_s is expressed as a function of radius ratio; i.e., with ψ = 1/2, η_{hy} = 3/4, and ϕ_e = 0.4, Equation (15) reduces to the following:

$$\Omega_s = 0.4854 \cdot \left[\frac{(r_3/r_2)_o}{r_3/r_2} \right]^{9/4} \qquad (22a)$$

or

$$N_s = 1327 \cdot \left[\frac{(r_3/r_2)_o}{r_3/r_2} \right]^{9/4} \qquad (22b)$$

This relationship is plotted in Figure 3, where it is noted that a smaller cutwater-to-impeller radius ratio produces greater speed and shorter life. In fact, if Equation (22a) is substituted into Equation (21), we get an expression for pump life that implicitly contains speed and sizing information together with a direct statement of synfuel plant scale effect: namely,

$$\text{Life} = \frac{k_{g,c}}{0.2356} \left[\frac{r_3/r_2}{(r_3/r_2)_c}\right]^{7.5} \frac{\rho V_f Q}{\rho_f \left(\frac{\rho_s}{\rho_f} - 1\right)^2 C_v (gH)^{5/2} d_p^2} \qquad (23)$$

where speed is found from

$$\Omega = \Omega_s \cdot (gH)^{3/4} / \sqrt{Q} \qquad \left.\right\} \qquad (24)$$

$$\left(\text{or } N = N_s \cdot H^{3/4} / \sqrt{Q}\right) \qquad \left.\right\}$$

and $\left(\frac{r_3}{r_2}\right)_c$ is found from Equation (22a);
and

$$r_2 = \frac{1}{\Omega} \sqrt{\frac{gH}{\psi}} \qquad (25)$$

$$(\psi \approx 0.5)$$

and $(r_3/r_2)_c$ typically equals 1.3.

Figure 4 is a plot of Equation (23) which illustrates the powerful effect of cutwater-to-impeller radius ratio r_3/r_2 on slurry pump life. Here specific speed is reduced at larger r_3/r_2 to take full advantage of equalizing W_1 with the correspondingly lower V_3. This, of course, leads to a larger, slower pump for a given head and flow rate, (Equation 24 and 25), and corresponding speed and

Shown are optimum values that equalize velocities relative to cutwater V_3 and impeller blade leading edge W_1. (Note that a larger cutwater radius, r_3, reduces V_3; maintaining $W_1 = V_3$ then produces a lower rotation speed N and greater life.)

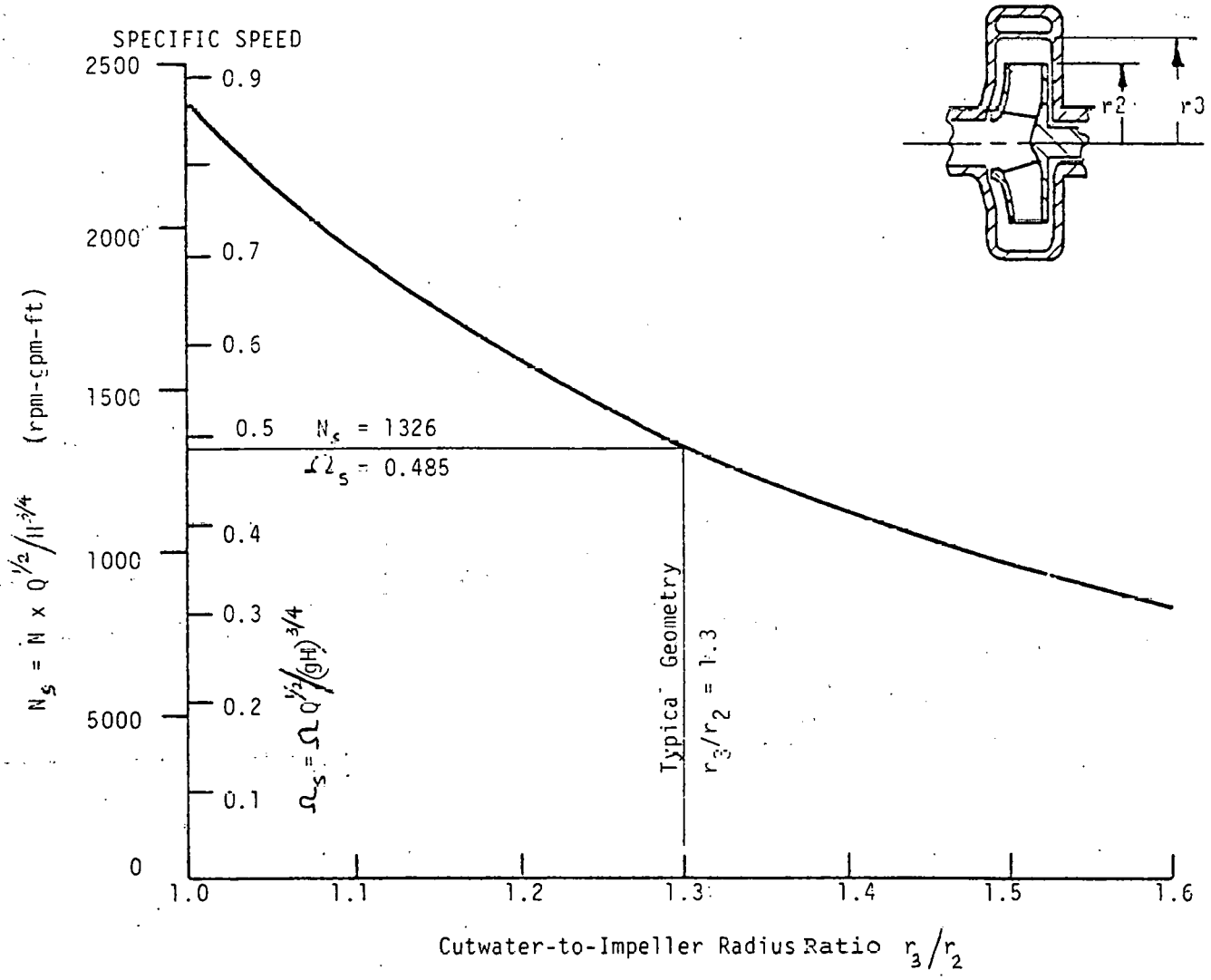

Figure 3: Slurry Pump Specific Speed vs. cutwater-to-Impeller Radius Ratio.

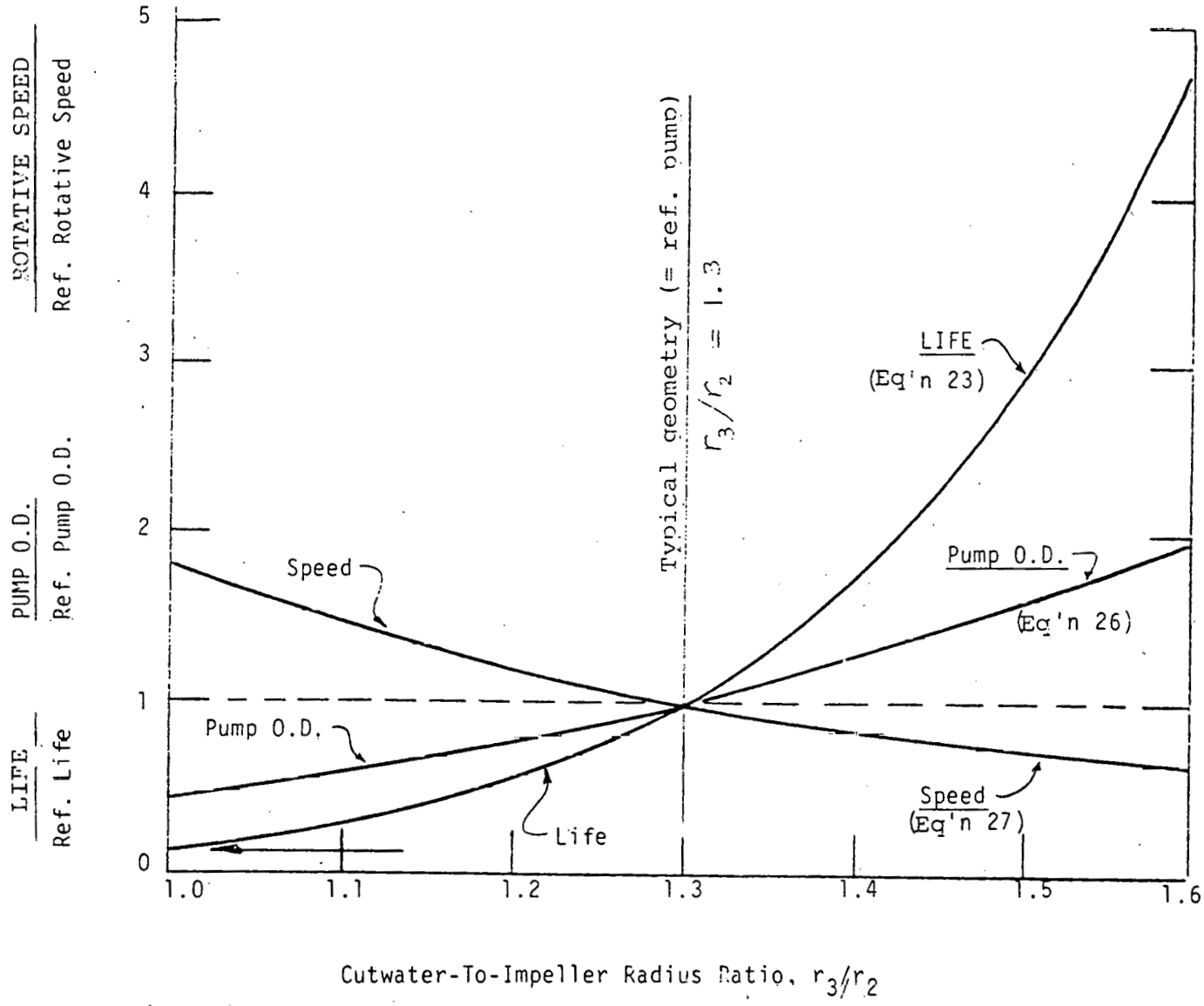

Figure 4: Slurry Pump Life, Size and Speed Relationship
(Head and Flow Rate Fixed)

For each value of the cutwater-to-impeller diameter ratio, the specific speed is chosen that equalized the inlet relative velocity W_1 and the cutwater-approach velocity V_3.

pump O.D. curves are also shown on Figure 4, where it has been assumed that pump O.D. is proportional to r_3. Thus with Equations (22a) and (25), at constant head and flow rate,

$$\text{Pump O.D.} \propto \left(r_3/r_2\right)^{13/4} \qquad (26)$$

since

$$\text{Speed} \propto \frac{1}{\left(r_3/r_2\right)^{9/4}} \qquad (27)$$

While Equation (23) may appear to be different from Equation (8) and the trend shown in Figure 2, this is not so. Inspection of Equation (24) and (23) show that for constant specific speed (as was the case, approximately, for Figure 2) $Q \propto H^{3/2}$, yielding the inverse dependence on head expressed in Equation (8).

3.2.1.5 Scaling

Equation (23) also shows that life of slurry pumps improves directly with flow rate so that when we scale a given geometry, holding head constant, the full-scale plant will have better life in direct proportion to flow rate; and, for the same specific speed, the speed will be lower by the inverse square root of the flow rate, and the size will be in proportion to square root of flow rate (Equations 24 and 25).

Obviously the larger pump of the full-scale plant will be more costly. If it is desired to reduce pump size, the radius ratio r_3/r_2 is reduced; speed is increased accordingly; and pump radius r_2 (and r_3) is reduced. For example if it is also desired to duplicate the life of a model full-head pump; the radius ratio can be reduced by a small amount (Equation 23) to compensate for the favorable life effect of the flow-rate increase.

These conclusions about life arise from the effects of particles crossing streamlines, which phenomenon in turn depends on streamline curvatures that decrease with increasing size. See the development of Equation (8). In all of this, the ususal assumption that solid particle sizes stay relatively constant from pilot plant to full-scale plant has been applied.

The usual way to scale up a pump is to do so while maintaining head and specific speed. Thus the large and small machines require the same NPSH, since

$$\text{NPSH} = \left(\frac{\Omega}{\Omega_{ss}}\right)^{4/3} \frac{Q^{2/3}}{g} \qquad (26)$$

where the suction specific speed

$$\Omega_{ss} = \Omega Q^{1/2} / (g\,\text{NPSH})^{3/4} \qquad (27)$$

is also constant, and from Equation (24)

$$H = \left(\frac{\Omega}{\Omega_s}\right)^{4/3} \frac{Q^{2/3}}{g} \qquad (28)$$

and dividing Equation (26) by (28) yields NPSH $\propto$ H. However, if more NPSH is available, the prototype full-scale machine does not need to be so large and slow running as Equations (22) and (25) would dictate, provided that the life-consequences (Equation 8 or 23) are acceptable.

3.2.2 TEST FACILITY AND PROCEDURE

A Small-Scale Test (SST) Loop was designed and fabricated in order to provide rapid screening of hydraulic concepts for slurry pump design. The use of sand/water as the primary slurry was selected in order to obtain accelerated wear data. Various particle sizes and viscosity fluids may be used. Small-scale hydraulic components (impeller sizes 4"-5" O.D.) are used for ease of fabrication and handling. Two pump rigs may be run off of a common drive shaft for side-to-side comparisons of designs in common test conditions. The pump rig speed may be adjusted to match blade speed and specific speed requirements. Hydraulic performance of different designs in various concentrations and types of slurry can also be obtained. Finally the effects on wear and performance due to size scale-up can be evaluated when a design is evaluated in the SST Loop as well as a Large-Scale Test Loop.

The slurry test loop is shown in Figure 5 and the schematic is presented in Figure 6. The key elements of the loop are:

a. Agitation/Mixing
b. Heat Rejection
c. Head Breakdown
d. Drive System
e. Sampling System

The slurry mixing tank (T101) is a 55-gallon drum with a rubber liner material. Agitation is accomplished by using a 1/2" sand blast nozzle (N101)jetting against a tungsten carbide plate secured to the bottom of the tank. Interruption of

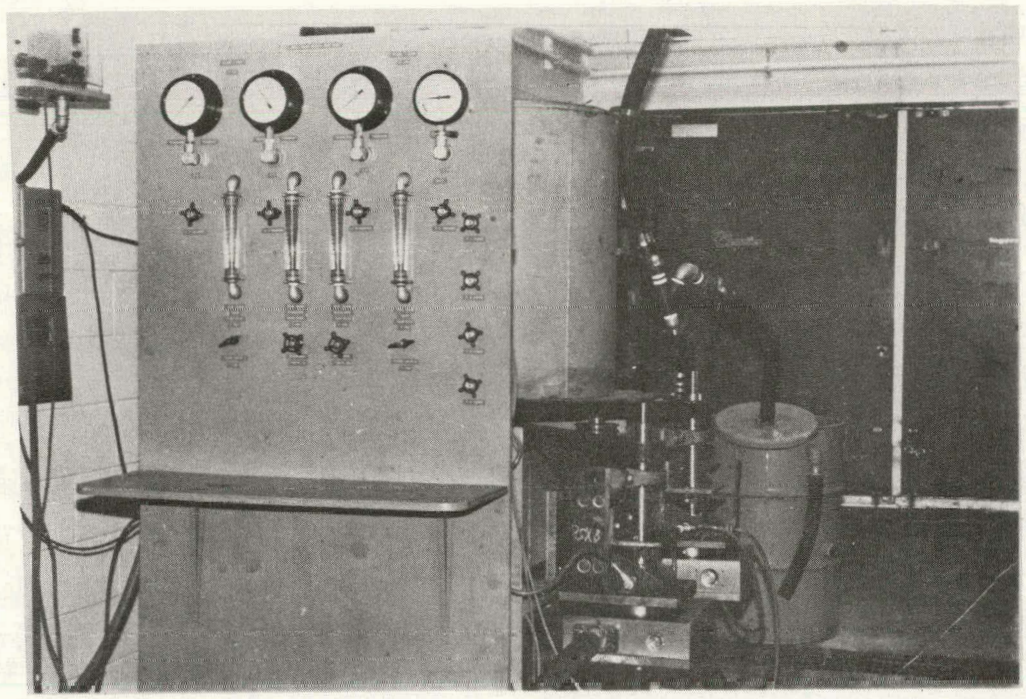

FIGURE 5: VIEW OF SST LOOP

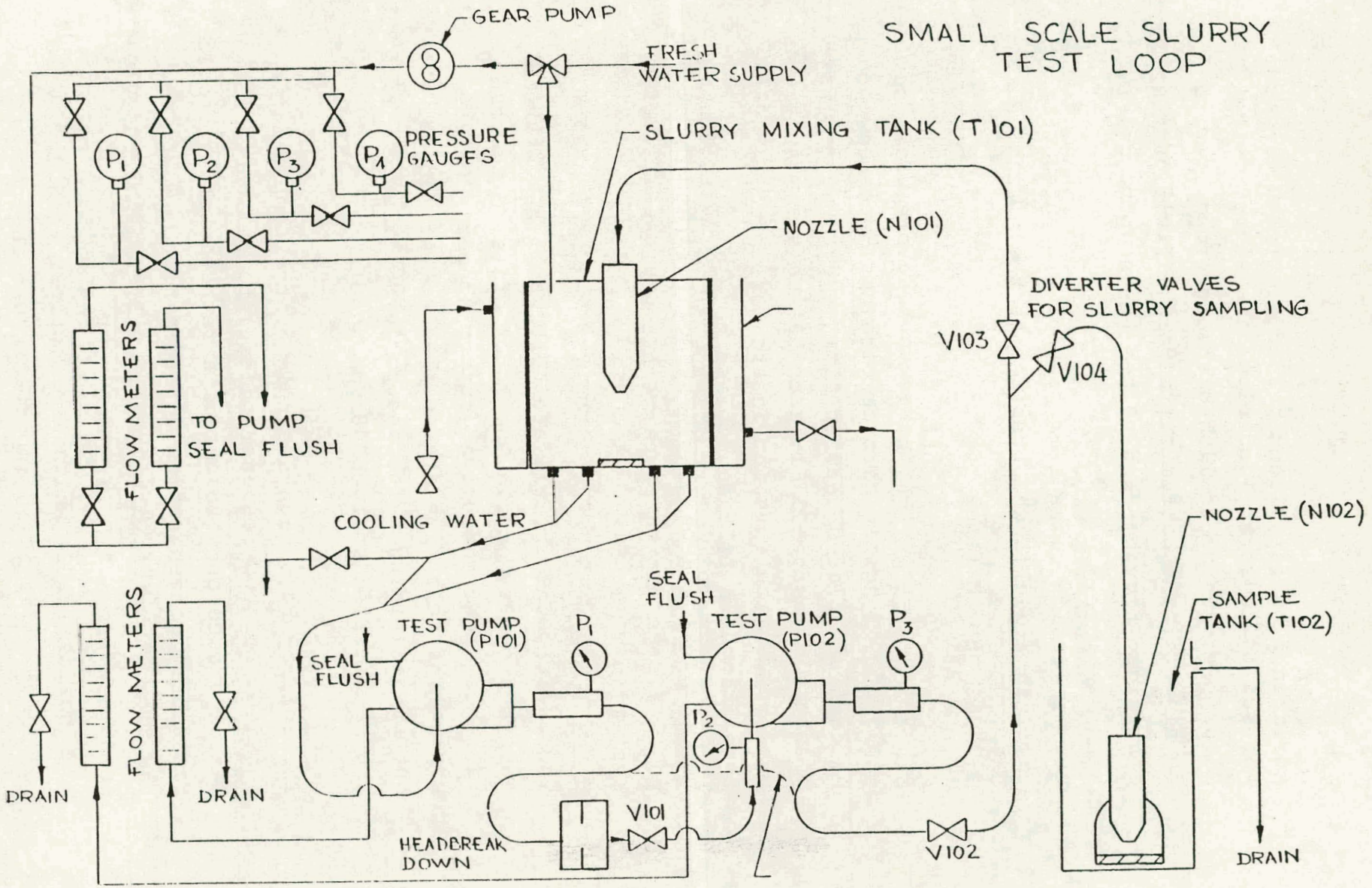

Figure 6: Small Scale Slurry Test Loop Schematic

the main flow for a long period of time will cause the solids to settle and block the slurry feed lines. Slurry feed is accomplished through four 1" pipe openings in the bottom of the tank (T101), which are manifolded together and routed to the pump inlet.

Heat rejection comes from providing treated cooling water to a jacket which surrounds the mixing tank (T101).

Several different approaches to head breakdown can be employed. Tungsten carbide bushings, pressed into holders and placed between flanges are used as main pressure breakdown. Clarkson "B" valves, knuckle pinch-type with a rubber insert, are used for fine throttling. A 1/2" sand blast nozzle (with a tungsten carbide coating) is used for head breakdown nd is also an integral part of the slurry agitation system in T101.

The shaft power is delivered from a 15 Hp, 3600 rpm AC synchronous motor. The motor drives a Reeves-variable speed motodrive (output speeds 400-3980 RPM). The test rigs are coupled to the motodrive output via timing belts and pulleys. The test rigs can be operated up to 6000 rpm.

The ability to obtain a sample of the pumped fluid is required for two reasons: first, to calibrate flow meters and second, to obtain a representative sample for slurry concentration determination. To divert the flow, two fast acting ball valves (V103 and V104) are placed in a "Y" fitting. The sample line leads to a nozzle (N102) which is identical to N101. In the sample mode it is important that the resistance of the sample branch be the same as the slurry return

line to T101 so that when doing a flow calibration or slurry sample, the operating point of the pumps is not changed due to a significant change in system resistance. The sample line nozzle, N102 discharges into a tank, T102 which is calibrated for volume. The sample may be weighed for concetration determination or timed for flow rate check.

A high pressure, low flow gear pump (P103) is used to provide clear water for seal flush injection and instrument line purge.

The size of the hose and piping, used in the loop, is determined on the basis two factors, both a function of slurry velocity (i.e. flow rate and pipe diameter). High velocities promote rapid wear at fittings and other discontinuities but inhibit slurry settling or clogging at bends and vertical sections. Low velocities would allow fittings to wear indefinitely but clogging problems will occur. For the expected flow rates, 30 to 60 gpm, 1.25" I.D. hose and 1" Sch 80 pipe was selected. This corresponds to hose velocities of 7.8 to 15.7 feet/second and pipe section velocities of 14 to 28 feet/second.

A primary consideration in the design of the pump test rigs was to provide a vehicle which makes an introduction of hydraulic design changes fast and simple. The modular approach shown in Figure 7 was selected. The typical test hardware is shown in Figure 8. Three stator pieces are required for each build: suction nozzle, front wall and volute liner. The impeller is the fourth component of the build. All four pieces are subject to wear. The other components are common for all builds.

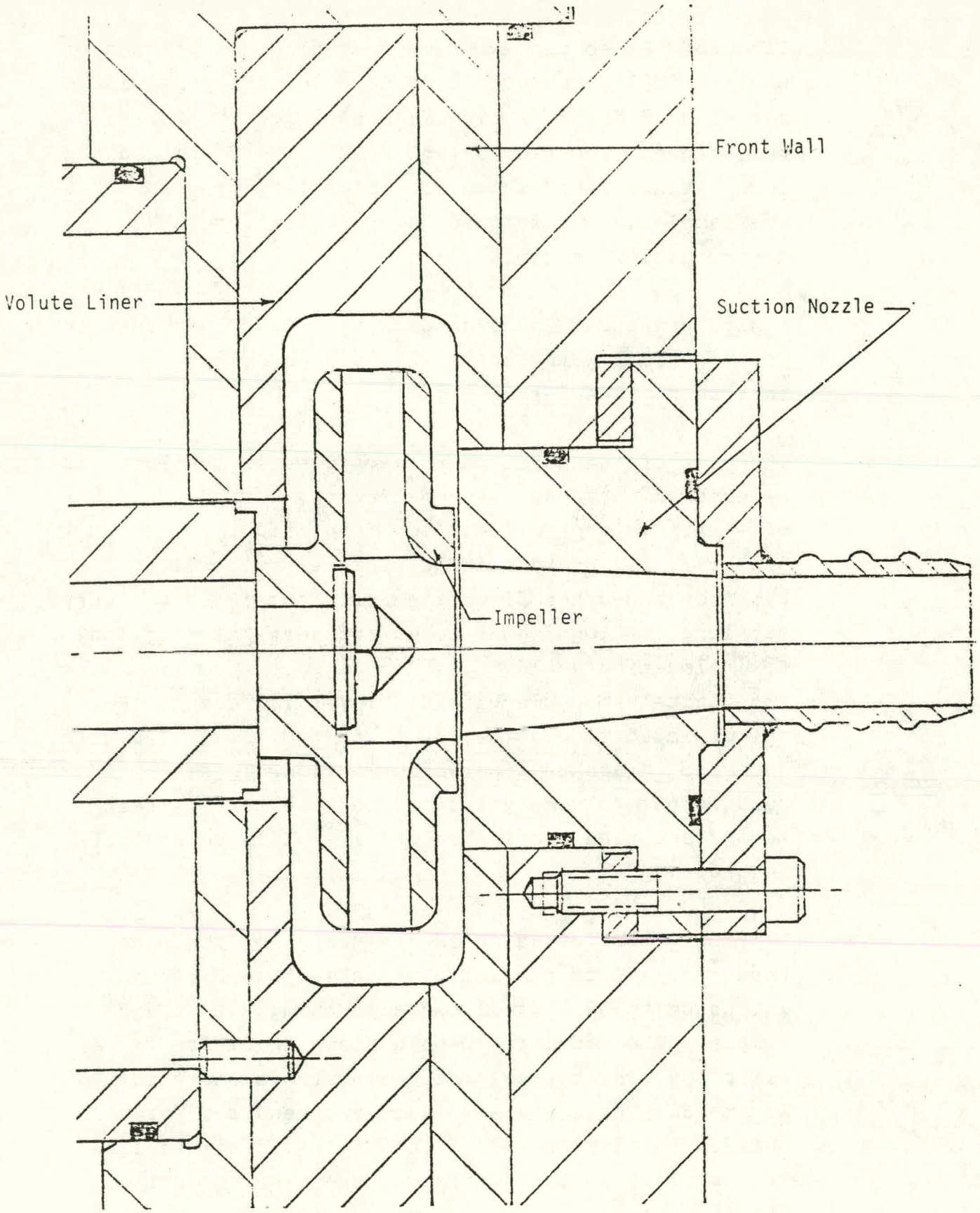

Figure 7: SST Pump Rig Hydraulic Components

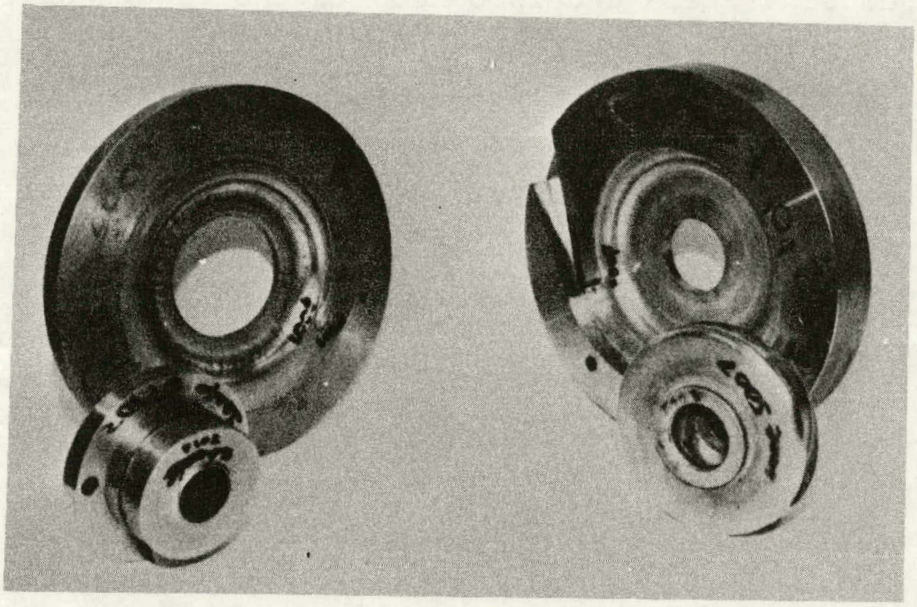

FIGURE 8: TYPICAL SST HYDRAULIC COMPONENTS

Several compromises are made in order to make fabrication and assembly of test components easier and less time-consuming. The present volute designs call for two-dimensional, rectangular corss sections. They are machined parts. The front wall mounting does not allow for a fillet along the mating surface with the volute piece. A two-dimensional diffuser is milledd into the volute ring. The impellers are also two-dimensional, machined parts. The front shroud is machined separately and is bonded to the bladed half of the impeller with a high-strength epoxy. The whole impeller is then finished machined. The front shroud piece may be removed later for inspection of the blade passages. The mating of the front shroud piece to the blade forms a 90 degree fillet. Consideration of this type of git is important when identifying and evaluating impeller wear.

In order to avoid an elaborate seal design effort a simple, single, pressure balanced carbon face seal was selected (Figure 9). Adequate seal flush and flush drain provisions are requuired 3to prevent sand from entering the seal cavity. The orientation of the test rigs also prevents trace sand from settling into the seal area following pump shutdown. The seal ring package rotated with the shaft and the hard mating ring is stationary. Installaation is typical of process pump application.

Grease packed, pillow block-type ball bearings are used to support the shaft. The life of these easily replaced bearings is not an important factor. Shaft speeds of 6000 rpm represent the maximum speed for these bearings; and thus, compromises life.

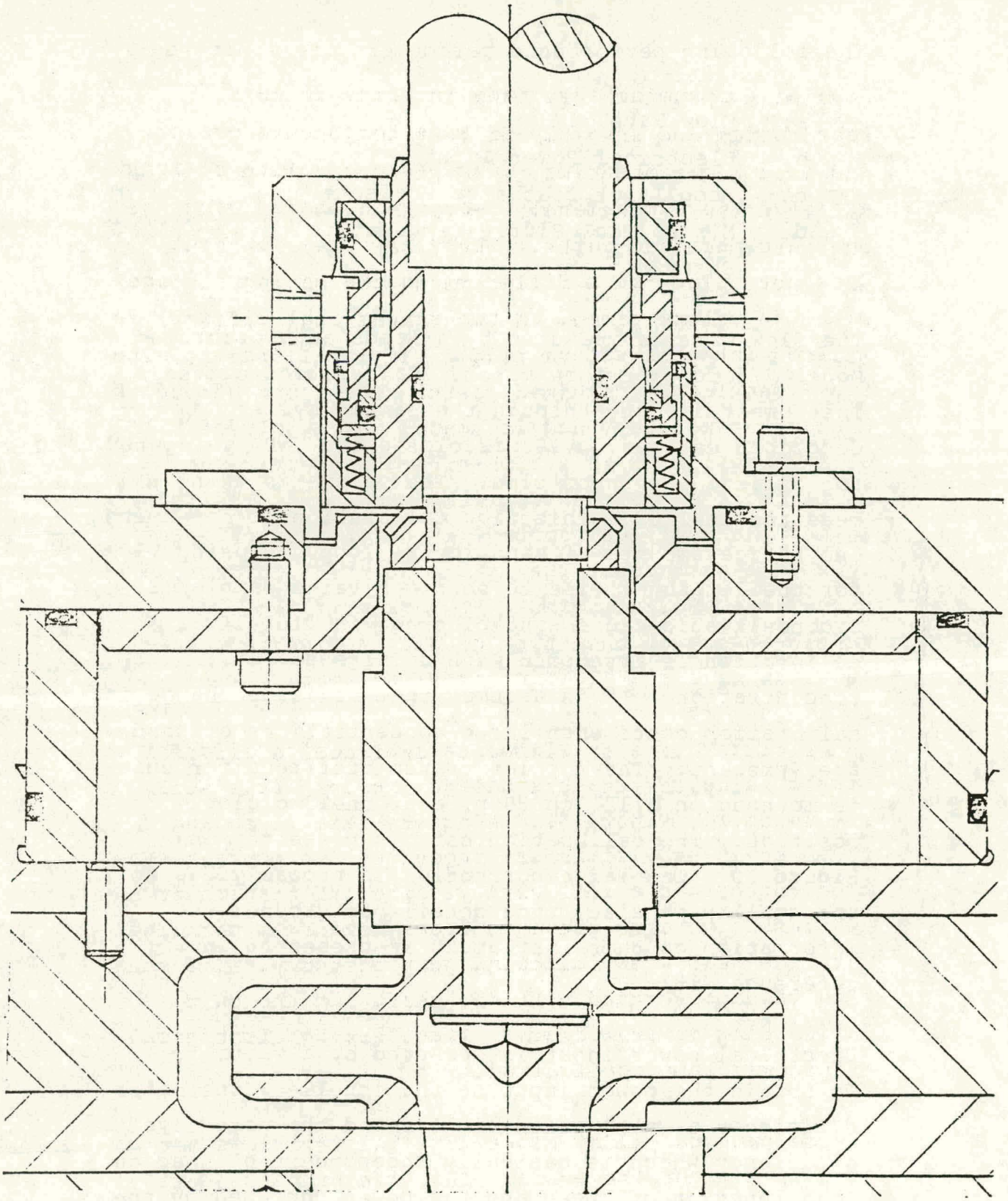

Figure 9: SST Seal Arrangement

The following performance parameters are monitored:

a. Flow Rate
b. Electrical Power Input
c. Pump Inlet/Discharge Pressure
d. Mixing Tank Slurry Temperature
e. Shaft rpm

The flow rate is measured by a Leeds and Northrup Model 775 doppler flow meter. Calibration of the instrument is done through the sample system described earlier. V103 is closed and V104 is opened for a fixed length of time. The volume is then measured in T102. This flow calibration is done with only trace amounts of sand in the loop. Closing V103 for the length of time to obtain a valid sample (20 seconds) would cause sand blockage in T101 if calibration is attempted with a large solids concentration. It is assumed that no large change in calibration occur when large concentrations of sand are present. The doppler transmitter/receiver unit is mounted on a 1" Sch 80 pipe at the 3 o'clock position. The calibration data is presented in Figure 10. The large correction is probably due to the small pipe size. the detail background information on this instrument is presented in reference (18).

Electrical power input is measured by a wattmeter. To obtain the power input to the impeller, the motor efficiency as a function of load and the motodrive efficiency which is basically independent of load but is a function of speed and the power consumed by the seal must be considered. Since the seal is pressure balanced, its power consumption versus speed may be measured by running it in water with no impeller.

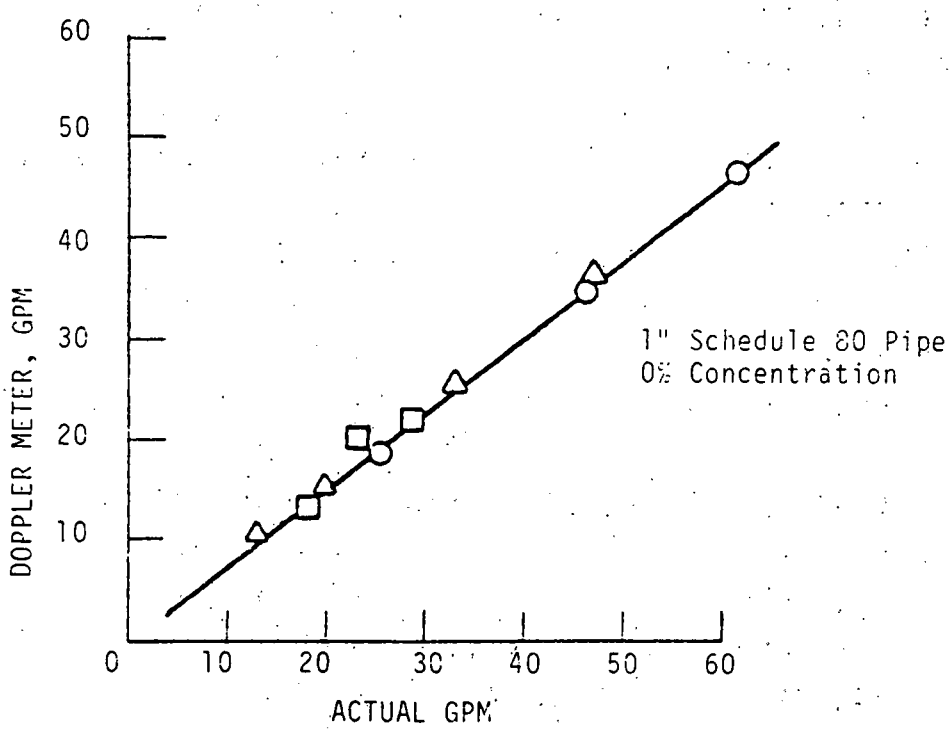

Figure 10: Doppler Flowmeter Calibration

Inlet and discharge pressures are measured at 1" Sch 80 pipe sections upstream and downstream of the pump. The slurry temperature of T101 is measured with a mercury thermometer. The shaft speed is measured with a portable, digital strobe.

The results of three separate doppler flow meter (DFM) calibrations is shown in Figure 10. The calibration runs were done with only trace amounts of sand and with accumulation times between 10 and 20 seconds. The linear nature of the calibration results in applying a constant correction factor is as follows:

$$\frac{\text{Doppler GPM}}{\text{Actual GPM}} = 0.75$$

Sampling for slurry concentration is more difficult than flow rate determination. Since closing V103 stops the slurry return to T101, the agitation is altered thus changing the concentration at the slurry feed lines in the bottom of the tank. Because of this, sampling is done for a very short period of time (approximately 2-3 seconds) or just enough time to collect the slurry which is resident in the lines and pump at the time V103 is closed and V104 is open. The results of two runs are shown in Figure 11. The loop conditions such as net flow through N101 and the starting volume of water (before sand addition) are noted. It is expected that with less nozzle flow, less agitation will results and a higher concentration will result for a given amount of sand added. Samples must be obained to verify this.

The test pumps are started with clear water.

Instrument lines are purged, seal flush injection and drain flow rates are set, the cooling water jacket is filled, and supply and return flows balanced off. When the desired speed and clear water flow rates are established, sand is added. If the flow rates are between 50-60 gpm, the curve in Figure 11 may be used to determine the amount of sand to be added for the desired slurry concentration. For other flows, gradual addition of sand with sampling may be necessary to obtain the desired concentration. Removal of sand from the loop is accomplished by running the pumps with V103 and V104 open and adding clear water to T101. In this process, T102 serves as a settling tank. The dilution process takes to to 10 minutes after which time the loop is shut down with no chance of clogging.

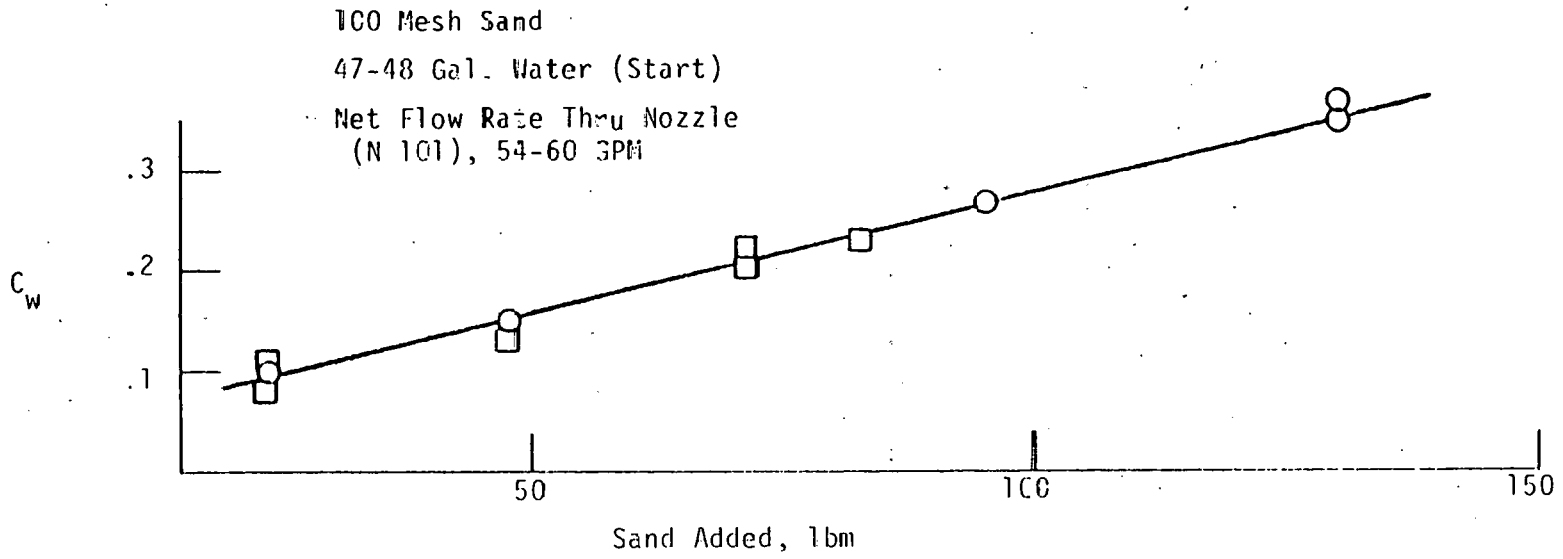

Figure 11: SST Loop. Sand Concentration (Mass Ratio)

3.2.3 TEST HARDWARE DESIGN, RESULTS & DISCUSSION

The Small Scale Test (SST) Loop, described previously in this report, provides a means of evaluating hydraulic design concepts for wear and performance on slurries of varying characteristics. The hydraulic components tested include impeller, front suction nozzle and volute liner (See Figure 7). The small scale of the components allow for rapid assembly, thus making it possible to evaluate redesigned components quickly. This part of the overall program is intended to screen several initial hydraulic concepts and refine a selected set of hydraulic components thru design modifications. The result will be a set of design criteria which will be applied to pilot plant size slurry pumps.

The following list summarizes the major factors which need to be considered when designing a slurry pump for minimum wear:

- Wear as a function of design & off design operation
- Volute cutwater damage
- Impeller trailing edge damage (related to blade loading)
- Slurry carrier viscosity (affects particle dynamics)
- Front shroud and ring wear
- Material hardness
- Specific speed effects
- Particle size

A test program which investigates the above factors, and allows for design improvements in those areas requires a set of hardware. Four base line impeller

cncepts were designed, all intended to be 900 specific speed machines in clear water:

SST 3 5V	- A traditional slurry pump design with 5 blades
SST 3 4V	- SST 3 impeller with only 4 blades
SST 5	- A new approach, low blade loading accomplished by maintaining a constant relative velocity passage (achieved by controlling blade angle, not axial passage width)
SST 7	- Conventional clear water hydraulic design with Quasi-francis type inlet blading

All impellers were initially designed with radial front wear ring lands. Figures 12 thru 15 show the designs for these and are designated as MKI. The volute liners are log spiral types with the throat area designed to match the impeller flow at 50 gpm. The radius ratio from impeller exit to volute cutwater is 1.2 for all SST MKI hardware. Figures 16 and 17 show MKI volute design drawings. Table I summarizes the main design parameters for each configuration.

To provide guidance in designing the traditional slurry pump (SST 3) a correlation was made, including several different commercial slurry pumps, of the ratio of inlet eye dia. to impeller O.D. and ratio of impeller exit blade width to impeller O.D. versus specific speed. This correlation is shown in Figure 18, with points displayed for SST 3 and SST 5. The deviation of SST 3 and SST 5 from the D /D correlation is intentional. Reducing the impeller eye diameter, lowers the inlet blade speeds, and will

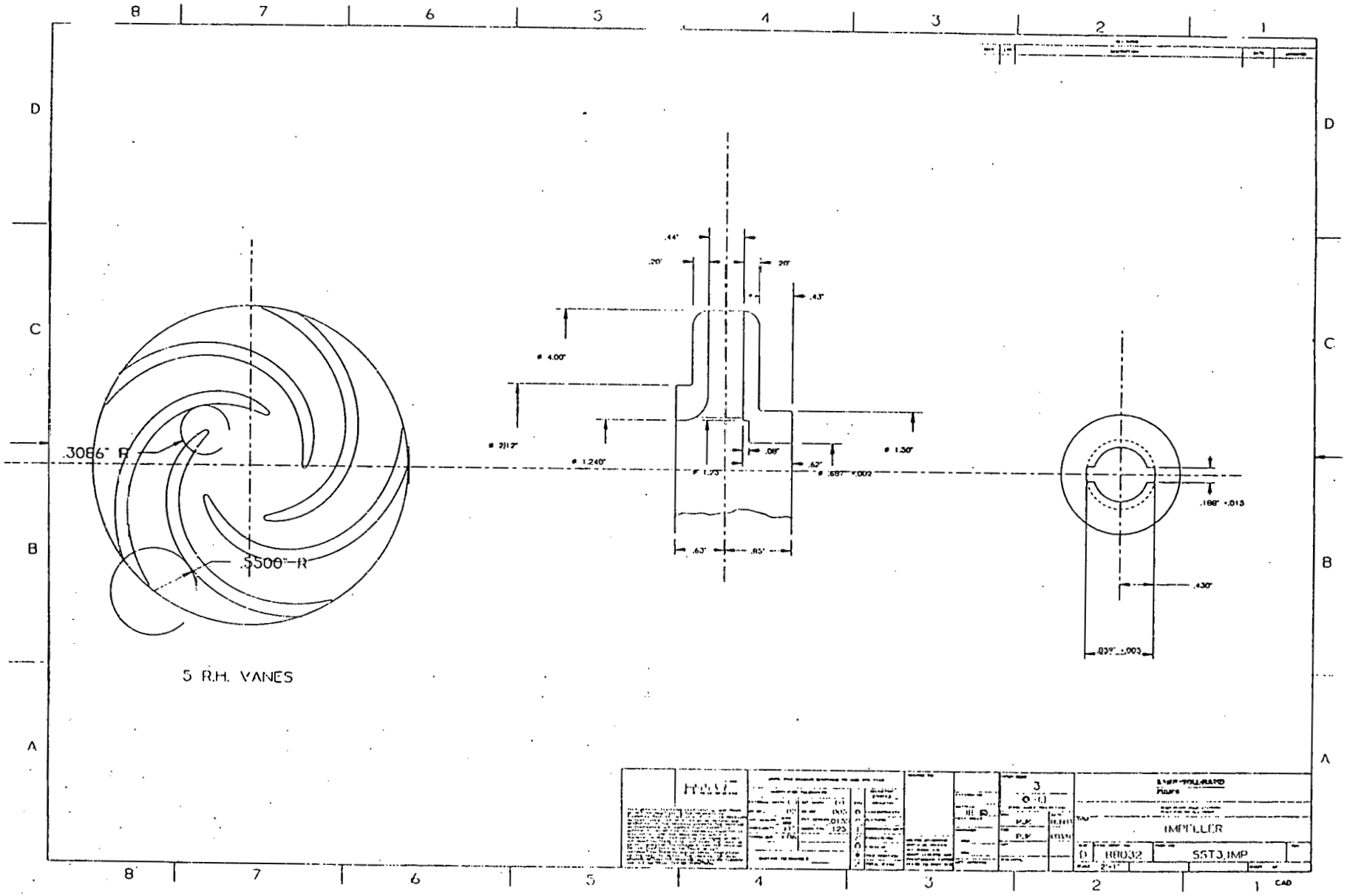

Figure 12: SST 3 (5 Vane) Impeller

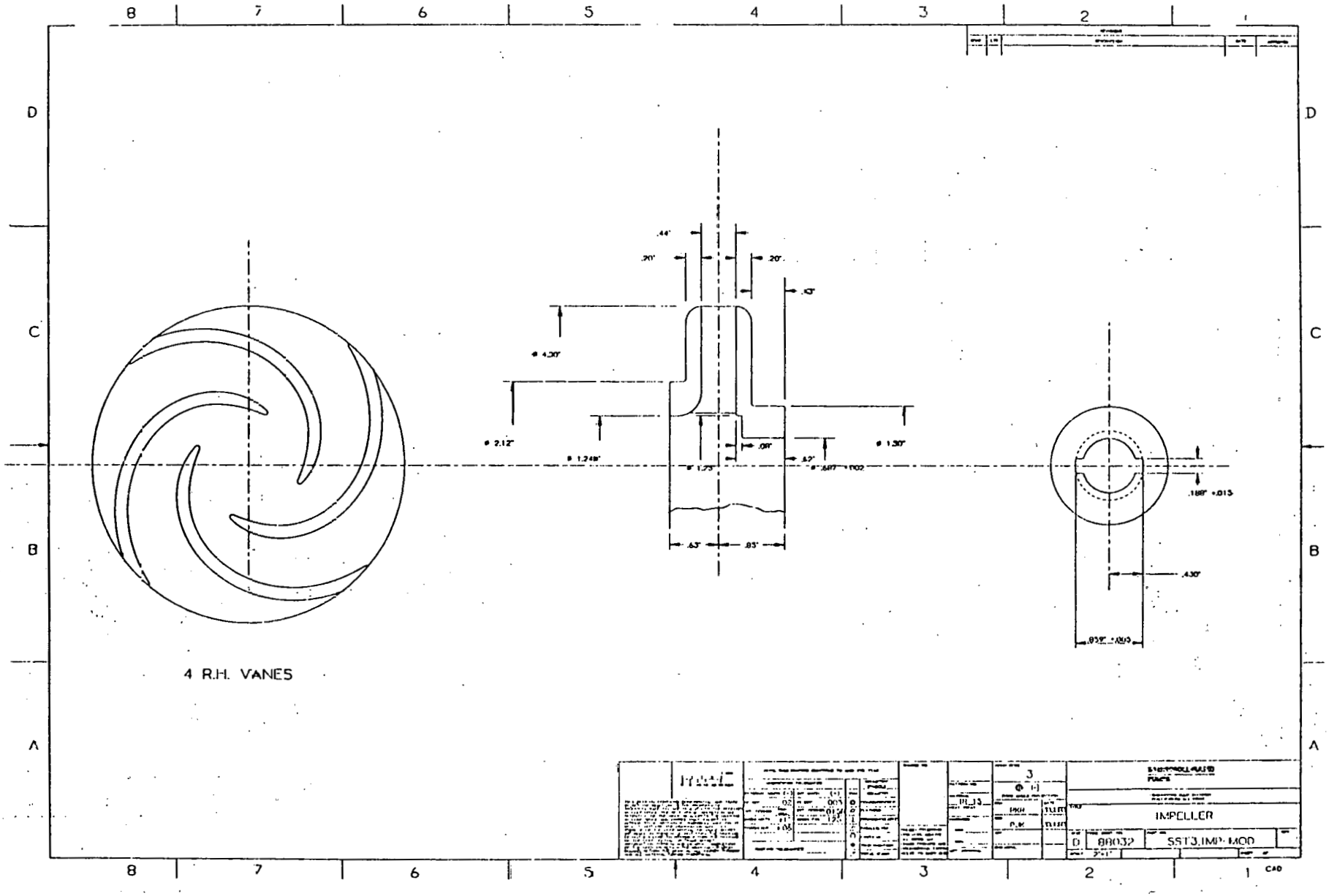

Figure 13: SST 3 (4 Vane) Impeller

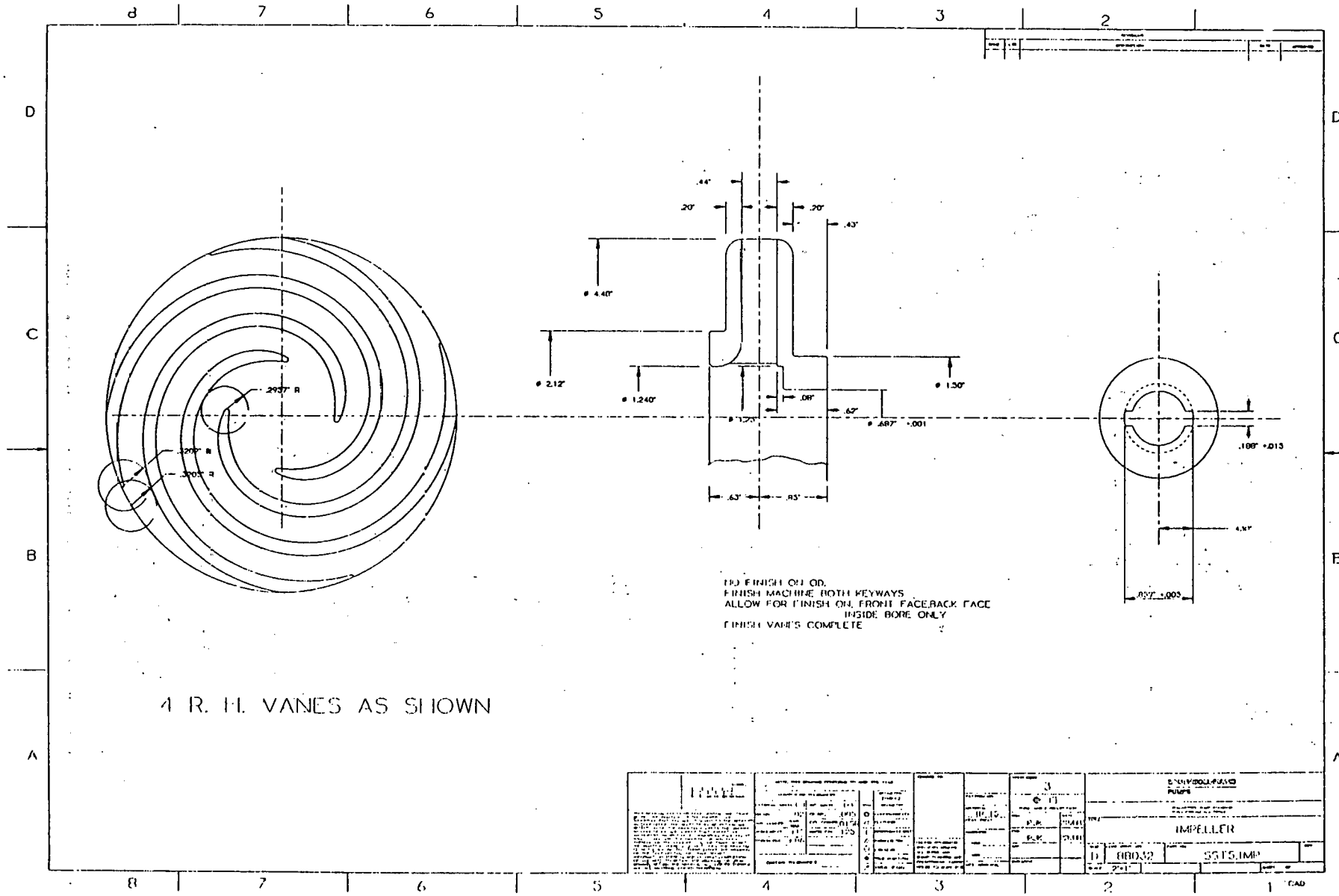

Figure 14: SST 5 Impeller

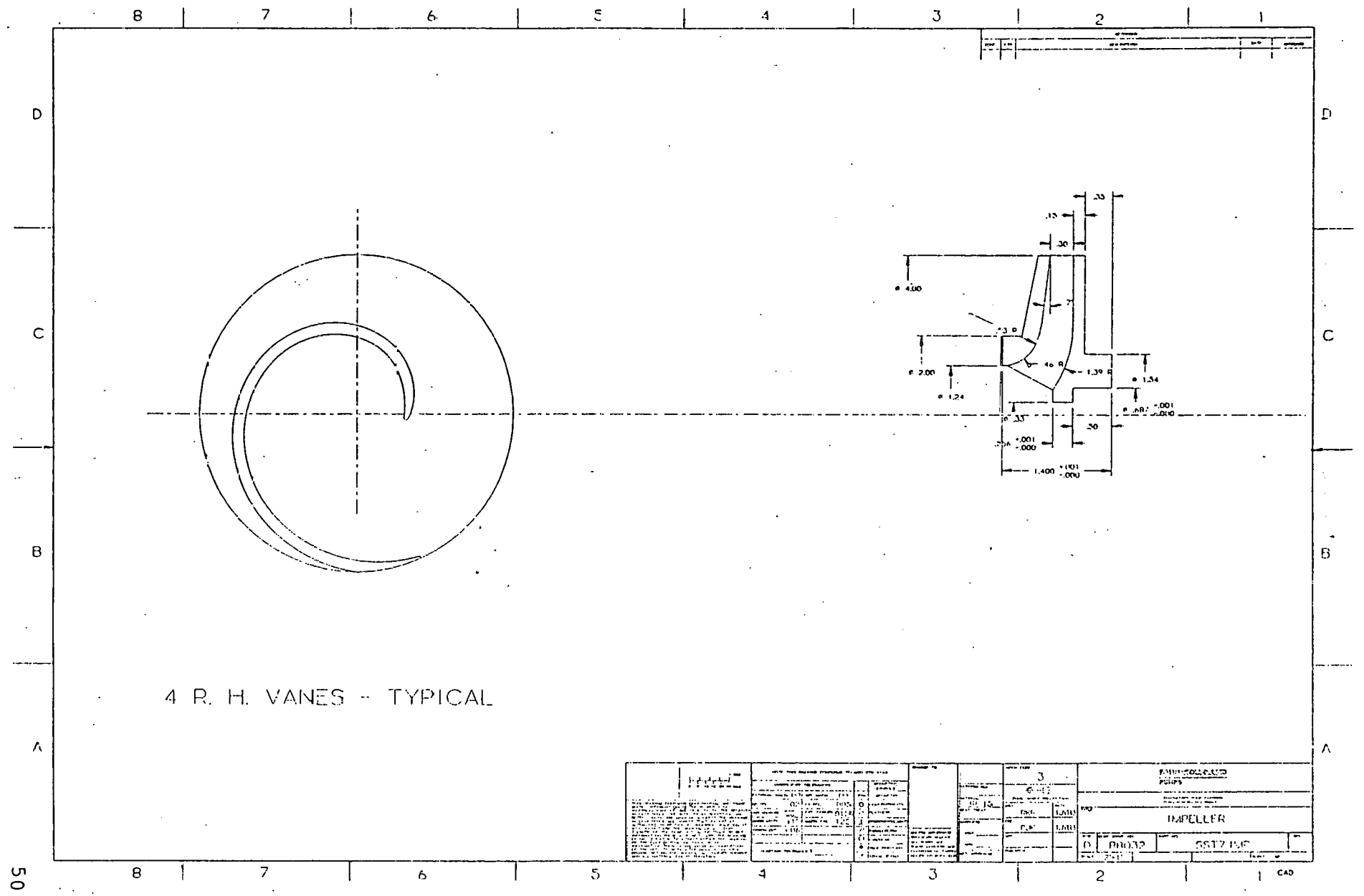

Figure 15: SST 7 Impeller

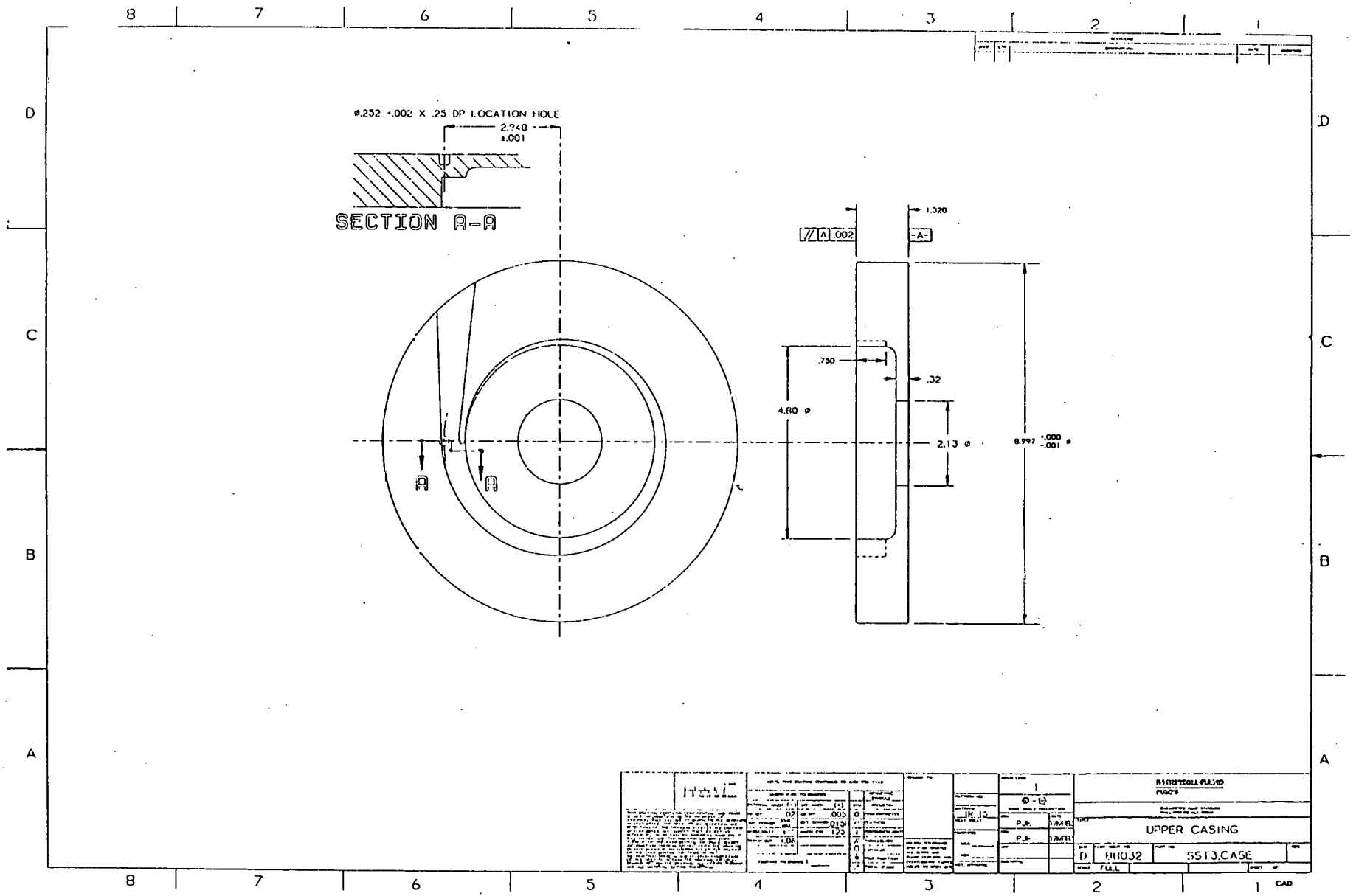

Figure 16: Volute For SST 3

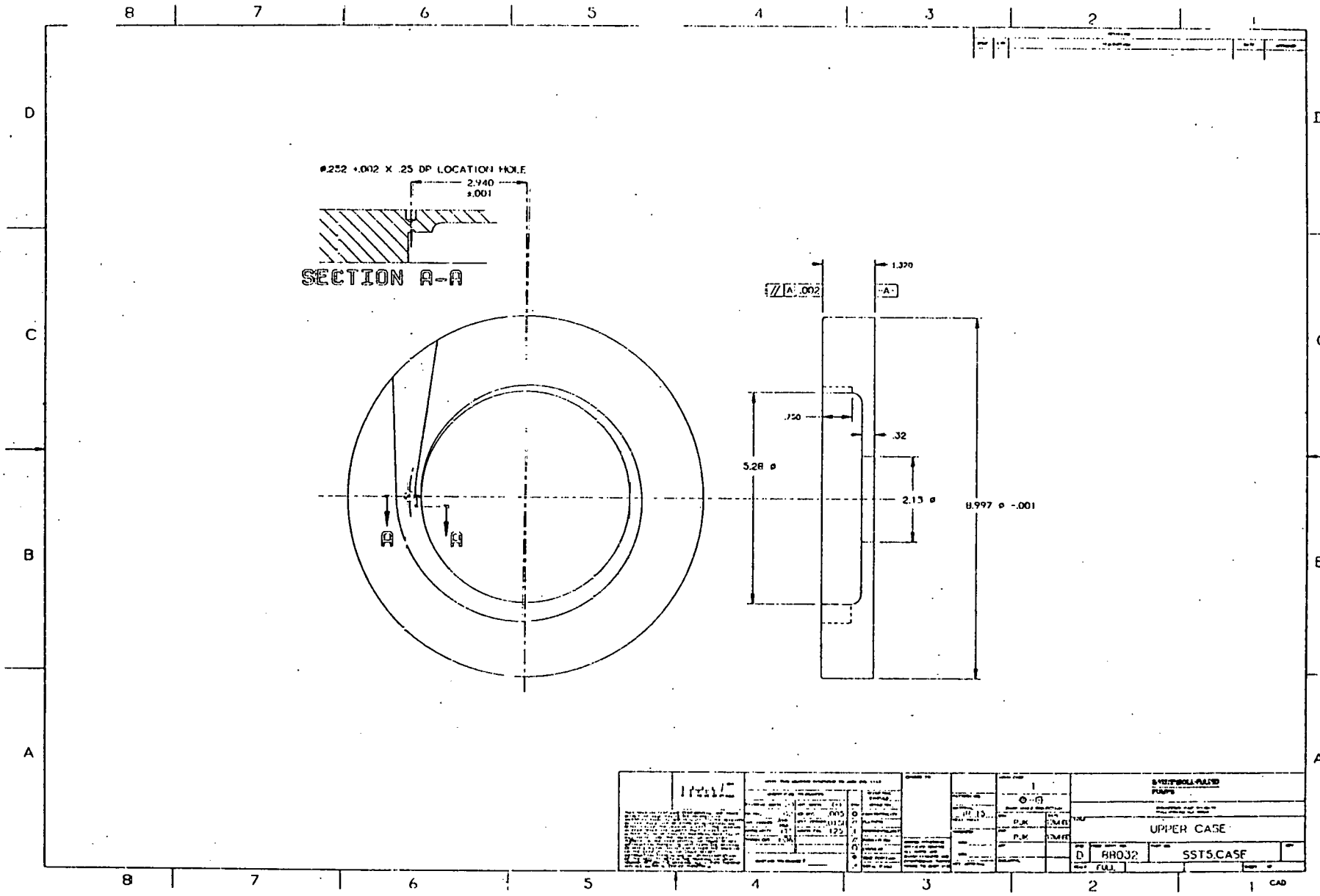

Figure 17: Volute For SST 5

TABLE 1

SST MK I DESIGNS

	TRADITIONAL SLURRY PUMP		LOW BLADE LOADING	CONVENTIONAL CLEAR WATER
	SST3	SST3 Mod.	SST5	SST7
De (in)	1.24	1.24	1.24	1.24
D_1 (in)	1.25	1.25	1.25	1.36
U_1 (fps)	32.7	32.7	32.7	35.6
β_1	27.6°	27.6°	25.1°	25.31°/27.06°
D_2 (in)	4.0	4.0	4.4	4.0
U_2 (fps)	104.7	104.7	115.2	104.7
β_2	17.0°	17.0°	8.0°	18.7°
Z blade	5	4	4	4
b_2 (in)	.442		.442	.300
A_{th} (in^2)	.326	.326	.364	-
b_3 (in)	.750	.750	.750	-
D_3 (in)	4.8	4.8	5.280	-
D_3/D_2	1.200	1.200	1.200	-

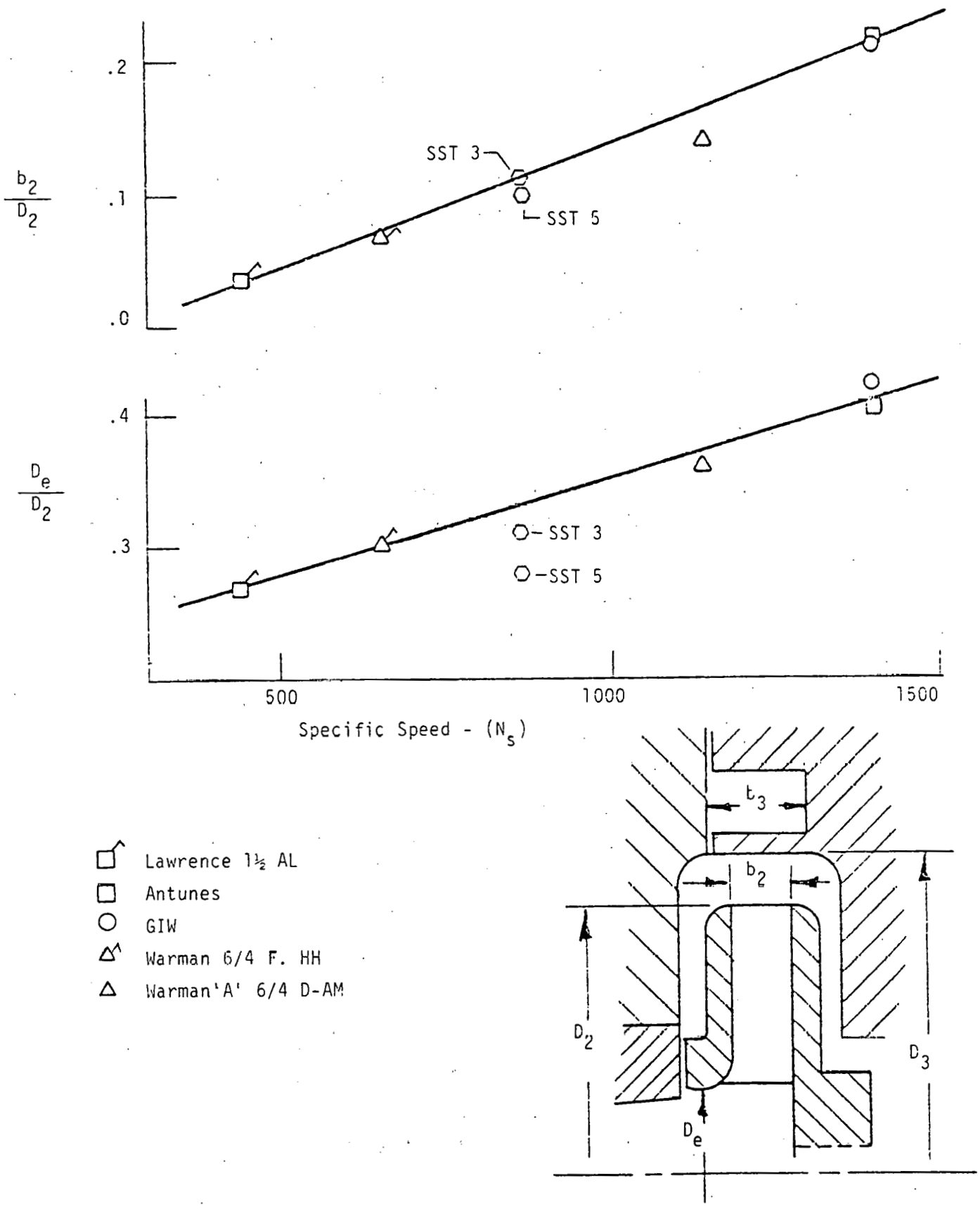

Figure 18: Slurry Pump Design Correlation

improve the wear characteristics of the pump inlet.

The penalty comes in poorer suction performance (larger NPSHR). For the synfuel applications it was decided to design for best life, not ultimate suction performance.

The impeller inlets of SST 3 and SST 5 were designed for 55 gpm, and maintain constant relative velocity at the stations just outside and just inside the blade (using full blade thickness).

The SST 7 impeller was designed along conventional clear water guidelines. The inlet diameter was made equal to the SST 3 design. The blade angle at the mean streamline was selected to provide zero work addition to the flow at the blade inlet. This design effectively unloads the inlet. However, acceleration of the relative velocity occurs. This design also lowers the angle of incidence at design flow rate.

The actual blade leading edge does not remain at full thickness. In order to obtain the best suction performance for the given eye diameter a suction side fairing is added which approximates the upstream flow angle.

The dynamics of the flow inside an impeller passage are connected with the angular momentum that is being delivered to the fluid. The torque therefore applied by the impeller blades is created by circumferential blade-to-blade pressure difference across the blade passage. This pressure difference may be converted to a corresponding relative velocity difference across the passage (using Bernoulli's equation, taken relative to the impeller motion). The distribution

of this pressure difference through the passage is commonly referred to as blade loading. Four different "loading" diagrams are shown in Figure 19 (a to d) for four basic impeller types.

The diagrams are in the form of blade surface relative velocities on the pressure side of blade and the suction side of blade. The larger the difference in relative velocity from scution to pressure surface, the larger the pressure difference and the higher the blade loading. Large decelerations of relative velocity usually indicate that the flow will be separated. Details regarding the relationship of particle dynamics and blade loading have been discussed in a previous section. All four impellers are designed to provide approximately the same head and same flow.

The actual head coefficient (gH/U^2) for SST 3 and SST 7 was chosen to be 0.5. The SST 5 has a lower head coefficient, 0.415, due to its lighter blade loading (a larger diameter is required to make the same head as SST 3 and SST 7).

Blade thickness was chosen using conventional slurry pump design practice as a guide. Clear water pumps typically have the blade thickness equal to 2% of the impeller diameter. For slurry service, a ratio of thickness to impeller diameter of 4% was chosen. The 4% figure being somewhat typical of slurry pmps currently in the field.

The base line impellers were designed with radial front wear surfaces, and nominal running clearance with the front suction nozzle of .020". This results in a volumetric efficiency of about 90% for a pump of

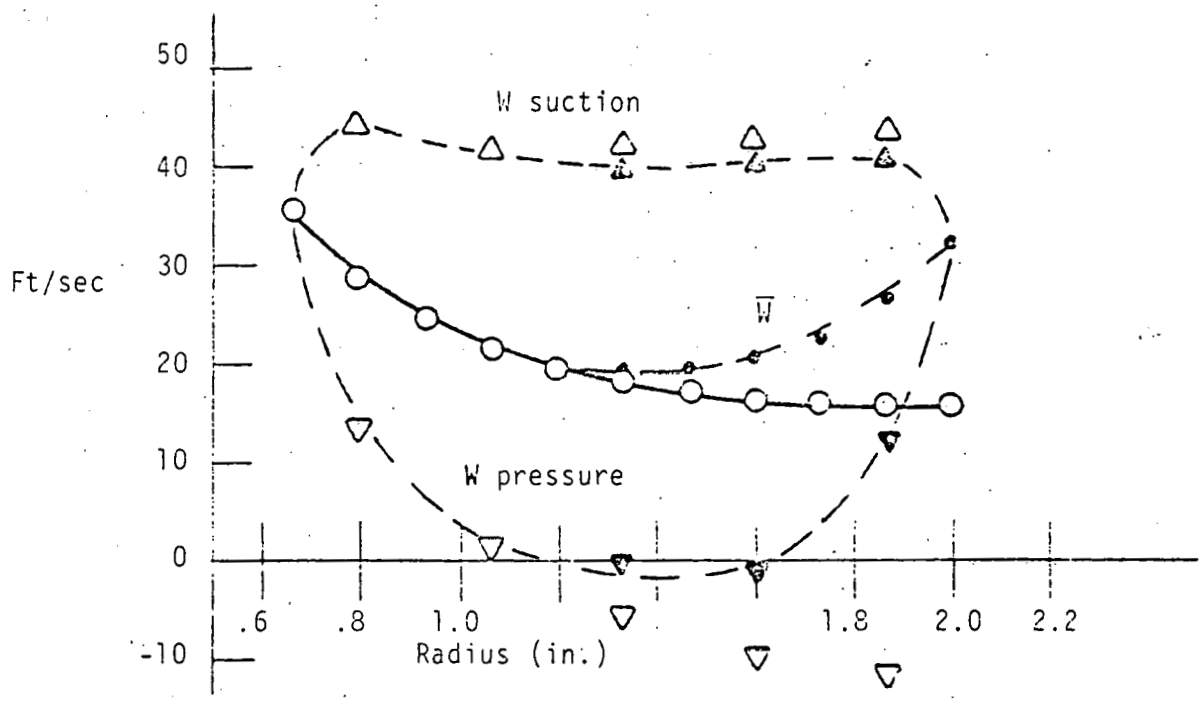

Figure 19_a: SST 3 (5 Vane) Impeller Blade Loading

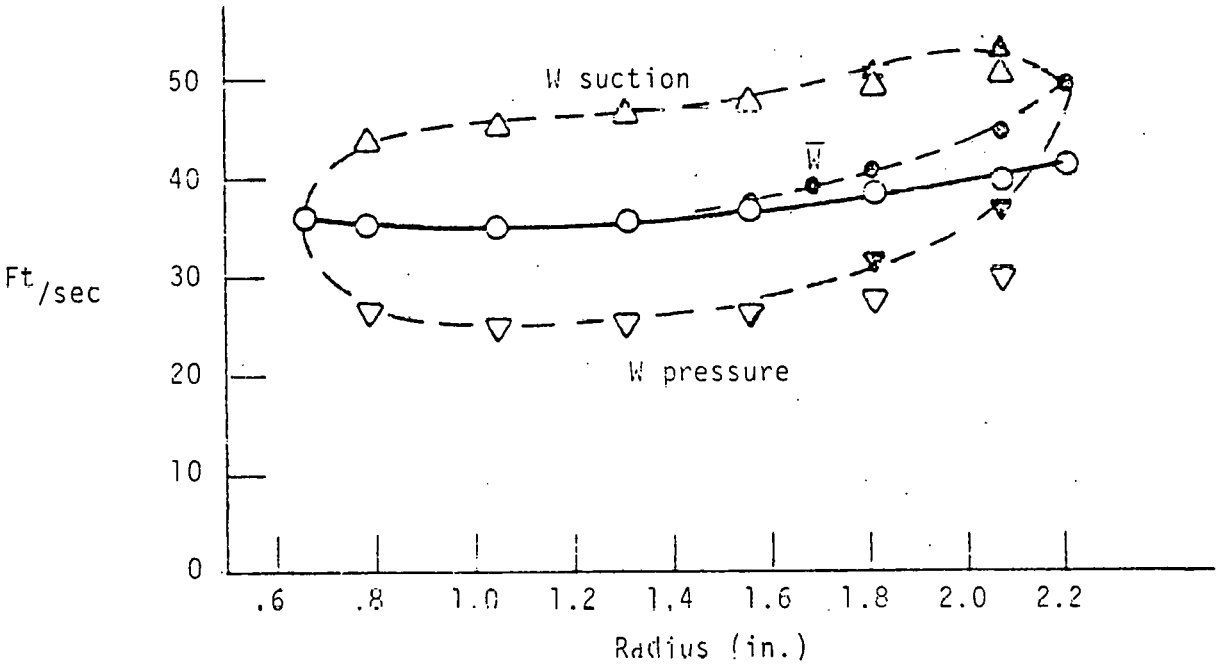

Figure 19_h: SST 5 Impeller Blade Loading

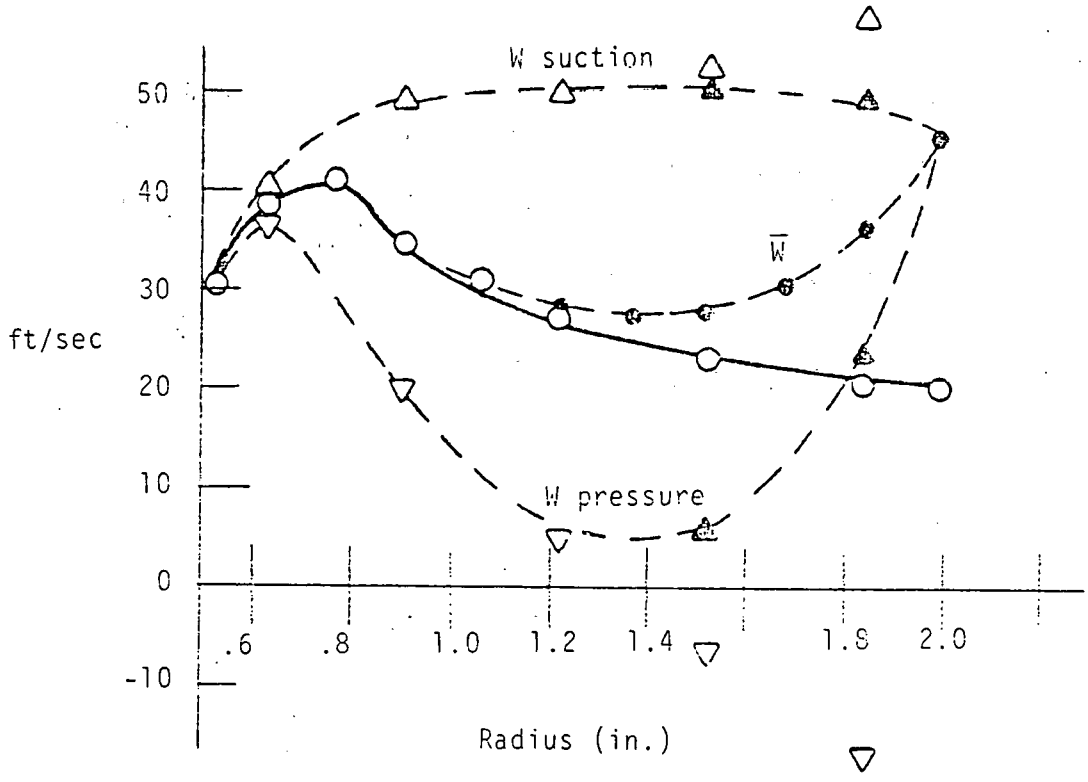

Figure 19_c: SST 7 Impeller Blade Wading

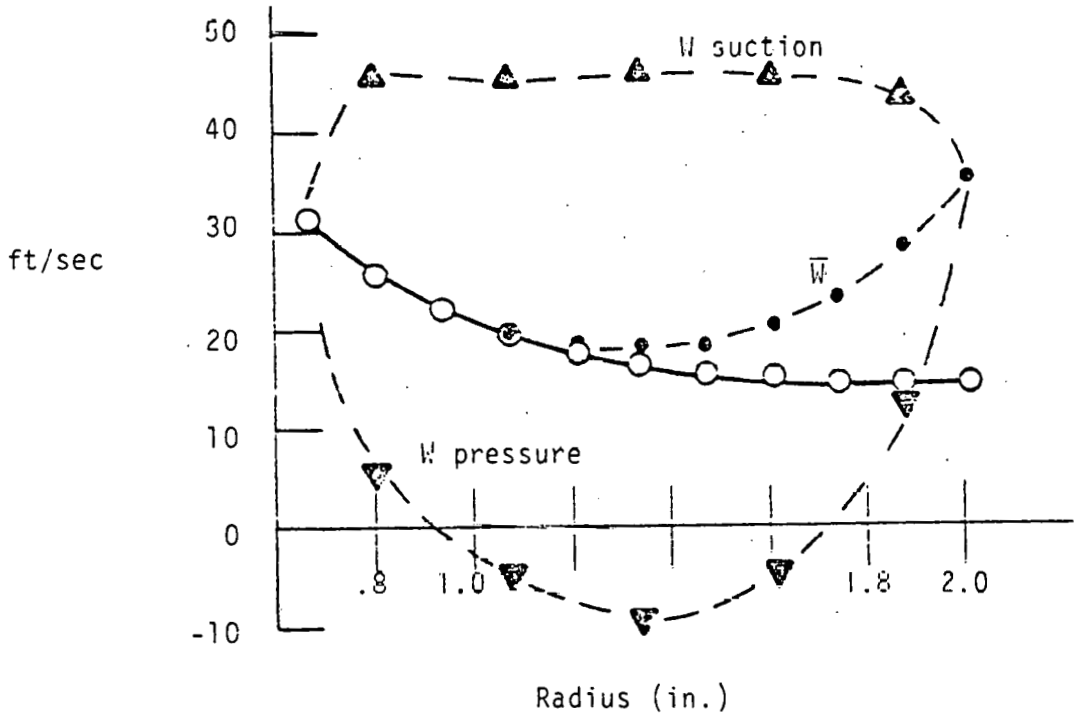

Figure 19_d: SST 3 (4 Vane) Impeller Blade Loading

this size.

All impellers were designed with axial element blades. This means that at any circumferential station, the blade angle from hub to shroud remains constant.

Volute type collectors were selcted for base line SST configurations. It was felt that volute offered performance benefits in the area of efficiency and radial thrust, (even though at large cutwater clearance ratios the benefit of volute vs concentric collector decreases) over concentric collectors. Multivane diffusers offered no benefit in terms of performance or packaging considerations (in fact, multivane diffusers significantly increase the complexity of hydraulic design). The throat area of the volute exit was sized to match the impeller at a net flow of 50 gpm or 55 gpm impeller flow. Throat areas of the various designs are summarized in Table I. A conventional clear water volute cutwater was used in the MKI hardware. A log spiral surface connected the cutwater to the outside volute throat. In order to facilitate fabrication a rectangular type volute cross-section was used. Downstream diffusion was accommplished thru a w simple two dimensional, straight wall diffuser.

Cutwater distance from the impeller is a key factor in cutwater wear in slurry. The two MKI volutes (one for SST 3 and one for SST 5) maintained a cutwater radius to impeller radius ratio of 1.2. This implies a 10% lower cutwater velocity for the SST 5 configuration than for the SST 3 configuration. This is because both impelles are designed to produce the same angular momentum change ($\Delta r V_\theta$) with the

SST 5 achieving it at a larger exit radius. this means a 10% smaller V_θ for the SST 5.

The volute section width is a constant .750" for MKI volutes. The vaneless space between impeller O.D. and cutwater is 1.250" wide. The clearance between the outside of the impeller shrouds, and the stationary sidewalls is .220".

Clear water performance for SST 3 (5 vane) and SST 5 is shown in Figure 20. Various builds of the same design were tested and head vs flow characteristics show good repeatability. The only exception being build 3001. This build was found to have the impeller running eccentric to the inlet suction nozzle by about .100". This misalignment altered the leakage path, increasing the leakage flow and shifting the H Q curve. The efficiency curves show significant variation. This is because of non-repeatable power data. Power is measured from a wattmeter connected to the drive motor with corrections made for motor and speed increasre losses and seal drag. The variation in power curves from test to test may involve changes in seal drag or variations in belt losses. Time did not allow tracking down the exact cause, however the problem did not severly alter the determination of the pumps best efficiency flow. As seen from Figure 20, both pumps peak at about 55 gpm and both produce about 192 ft. of head at this flow. Comparison of this clear water performance versus the clear water design condition follows:

	DESIGN	ACTUAL (SST 3 & SST 5)
RPM	6000	6000
Flow (ft)	50	55

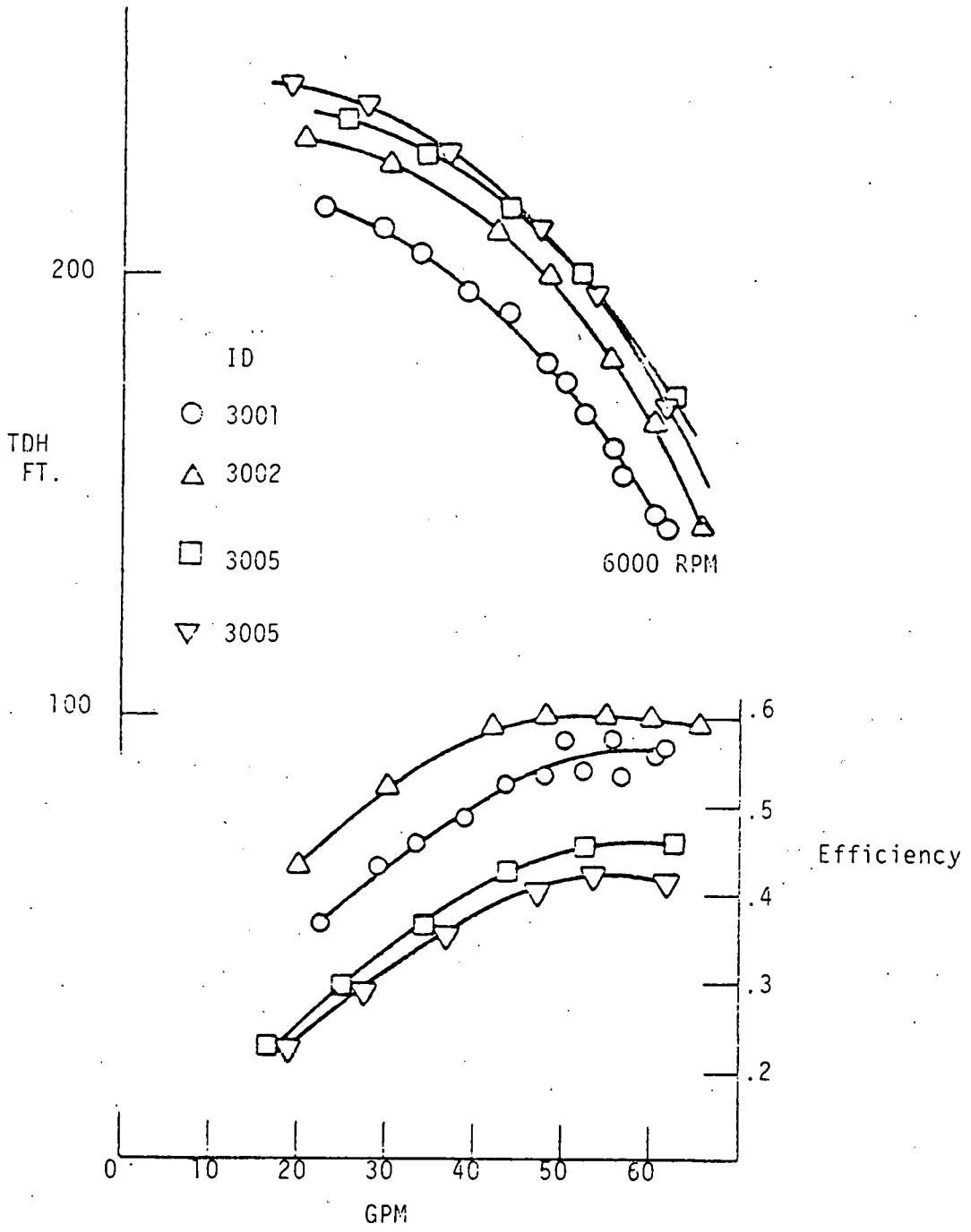

Figure 20_a: SST 3 (5 Vane) Clearwater Performance

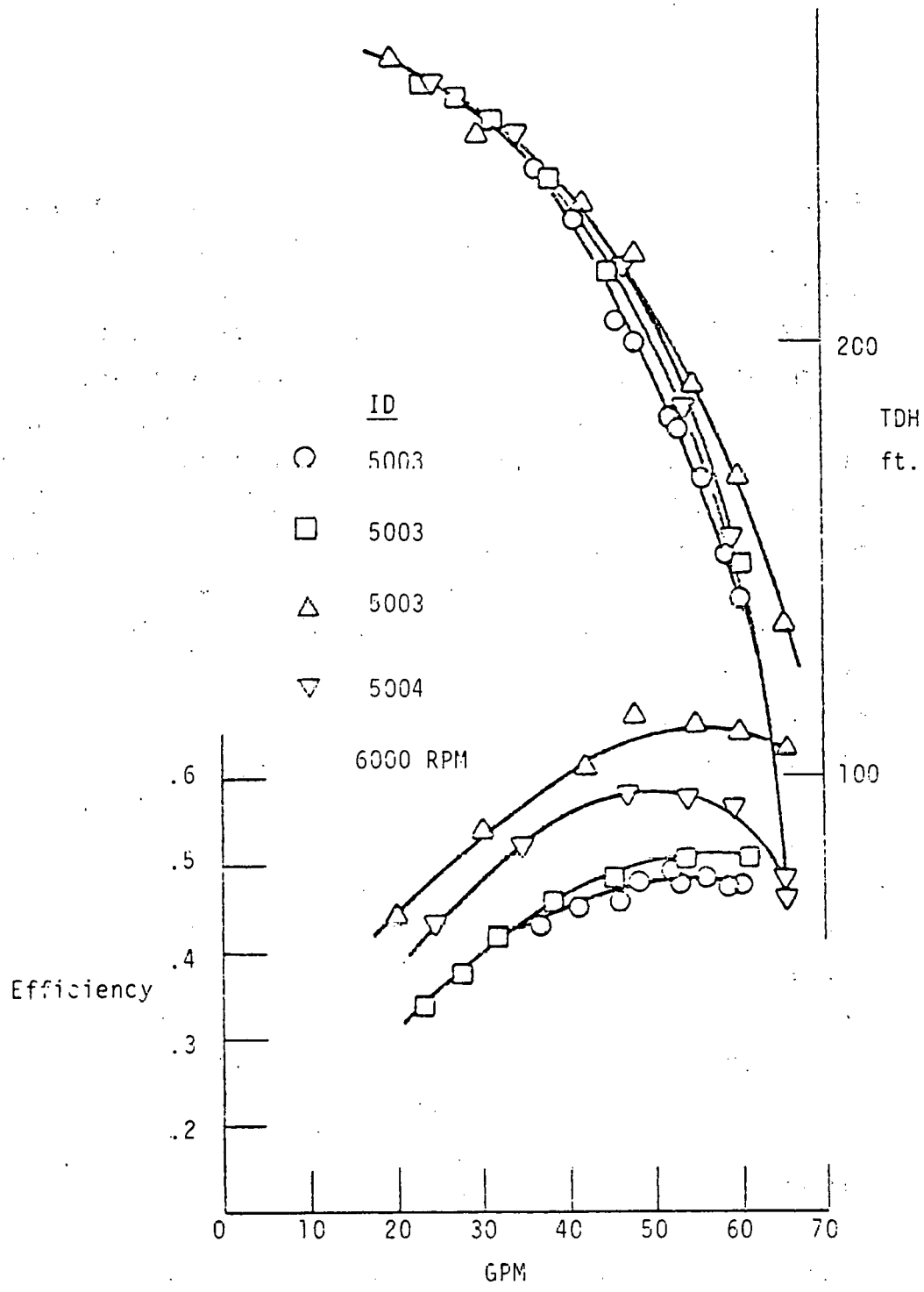

Figure 20_b: SST 5 Performance (Clearwater)

Head (gpm)	170	192
Ns	900	860

Performance of the two impeller types in sand-water slurry is presented in Figure 21. It should be noted that the lightly loaded SST 5 wheel suffers from twice as much head fall off (from clear water performance) as the SST 3 for a given concentration of sand (Figure 22). The performance change in sand was measured at a constant system resistance setting. performance of the SST 3 impeller in high viscous slurry (Appendix C, SCMC additive) is shown in Figure 23. Changes in Hvs Q curve are as expected, with the addition of the 1.4% (WT) SCMC not having a large impact on performance, in fact improving it. The 2% solution SCMC, corresponds to a viscosity of about 80 centistoke based on the shear rate seen in impeller passage. Good correlation with Stepanoff's (19). Test Data, when pumping oils of varying viscosity, is obtained. The addition of 15% sand in this high viscosity solution severely affects performance and the flow drops in half. Changes in efficiency noted in Figure 23 are valid as all the data comes from one test, thus providing consistency of power measurements.

After evaluating SST 3 and SST 5 it was concluded that there is no need to evaluate SST 7 design and therefore the hardware was not fabricated.

Appendix B contains wear test summary and reports which provide a summary of configuration, operating conditions, and observations. the numbers under test observation correspond to numbers shown on respective wear location diagram. All endurance testing was done with front ring clearances of nominally 0.020".

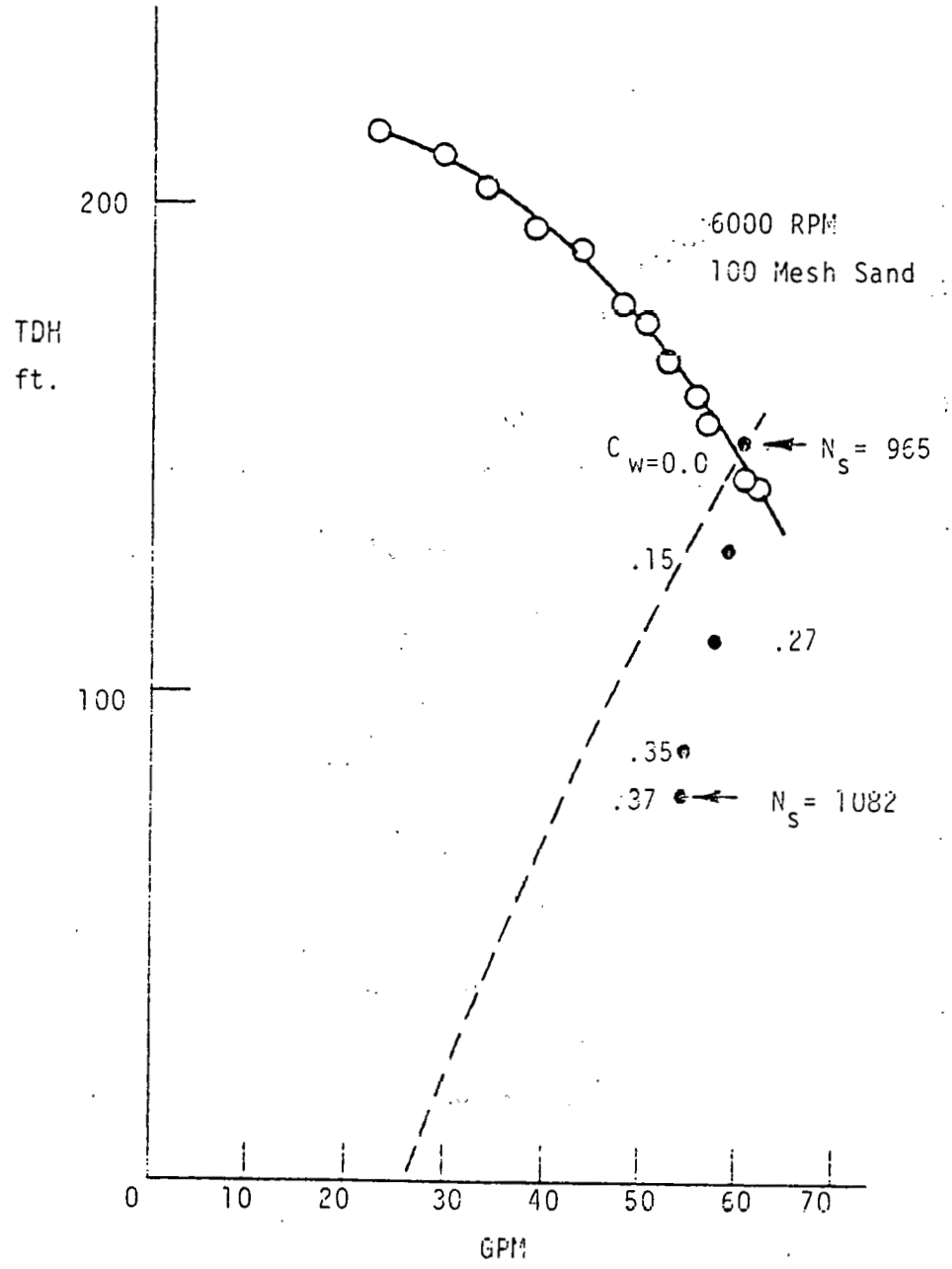

Figure 21a: SST 3 Performance (5 Vane)
(In Slurry)

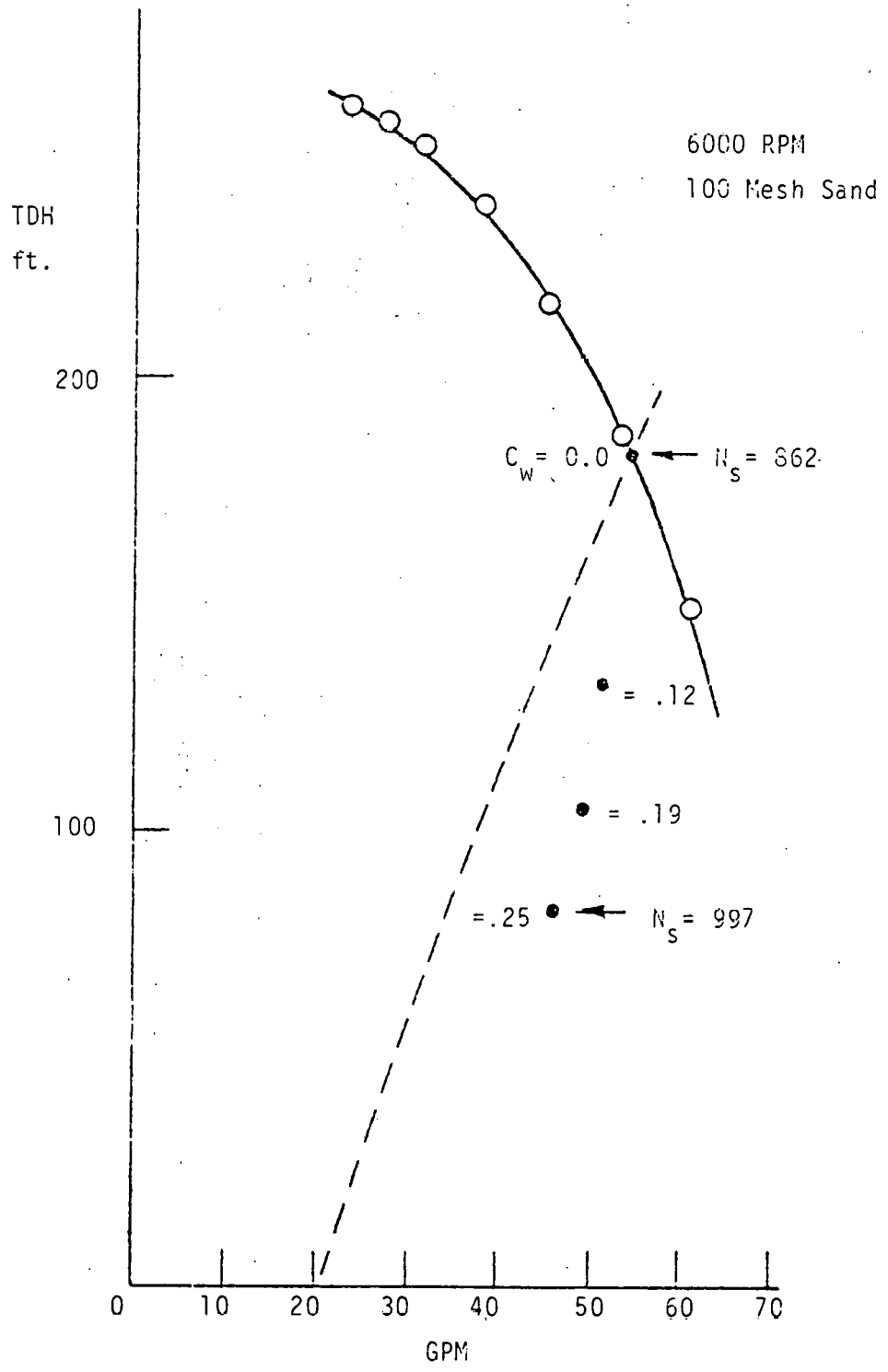

Figure 2.1b: SST 5 Performance (In Slurry)

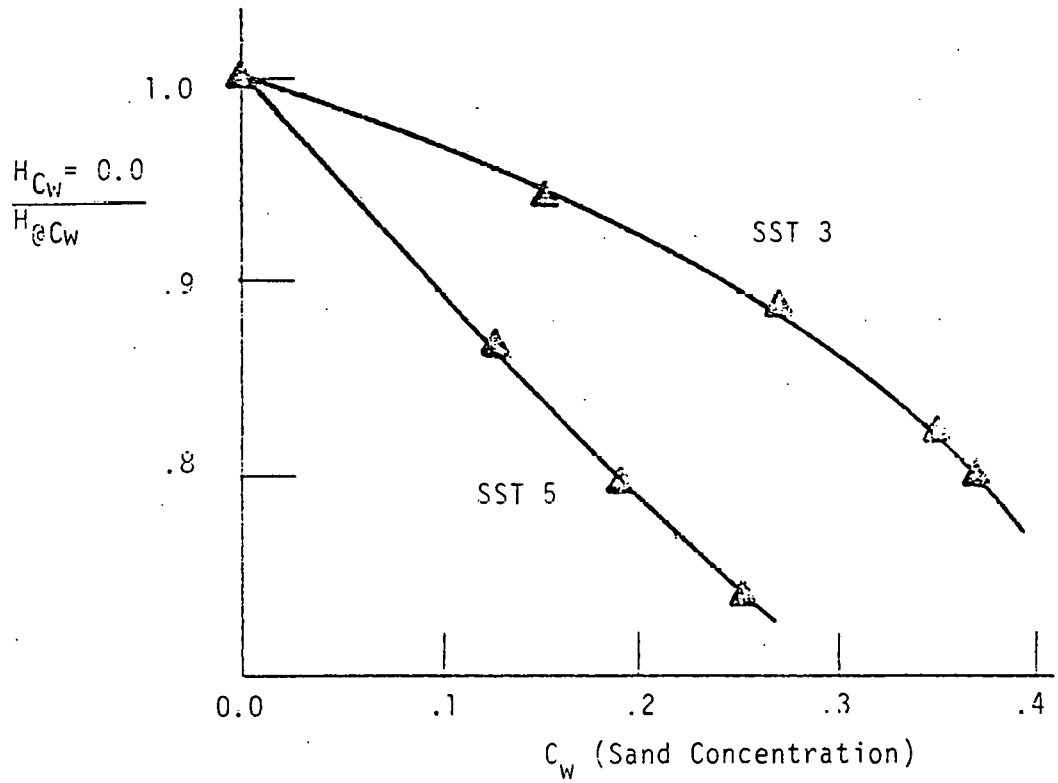

Figure 22: Head Falloff Comparison

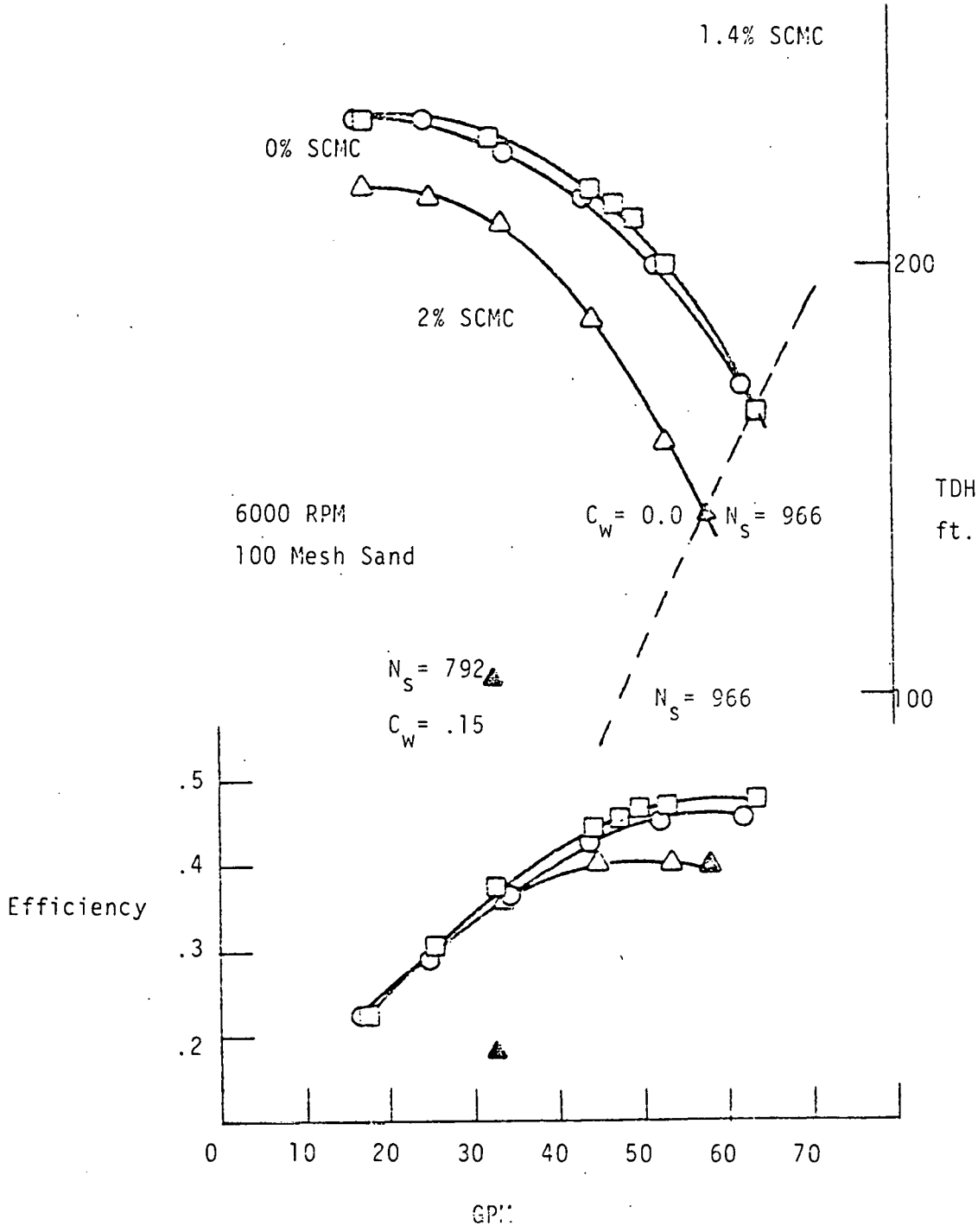

Figure 23: SST 3 Performance, Viscous Slurry

The clearances were adjusted, and new slurry added at 2 hr. to 4 hr. intervals. The flow control valve was not adjusted throughout this period. Although flow varied due to increased front ring clearances. When the test purpose is stated as a side by side comparison, both pumps were running in series, on a common slurry at the same flow rate.

3.2.4 DEVELOPMENT OF CRITICAL WEAR AREAS

Through the course of the pilot plant field trips and the initial SST (MKI) Tests, six major critical design areas were defined. These areas were investigted and optimized to minimize wear. They are:

1. Collector Configuration
2. Impeller Front Leakage Path
3. Impeller Blade Shape
4. Collector Sidewall Configuration
5. Pumpout Vanes
6. Impeller Shroud Configuration at O.D.

Each of these areas will be discussed and details of the evolution of design follows:

COLLECTOR CONFIGURATION

Constant pressure volute type collectors are known to be desirable for application to centrifugal pumps for several reasons. The provide for continuous, uniform fluid collection from the impeller, maintain a uniform circumferential pressure distribution around the O.D. of the impeller at the design point, exert minimal radial thrust loads on the bearings at the design point, and maintain a uniform, circumferential leakage flow, past the front impeller ring. At off design flows, volutes do create a circumferential pressure gradient which comprises the above mentioned qualities. Volute pumps have mechanical designs which accomodate the thrust loads due to varying flow rates imposed on the pump. From a wear standpoint, the behavior of

the fluid in the collector is very important.

The conventional appearing volute in Figure 24 is representative of the volutes tested in the SST. The major area of wear on this volute is on and around the region of the cutwater. The issue of cutwater survivability is the most important design consideration. On the baseline volutes, horsehoe vortex wear on the endwalls around the cutwater was obvious, as well as endwall grooving, parallel to the cutwater on the diffuser and impeller side. Sharpening and wear back of the leading edge also occurred. The horseshoe vortex was minimized by designing large radius on the cutwater leading edge (Section B-B, Figure 24). This eliminates the vortex formed due to the interaction of the stagnation streamline and the endwall boundary layer which causes the grooving in front of the cutwater. The side grooves persisted as well as sharpening and wearback. Altering this wear could be done by moving the cutwater radially away from the impeller. This approach for conventional volute will increase the overall outside diameter of the casing, which results in a larger pump package.

The next volute configuration, shown in Figure 25, addresses the packaging question while moving the cutwater to a radius of 2.98". Trimming of the cutwater to 70 angle of sharpness was done, along with applying a concave type trim to the leading edge. The diffuser length was shortened which altered the design. However, since cutwater wear was the primary concern (diffuser performance was secondary) it was considered satisfactory. Wear testing resulted in no horse-

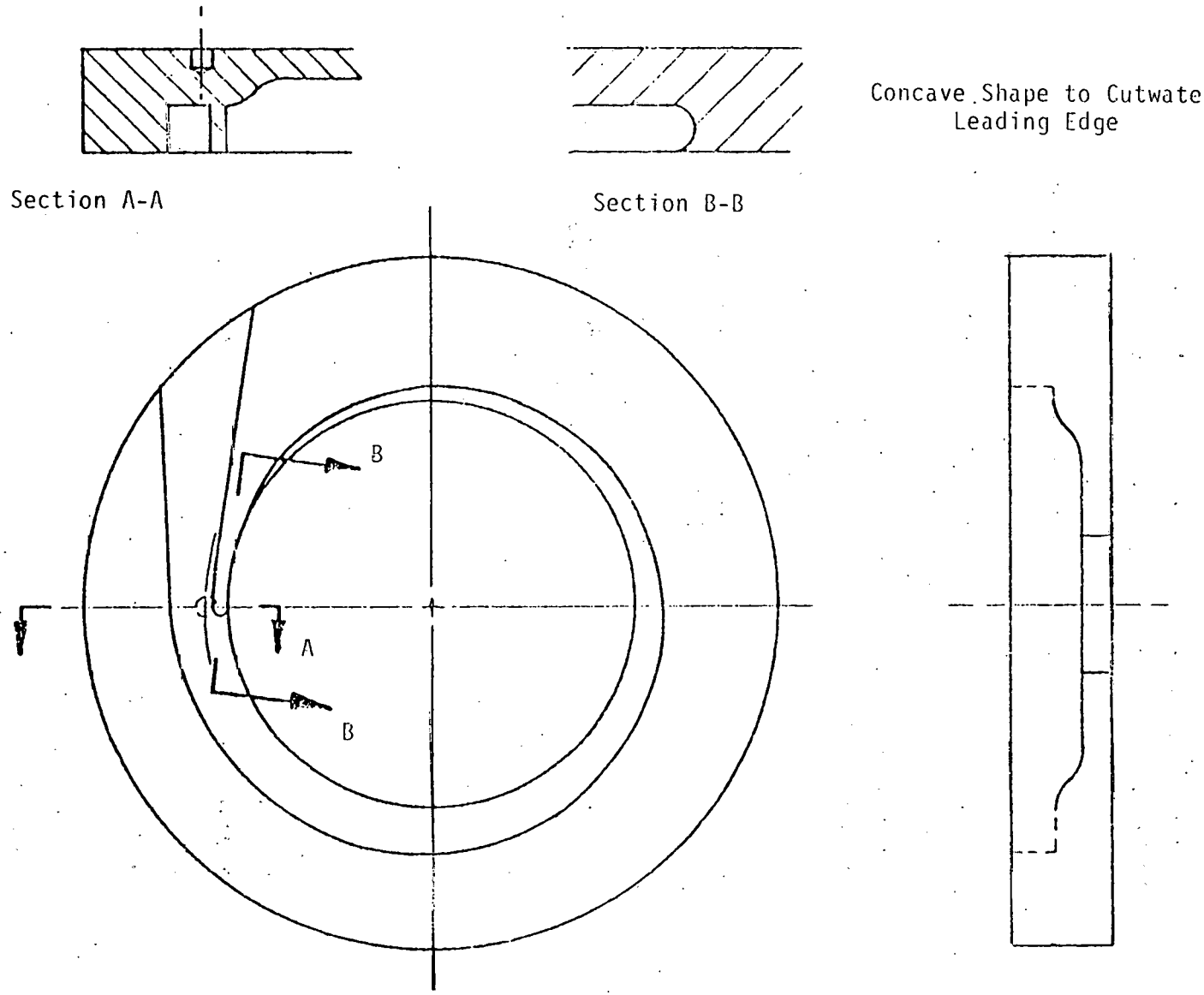

Figure 24: Typical Volute with Concave Cutwater Trim

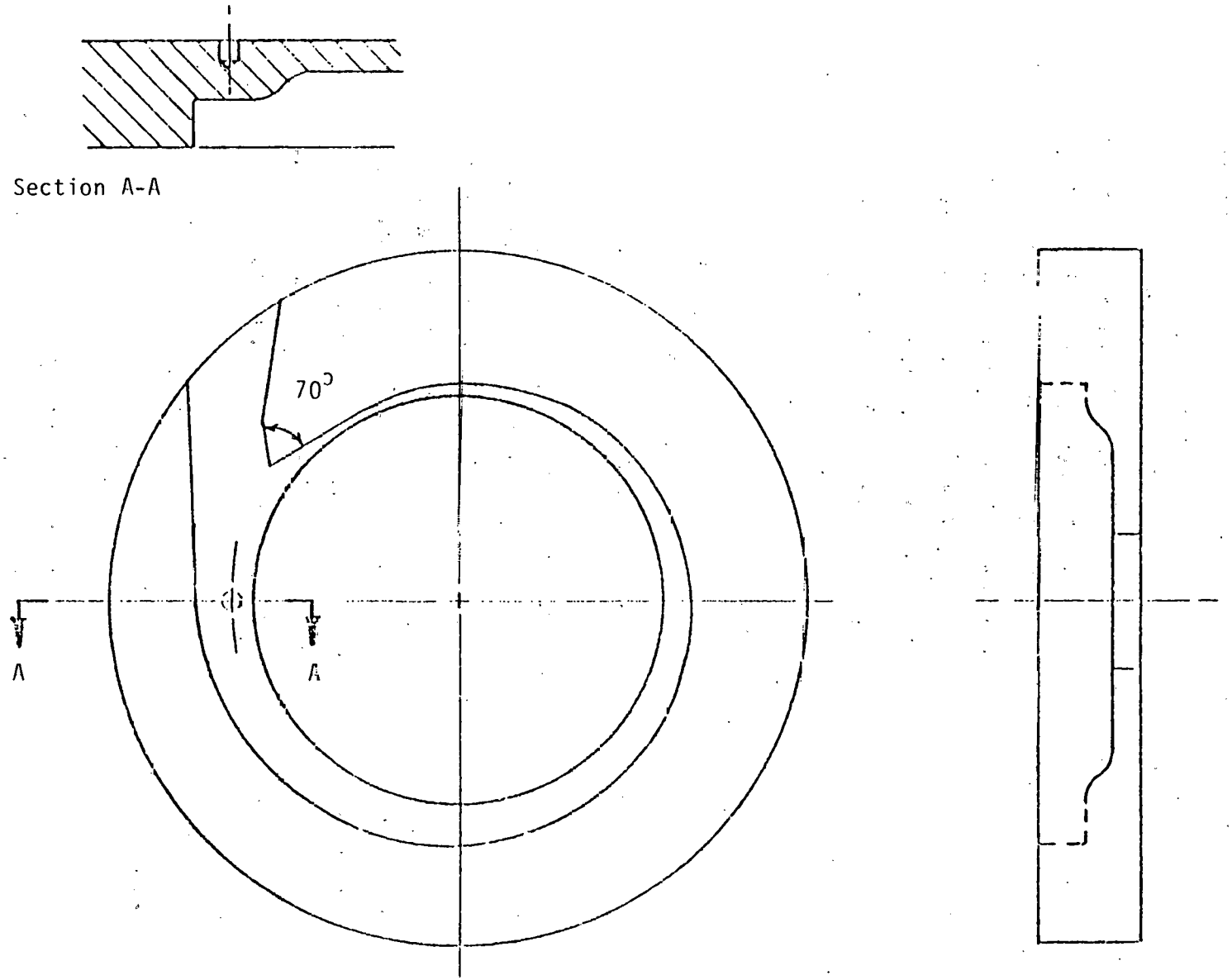

Figure 25: Volute with Cutback Cutwater

shoe vortex, but some sidewall grooving on the impeller side of the cutwater did occur.

The most effectively packaged collector is that of a concentric volute collector. The cutwater radius is equal to the collector ID. The configuration tested is shown in Figure 26. The oval shape of the diffuser throat forms a concave type trim to the cutwater when intersecting with the collector outer wall. The mean throat velocity for this collector at 55 GPM was 26.9 fps as compared to 53.2 fps for the volute in Figure 24. As would be expected from dropping the throat velocity (and hence cutwater velocity) wear around the concentric collector's cutwater was negligible. The disadvantage of this design is slightly poor efficiency as compared to a volute design, and uneven leakage flow past the front impeller ring. This uneven flow manifeted itself in uneven wear on the suction nozzle.

The design ideas resulting from this testing include designing a volute with large cutwater clearance. The ratio of the cutwater to impeller radius should be about 1.5. In addition, the diffuser throat area should be of oval shape as shown in Figure 26, and sized to match the impeller at design flow. The cutwater should be connected to the outside wall by a log spiral shape.

IMPELLER FRONT LEAKAGE PATH

SST indicated that the front leakage area constitutes as significant a wear problem as the cutwater. At the exit of the leakage path the

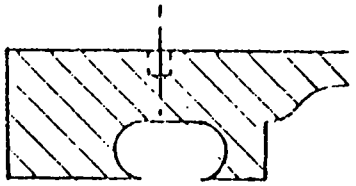

Section A-A

Note: Intersection of Diffuser Throat with Collector, form concave type trim on cutwater

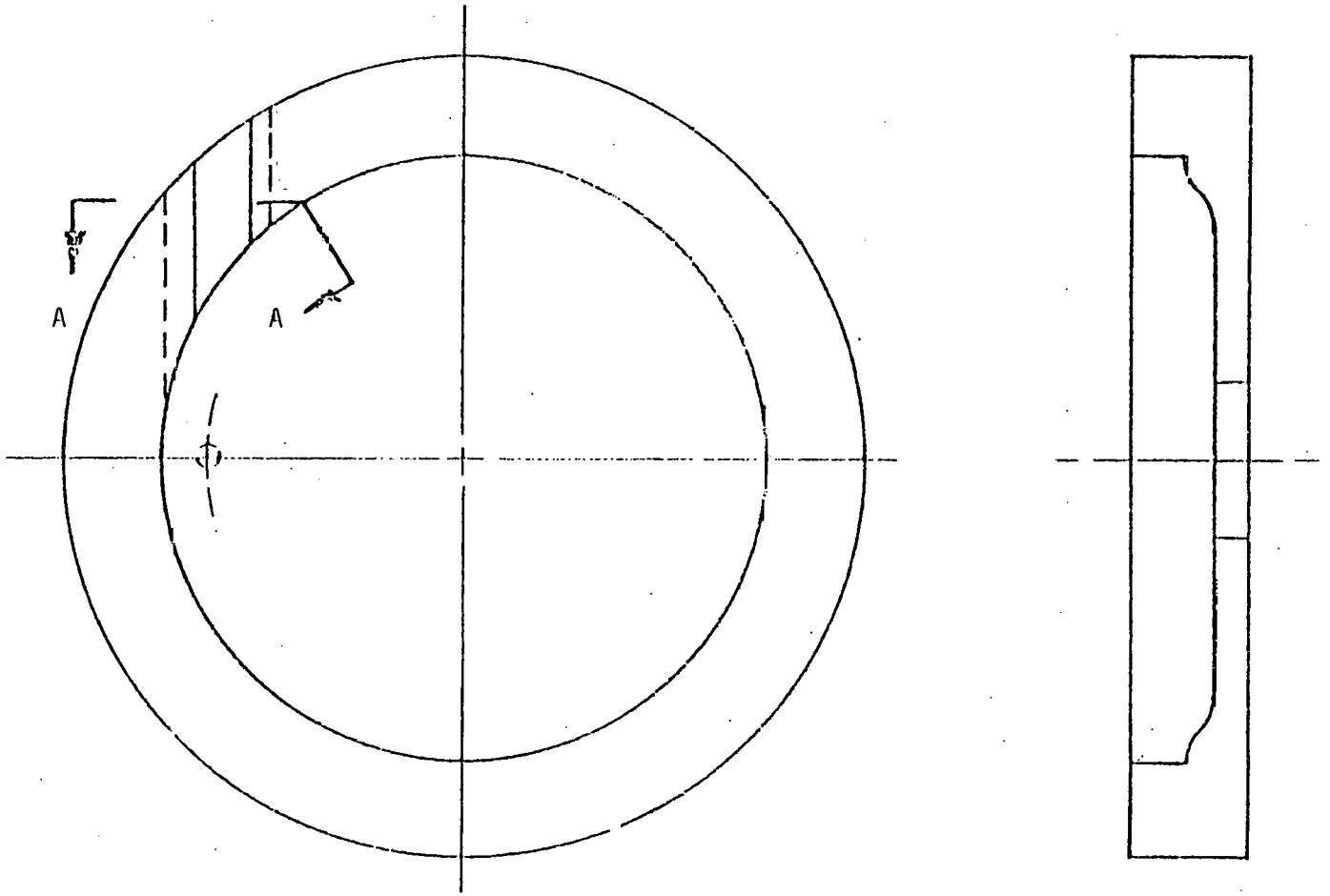

Figure 26: Concentric Type Collector

meridional through flow is about two thirds the impeller speed.

The particles in this flow stream also have a large tangential component. This results in more wear on the stationary suction nozzle than on the rotating impeller. Various flow phenomenon exist in this region of the pump, and provide a variety of wear problems. The overall impact on wear in this area is not only affected by the leak path arrangement, but also by the effect of pump out vanes, density differences between particles and carrier fluid, and the viscosity of the carrier.

The initial SST (MKI) leak path arrangement was typical of general slurry pump practice. This is characterized by a radial, close clearance leak path, terminating at the ID of the inlet nozzle, just upstream of a sharp cornered edge of the impeller ID and just downstream of a sharp cornered suction nozzle. The SST configuration differed from traditional practice in that the suction nozzle wall diverged 2.75 degrees in order to provide transition from hose to impeller ID.

The MKI impeller configuration is shown on the right hand side of Figure 27. Three areas of wear were observed with this base line configuration. First (occurring on all close clearance surfaces) is a gradual wearing of the stationary wear surface; second, chewing of the corner on the suction nozzle, at the leak path exit; and third, ripple wear on the ID of the impeller, with the axis of the ripples approximately matching the direction of the inlet relative

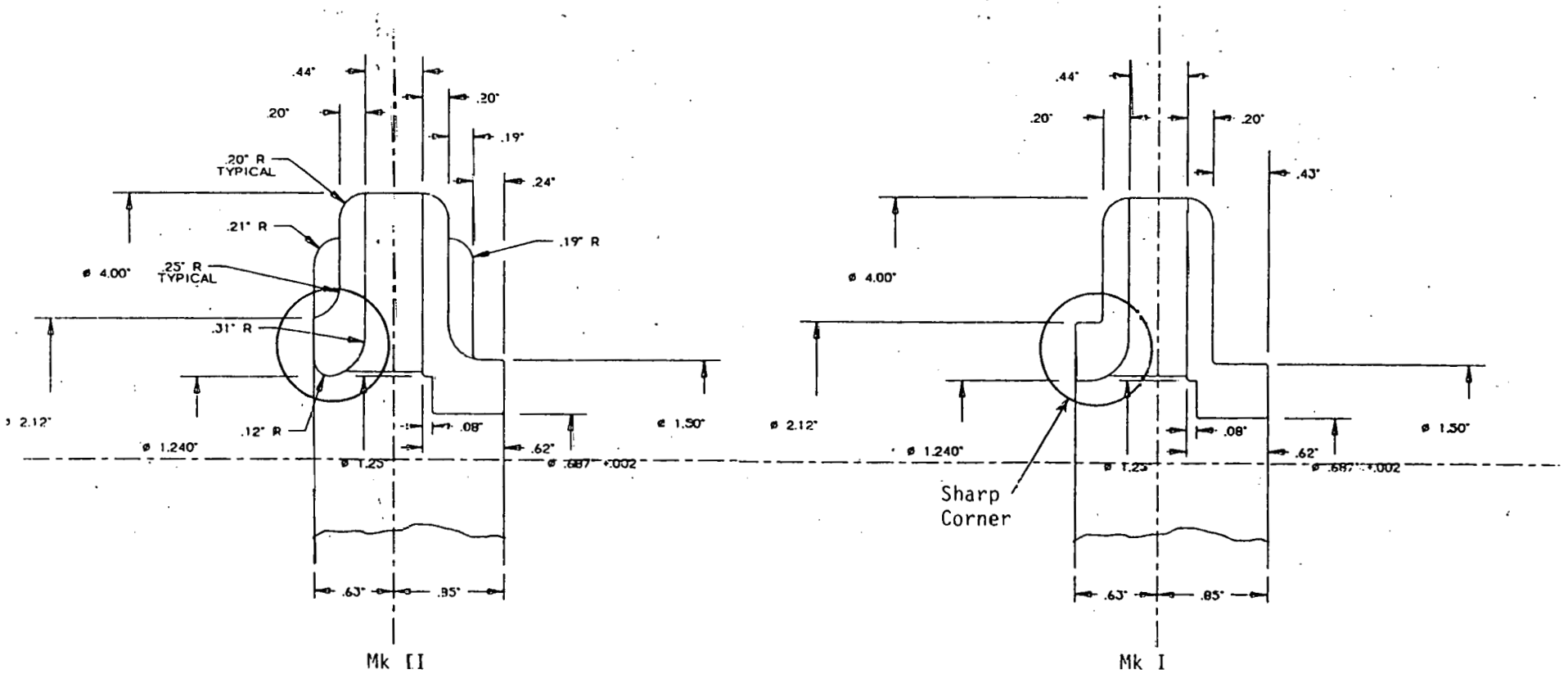

(II)

IMPELLER WEAR RING CONFIGURATIONS

Figure 27

velocity vector.

An attempt to improve the wear on the impeller ID consisted of rounding the radius which had been sharp on the MKI. This is shown on the left hand side of Figure 27. It was thought that this radius would keep the leakage flow attached to the impeller surface as it rounds the corner. Keeping the flow attached helps prevent the formation of vortices, and the throwing of particles against hard surfaces.

The improvement, however, did not occur, in fact wear may even have been increased on the impeller ID with the MKII radius. Apparently vortices are still being formed and particles thrown against the surface, thus causing wear.

In order to eliminate wear on the suction nozzle, a small radius lip was built into the nozzle at the leak path exit, which turns the leakage flow nearly axial (see left half of configurataion in Figure 28). This change of direction alters the interaction of the high energy leakage flow with the incoming mainflow and stopped the wear on the corner of the nozzle. The turning of the leakage flow resulted in very high particle loading on the radius itself, causing the lip to wear away on some SST builds. This shows that the change of direction of the leakage flow must be gradual, so that particle loadings on the outside of the turn may be kept low.

In order to reduce these loadings either the turn can be made very gradually, or the velocity of the fluid in the turn can be dropped. These

SST 3008

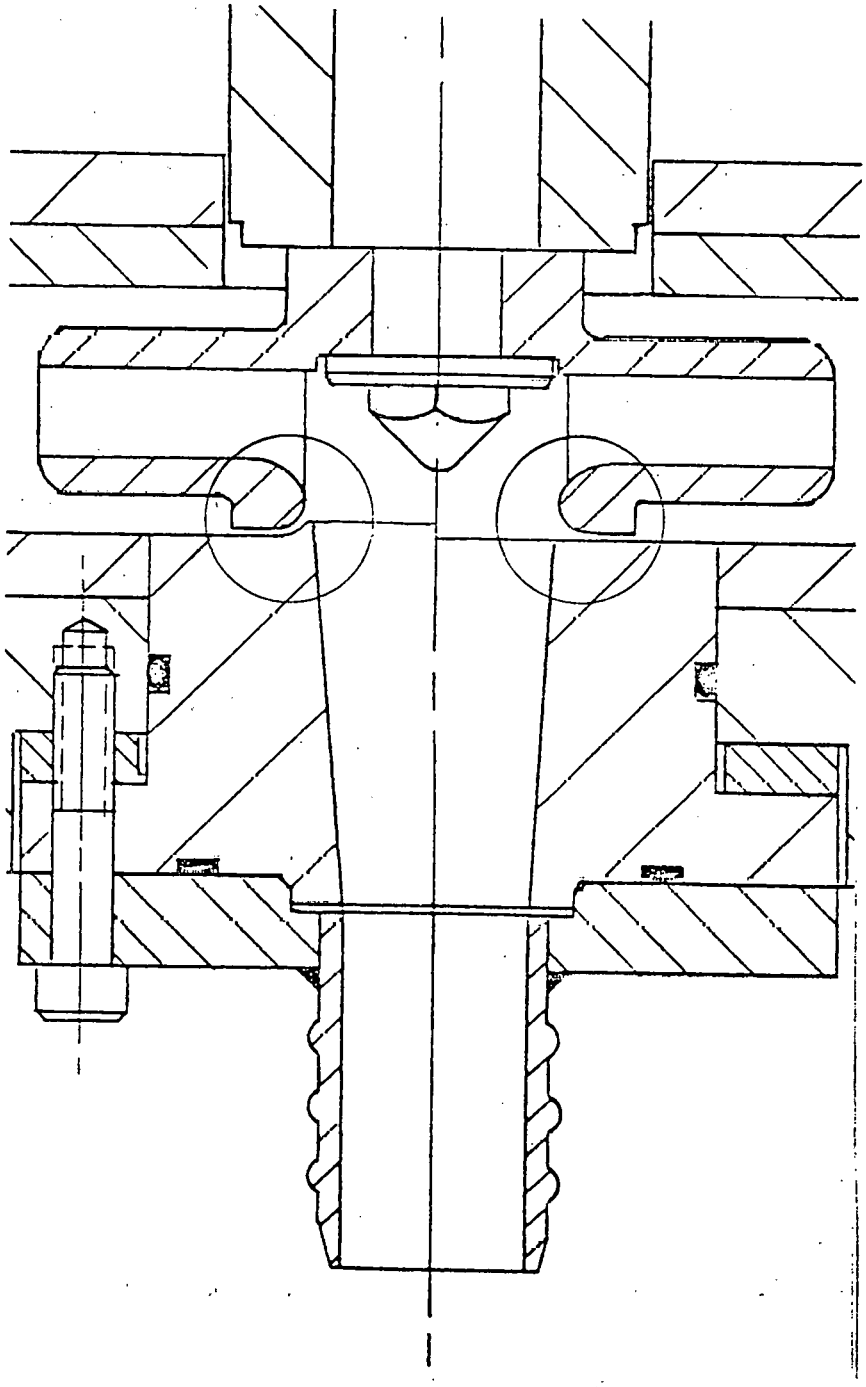

SST 3009

(II)

Figure 28: Two Leakage Path Arrangements

ideas prompted the two directed leakage "path" approaches shown in Figure 29. the bottom configuration collects the leakage flow and directs it into a 30 from axial clearance space. Wear did occur at the entrance, on the suction nozzle itself, indicating that the entrance design caused particles to turn suddenly. The configuration on top turned the flow over a larger radius, and due to more open area, did the turning with a lower flow velocity. Some wear did occur at the outside of the turn on the suction nozzle. Unusual wear was seen on the suction nozzle, in the close clearance section, but only over about a 30 arc. This was thought to be caused by the non-symmetric distribution of the front leakage flow due to the pressure distortion at the impeller ID caused by the circular type collector. The nature and location of the wear lead to this conclusion. Discounting this unusual wear, it was concluded that both configurations provide acceptable suction nozzle designs. Wear, however, was observed at impeller I.D.

The impeller I.D. wear seemed most severe on the bottom configuration (Figure 29). Chewing of the sharp corner, extending into the blade itself occurred. Also, ripple type wear at the I.D. of the impeller was observed right at the clearance exit. The separation that occurs with the bottom path configuration also caused a worse wear groove on the suction side, shroud side of the blade, as compared to the top configuration.

A directed leakage path has been shown to be a desirable feature. The 30° from radial approach,

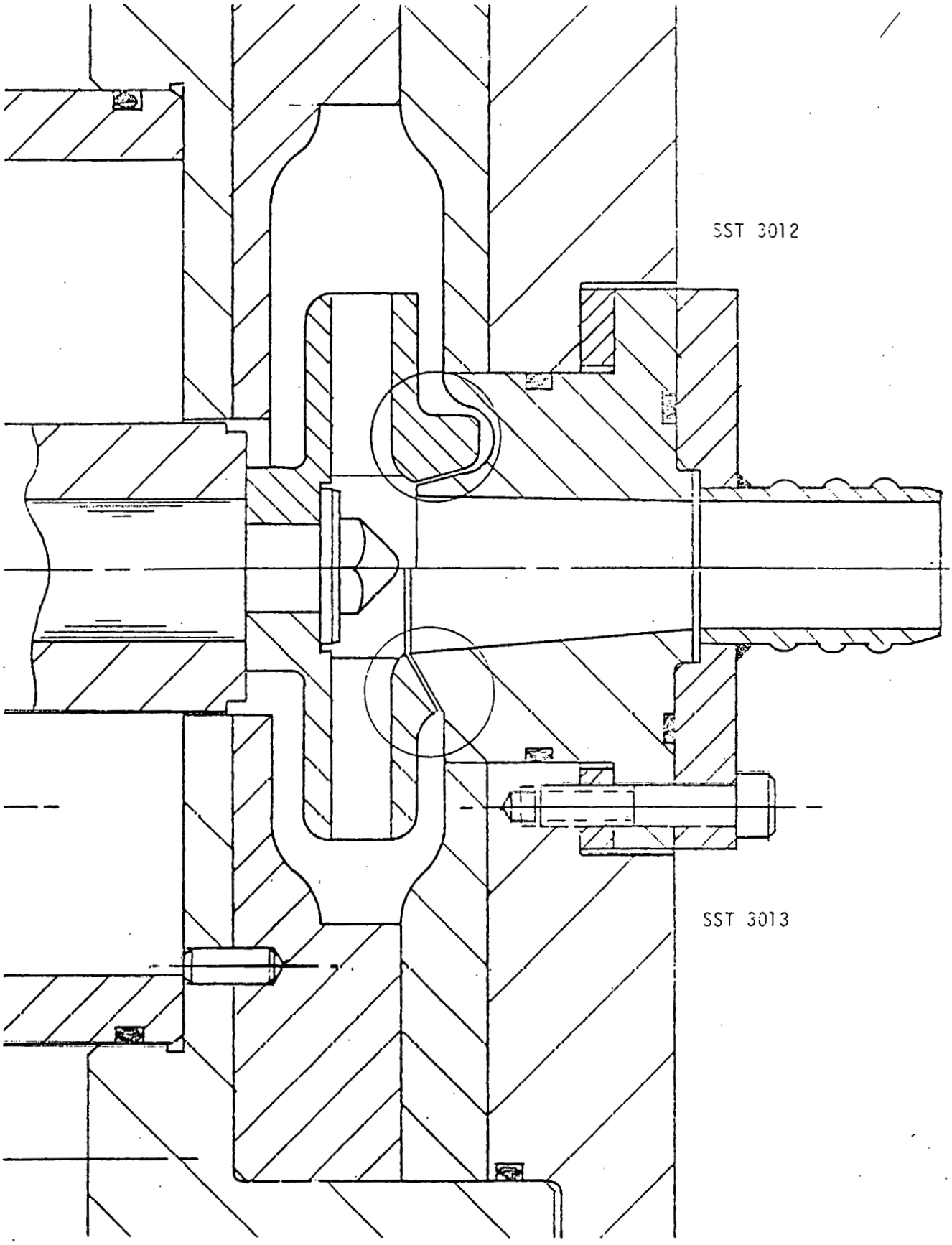

Figure 29: Two Directed Leakage Path Concepts

with an inlet designed to gradually turn the leakage flow is a practical design solution with respect to fabrication and assembly. The exit of the close clearance path should not be immediately adjacent to the blade tip. A sharp corner, with a short radius section to the blade seems desirable (similar to MKI, Figure 27).

IMPELLER BLADE SHAPE

The motion of a particle in an impeller is influenced largely by the blade to blade pressure distribution. This has been discussed previously. Three configurations shown in Figures 30, 31 and 32 were tested. The corresponding blade loading diagrams are presented in Figure 19 a, b and d.

The impeller shown in Figure 30, SST 5, has a very light blade loading. The nearly constant relative flow area results in non-separated flow. Unfortunately, ripple wear, similar to what is observed in a channel flow situation was observed on the suction side of the blading, over the latter two thirds of the blade length. Sidewall grooving in the passage and grooving on the pressure side was also observed. A large drop in performance when sand was added was also observed. (See Figure 21b).

It is believed that the lack of mixing, which would have occured had the flow separated within the blade passages, allowed the solids to be concentrated on the pressure sides of the blades. This would have led to slower movement of those solids which would have then piled up

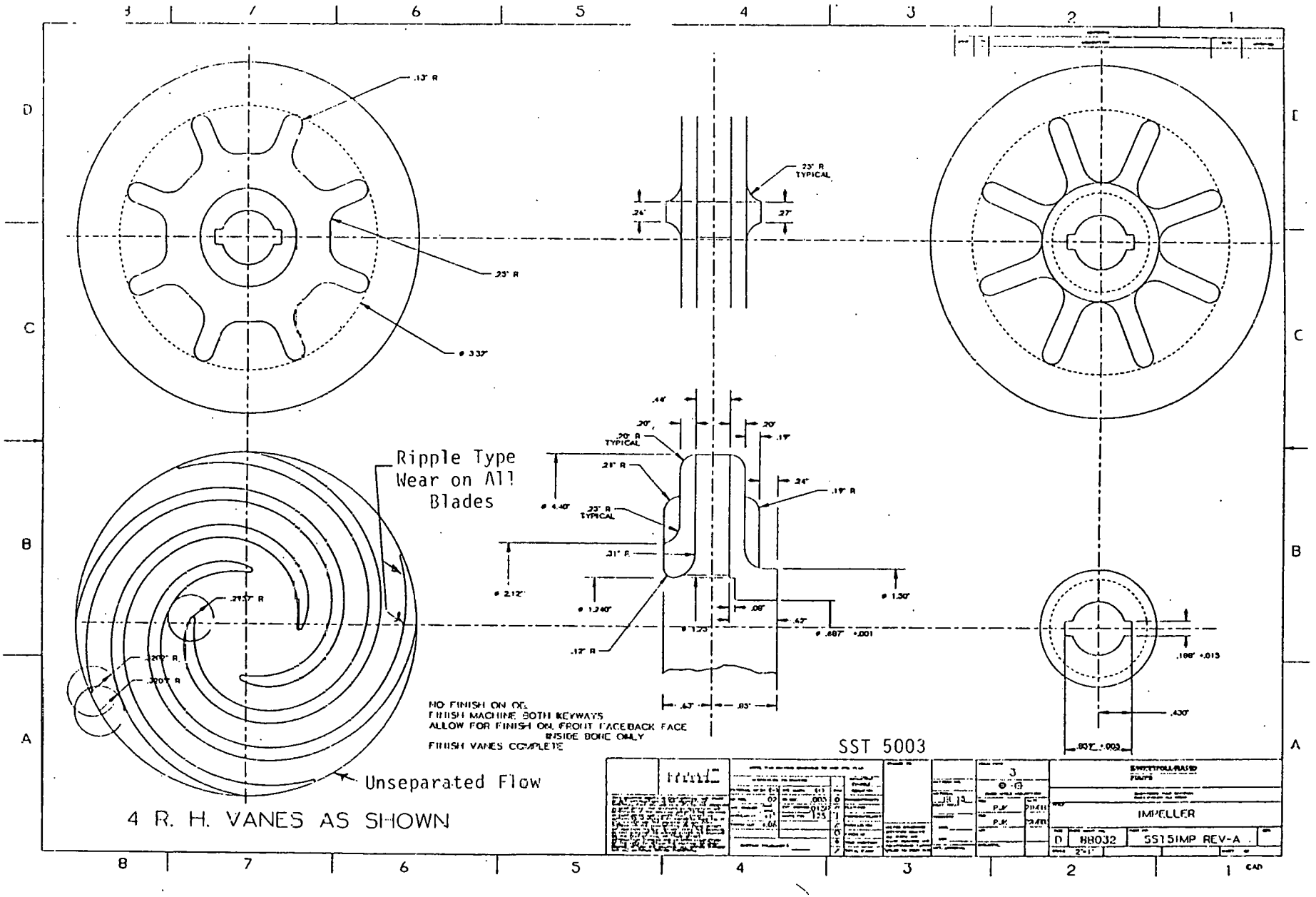

(III)

Figure 30: SST 5 Impeller

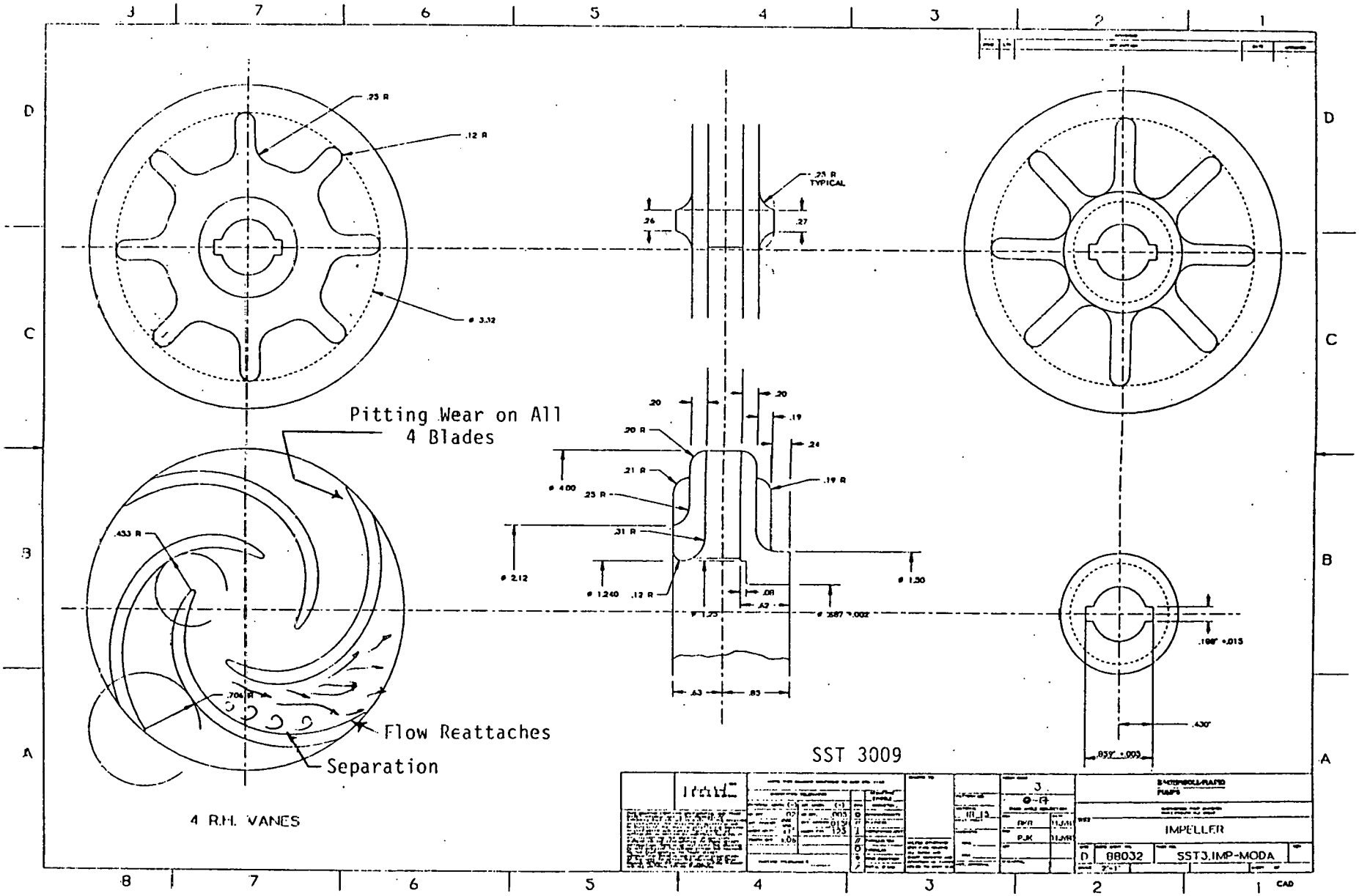

(III)

Figure 31: SST 3, 4 Vane Impeller

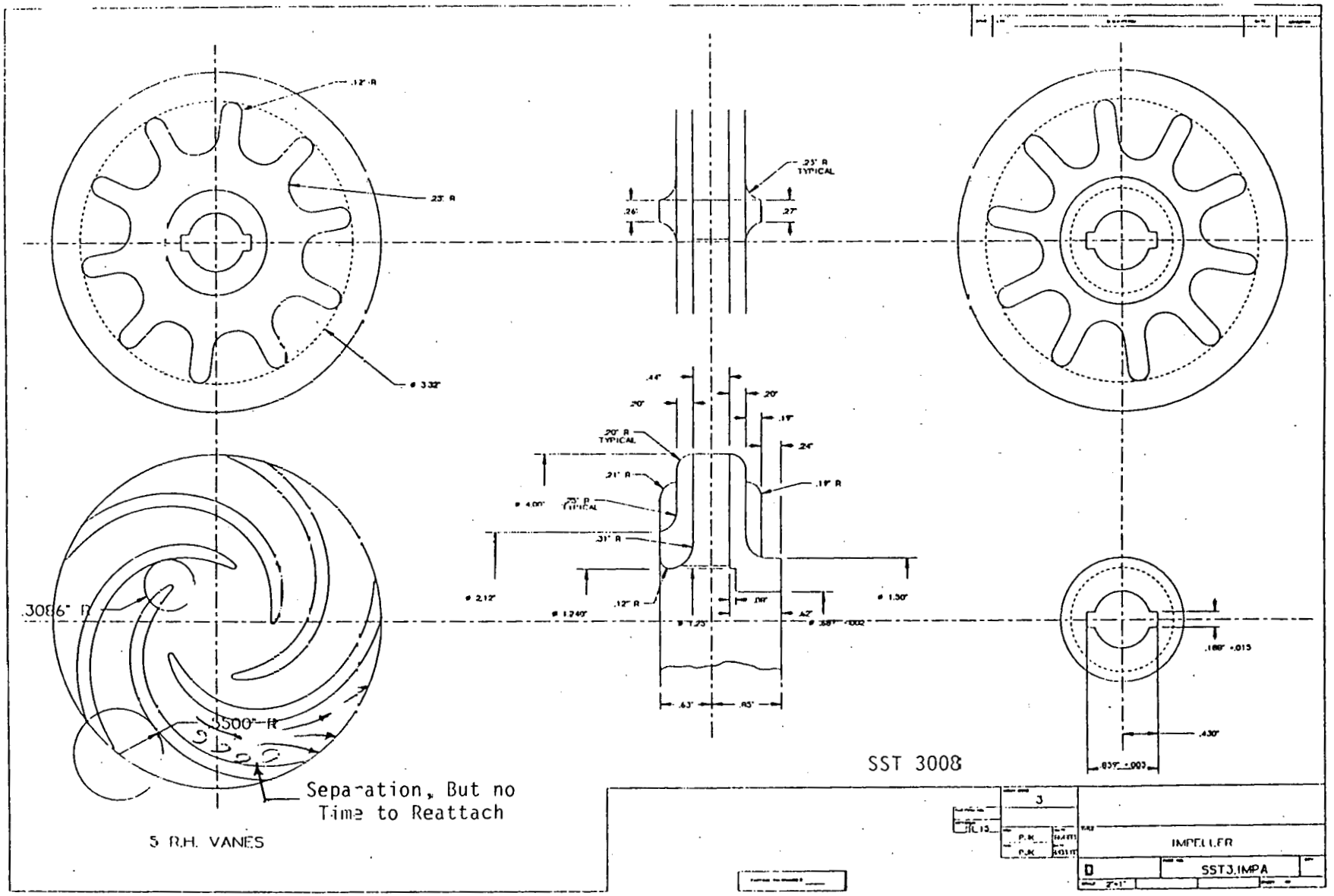

(III)

Figure 32: SST 3, 5 Vane Impeller

and blocked the passages enough to reduce the head.

Figure 31 shows a 4-vane, SST 3 type impeller with a very heavy blade loading. Here the relative flow area diverges so rapdily, that separation occurs well near the leading edge of the passage on the pressure side of each blade. On this design, the flow seems to impinge on the suction side of each blade just before the impeller exit. At this location pitting type wear was observed, which seems to indicate that particles were hitting this area with high enough energy to cause damage. The blade design was satisfactory in other aspects.

The impeller in Figure 32 is a 5-vaned SST 3, which has a higher solidity than the 4-vane and hence a lighter blade loading. Separation occurs farther back in the passage than with the 4 vane, and apparently does not have the time to impinge on the suction side, since the pitting wear on the suction side of the blade at the trailing edge is hardly noticeable. Some side wall wear (axial wear) is noticeable in the vicinity of the wake (separated zone), where the blockage due to the wake causes a local increase in relative velocity in the passage. It is possible that sand packs up in this separated zone and forms a Hydraulically Preferred" passage, effectively decreasing the blade loading.

The mixing which accompanies the separated flow, which exists in both the SST3 impellers, tends to reduce the layer of particles on the pressure side of the blades. This may reduce the blockage

effect which existed on the non-separated SST5 and caused the decay in head-flow performance. Furthermore, this reduction in solids layer thickness could also lead to a more favorable wear life, particularly if the wear is related to this layer thickness as Tuzson reports (4).

All the impellers tested showed blade leading edge wear, and wear back (shortening of blade). Also smooth groove type wear on the suction side of the blades, along the shroud, from the inlet to about one quarter blade length. This groove may be caused by separated flow resulting from flow trying to get around the shroud radius and into the blades.

A superior impeller configuration would include an SST 3 type blade shape with 5 vanes (tangent of the blade angle is a linear function of radius). Careful attention to the impeller inlet and shroud profile will minimize the tendency for flow to separate off the shroud radius. The inlet blading should not have axial leading edges. The leading edge should have a concave shape (in the meridional view) similar to the concave trim shown on the volutes. This shape would pull the hub side of blade to a smaller radius (hence lower tip speed) and minimize formation of horseshoe vortices.

COLLECTOR SIDEWALL

The sidewall configuration shown on the top of Figure 33, referred to as MKI sidewall served as the baseline design for early SST work. The edge formed by the collector radius and volute side-

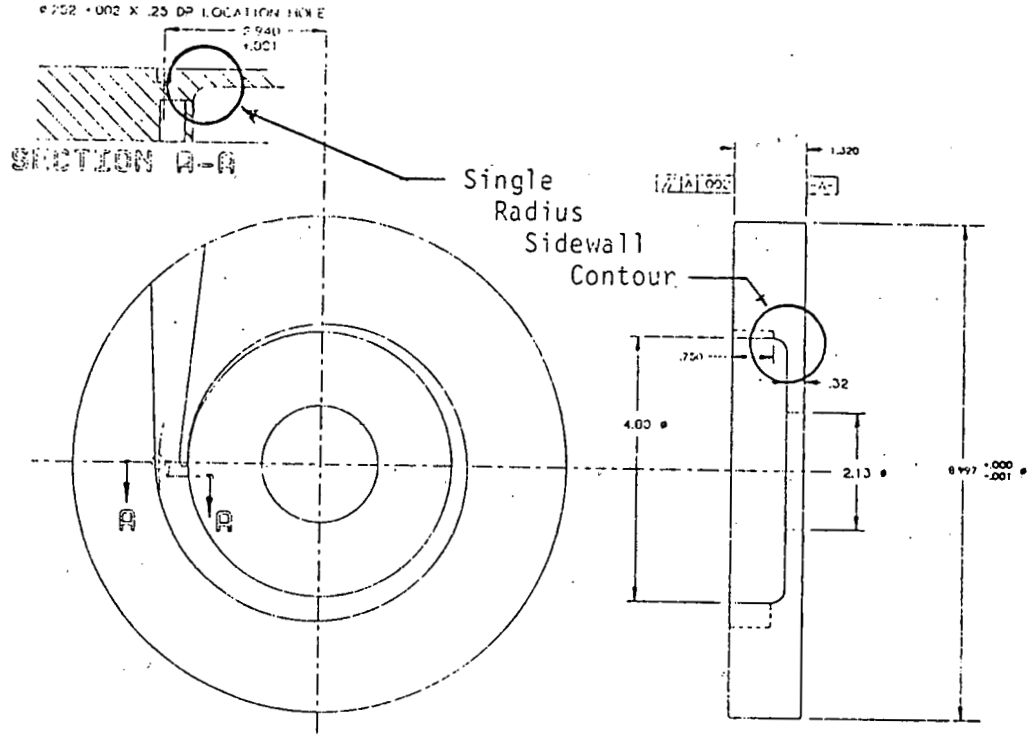

SST Mk I

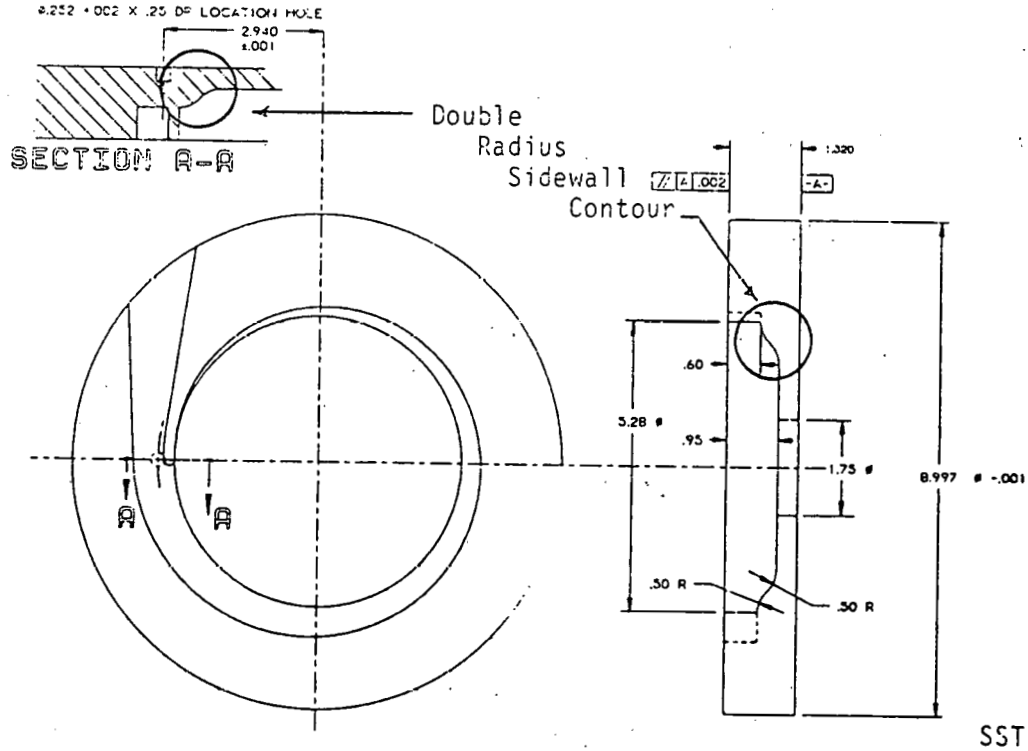

SST Mk II

Figure 33: Two Sidewall Configurations

(IV)

wall caused the volute sidewall boundary layer flow (radially inward, but with a large tangential component) to separate as it passed over this boundary. The vortices formed by this separation cause sharpening and undercutting of the edge, from the collector side. This wear, coupled with the flow phenomena around the cutwater, caussed severe undercutting of the cutwater.

The double radius contour, shown in the lower half of Figure 33, solved this wear problem. The secondary flow still exists from the volute, but since no sharp corners exist, no separation occurs. Undercutting in the cutwater region was eliminated, and was replaced by sidewall grooving on both sides of the cutwater.

The double radius contour appears to be the most desirable configuration. Besides eliminating undercutting type wear, it also appears that ripple wear long the collector sidewalls is reduced.

PUMP OUT VANES

Pump out vanes are used to reduce the pressure differences across the front impeller ring clearance and hence drop the leakage flow passing through this close clearance. Pump out vanes on the rear shroud of the impeller are important since they help equalize the pressure on both sides of the impeller, and balance axial thrust, i.e., balance the effect of the pumpout vanes on the front. The rear vanes may also serve to protect the rear seal from particle laden flow

activity. Pump out vanes also consume power with a typically negative effect on pump efficiency.

The design shown in Figure 34 was tested on an SST 5 type impeller. The design of the two most obvious features are related to each other. First, the vanes are radial and second, they do not extend to the full diameter of the impeller. Assuming that the flow along the sidewalls and entering the pumpout vane maintains constant angular momentum, by designing a 90 degree vane at the proper diameter (based on blade speed consideration) an approximately 0 degree angle of incidence may be achieved at the tip of the vane. This should extend the life of the pump out vane. Another benefit is a smaller power consumption penalty due to the short pumpout vane (horsepower is proportional to fourth power of radius).

The results of the testing of this design showed that the leakage flow was cut down considerably (Figure 35 for the H-Q performance). The reduced leakage also meant longer life for the directed leakage lip (see Figure 28). Some wear was also evident on the impeller shroud at the tip of the pumpout vane. The reduced front ring leakage was also seen in the wear pattern at the exit of the leakage lip. The reduced leakage flow apparently remains attached to the impeller I.D. radius. The axis of the wear ripples indicate particle velocities greater than the local wheel velocity (this means flow in the gap is characterized as being somewhere between free vortex and solid body rotation). On the blade side of the radius, the ripple axes are oriented in a way which corresponds to the angle of the inlet relative

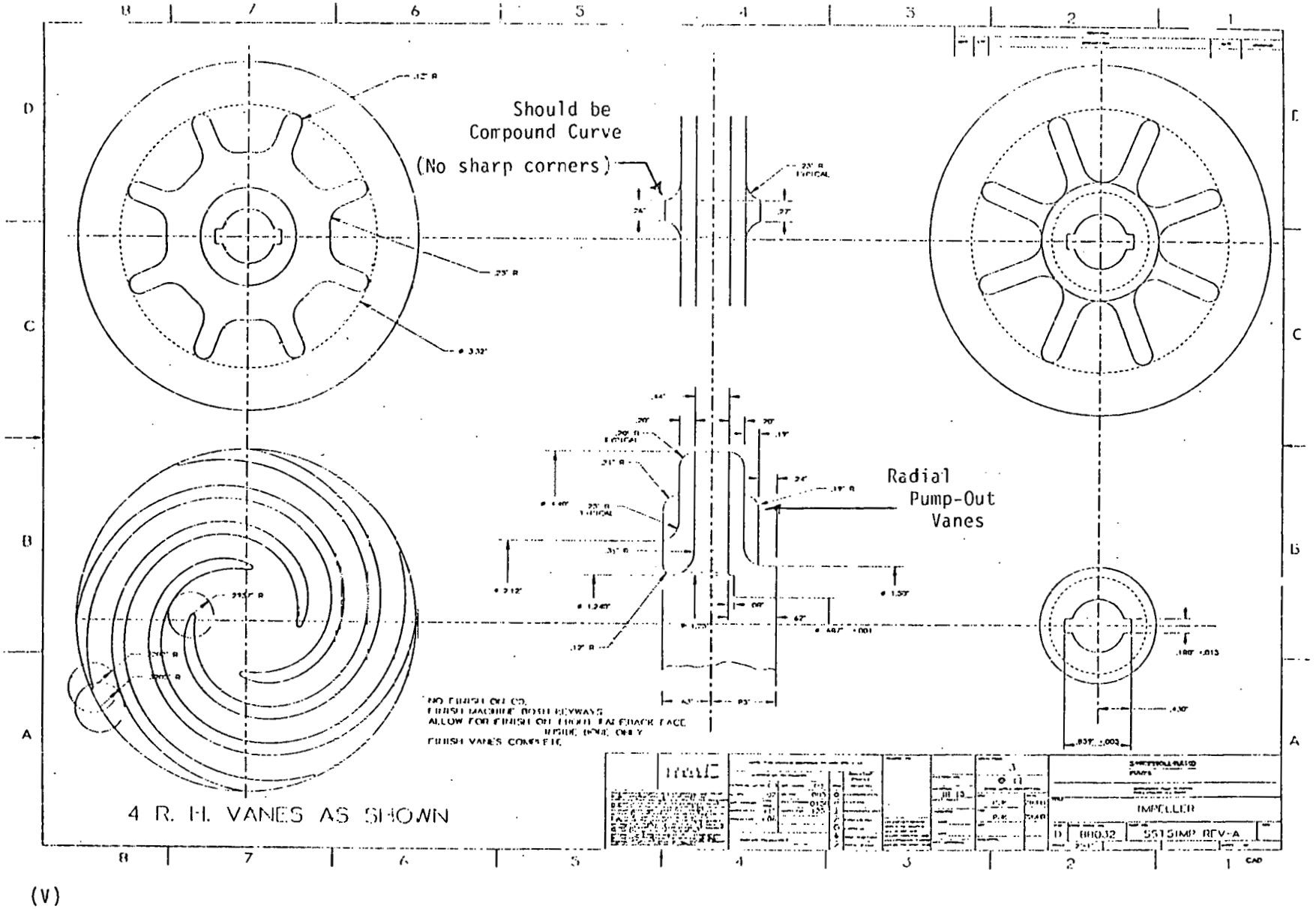

(V)

Figure 34: SST 5 Impeller With Pump-Out Vanes

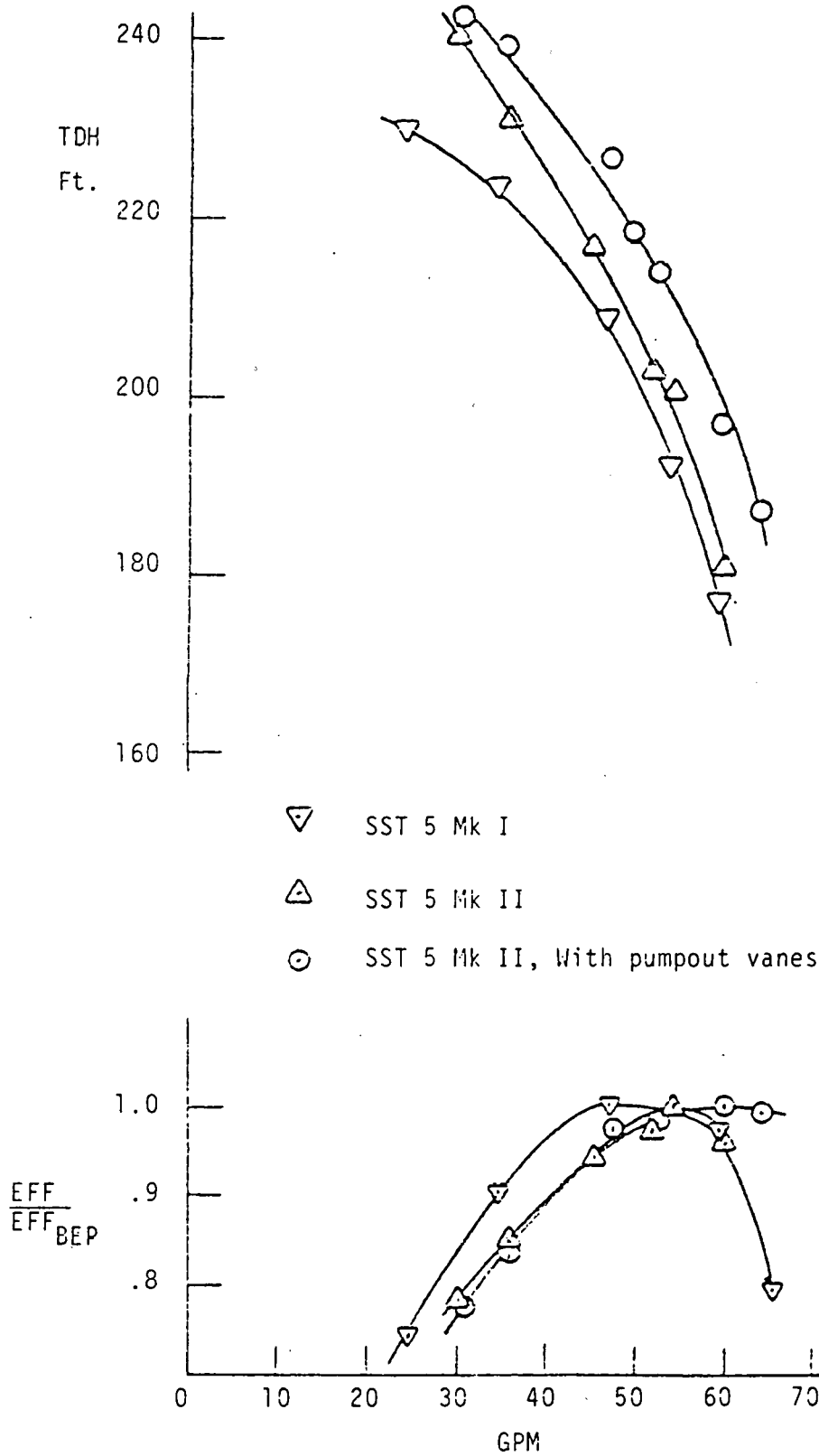

Figure 35: SST 5 Impeller, With and Without Pumpout Vanes

velocity vector. The resultant wear pattern on the I.D. of the impeller is best described as "Herringbone". (See Test Report 5006 in Appendix B).

Pump out vanes are desirable in slurry pumps to minimize front seal wear. The design tested, with the exception of changing the O.D. blade trim, appears acceptable.

IMPELLER SHROUD CONFIGURATION

Trailing edge damage in the form of two grooves across the blade land, with the groove originating at the corner sidewall, has been observed on slurry pumps in the field. SST MKI and MKII impeller designs have never shown such wear. After considering this difference it was noticed that field pumps had square edges on the outside impeller sidewall while SST impellers had round edges.

A possible explanation is that the flow being dragged along the outside of the impeller remains attached to the impeller as it follows the radius (on SST) at the O.D. This flow mixes with the corner vortex, from the blade passage, in a manner which eliminates the dragging of the vortex across the blade land. To test this theory an SST impeller was tested with a square front shroud (see Figure 36). No damage on the blade land was observed with this square edge; so apparently, the interaction of the radially outward impeller sidewall flow with the main impeller is not responsible for the blade land damage observed in field pumps.

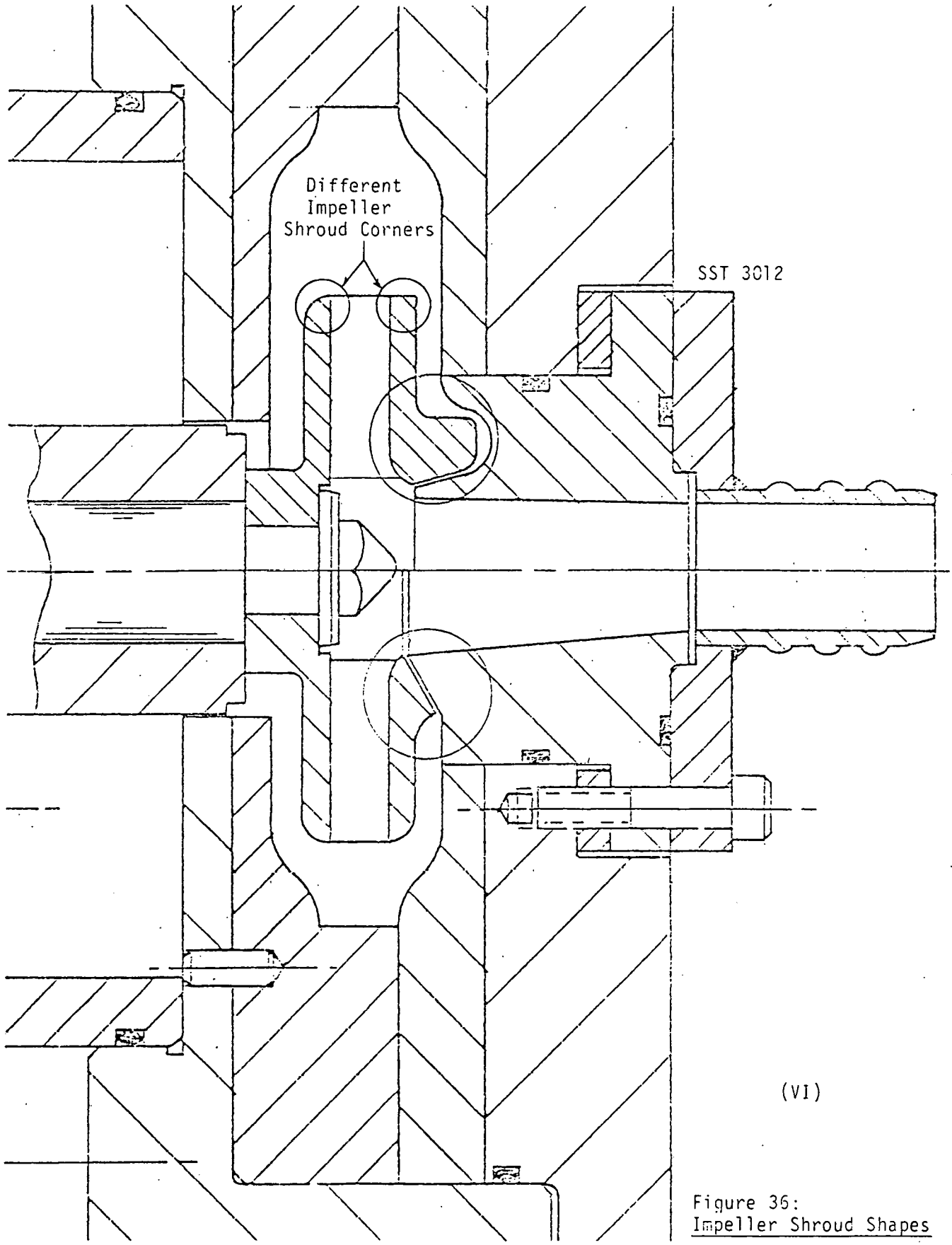

(VI)

Figure 36:
Impeller Shroud Shapes

3.2.5 PROTOTYPE PUMP HYDRAULIC DESIGN FEATURES

The SST Development of the six critical design areas, described previously, has evolved a set of design features for the prototype size pump. Some of the features come directly from component design in SST while other design features are based on observations made of wear phenomena in various parts of the pump.

A volute type collector will be used to provide for continuous fluid collection, at the design point, with all the hydraulic benefits this entails. The cutwater wedge angle should be as large as possible, while maintaining acceptable throat dimensions and holding to overall envelope requirements. A circular shape to the diffuser throat and the volute sectional cross-section, assures the concave type trim used to prevent horseshoe vortex will be provided. The ratio of cutwater radius to impeller radius will be 1.5 with a cutwater wedge at the cutwater tip of 34 .

The directed leakage path will be oriented 30° from radial. The entrance to the close clearance leak path is entered from a large annular plenum, which slows down the leakage flow, tangentially and radially. The clearance will be capable of external adjustment. The joint where adjuster piece mates with the stationary front wall is placed as closely to the inside of a radius as possible. This placement discourages particles from attacking this joint, since the normal forces tend to push the particles to the outside of the turn. At the exit of the leak path, on the impeller side, a MKI type square edge is used.

The Hub/Shroud, meridional profile of the impeller

inlet must be designed to avoid separation of flow from the shroud radius. The meridional profile of the blade shows a concave trim (similar to the volute cutwater) to the leading edge. This discourages the formation of the horseshoe vortex on the hub and shroud walls. This trim, coupled with suction side fairing which matches the unblocked flow angle, form a quasi-francis type inlet blade design. The blading used on SST 3, 5-vane impeller appears to provide the best wear characteristics. The blade itself is defined by making the tangent of the blade angle, a linear function of radius.

The collector sidewalls will have the double radius contour characteristic of the MKII SST configuration. Using this approach, eliminates any sharp corners which provide areas of potential separation. These separation zones cause undercutting and grooving.

Radial pump out vanes, similar to the type tested in SST will be used. The vanes will not extend to the full diameter of the impeller. Design criteria in terms of matching the flow angles at the vane O. D. are as described in the SST results.

3.3 MATERIALS INVESTIGATION

The objective of the materials investigation is to find a pump material(s) that is more wear-resistant than currently commonly used material (HC250) for synfuel slurry application.

The results of the materials study are described in this section which includes: selection of the best candidate slurry pump materials, experimental testing of these materials at Ingersoll-Rand, Battelle Columbus Laboratories and Oak Ridge National Laboratories, and the final selection of the material(s) for test pumps.

3.3.1 CANDIDATE MATERIALS SELECTION

Based upon the literature survey, pilot plant experience and inhouse experience of slurry pump materials, several materials were selected for test evaluation. A list of these candidate materials is shown in Table 2. As can be seen, four different categories of materials were selected for investigation - structural alloys, ceramics, coatings and weld deposits (or hard facings). Weld deposits were selected for high wear areas only.

Alloys

The three most commonly used erosion-resistant slurry pump alloys are Ni-Hard 4, HC250 and 1503. Since hot coal-oil slurry could be corrosive and the previous works show that the rate of corrosion decreases with increase in the chrome level of the alloys and levels off at about 12% Cr, only HC250 (28% Cr) and 1503

TABLE 2

CANDIDATE MATERIALS

ALLOYS	CERAMICS	COATING	WELD OVERLAY
EXISTING 1) 28% Cr Iron A) Fully Hardened B) Semi-Annealed C) Fully Annealed 2) 1503 Iron NEW 1) Higher Cr Iron 2) High P, High Cr Iron	1) SiC (Solid)	1) BORONIZED	1) EUTECTIC 6715

(15% Cr) were selected. Ni-Hard 4 has only 8% Cr.

The pilot plant experience indicates that a fully hardened HC250 may be too brittle to withstand thermal shocks that the pumps experience during start up and shut down, whereas, a fully annealed HC250 has enough ductility to withstand these shocks. Therefore, HC250 was studied for the effect of annealing on its erosion properties at three different heat-treated conditions - fully hardened (about 600 BHN), semi annealed (about 450 BHN) and fully annealed (about 350 BHN).

The two new alloy compositions are, 1) above 30% chrome iron and, 2) high phos high chrome-iron. They are based upon the formation of more hard carbides and hard phosphides phases.

Ceramics

Ceramics are generally too expensive to fabricate slurry pumps. However, they are much more erosion resistant than alloys. Several pump manufacturers have developed low grade all-ceramic pumps for some limited applications (low speed and small particle water base slurries). Refrax, a slurry-cast silicon carbide made by Carborundum Co., has been used successfully in these pumps. Since refrax has a very low tensile strength , it should be evaluated only for stationary wear parts in pumps. Its application in hot coal-oil slurry may be questionable due to its poor thermal shock resistance. Other higher strength ceramic materials and cermets, such as hot-pressed silicon carbide, silicon nitride, tungsten carbide, etc., were not considered, due to their high cost.

Coatings

Various diffusion bonded coatings were considered such as, surface boronizing, TiB_2 (including TMT coatings), Si_3N_4, SiC etc., but only surface boronizing was selected for evaluation. The HC250 was selected as the substrate for boronizing. Most of these coatings either cannot be effectively deposited on HC250, or can be deposited only to a very small thickness, normally less than 0.001" by the existing commercial processes. Some coatings are too expensive to use. Boronized coating can be deposited to over 0.001" successfully on HC250. Previous laboratory tests also indicate that its erosion resistance is extremely good.

Non-diffusion type coatings such as plasma and D-gun coatings were not considered due to their poor bond strength and their thermal mismatch with HC250 base material. Moreover, most of the tests run in the pilot plants with these types of coatings were not successful.

Weld Overlays

Weld overlays or hard facings were considered for the following two reasons:

1. Convenient to apply selectively in the high-wear areas in the pump to prolong the over-all pump life.

2. Convenient to repair worn pumps.

Various hard facing alloys were considered, such as Eutectic 6715, Stellite 6, Stellite 12, Ferro-Tic M6, etc. Eutectic 6715 was selected because of its superior erosion resistance, as shown by lab tests, as well as pilot plant experiments. Hard facing of HC250 with Eutectic 6715 causes severe cracking problem, but by using an intermediate layer of carbon steel weld deposit, the cracking problem can be minimized.

Insert Materials

In addition to the above materials, six other materials were selected for evaluation for possible application as inserts in the pumps. By using inserts in the high-wear areas, such as cut-water, the overall life of the pumps can be improved. These materials are mostly ceramics and coatings and cannot be used for fabricating the pump components, due to either high cost or manufacturing problems. The following six materials were selected.

1. Kennametal K3883 - It is cobalt bonded WC, similar to K701 or K703. Although K701 and K703 have higher erosion resistance, K3833 was selected because of its superior toughness and thermal shock resistance.

2. TMT-745B3 coating on K3833 - This TiB coating on K703 has shown almost no wear in previous Battelle coat-oil slurry erosion tests.

3. CVD SiC on graphite - It showed extremely high wear resistance in previous Battelle

lab tests.

4. Partially stabilized zirconia - The toughness and thermal shock resistance of this material is higher than most of the ceramic materials. It may be used to fabricate pump components also. Several laboratories are currently working to further improve the wear resistance of this material.

5. CVD TiB_2 on 410 stainless steel - This coating showed excellent erosion resistance in previous Battelle lab tests.

6. Sintered SiC - This material also exhibited excellent erosion resistance in previous Battelle lab tests. However, its poor thermal shock resistance could limit its application.

The use of inserts in pumps will require changes in pump design to fasten the inserts in place and also to accommodate the mismatch of thermal expansion of the insert and pump material.

3.3.2 TEST METHODS

The purpose of the tests is to obtain quantitative erosion, corrosion and erosion-corrosion data on the candidate materials and to select the best material/ materials for the pump. The materials' evaluation was done by three types of tests as shown in Table 3.

1. Erosion tests at Ingersoll-Rand.
2. Corrosion tests at Oak Ridge National Lab.
3. Erosion-corrosion tests at Battelle Labs.

The erosion tests were run in a nozzle tester, using a high velocity sand-water slurry jet at room temperature. The nozzle diameter was 0.187" and a slurry concentration of 40 wt. pct. sand was used. These tests were run using:

1. Regular sand-water slurry of 42 mesh average particle size.

2. Viscous sand-water slurry of 100 mesh average particle size with 2 wt. pct. sodium carboxy methyl cellulose added to the water to increase the viscosity.

The regular sand-water slurry tests were run at two different velocities, 100 ft/sec and 150 ft/sec to study the effect of velocity on erosion wear. At 100 ft/sec velocity, three different impingement angles were used, 10 deg., 20 deg., and 75 deg., to study the erosion wear at different angles. However, at 150 ft/sec velocity, only 10 deg. impingement angle was used.

TABLE 3

MATERIALS TEST

EROSION (IR)	CORROSION (ORNL)	EROSION-CORROSION (BATTELLE)
A. Sand-Water Jet 1) 100 Ft/Sec. A) 10^{o} B) 20^{o} C) 75^{o} 2) 150 Ft/Sec. 20^{o} B. Viscous Sand-Water At 500^{o}F. & 550^{o}F. Jet 100 Ft/Sec. 20^{o}	A. T102 Bottoms At 550^{o}, 570^{o}F. & 625^{o}F. B. V-131 B Solvent	50% T-102 Bottoms At 550^{o}F. & 20^{o} 1) 100 Ft/Sec. 2) 150 Ft/Sec.

The viscous sand-water slurry tests were used to simulate the synfuel slurry in terms of viscosity and particle size. Only 100 ft/sec velocity and 20 deg. impingement angle were used for these tests.

The corrosion tests were run by static immersion of the specimens in the corrosive medium. Both T-102 bottoms and V-131B solvents from Wilsonville plant were used to study the corrosive properties of the candidate materials. The test temperatures were as follows:

1. T-102 bottoms test - 550, 570 and 625 degree Fahrenheit.

2. V-131B solvent test - 500 and 550 degree Fahrenheit.

Some carbon steel specimens were also tested for comparison.

The erosion-corrosion tests were run in a nozzle tester using a high velocity synfuel slurry jet at a high temperature. The T-102 bottoms diluted with 50 wt. pct. of anthracene was used, the net solid concentration of diluted slurry was about 5 pct. All tests were run at 550 deg. F., 20 deg. impingement angle, and two different velocities, 100 ft/sec and 150 ft/sec.

3.3.3 DESCRIPTION OF TEST APPARATUS

I-R Nozzle Tester

The IR nozzle tester is used to run slurry erosion tests of materials to evaluate their erosion properties. The test system uses water-base slurries as the eroding medium. The tester is shown in Figures 37 and 38, and a schematic drawing is shown in Figure 39.

The nozzle tester consists of a 72 gallon slurry tank that can be pressurized up to 350 psi by air to drive the slurry through a nozzle in the test chamber. The tungsten carbide nozzle produces a 3/16" diameter high velocity jet that impinges on a rectangular specimen. The specimens can be set at angles ranging from 7 degrees to 90 degrees with the jet. The slurry, after impinging on the specimen, is collected in a receiving tank and then pumped back into the slurry tank at the end of the test cycle. Slurries containing up to 50 wt. pct. of sand or coal have been used, and the maximum jet velocity obtained at this concentration, using sand, was about 160 ft/sec at 350 psi operating pressure. The test duration for each cycle for 160 ft/sec jet velocity is about 5 min., 30 sec.

Both the pressure tank and receiving tank are rubber lined and provided with mixers to keep the slurry in suspension. The transfer pump is a 60 gpm, 40 ft head and 1.5 HP slurry pump. Rectangular specimens of 2.5" x 0.75" x 0.25" dimensions were used with a surface finish of 32 microinches. The material

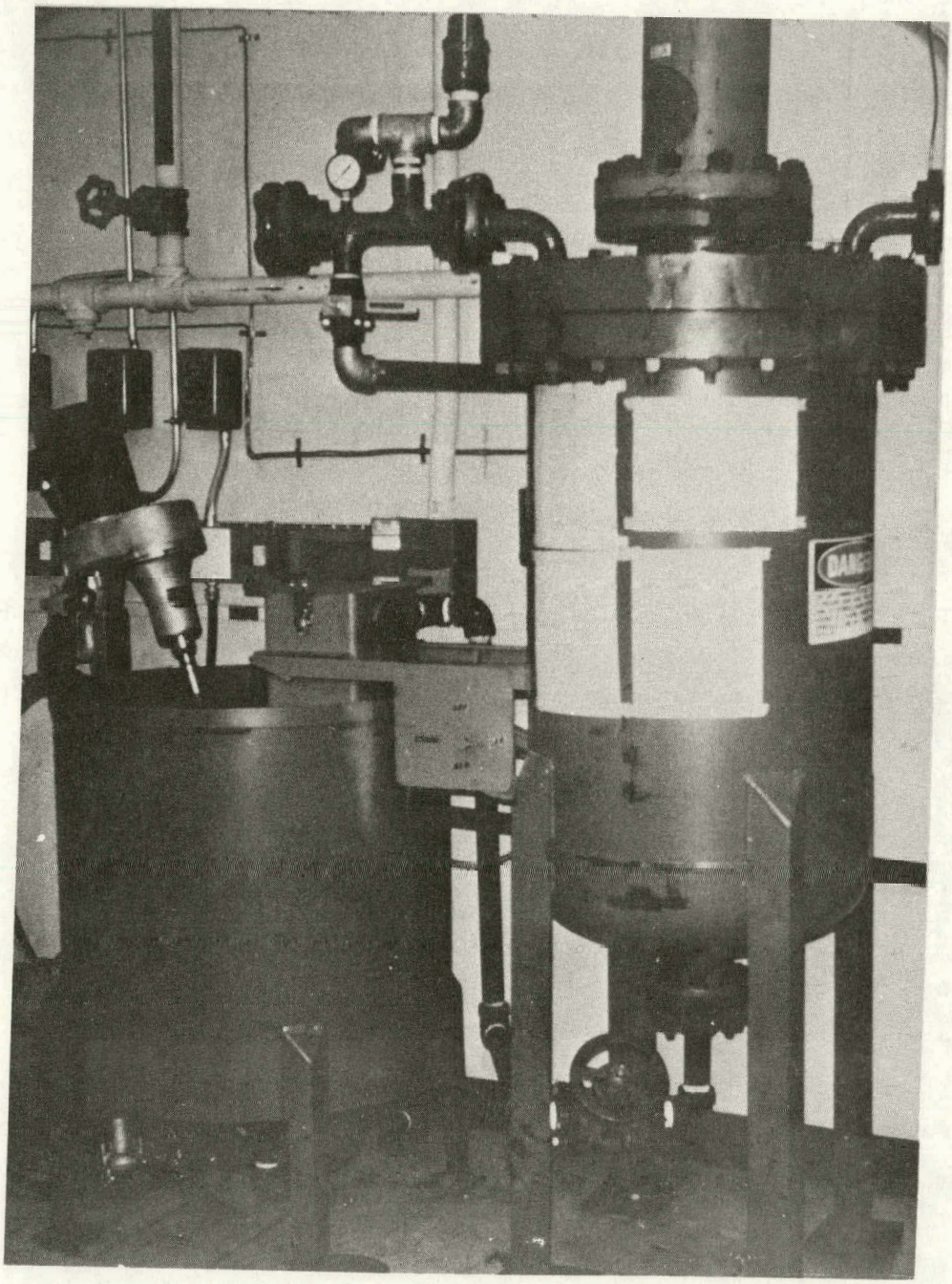

Figure 37: IR Nozzle Tester

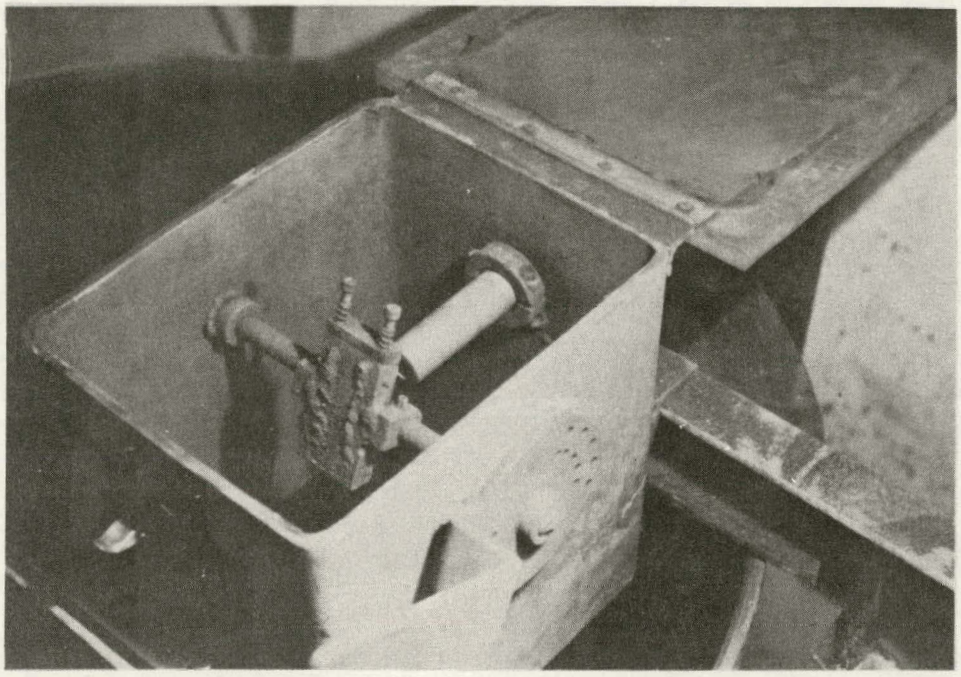

Figure 38: Nozzle Test Chamber

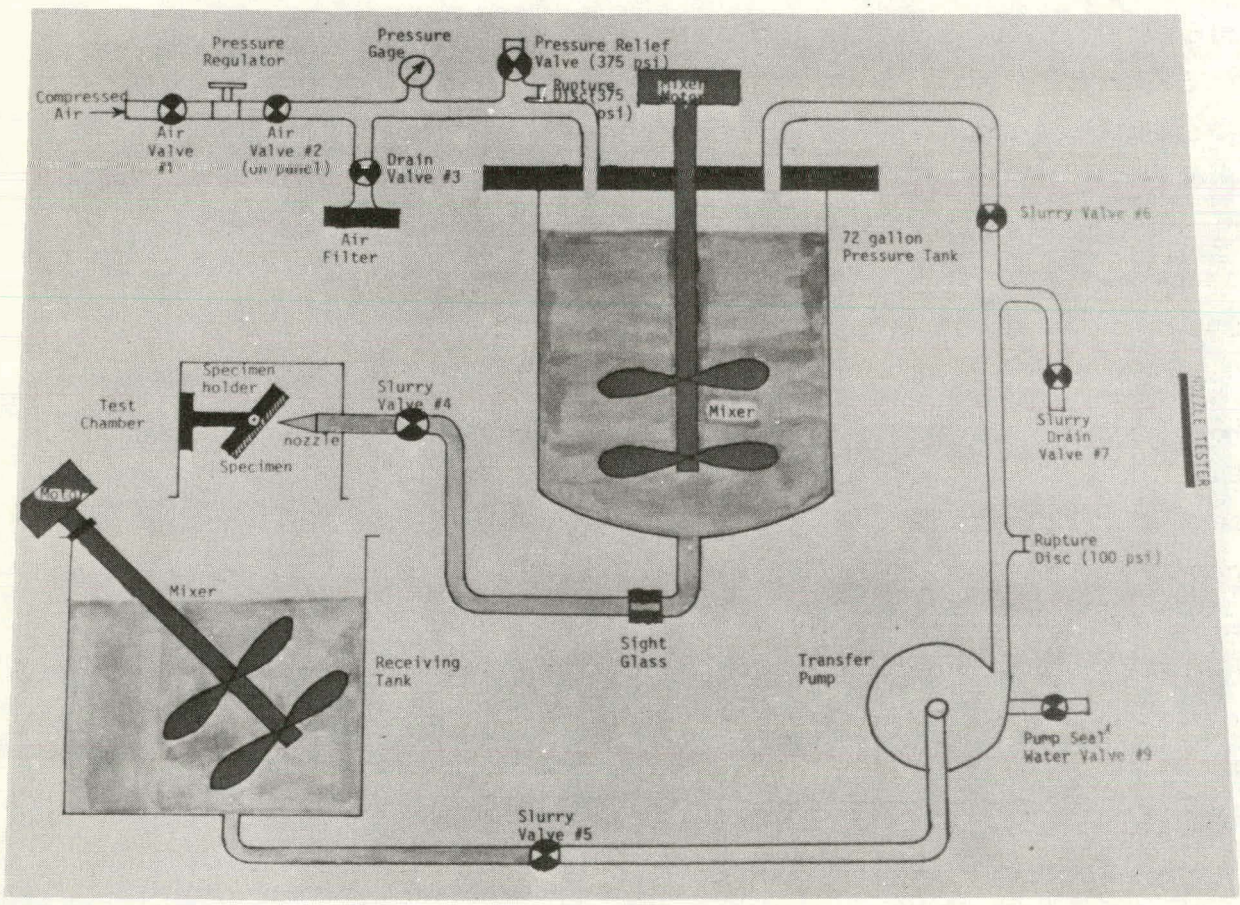

Figure 39: IR Nozzle Tester Schematic

performance was evaluated by determining the maximum erosion depth and the weight loss of the specimen.

ORNL Corrosion Tester

The ORNL corrosion tester is used to evaluate materials for their corrosion properties in a liquid medium at high temperatures. Hot coal process solvent is commonly used as the corrosive medium.

The corrosive tester is a very simple device consisting of a 1000 ml flask placed inside a furnace, as shown in Figure 40. The stem of the flask is provided with a water cooling jacket outside the furnace. Any vapor produced due to the boiling of the low boiling constituents condenses in the stem and trickles back in the flask maintaining the composition of the corrosive medium. An inert cover gas, normally argon, is used at the top of the flask. A thermocouple is inserted into the flask to measure the solvent temperature and two specimens are hung from a hook at the end of the thermocouple. The temperature of the furnace is maintained constant during the test by thermocouples.

Specimens of 1" x 1/2" x 1/4" dimensions are used with a highly polished surface. The corrosion rates are calculated on the basis of the weight loss of the specimens.

Battelle Nozzle Tester

The Battelle nozzle tester is used to evaluate test materials for their erosion properties at high

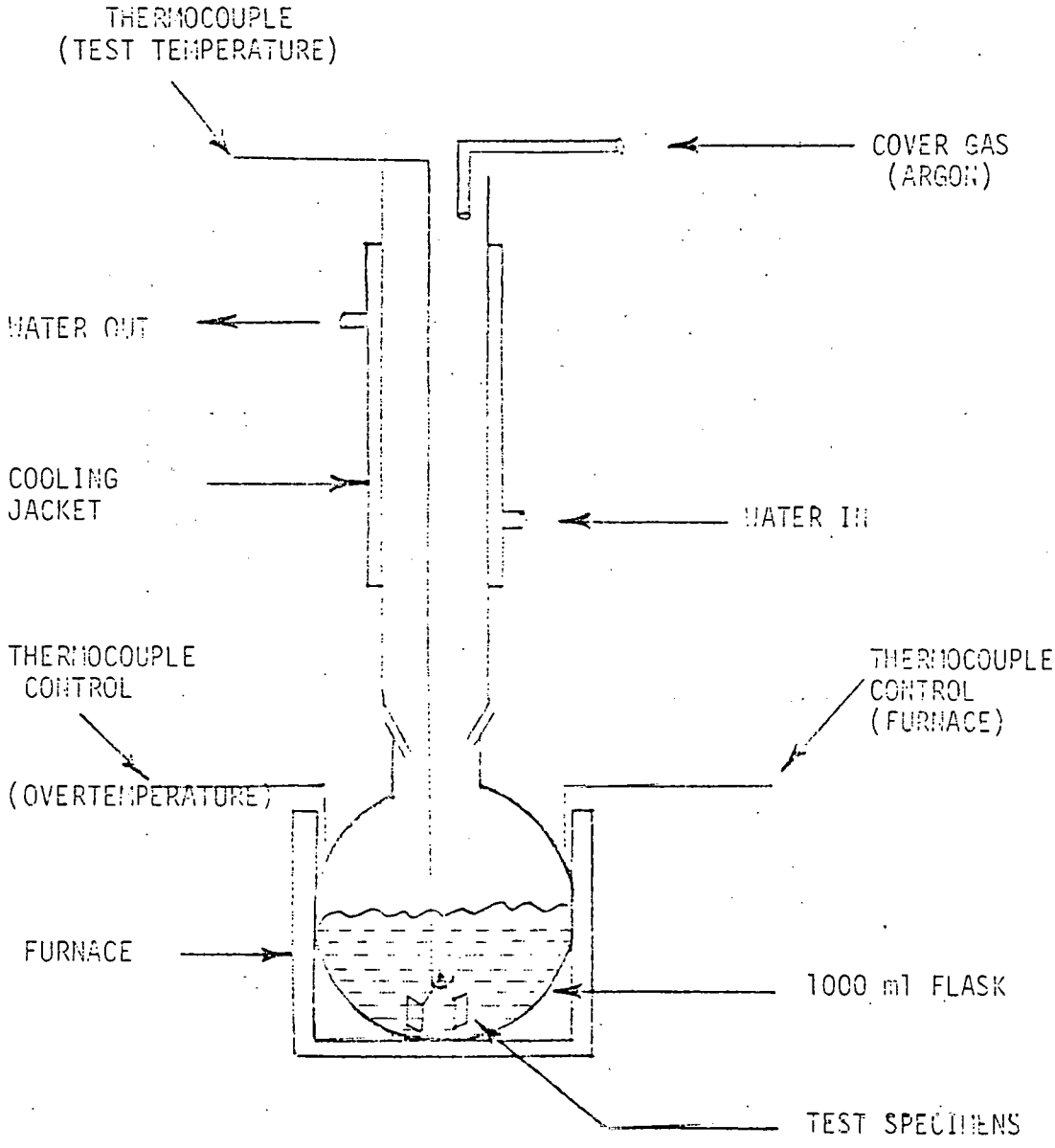

Figure 40: ORNL Corrosion Tester

temperatures. Hot coal-oil slurry is commonly used as the eroding medium in this system. The detailed description of this wear tester has been published in several reports.

The system consists of a bellows-type pump, mixing vessel, and test chamber and relies on gas pressure to drive the slurry through an orifice in the test chamber. A bellows pump is used to fill the mixing vessel with slurry (which enters the vessel from the bottom) and to mix and maintain suspension of solid particles during operation. The pressurized mixing vessel feeds the test chamber and orifice through a high pressure line. The high pressure slurry is uniformly heated to a high temperature just before it reaches the test chamber. The cemented carbide orifice of 0.020" diameter produces a high velocity jet that impinges on a material specimen. The angle of impingement is obtained by adjusting the specimen holder.

Rectangular specimens of 1.5" x 0.375" x 0.25" dimensions were used with a surface finish of 32 microinches. The material performance was evaluated by determining the maximum erosion depth and the average erosion depth by means of surface profilometer.

3.3.4 SAND-WATER NOZZLE TESTS

The purpose of the sand-water nozzle tests is to compare and rank the candidate materials purely on the basis of their erosion resistance. It is believed that most of the wear in the synfuel slurry pumps is due to erosion. Sand was selected as the erodent because in coal-oil slurry, most of the erosive wear is due to the ash content of the coal and both sand and coal-ash contain silica as the principal constituent. Coal itself does not cause much wear since it is very soft compared to the pump materials. The ranking of the materials obtained in the pure erosion test will, however, be compared with the ranking obtained in the hot coal-oil nozzle tests.

A slurry consisting of 40 wt. pct. sand in water was used because of maximum solid content of the synfuel slurry in the pilot plants is about 38 wt. pct. Foundry grade sand of average particle size, 42 mesh, (380 microns), was used and its particle size analysis is given in Table 4. The 100 ft/sec velocity was chosen because it is close to the tip speed of a typical slurry pump impeller and the 150 ft/sec velocity was used to study the effect of velocity on the wear rate. Low impingement angles of 10 degrees and 20 degrees and a high impingement angle of 75 degrees were chosen because most of the slurry flow inside a pump is of low angle sliding type, except at the cut-water where a high angle impingement occurs. Initially, only 10 degree and 75 degree angles were chosen. But, in Batelle's test, it was found that a 10 degree angle produced

TABLE 4

PARTICLE SIZE ANALYSIS OF SAND

MESH	Percent
+20	0.6
+30	5.3
+40	16.7
+50	44.8
+70	26.6
+100	5.6
+140	0.3
Pan	0.1

Average Size - 42 mesh (380 microns)

extremely small wear even after two hours of test, whereas a 20 degree angle produced a measurable wear in two hours. Therefore, all the Batelle tests were run at 20 degrees instead of 10 degrees. IR also ran a series of tests at 20 degrees for direct comparison with the Batelle tests.

The erosion wear of the specimens was measured by both maximum wear depth and the weight loss of the specimens. The initial thickness of the specimens was measured at three points on the specimens and the difference between the readings did not exceed 0.001". The final thickness was measured at the point of maximum erosion. Since silicon carbide specimens contain about 14% porosity, these specimens were always weighed after soaking in water for about 10 minutes.

In spite of severe mixing of the slurry inside the pressure tank, it was found that there was concentration gradient in the tank -- the slurry near the bottom being 10 pct more concentrated than that near the top. In order to avoid such a large variation in concentration, only half of the slurry was used in each test cycle. It takes about four minutes to empty the tank 50% at a 100 ft/sec jet velocity. Each specimen was tested for 8 minutes (2 cycles) at 100 ft/sec velocity and 5 minutes 30 seconds (2 cycles) at 150 ft/sec velocity. After every 20 cycles of test, a new batch of slurry was prepared. No change in the particle size distribution, due to grain fragmentation, nor any rounding of the edges and corners of grains was observed after 20 cycles of test. In most cases,

each material was tested twice. The wear ratios were calculated on the basis of the maximum erosion depth, and the materials were ranked according to their erosion resistance.

Results and Discussions

The results of the sand-water nozzle tests are shown in Table 5 in terms of wear ratios. The wear ratios were calculated as the ratio of the maximum wear depth of the material to that of the fully hardened (F.H.) HC250 since HC250 (F.H.) was used as the baseline with a wear ratio of 1.0. The average maximum wear depths of HC250 (F.H.) are:

100 ft/sec at 10 degrees - 0.0176"
100 ft/sec at 20 degrees - 0.032"
100 ft/sec at 75 degrees - 0.0415"
150 ft/sec at 10 degrees - 0.042"

Although the wear ratios are different for different series of tests, the ranking of the materials is the same for all four different test conditions, as shown below (only exception being the wear ratio of SiC at 100 ft/sec and 10 degrees):

1. Boronized HC250
2. Eutectic 6715
3. Silicon carbide
4. 1503
5. HC250 (F.H.)
6. HC250 (S.A.)
7. HC250 (F.A.)

TABLE 5

SAND-WATER NOZZLE TEST RESULTS

MATERIAL	WEAR RATIO			
	100 ft/sec			150 ft/sec
	10^{o}	20^{o}	75^{o}	10^{o}
1. HC250 Iron				
a) Fully hardened (600 BHN)	1.00	1.00	1.00	1.00
b) Semi annealed (450 BHN)	2.02	1.81	1.57	2.11
c) Fully annealed (350 BHN)	2.51	2.45	1.83	2.32
2. 1603 Iron (650 BHN)	0.87	0.95	0.69	0.66
3. Eutectic 6715	0.39	0.59	0.46	0.36
4. Silicon Carbide	1.11	0.73	0.49	0.39
5. Boronized HC250	-	0.016	-	-

Figure 41 represents a graphical representation of the ranking. The vertical axis represents the wear ratios and the horizontal axis shows the ranking in the order of decreasing wear resistance to the right. Boronized HC250 was the most wear resistant, about 60 times better than HC250 (F.H.). It was tested only at 100 ft/sec and 20 degrees since it was not available during the other tests.

The results also indicate that 1503 is slightly more erosion resistant than HC250 (F.H.) and the erosion resistance of fully hardened HC250 decreases rapidly with annealing.

In the 100 ft/sec and 20 degrees test series, the baseline material HC250 (F.H.) was tested after each material to check the consistency of the tests and determine the rate of degradation of the slurry, if any. It was tested five time all together, and the results were very consistent; the maximum erosion depths obtained in sequence were: 0.032", 0.030", 0.031", 0.030" and 0.033".

The weight loss of the materials was also recorded. Although the wear ratios obtained from the volume loss were different, the ranking of the materials remained the same.

The results in Table 5 indicate that the wear is higher at larger impingement angle for the same velocity. This was expected since these are all brittle materials. Also, the wear is higher at higher velocity. The velocity exponents at 10 degrees were calculated as follows:

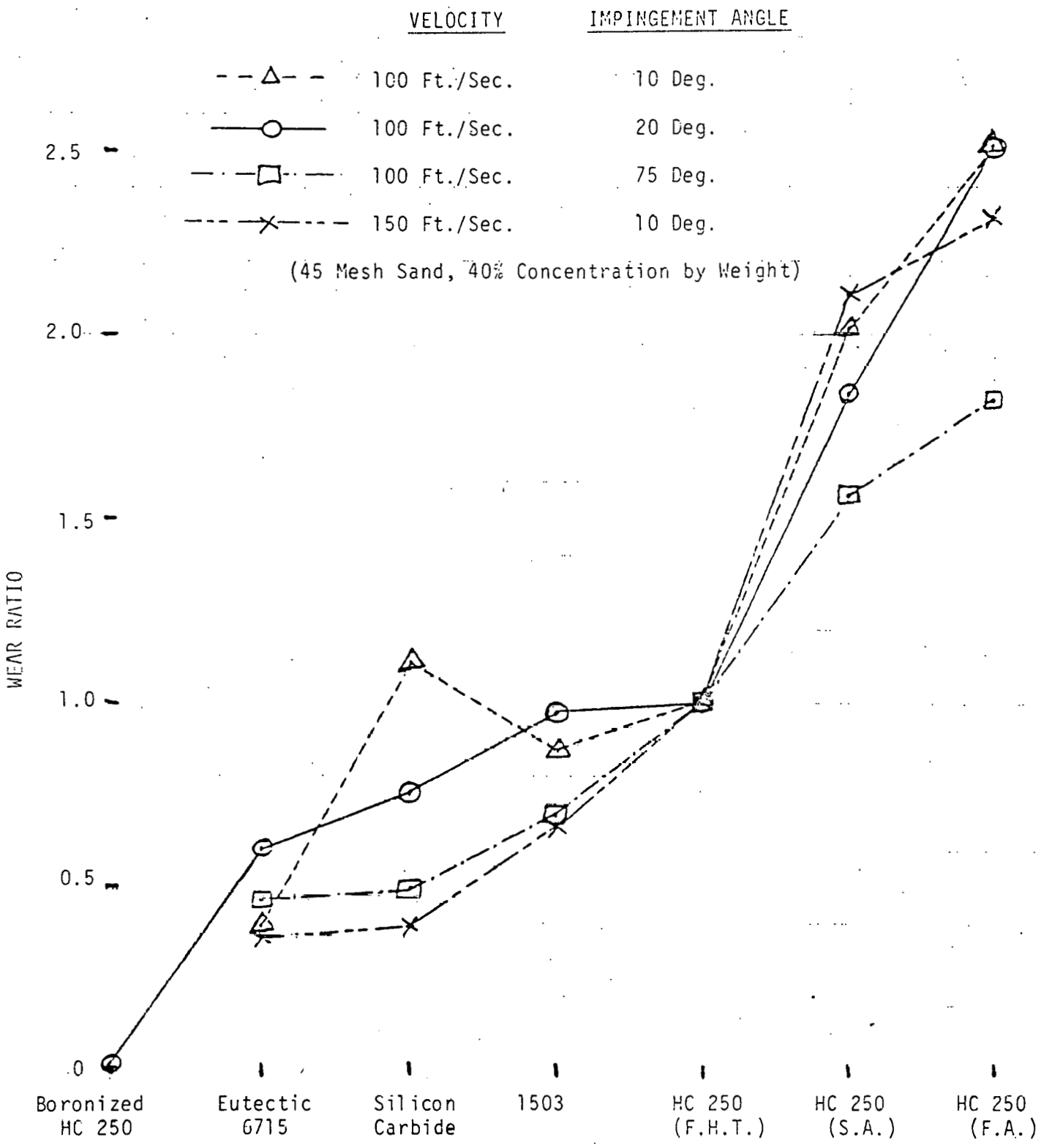

Figure 41: Results of Sand-Water Jet-Impingement Tests

Materials	Velocity Exponent
HC250 (F.H.)	2.15
HC250 (S.A.)	2.25
HC250 (F.A.)	1.95
Eutectic 6715	1.95
1503	1.47
SiC	Could not be calculated since wear at 100 ft/sec and 10 degrees is too high.

3.3.5 CORROSION TESTS

The corrosion tests were performed by immersing the preweighed material specimens in the hot solvent/slurry inside a 1000 ml flask for 40 to 50 hours. Following exposure, the specimens were cleaned and reweighed, and then corrosion rates were calculated on the basis of weight change. The test conditions are as follows:

Materials	- HC 250, 1503 and Carbon Steel (ASTM A366)
Temperature	- 500 degrees F., 550 degrees F. and 625 degrees F.
Time	- 40 to 50 hours
Medium	- T-102 bottoms and V-131B process solvent from Wilsonville
Analysis of Medium	- T-102 bottoms - 1.15 S & 337 ppm cl V-131B solvent - 8 ppm cl

These tests are basically static in nature, although there is some boiling action inside the flask at the test temperatures. Other candidate materials were not tested because it was found very early in this test series that the corrosivity of the solvent/slurry was extremely low.

Results and Discussions

The tests results are listed in Table 6. These results show that both HC250 and 1503 have very low corrosion rates, less than 1 mil per year. Carbon steel, however, showed a maximum corrosion rate of

TABLE 6

ORNL CORROSION TEST RESULTS

		Corrosion Rates (mpy)		
		HC250	1503	C-Steel
T-102 Bottoms	550°F.	< 1	< 1	2
	570°F.	-	-	5
	625°F.	< 1	-	5
V-131B Solvent	500°F.	< 1	-	< 1
	550°F.	< 1	-	< 1

about 5 mils per year only. Previous results from in-plant coupon studies as well as ORNL laboratory studies showed higher corrosion rates for carbon steel in both the media but not significantly different for alloys with 12% or more chromium.

Since the corrosion rate of HC250 and 1503 in synfuel slurry is insignificant, most of the wear of the coal-oil slurry pumps is probably due to erosion alone.

3.3.6 VISCOUS SAND-WATER NOZZLE TESTS

The purpose of this test is to simulate the hot synfuel slurry, in terms of viscosity and particles size, and run erosion tests at room temperature for materials evaluation. This slurry consists of viscous water and 40 wt. pct. sand of 100 mesh average particle size. The viscosity of water was increased by adding 2 wt. pct. of sodium carboxy methyl cellulose (Hercules SCMC-9M31) in the water.

In hot coal-oil nozzle tests (Section 3.3.7) SiC consistently showed no wear, whereas it ranked third in sand-water nozzle tests. This indicates that the viscosity and/or particle size may have effect on erosion properties of materials and, therefore, their ranking. In addition, since ORNL tests showed that the corrosive wear of high chrome alloys and ceramics is insignificant, it was decided to use viscous sand-water slurry to simulate only the erosive properties of synfuel slurry for nozzle testing. The test conditions were:

Jet Velocity	-	100 ft/sec
Impingement Angle	-	20 degrees
Viscosity of the carrier water	-	60 cp at 1130 sec^{-} shear rate.
Test duration	-	8 minutes

The results of viscosity measurements are presented in Appendix C.

Results and Discussion

The wear patterns obtained with this slurry were significantly different from those obtained with the sand-water slurry, as shown in Figure 42. The wear depths were also less with this slurry. the test results, shown in Table 7, indicate that there was no measureable wear in boronized HC250. A repeat test of this material also showed no measurable wear. The materials ranking obtained in this series of tests was slightly different from that obtained with the sand-water slurry. The two rankings obtained at 100 ft/sec and 20 degrees angle are compared in Table 8. Boronzied HC250 was the best material in both cases, and it was far superior to the rest of the candidate materials. Silicon carbide appeared better in the viscous slurry and also HC250 (F.H.) showed better wear resistance than 1503 in this slurry. The annealing reduces the wear resistance of HC250 more significantly in the viscous slurry. Fully annealed HC250 wears about 3.7 times faster than fully hardened HC250 in this slurry. The wear ratios, as shown inside the parenthesis, were quite different in these two slurries. Therefore, viscosity and/or particle size has at least some effect on the wear behavior of the materials.

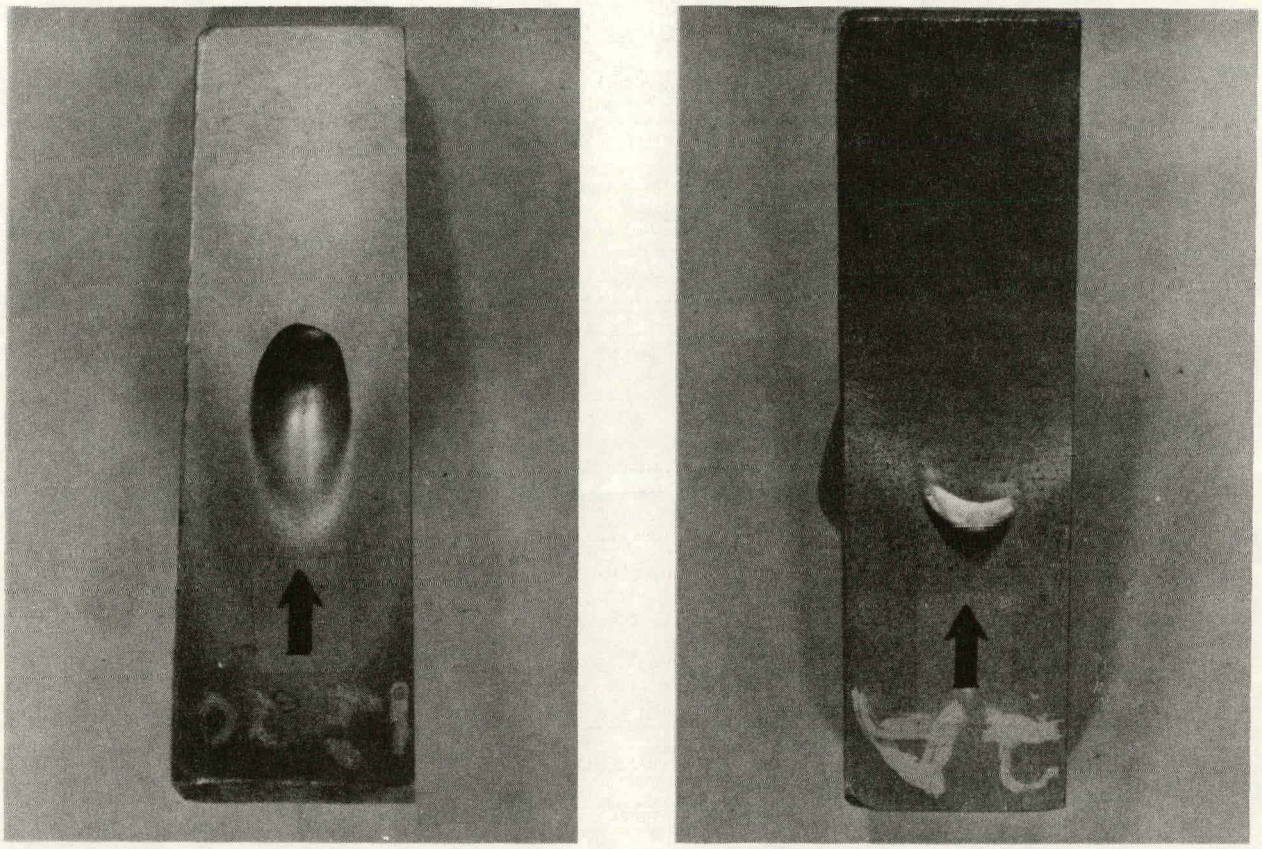

(a) Sand-water Test Specimen

(b) Viscous Sand-water Test Specimen

Note: Arrows indicate the direction of the jet

Figure 42: Wear Patterns Obtained in the IR Nozzle Tests

TABLE 7

VISCOUS SAND-WATER NOZZLE TEST RESULTS

MATERIAL	MAX. WEAR DEPTH(In.)	WEAR RATIO
1) HC250		
a) Fully Hardened	0.009	1.00
b) Semi Annealed	0.021	2.33
c) Fully annealed	0.024	2.67
2) 1503	0.013	1.44
3) Eutectic 6715	0.008	0.89
4) Silicon Carbide	0.006	0.67
5) Boronized HC250	0	0

TABLE 8

COMPARISON OF MATERIALS RANKING

Ranking With Sand-Water		Ranking With Viscous Sand-Water	
1) Boronized HC250	(.016)	1) Boronized HC250	(0)
2) Eutectic 6715	(.59)	2) SiC	(.67)
3) SiC	(.73)	3) Eutectic 6715	(.89)
4) 1503	(.95)	4) HC250 (F.H.)	(1.00)
5) HC250 (F.H.)	(1.00)	5) 1503	(1.44)
6) HC250 (S.A.)	(1.81)	6) HC250 (S.A.)	(2.33)
7) HC250 (F.A.)	(2.45)	7) HC250 (F.A.)	(3.67)

- Numbers inside the parentheses indicate wear ratios
- 100 ft/sec and 20^{o}

3.3.7 HOT COAL-OIL NOZZLE TESTS

The purpose of these tests is to establish the ranking of the candidate materials by nozzle tests, using hot synfuel slurry. This will determine the erosion-corrosion properties of the candidate slurry pump materials.

The slurry used in these tests was prepared from T-102 bottoms (solid at room temperature) obtained from the Wilsonville pilot plant. The T-102 bottoms contained about 10 wt. pct. solid which consists of ash, unreacted coal etc. The solid T-102 was first reduced to -14 mesh size in a jaw crusher and a rolling mill and then mixed with 50 wt. pct. anthracene to improve flow characteristics in the nozzle tester. The slurry mixture was agitated in a rolling drum for 48 hours to insure dissolution of the organic constituents in the anthracene. The undissolved ash particles were minus 325 mesh size.

Another set of nozzle tests, using hot solvent (V-1067) and coal slurry, was originally planned, but was not completed since the test results for T-102 slurry were not consistent.

The T-102 slurry test conditions were:

Slurry Temperature	: 500 degrees F
Slurry Velocity	: 100 ft/sec & 150 ft/sec
Impingement Angle	: 20 degrees
Test Duration	: 2 hours
Nominal Solid Content	: 5 wt. pct.
Particle Size	: minus 325 mesh

Capacity of Tester : 2 gallons

The slurry was essentially recycled during testing. About 15 volume percent of the slurry (0.3 gallons) was replaced by fresh slurry after each of the 2-hour test to compensate for the degradation of the slurry. The erosion wear of the specimens was determined by measuring the maximum (d max.) and average (d avg.) depths of the craters generated on the specimen surfaces. These crater depths were measured from surface-profilometer (Talysurf) traces taken through the deepest point of the crater along a direction perpendicular to the slurry jet direction. Figure 43 shows a typical trace on the fully hardened HC250. The sensitivity of the profilometer is 1 X 10^{-6} inches, but the accuracy in the crater depth measurement is usually limited by the roughness and curvature of the reference.

Results and Discussion

The results of the hot slurry nozzle tests are given in Table 9. The test numbers indicate the sequence in which tests were run for each velocity. The following conclusions were made:

1. Silicon carbide showed extremely high wear resistance. The wear was virtually zero. This result is not unexpected since SiC, particularly the sintered grades, is one of the more wear resistant materials among ceramics. Sand-water nozzle tests (at IR), however, did not show SiC to be extremely wear resistant. The differences in the results of the two tests are probably

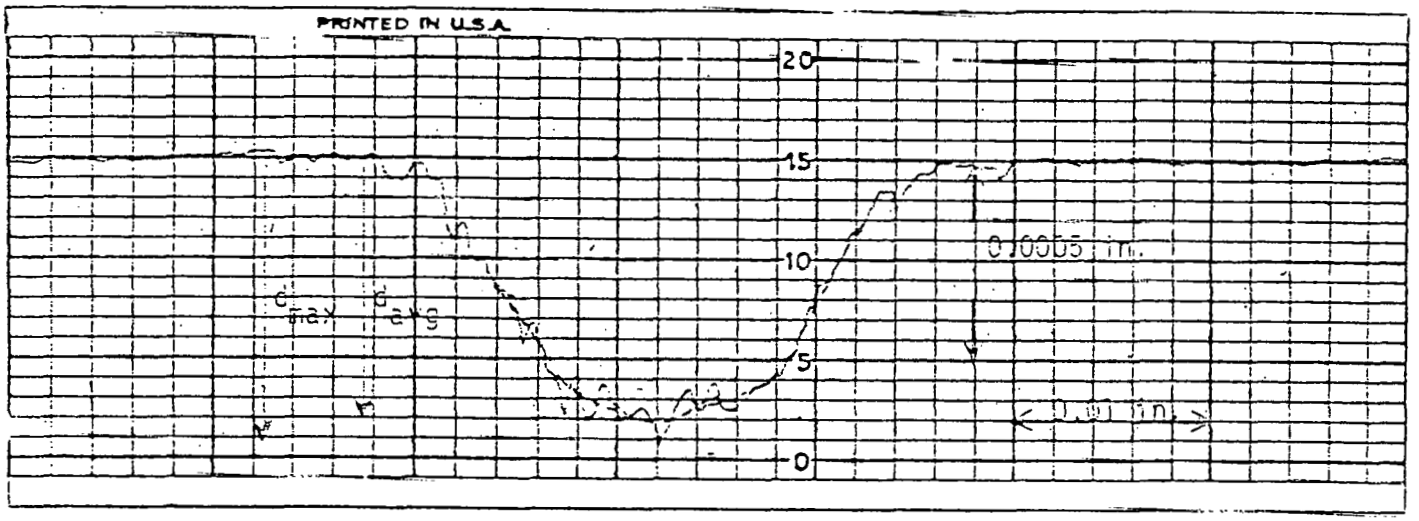

Figure 43: Profilometer Trace Through The Deepest Point of the Crater On A Fully Hardened HC 250 Specimen. (Test #1 at 100 ft/sec)

TABLE 9

HOT COAL-OIL TEST RESULTS

20^{o}, 550^{o}F., 2 hrs. & 50% T-102

Test Material	V = 100 ft/sec. d max 10^{-3}in.	V = 100 ft/sec. d avg. 10^{-3}in.	V = 150 ft/sec. d max 10^{-3}in.	V = 150 ft/sec. d avg. 10^{-3}in.
*1) HC250 (F.H.)	0.71(0.10**)	0.65(0.10**)	0.30	0.17
2) HC250 (S.A.)	0.50	0.38	0.23	0.21
3) 1503	0.50	0.37	0.70	0.50
*4) HC250 (F.H.)	-	-	0.18	0.06
5) Entectic 6715	0.07	.05	0.20	0.17
6) Sic	No Measureable Wear----------			
*7) HC250 (F.H.)	0.15	0.10	0.65(0.25**)	0.54(0.20**)
*8) HC250 (F.H.)	0.14	0.10	- -	- -
9) Boronized HC250	0.20	-	- 0.20	0.18

*Baseline tests
**Numbers inside parenthesis indicate repeat test data

related to the differences in the severity of the erosion conditions. Sand-water tests employed larger and higher density sand particles in both high viscosity and low viscosity medium. In sand-water tests, an increase in viscosity and decrease in sand particle size reduced the wear depth of SiC significantly. The smaller particle size and lower particle density in the hot slurry testing may have reduced the wear of SiC to an almost negligible level. Therefore, one can conclude that as the severity of the impact conditions is reduced, or the kinetic energy of the impacting particles is reduced, the wear of the SiC is also reduced. It is probably related to the transition in wear mechanisms due to various impact conditions. Brittle ceramic materials often erode at very low rates under conditions of deformation wear, i.e., cutting, ploughing, or flaking. But, because of their low fracture toughness, they can erode by a severe brittle chipping mechanism when the impact conditions are severe.

2. In general, d avg. values are slightly smaller than d max. and the material rankings obtained using these two values are identical. Therefore, only d max. values are used to calculate wear ratios (W.R.) and establish material ranking. Table 10 shows the calculated wear ratios using HC250 (F.H.) as the baseline. It also shows ranking of the materials in decreasing order of wear resistance for 100 ft/sec and 150 ft/sec velocity. A comparison of

TABLE 10

BATTELLE RANKINGS AND WEAR RATIOS

Ranking at 100 ft/sec				Ranking at 150 ft/sec			
1)	Silicon Carbide		(0)	1)	Silicon Carbide		(0)
2	Eutectic	6715	(0.54)	2)	Eutectic	6715	(0.83)
					Boronized	HC250	(0.83)
3)	HC250	(F.H.)	(1.00)	3)	HC250	(S.A.)	(0.96)
4)	Boronized	HC250	(1.54)	4)	HC250	(F.H.)	(1.00)
5)	1503		(3.85)	5)	1503		(2.92)
	HC250	(S.A.)	(3.85)				

Numbers inside the parentheses indicate wear ratios

the wear ratios at two velocities shows that the rankings are different at these two velocities. The HC250 (S.A.) is the worst material (5th best) at 100 ft/sec with the W.R. of 3.85, whereas it is the 3rd best material at 150 ft/sec with the W.R. of 0.96. In sand-water nozzle tests, HC250 (S.A.) consistently ranked 6th (Table 11). It is disturbing to note that semi-annealed HC250 with a hardness of 450 BHN performed better or equal compared to the fully hardened HC250, with a hardness of 600 BHN. This is contrary both to the general understanding of the erosion process and the test results reported in the literature. Further, the pilot plant experience indicated that annealing of HC250 reduces erosion resistance. Another disturbing observation in the hot coal-oil slurry test is that the boronized HC250 is the 4th best material at 100 ft/sec with a W.R. of 1.54, whereas it is the 2nd best at 150 ft/sec with a wear ratio of 0.83. Contrary to this, in sand-water nozzle tests, boronized HC250 showed very high wear-resistance, particularly in the viscous sand-water test, where the wear was almost zero (Table 11). Boronized coating is known to have very high erosion resistance. It is not clear why the boronized HC 250 with a surface hardness of 1800 Knopp will wear 50 pct faster than the uncoated HC250 with a hardness of 600 BHN at 100 ft/sec velocity.

Due to these discrepancies, Battelle decided to re-evaluate the three types of HC250 (boronized,

TABLE 11

COMPARISON OF IR AND BATTELLE RANKINGS
AT 100 FT/SEC. AND 20

IR RANKING (With Viscous Slurry)		Battelle Ranking	
1. Boronized HC250	(0)	1. Silicon Carbide	(0)
2. Silicon Carbide	(.67)	2. Eutectic 6715	(0.54)
3. Eutectic 6715	(.89)	3. HC250 (F.H.)	(1.00)
4. HC250 (F.H.)	(1.00)	4. Boronized HC250	(1.54)
5. 1503	(1.44)	5. 1503	(3.85)
6. HC250 (S.A.)	(2.33)	6. 1503	(3.85)
7. HC250 (F.A.)	(2.67)		

Numbers inside the parentheses indicate wear ratios

fully hardened and semi-annealed) as part of their on-going screening tests for evaluation of the slurry let-down valve materials. The test slurry, test conditions and wear depths obtained are summarized in Table 12. The only major difference in the test conditions is the higher jet velocity (330 ft/sec). Therefore, the wear depths were higher. The ranking of the three materials was very different from the ranking for 100 ft/sec, but very similar to the ranking for 150 ft/sec. Boronized HC250 showed the highest wear resistance with a W.R. of 0.35. However, semi-annealed material showed significantly better wear resistance (W.R. = 0.62) than fully hardened HC250. It is not clear why a material when annealed to a 150 BHN lower hardness will become 40% more wear resistant. But, it is interesting to note that the semi-annealed HC250 material became progressively better than fully hardened HC250 as the jet velocity was increased as shown below:

Velocity (ft/sec)	Wear Ratio
100	3.85
150	0.96
330	0.62

This was not the case in sand-water tests, where the wear ratios were very similar, as shown below:

Velocity (ft/sec)	Wear Ratio
100	2.02

TABLE 12

EVALUATION OF HC250 MATERIALS IN THE BATTELLE SCREENING TESTS

Slurry	SRC + 75 Wt. Pct. Anthracene
Temperature	550°F.
Impingement Angle	20°
Jet Velocity	330 ft/sec.
Test Duration	1 hour

Material	d max (10^{-3} in.)	Wear Ratio
Boronized HC250	22.6	0.35
HC250 (S.A.)	40.0	0.62
HC250 (F.H.)	64.6	1.00

3. The test results appear to have large scatter. The baseline material HC250 (F.H.) was tested four times at each velocity as checkpoints to determine the consistency of the tests and/or degradation of the slurry.

   The maximum wear depths obtained in the order of testing are:

   100 ft/sec - 0.71", 0.15", 0.14" & 0.10"
   150 ft/sec - 0.30", 0.18", 0.65",& 0.25"

   Two results, 0.71" depth for 100 ft/sec and 0.65" depth for 150 ft/sec, were rejected since it was suspected that the slurry flow was not consistent during these two tests. Still, the scatter is large, as calculated below:

   100 ft/sec-50% between the max. and min. depths
   150 ft/sec-67% between the max. and min. depths

4. The wear and velocity relationships were calculated and the velocity exponents are:

Material	Velocity Exponents
HC250 (F.H.)	1.51
HC250 (S.A.)	Negative
Boronized HC250	0
Silicon Carbide	Not Applicable
Eutectic 6715	2.60
1503	0.83

It is surprising to note that the HC250 (S.A.) produced a negative exponent; boronized HC250 produced 0 exponent and 1503 produced an exponent less than one.

In an effort to explain these discrepancies it was decided to measure viscosity and solid fraction on three slurry samples, taken during the course of the tests. Unfortunately, no definite answer was found, since both viscosity and solid concentrations were found not to change significantly during the tests.

The viscosity of the test slurry was measured in a Brookefield rotating spindle viscometer. A shear rate of four per second was used (Spindle #4 at 100 rpm) and the tests were run at temperatures close to 550 degrees F. The viscosity did not change very much during the test as shown below:

Slurry Sample	Temp. Degrees F	Mean Viscosity (Centi-poise)
Initial Fresh Slurry	534	48.8
Slurry After Test #7 (100 ft/sec)	543	40.8
Slurry After Test "15 (100 ft/sec)	511	40.0

The solid concentrations in the test slurry were determined by a Soxhlet extraction technique using pyridine as the solvent. There was a small variation in the solid concentration during the test as shown below:

Slurry Sample	Wt. Pct. Insolubles
Initial Fresh Slurry	5.35
Slurry After Test #7 (100 ft/sec)	3.99
Slurry After Test #15 (100 ft/sec)	4.54

The Wilsonville plant data showed that the wt. pct. of the insolubles in the T-102 bottoms sample was only 10. Therefore, a 50% dilution would produce about 5% solid concentration as obtained in this analysis. In the SRC process, the insolubles in the T-102 bottoms normally vary from 10 to 25%.

3.3.8 NEW ALLOY DEVELOPMENT

The objective of the new alloy work is to develop a new pump alloy that is more erosion resistant than fully hardened HC250 for synfuel slurry application. This work is being carried out in the IR experimental casting lab, using a 75 KW-50 pound melting furnace.

The IR laboratory casting facility consists of a high frequency 75 KW, 3000 HZ solid state induction melting power supply with a 50 pound hand-tilt type furnace and MgO crucible (see Figures 44 and 45). An electric winch with a remote control is used to tilt the furnace for pouring.

Test blocks of 4" x 4" x 1.5" dimensions are being cast for the experimental alloys. Sand molding with a no-bake binder system is used for casting test blocks. The sand mix consists of:

Sand	-	Foundry grade of 45 AFS number
Binder	-	Linocure AW (1.5 wt. pct. of sand)
Catalyst	-	Linocure C (20 wt. pct. of Linocure AW)

The sand, binder and catalyst are mixed in a 30 pound capacity Sampson Lab Muller for about 10 minutes before making the mold. The mold cure time was established at about one hour.

High purity 0.08 pct. carbon steel punchings are used for the furnace charge and the alloying ingredients are added in the form of either pure metal or ferroalloys after melt-down of the base charge.

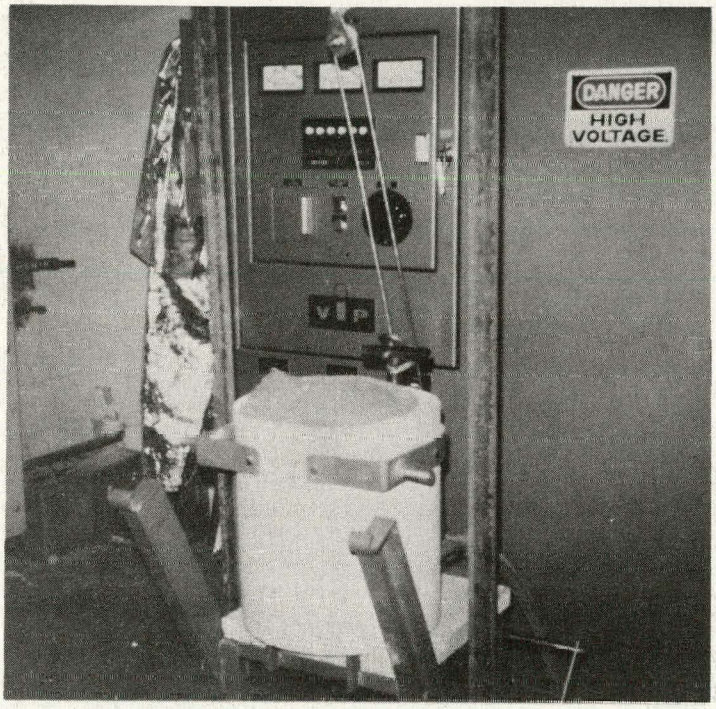

Figure 44: Casting Laboratory Showing Power Supply and Furnace

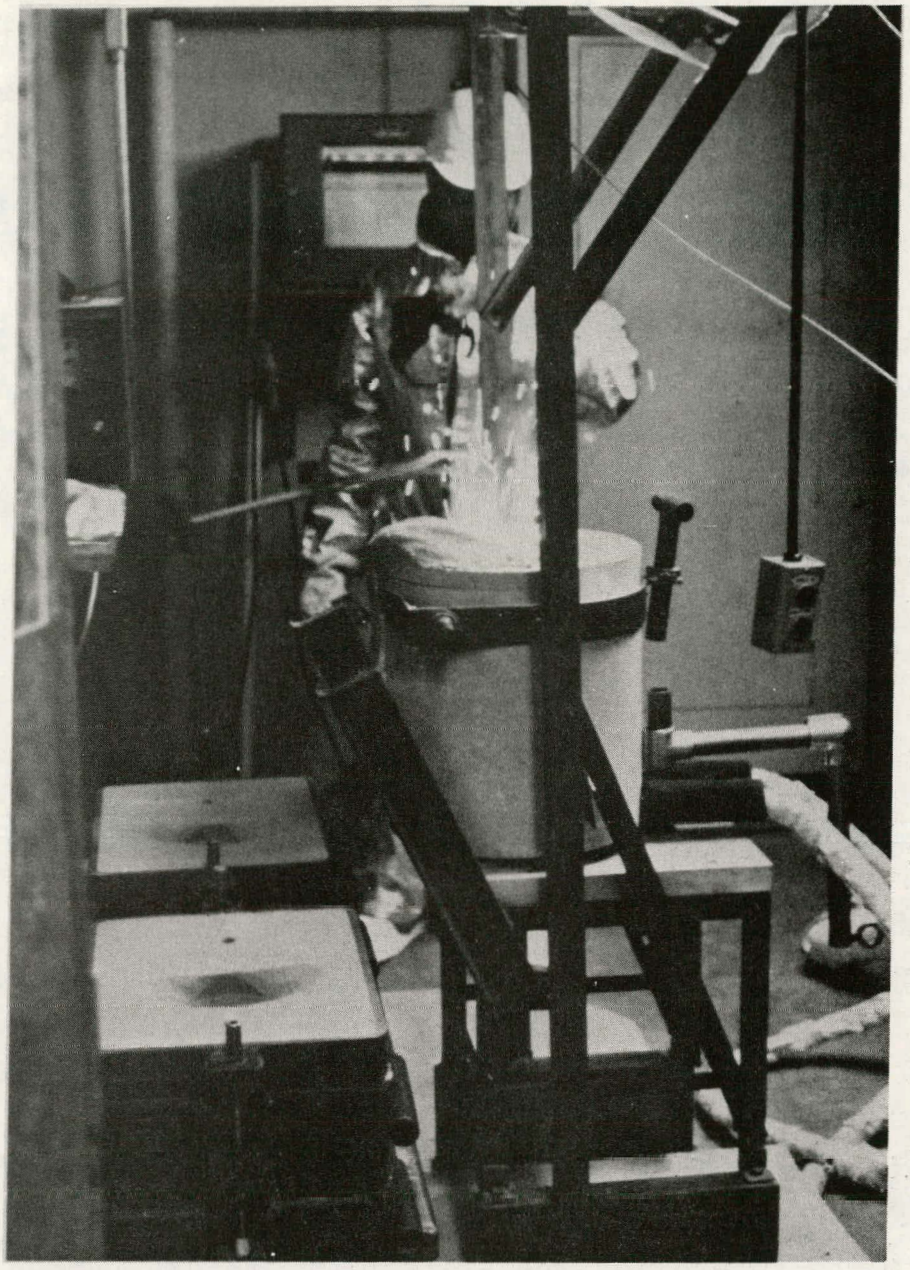

Figure 45: Casting Laboratory Showing Molds and Furnace

Graphite is added to increase the carbon level. After all the alloying additions are made, metal temperature is recorded and freeze point is determined. Pouring is done at about 200 degrees F superheat and spectro analysis samples are taken just before pouring.

Chemical analysis, microstructural analysis and hardness study are done for each casting. The nozzle testing is done only when the above analyses are satisfactory.

Two basic approaches were taken:

1) Higher chrome (>30 pct.) iron
2) High phos-high chrome iron

In HC250, the chrome level is 26 to 28 percent and the microstructure contains massive primary carbides in a matrix of fine secondary carbides and martensite with or without some austenite. The approach would be to increase the amount of primary carbides by about 10 vol. pct. (from 35 vol. pct. to 45 vol. pct.) by increasing the chrome level. However, a higher chrome level tends to stabilize a ferritic matrix which is inferior to a martensitic matrix, with regard to erosion resistance. Therefore, other alloying additions would have to be made to form a martensitic matrix.

For high phos-high chrome iron, preliminary attempts were made to form massive chromium carbides in a predominately steadite matrix. Steadite consists of iron phosfide, iron carbide and pearlite and/or

ferrite. Iron phosfide and iron carbide matrix is expected to make the alloy highly erosion resistant. The presence of chrome will also provide corrosion resistance to the alloy. Two formulations were cast and analyzed.

3.3.9 DISCUSSION AND MATERIALS SELECTION FOR PILOT SCALE PUMP

A comparison of materials ranking obtained with sand-water, viscous sand-water and coal-oil slurries (at 100 ft/sec) is shown in Table 13. For sand-water tests there is a direct correlation between the hardness of the materials and their erosion resistance, as shown below in the order of decreasing wear resistance (the hardness of SiC could not be determined due to its porous structure):

Material	Hardness
1) Boronized HC250	1800 Knoop
2) Eutectic 6715	750 BHN
3) SiC	Could not be determined
4) 1503	650 BHN
5) HC250 (F.H.)	600 BHN
6) HC250 (S.A.)	450 BHN
7) HC250 (F.A.)	350 BHN

A quantitative correlation between the hardness and wear resistance, however, could not be established. Viscous sand-water test results also show the same correlation with the only exception of 1503 which is 50 BHN harder, but shows a poorer wear resistance than HC250 (F.H.). The hot coal-oil results, however, do not show any such correlation.

In any slurry erosion test, the erosion rate does not remain constant; the rate decreases in the beginning and then tends to stabilize after a period of time. This "saturation effect" is important when a very

TABLE 13

COMPARISON OF RANKING OF MATERIALS

IR Sand-Water	IR Viscous Sand-Water	Battelle T-102 (100 Ft/Sec)
1) Boronized HC250	1) Boronized HC250	1) SiC
2) Eutectic 6715	2) SiC	2) Eutectic 6715
3) SiC	3) Eutectic 6715	3) HC250 (F.H.)
4) 1503	4) HC250 (F.H.)	4) Boronized HC250
5) HC250 (F.H.)	5) 1503	5) 1503
		HC250 (S.A.)
6) HC250 (S.A.)	6) HC250 (S.A.)	
7) HC250 (F.A.)	7) HC250 (F.A.)	

small material thickness is removed from the specimen during the test. In the hot coal-oil test, the thickness removed was very small, considerably smaller than in sand-water tests. It is not known how much effect this "initial erosion rate" had on the "overall erosion rate", Since the erosion depth was not determined as a function of time.

The selection of material(s) for the prototype pilot scale pump was made on the basis of sand-water tests. Both sand-water and viscous sand-water tests showed the same three best materials-boronized HC250, Eutectic 6715 and SiC. Thermal shock resistance is a primary consideration for the structural materials for synfuel slurry pumps. Impact resistance or toughness is also an important consideration. Both these properties are very poor in SiC and have not been determined. Therefore, only boronized HC250 and Eutectic 6715 have been selected for the test pump. HC250 will be used as the structural alloy since it has been used in the pilot plants, and it is one of the best pump alloys for water-base slurry services. Furthermore, it is also corrosion resistant due to its high chrome level. HC 250 will be used in the fully hardened conditions and it is recommended that the thermal shock resistance of HC250 be examined in three different heat treated conditions -- fully hardened, semi-annealed and fully annealed. In these tests, the maximum heating and cooling rate of HC250 in these three conditions should be established. Although semi-annealed and fully annealed HC250 will not be evaluated in the test pump, the life of these pumps can be estimated from the life of the fully hardened test pump by using their relative wear

ratios established in the nozzle tests.

The weld deposition of Eutectic 6715 on HC 250 requires an intermediate layer of carbon steel weld deposition to reduce cracking of the weld deposit. In the Wilsonville plant, this type of weld deposition has been successfully made in HC250 pumps. Eutectic 6715 will be used only in the volute cut water area to a thickness of about 0.050".

Surface boronizing is a diffusion-type coating and it can be applied uniformly over the entire surface of near-finished pump components. It is not a line-of-sight process. Surface boronizing of the test specimens was done by a proprietary process developed by Materials Development Corporation at Medford, Massachusetts. Their experiments revealed that the maximum diffused case thickness on a HC250 substrate was of the order of 0.0015" beyond which the coating tends to develop cracks. Further experiments should be done to study if a deeper diffused case can be achieved by using lower chrome alloys such as 1503 or Ni-Hard iron. All the wet parts of the test pump will be surfaced boronized to a 0.0015" depth.

3.4 PROTOTYPE PUMP TEST FACILITY

The pilot scale prototype pump test facility shown in Figure 46 is designed to evaluate pumps on sand-water slurry with flows up to 300 GPM and heads up to 300 feet. Two pumps can be tested in series simultaneously to directly compare performance and wear characteristics for differrent designs or materials. Centrifugal as well as other types of pumps can readily be tested in this facility. The installed test pump motor is rated for 200 hp and 3550 rpm. This motor is used to drive two centrifugal pumps using belt drives. A photograph of the test bedframe is shown in Figure 47. The loop is designed to handle slurry concentrations up to 40% by weight. It is also possible to test at higher viscosities through the use of additive such as sodium carboxi methyl cellulose (SMCM), which increases the viscosity of water. Victaulic pipe connections are used throughout the slurry piping to minimize slurry erosion of the pipe connections and fittings, and facilitate rapid replacement of worn sections of the loop. The slurry pipe lines are 3 inch schedule 80 and were designed for proper slurry velocity to avoid settling. A majority of the tests are planned with 100 mesh foundry grade sand. The sand particles breakdown during testing, so periodic replacement of the slurry is necessary to maintain relatively uniform test conditions. Slurry concentration will also be monitored periodically and adjusted as required. The slurry concentration will decrease slowly as pump seal water leaks into the system. Clean water from the cyclone overflow is periodically bled from the loop to maintain proper slurry concentration. The cooling system rejects heat to the atmosphere with a design capcity of 135 hp

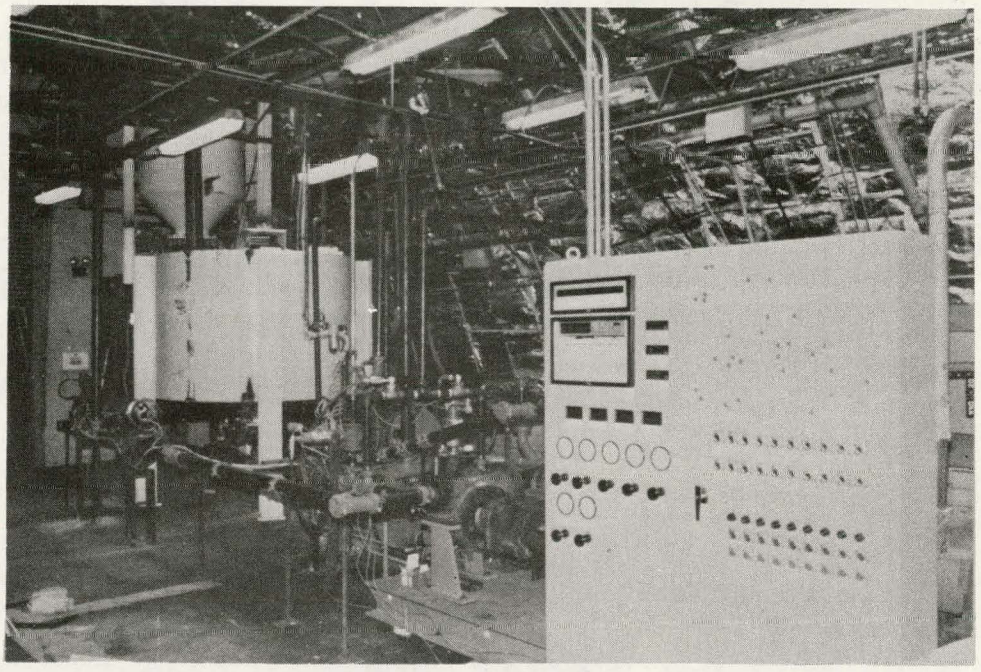

Figure 46: Prototype Pump Test Facility

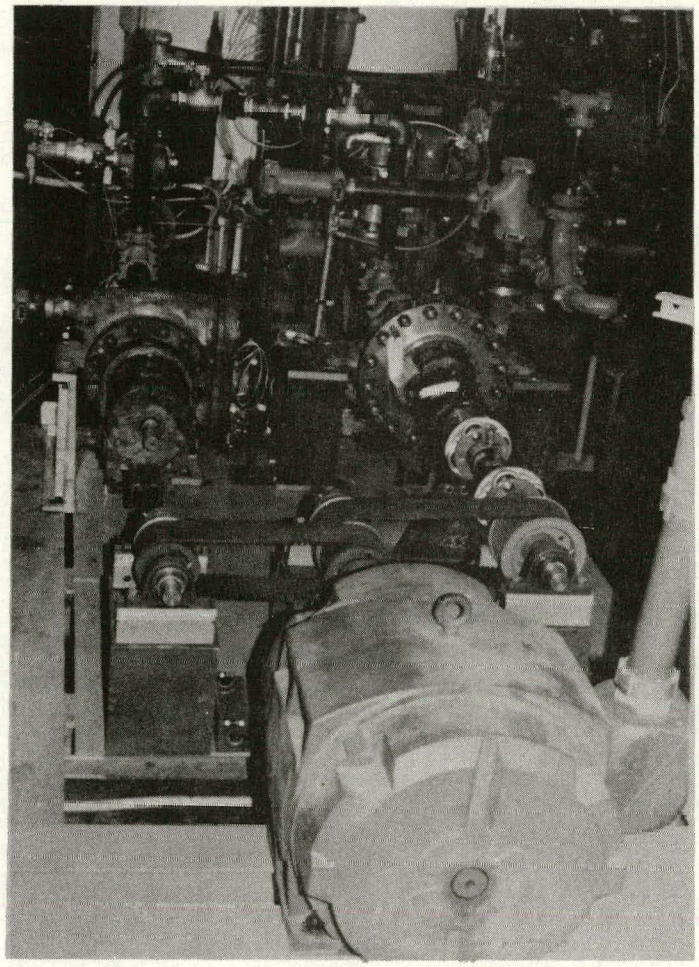

Figure 47: Pump Test BED Frame

assuming a 65 degree F. ambient temperature. All process parameters will be continuously monitored and recorded on a strip chart by a 30 channel programmable data logger. The data logger has an alarm/relay system that can automatically trigger a shutdown procedure if any parameter exceeds the value of the limits programmed into the logger. This allows the loop to be set up for 24 hour unattended operation. The test pumps will be monitored for inlet and discharge pressures, rpm and torque. Slurry temperature will also be monitored to insure proper operation of the cooling system.

SLURRY TEST SYSTEM

A schematic of the test system is shown in Figure 48. Each component in the loop will be referred to by its identification number. The detailed information on major equipment is presented in Appendix D. Details of the piping configuration are shown in Figures 49 and 50. The slurry mixing tank has a 1500 gallon brim-full capacity. The tank is 7 feet in diameter and has four 7-inch wide baffles spaced 90 degrees apart. The slurry tank as well as a general view of the piping is shown in Figure 51. An agitator, M3, is used to keep the slurry in suspension. The agitator is manufactured by Philadelphia Gear Corporation, who performed a laboratory simulation in order to determine the proper design. A 40 per cent sand/water slurry was evaluated in a scaled down tank that is geometrically similar to the one used in the loop. The slurry exits through the bottom of the mixing tank. A Clarkson KGA knife-gate valve, S1, is used for on/off flow control. All slurry valves are pneumatically actuated.

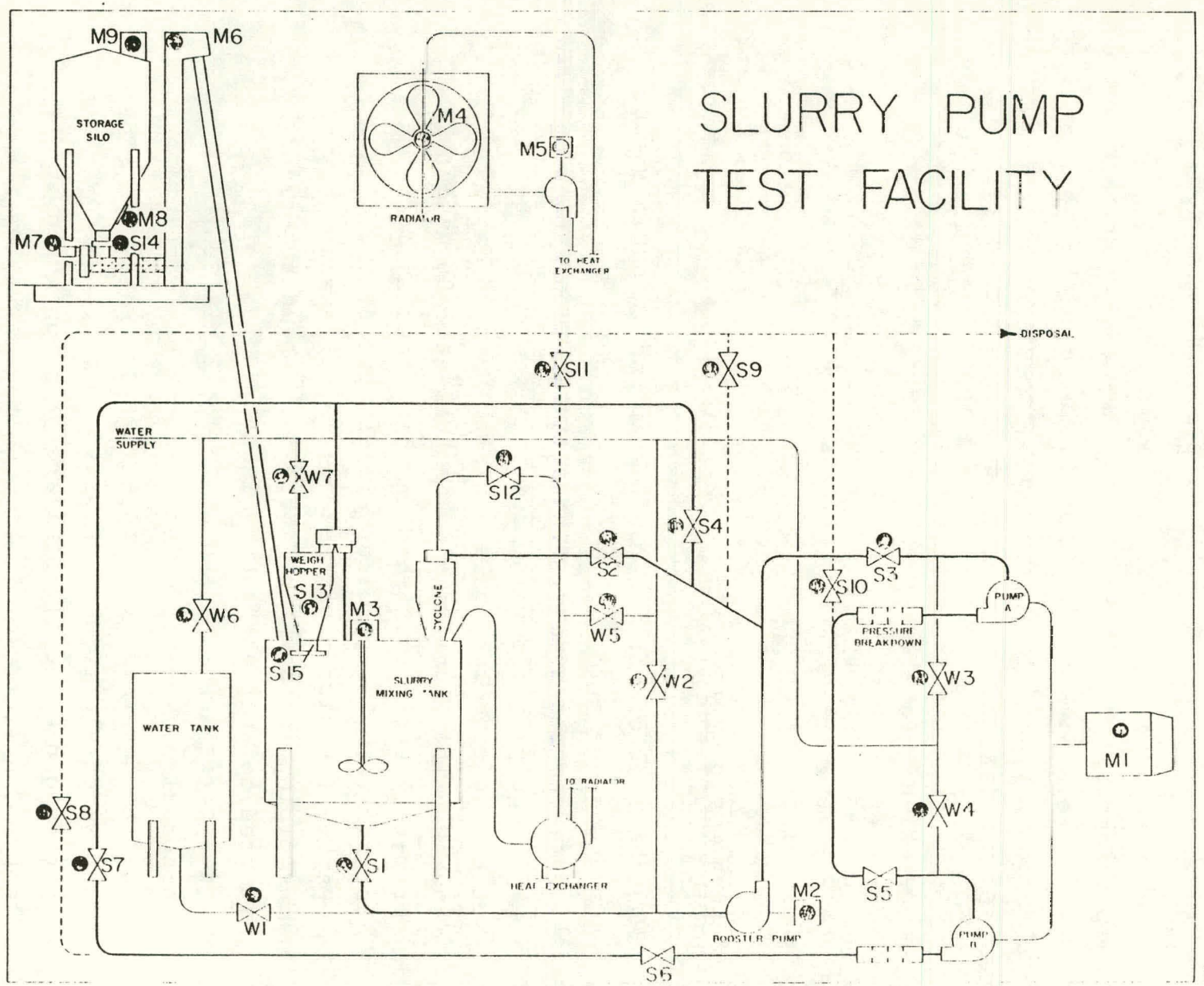

Figure 48: Test System Schematic

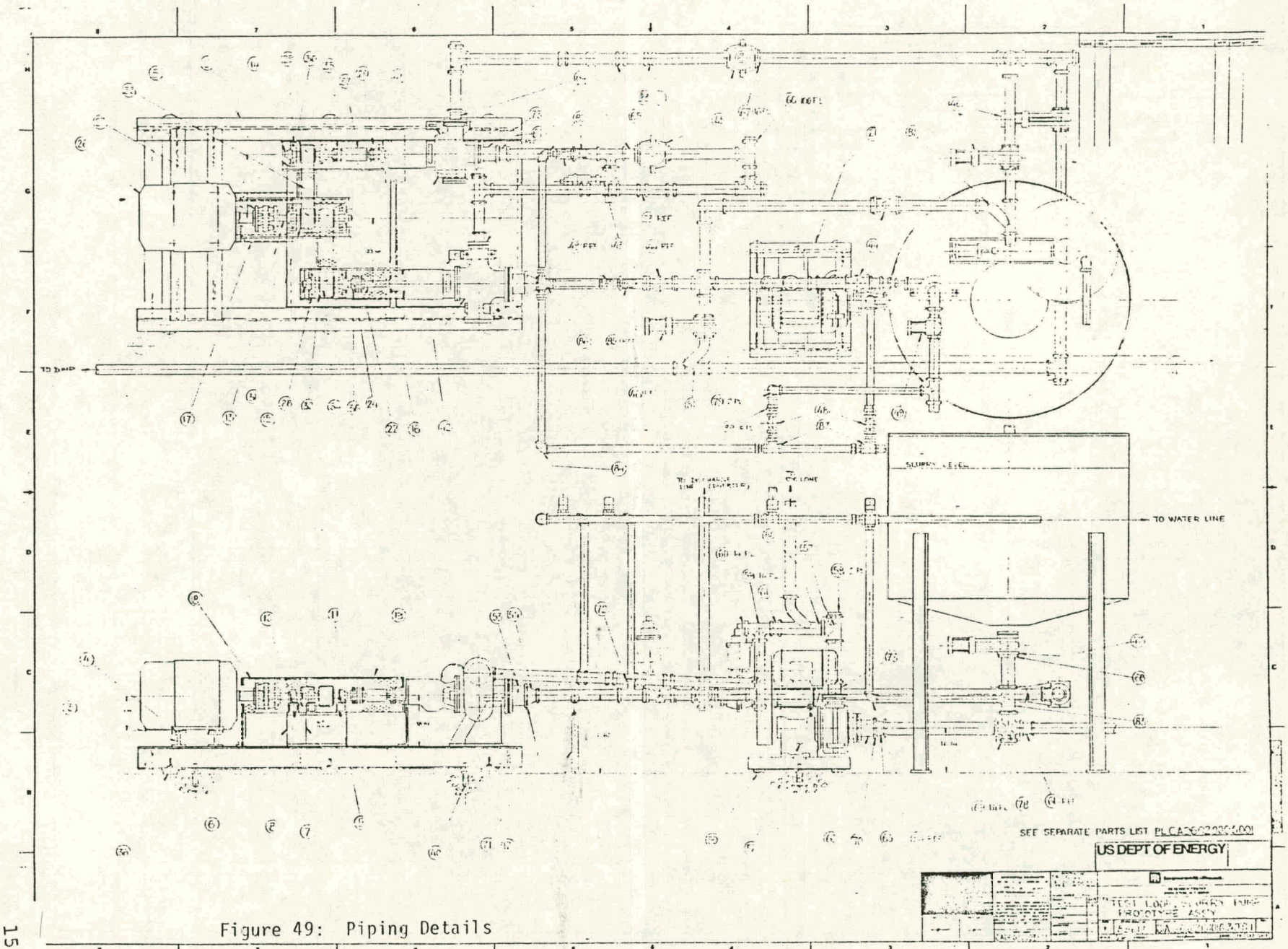

Figure 49: Piping Details

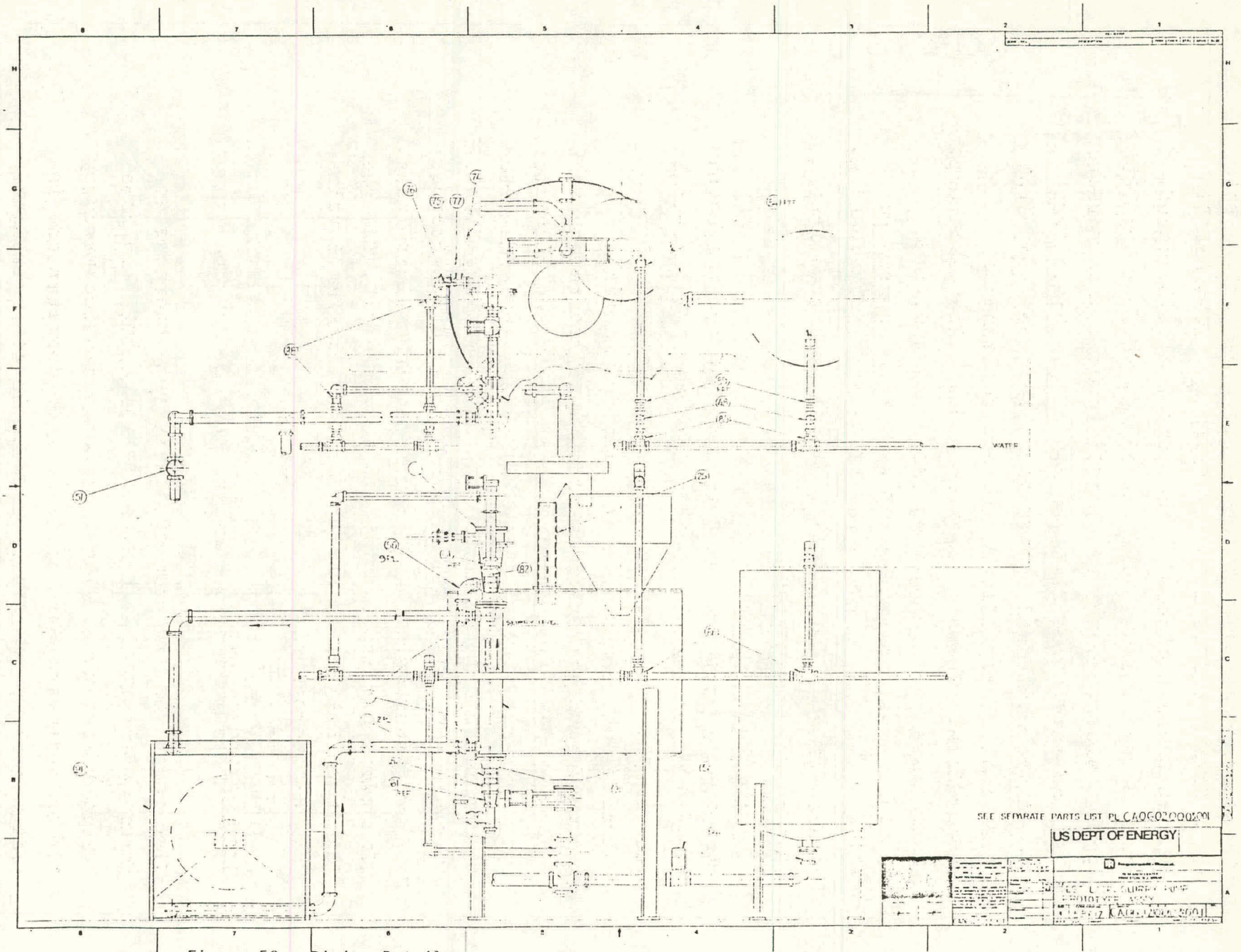

Figure 50: Piping Details

The slurry then goes to the booster pump, M2. this is a Warman rubber-lined slurry pump rated for 500 gpm at 80 feet of head. The pump is single speed, belt driven using a 30 hp motor. Approximately 300 gpm of slurry goes through a Clarkson B slurry valve, S3, and enters the test section of the loop. Two pumps are connected in series so that they pump the identical slurry allowing direct performance comparison. The head is broken down after each pump using fixed orifice plates, HBD1 and HBD2, and Clarkson C slurry valves, S5 and S6, are used for final trim adjustment. The fixed orifice plates are solid tungsten carbide drill bushings fitted into carbon steel housings.

The slurry exits the test section and returns to the slurry mixing tank through a Clarkson KGA knife-gate valve, S7. A diverter valve is located above the slurry tank. This valve is also pneumatically actuated and either allows the slurry to return to the tank directly, or diverts it to the weigh hopper, T3. The weigh hopper measures the weight of a given slurry volume to determine the sand concentration. A DeZurick butterfly valve on the botom of the hopper allows the sample to be returned to the slurry tank. In order to dump slurry to the outside pit, T4, the Clarkson KGA valve, S8, and/or the Clarkson B valve, S9, can be opened.

HEAT REJECTION SYSTEM

The additional 200 gpm of slurry from the booster pump goes through a Clarkson B valve, S2, and to a cyclone separator. The cyclone is manufacturred by Krebs Engineers. It has a 10 inch diameter and is rated for 200 gpm slurry feed up to 40% by weight.

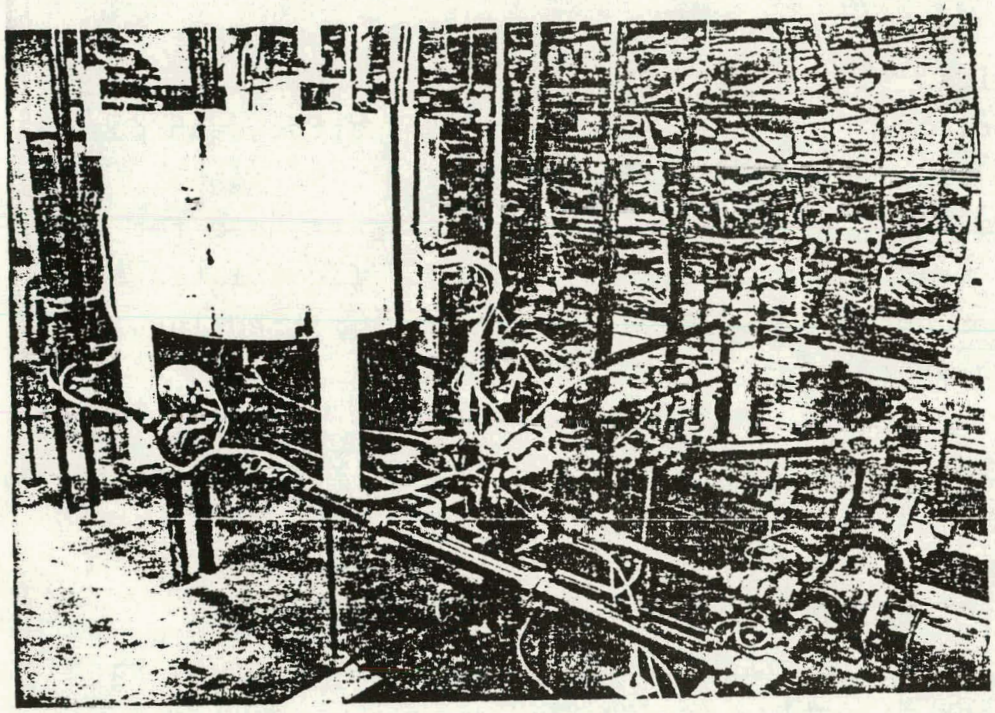

Figure 51: General View Of Slurry Tank and Piping

The predicted overflow is 120 gpm with 100% recovery down to 150 mesh. The cyclone requires a 20-25 psi pressure drop for proper operation.

The overflow is sent through a heat exchanger to be cooled and is then returned to the slurry mixing tank. The heat exchanger selected is an Alfa-Laval spiral heat exchanger. This equipment is capable of handling solids without plugging and features thick-walled construction to extend life. While shell and tube exchangers were considered, it was felt that they were prone to plugging during transient or upset conditions when appreciable solids are in the over-flow of the cyclone. Shell and tube exchangers are also harder to clean out. The cold side of the exchanger is connected to a closed 50% ethylene glycol loop. The ethylene glycol is cooled in an O&H Manufacturing vertical cooler. The cooler is a fan-driven radiator with direct drive motor. The fluid is circulated in this closed loop by an I-R 3x3x5 SMP centrifugal pump rated for 220 gpm at 45 feet ahead. A globe valve, W8, is used to throttle this pump to design conditions. The ethylene glycol temperature ranges from 90-94 degrees F. and the slurry temperature ranges from 125-130 degrees F. The cooling system is designed for a heat rejection capacity of 135 hp.

WATER INJECTION SYSTEM

Whenever slurry operation is suspended, water will be used to immediately flush the system to prevent sand settling and plugging of components. A 900 gallon reservoir, T2, is the reserve water supply that feeds the booster pump during this operation. Also, additional water can be supplied through electric

solenoid operated water valves, W2, W3, W4 and W6. when an emergency shutdown occurs, the slurry tank valve, S1, is closed and the water reservoir valve, W1, is opened. Also, return lines to the slurry tank are closed and all dump lines are opened. After approximately two minutes of flushing, the entire system will be shut down.

SOLID HANDLING SYSTEM

Solid (sand) is stored on site in a 25 ton storage silo located aside of the test facility building. The silo, 8 feet in diameter and 20 feet high, is shown in Figure 52 along with the bucket elevator, screw conveyor and radiator. It is equipped with a level indicator, dust collector, OSHA safety ladder, ground level fill connection, pneumatic operated rotary gate valve and skirted bottom. The silo is filled by a blower delivery truck.

A Kelly-Duplex screw conveyor and bucket elevator feed sand to the weigh hopper through a feed duct that goes through the roof of the test facility building. This equipment is rated for 10 ton per hour feeding capacity. By adding sand through the weigh hopper, the sand is first weighed so an accurate amount can be added to properly adjust slurry concentration.

CONTROL PANEL

A central control panel is used for complete operation of the test loop. A photograph of the panel is shown in Figure 53. The control panel allows manual remote operation of 20 valves and 9 motors. An operational schematic is included on the

Figure 52: Sand Handling System

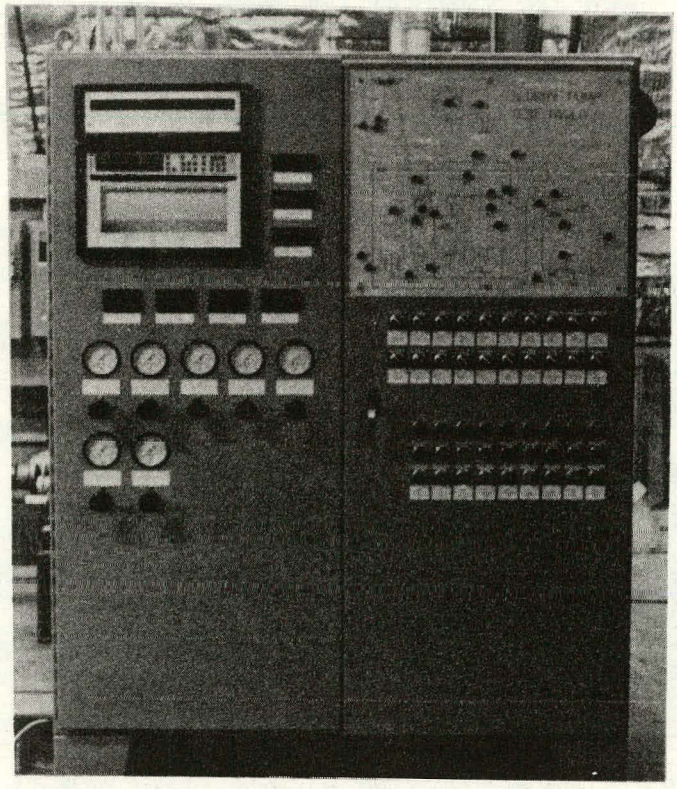

Figure 53: Central Control Panel

panel. This schematic, shown previously in Figure 48, uses lights to indicate if a motor is running and if a valve is open. The control panel also houses pump rpm, torque and pressure digital indicators as well as slurry valve throttle controls, weigh hopper and silo level indicators and a 30 channel data logger/ alarm.

APPENDICES

APPENDIX A

REFERENCES

1. Want, F.M. : "Centrifugal Slurry Pump Wear - Plant Experienced". Hydrotransport 7, BHRA, November 1980, Paper H1, pp. 301-314.

2. Wilson, G. : "The Design Aspects of Centrifugal Pumps for Abrasive Slurries". Hydrotransport 2, BHRA, September 1972, Paper H2, pp. H2-25 to H2-52.

3. Vocadlo, J.J., Koo, J.K., and Prang, A.J., : "Performance of Centrifugal Pumps in Slurry Service". Hydrotransport 3, BHRA, May 1974, Paper J2, pp. J2-17 - J2-32.

4. Tuzson, J.J. : "Laboratory Slurry Erosion Tests and Pump Wear Rate Calculations". Particulate Laden Flows in Turbomachinery, ASME, 1982, pp. 49 - 52.

5. Zarzycki, M. : "Influence of the Pump Material on Service Life of the Impellers of Rotordynamic Pumps in Transport of Mechanically Impure Fluids". Proc. 3rd Conf. on Fluid Mechanics and Fluid Machinery, Budapest (1969).

6. Bak, E. : "Construction Materials and Testing Results of the Wear of Pumps for Transporting Solids Media". BHRA, 12, (1966).

7. Wiedenroth, W. : "The influence of Sand and Gravel on the Characteristics of Centrifugal Pumps". Proc. 1st Conf. on the Hydraulic Transport of Solids in Pipes, E1, pp. 1 (1970).

8. Herbich, J.B. : "Modifications in Design Improve Dredge Pump Efficiency". Lehigh University, Fritz Engineering Laboratory, Project Report No. 36 (1962).

9. Welte, A. : "Wear Phenomena in Dredging Pumps". Translation by Lehigh University, Fritz Engineering Laboratory, Laboratory Report No. 310.17 (1966).

10. Vasiliev, V. : "On Evaluation of Wear of Centrifugal Pump Parts in Hydroabrasive Mixtures". Proc. 1st Conf. on the Hydraulic Transport of Solids in Pipes (1970).

11. Bergeron, P. and Dollfus, J. : "The Influence of the Nature of the Pumped Mixture and Hydraulic Characteristics on the Design and Installation of Liquid/Solid Mixture Pumps". Proc. 5th Conf. on Hydraulics, 2, pp. 597 (1958).

12. Ernst, R.: "Centrifugal Dredging Pumps". Proc. World Dredging Conf., pp. 305 (1967).

13. Warman, C.H. : "The Pumping of Abrasive Slurries". Proc. 1st Pumping Exhibition and Conf., London (1965).

14. Warring, R.H. : "Solids Handling Pumps". Pumps, 34, pp. 305 (1969).

15. Wong, G.S., et al: "Coal Slurry Feed Pump for Coal Liquefaction". Electric Power Research Institute AF-853, Project 775-1, Final Report, September 1978.

16. Schlicting, H. : Boundary Layer Theory . 4th Ed., McGraw-Hill, 1960, p. 16.

17. Truscott, G.F. : "A Literature Ssurvey on Abrasive Wear in Hydraulic Machinery". Wear , Vol. 20, pp. 29-50.

18. Faddick, R. : Pouska, G. ; Connery, J ; L. DiNapoli ; and Punis, G. : Ultrasonic Velocity Meter. In Hydrotransport 6 . Sixth International Conference on the Hydraulic Transport of Solids in Pipes, Paper B4. BHRA Fluid Engineering, Cranfield, Bedford, England, September 1979.

19. Stepanoff, A.J. : Centrifugal and Axial Flow Pumps , John Wiley and Sons, Inc., New York, 1957.

20. Murakami, M. ; Kikuyama, k. ; and Asakura, E.; "Velocity and Pressure Distribution in the Impeller Passages of Centrifugal Pumps". Trans. ASME, Journal of Fluids Engineering , Vol. December 1980, pp. 420-426.

APPENDIX B

SMALL SCALE TESTING (SST) DETAILS

- Test Summary
- Discussion of Results
- Test Reports

BUILD ID	DESIGN AREA OF INTEREST	SLURRY	DESCRIPTION
3001			3001 - SST 3 Mk I Hardware - All Original Design
3002 vs. 5003	Impeller Blading	25% Sand/Water	3002 - SST 3 Mk I - All Original - No Mods III 5003 - SST 5 Mk I - All Original - No Mods
5004	Collector Configuration	25% Sand/Water	5004 - SST 5 Mk I Impeller; Volute with Concave Cutwater Trim on L.E. I
3005		2% + 1% Mixture SCMC + WATER 1/3 .10 - .27 C_w Sand	3005 - SST 3 Mk I Hardware; No Mods
5006 vs. 5007	Collector Configuration Impeller Leakage Path Pump-out Vanes	25% Sand/Water	5006 - SST 5 Mk II Impeller with Radial P/O Vanes with Directed Leakage Lip II Straight Cutwater L.E. I 5007 - SST 5 Mk II Impeller - No P/O Vanes with Directed Leakage Lip V Concave Cutwater L.E.
3006 vs. 3009	Impeller Leakage Path Impeller Blading Collector Configuration	25% Sand/Water	3006 - SST 3 Mk II 5 Vane No PO Vanes, Cutback C_w with Directed Leakage III II 3009 - SST 3 Mk II 4 Vane No PO Vanes, Concave C_w L.E. III Radial Leakage Path
5010 vs. 3011	Impeller Leakage Path Impeller Blading	25% Sand/Water ½% SCMC	5010 - SST 5 Mk II Impeller Directed Leakage Path with Concave C_w III 3011 - SST 3 Mk II 5 Vane Impeller, Directed Leakage with Concave C_w II
3012 vs. 3013	Collector Configuration Impeller Leakage Path Impeller Blading Impeller O.D. Shroud	25% Sand/Water +½% SCMC	3012 - SST 3 Mk II 5 Vane with Square Edge on Impeller Shroud, Concentric Collector with Oval Throat Diffuser, Axial Leakage Direction III II 3013 - SST 3 Mk II 4 Vane Concave C_w L.E. on Mk II Volute I 39^0 From Radial Leakage Path IV

SST TEST SUMMARY

APPENDIX B

DISCUSSION OF WEAR RESULTS

The experimental investigation has provided many insights into slurry pump wear. Some of the wear can be attributed to peculiarities in the MKI design; however, much of the observable wear is typical slurry pump-type wear, which has been seen in the field. The following discussion will explain why wear took place at each location. When wear is associated with one particular design, discussion of the differences between hardware is presented.

1) Stationary and Impeller Front Ring Wear - Figure B1

The test experience shows that front clearance increases about .010" to .015" per every two hours of testing (starting clearance is .020"). Of that amount, only 1 to 2 mils is worn away from the impeller side of the ring -- the remainder comes from the stationary ring. The relative motion of the flow (and particles) with the stationary and rotating surface provides the answer. The tangential component of the main front leakage flow tends to follow half speed, solid body rotation; however, the flow adjacent to the impeller shroud is dragged along at blade speed.

Particles entering the clearance gap still have tangential velocity, and as these particles get "bumped" around in the gap and strike the adjacent walls, their relative velocity to the surface is higher for the stationary wall than for the impeller ring surface. The sliding velocities along the stationary wall are higher, and thus, the majority of metal removal takes place

there.

2) Suction Nozzle Erosion - Figure B1

The severe slurry erosion at the corner of the inlet suction nozzle is due to interaction of the high velocity leakage flow and the incoming fluid. When the leakage flow is injected radially into the main flow, toroidal vortices are created at the interfaces of the jet and main flow (the vortices have some tangential component due to the tangential nature of the leakage flow). The vortices trail off downstream (into the impeller) and upstream (actually into the boundary layer of the nozzle) causing the chewing evident in Figure B1.

3) Impeller I.D. Wear - Figure B2

The ripple-type wear observed on the impeller I.D. is the result of vortices formed as the leakage flow jets into the main flow and turns the corner at the impeller inlet. This vortical flow is mixed with the incoming axial flow and causes the axes of the vortices (as evidenced by the wear in the photograph) to become more axial thus causing the angle of attack shown on Figure B1. If the vortices had not been mixed, the wear pattern would have a more axial nature relative to the wheel indicating a large tangential component to the vortical flow.

4) Sidewall Thinning (SST3) - Figure B3

It was noticed after removal of the shroud from SST 3002 that the sidewall showed a depression due to metal removal about 2/3 of the way along the passage. Upon inspection of the impeller immediately following a test,

it was observed that sand had accumulated (tightly compacted) and adhered to the suction side of the blade in the same location as the sidewall thinning. This accumulation blocks the passage thus increasing the local relative velocity and thinning out of the wall boundary layer so that particles sliding against the wall carry almost the same velocity as the main flow field. The reasons for the sand accumulation involve separation of the main flow from the suction side of the passage and the movement of sand to the suction side of the blade in the separated zone. Apparently, the particles in the separated region respond to centrifugal force and are forced outward -- the Coriolis force being weaker in the separated region and therefore having less influence on the particles.

5) Groove Along Pressure Side of Blade (SST5) - Figure B4

As described earlier in this report, the Coriolis force is very powerful in determining the motion of particles inside the blades of an impeller. The wear in Photograph must have come from sliding wear of particles forced to the pressure surface due to Coriolis forces in an unseparated relative flow.

6) Ripple Wear, Suction Side of Blade (SST5) - Figure B5 and B6

Shown in these two photographs are the trailing edges, suction side, of two different impellers (SST3 and SST5) tested under identical conditions. The presence of ripple wear on the SST5 impeller and not on the SST3 is clear. The wear could be due to vortices formed when particles forced to the suction side of the blade inter-

act with the secondary flow from the endwalls, which meets at the suction side of the blade. The formed vortices have tangential and axial components and so their direction is neither perpendicular or parallel to the main flow. The secondary flow is quite well-behaved in the SST5 since the flow in the passage is not separated. In the SST3, the evidence of separation and local relative velocity increase tends to thin out boundary layers and reduce the action of secondary flow heading for the suction side of the blade. Without this strong secondary flow meeting and forming vortices on the suction side of the blades, no ripple-type wear can take place. Another theory for ripple wear is that standing transverse vortices develop in the boundary layer of an unseparated flow.

7) Ripple-Type Wear - Figure B7, B8, and B9

The ripple-type wear noticeable on both the SST3 and the SST5 on the sidewalls results from vortices forming from the interaction of secondary flow spiraling inward along the outer volute and sidewalls and flow being flung outward along the rotating impeller wall. This recirculatory-type motion (radially downward along the sidewall and radially outward along the rotating impeller wall) can cause particles to get caught up in vortices formed along the boundary of these two motions. The ripple-type wear is more noticeable on the rear or hub sidewall than on the front -- since leakage flow down the front wall influences the recirculatory flows going on in the space between impeller and wall. It should be noted that the formation of these vortices is influenced by viscosity of the carrier fluid. Figure B9 shows very little ripple-type wear on hardware run in 2%

mixture of SCMC, a viscotity additive.

8) Undercutting-Volute Base Circle (MKI) - Figure B7 & B8

From the photographs, notice the corner present at a radius equal to the cutwater radius. This edge suffered undercutting in all tests. The undercutting resulted from secondary flow moving inward with radial and tangential components. This flow separates as it goes over the corner and forms small vortices which sharpen and undercut around this circle. This edge is removed from all SST MKII designs.

9) Wear on Cutwater and Impeller Leading Edges- Figure B2 , B7 and B8

The wear on endwalls formed when flow is obstructed by a vane or cutwater perpendicular to the endwall is commonly known as a horseshoe vortex. It is really a complex interaction of the endwall boundary layer with the pressure distribution (caused by the main flow) around the leading edge of the surface.

The pressure distribution causes vortices to be created with two different directions of rotation. The vortex created by the high stagnation pressure at the nose actually removes material slightly upstream of the nose. This vortex is then swept around the vane by the main flow. The vortices (one on each side) caused by the low pressure (about 45 degrees from the nose) tend to groove parallel to the vane. The classic horseshoe vortex is evident in Figure B2. The photographs of cutwater wear show a deviation from the classic horseshoe vortex since the edge at the base circle of the volute complicates

the endwall flow.

It can also be seen that the main flow sharpens (and wears back) the leading edges. This is, of course, mostly sliding wear. Once sharpening begins, the character of the horseshoe vortex changes. The sharpening tends to lengthen the high pressure region along the vane leading edge causing the main flow to enter the endwall boundary layer and causing a vortex to be formed. This vortex is then carried downstream by the main flow. As sharpening occurs, the second mechanism of the horseshoe vortex formation becomes a smaller factor. The radiusing of the cutwater leading edge (parallel to the direction of flow) has proved successful in altering the pressure distribution around the nose of the cutwater and thus affecting the initiation of the horseshoe vortex. However, once sharpening occurs, it appears that a potential exists for interaction with endwall boundary layer and some vortex generation. Figure B10 and B11 show the effect of this change.

10) Blade Wear due to High Blade Loading - Figure B12

A noticeable difference in wear was observed between the SST 3 4 vane and 5 vane impellers. Figures 19a and 19d show the blade loading diagrams for these two designs. The information on the diagrams tend to indicate that the more severe deceleration of the relative velocity on the pressure side of the 4 vane probably leads to pressure side separation quite early in the passage. This separated flow transports solids outward and strikes the suction side of the blade at the trailing edge. The 5 vane does not suffer quite as severe a pressure side deceleration as the 4 vane impeller, and hence the

pressure side separation occurs farther on in the passage. The effect of this is to eliminate the collection of particles on the suction side of the blade (as in the 4 vane) and prevents the wear. The difference in blade trailing edge wear are quite noticable in Figure B12.

Further consideration may be given to pressure side separation by referring to Murakami (20).

11) Directed Leakage Lip and Impeller I.D. - Figure B13

The two MKII impeller shrouds and suction nozzles shown in Figure B13 represent wear with and without the directed leakage lip shown in Figure 28. The two units were run in a side by side comparison. It can be observed that 3008 still shows the remains of the lip which served to turn the leakage flow in a more axial direction. This direction of the leakage flow is important in the elimination of the interaction of the high energy leakage flow with the incoming main flow. It is this interaction which causes vortices which throw particles against the suction nozzle piece, as well as the impeller I.D. The configuration on the right shows the effect of no lip, severe wear on the stationary suction nozzle piece is obvious. The wearing away of the lip of SST 3008 shows that the abruptness of the turn results in a large loading of particles on the outside of the turn. These particles eventually wear away the direction lip.

12) Directed Leakage Paths - Figures B14 thru B17

Improvements over the leakage lip shows in SST 3008 are

shown in Figure 29, SST 3012 and 3013. SST 3012 attempts to turn the leakage flow to a more axial direction in a manner more gradual than SST 3008. Only wear as a result of the turn is evident in Figure B15 and impeller ID wear is evident in Figure B14. No ID suction nozzle wear was measured. Also, note the nonsymmetric spiral type groove on the injection land in Figure B15. This is believed to be a result of the non-symmetric peripheral pressure gradient around the OD of the impeller, due to the use of a concentric type collector. This pressure gradient causes non-uniform distribution of leakage flow in the close clearance zone.

Another approach to directed leakage is shown in Figures B16 and B17, SST 3013. Here the leakage flow makes an abrupt turn from a radial direction to a direction 30" from radial. Wear at the corner where this transition occurs is evident from Figure B16. No inlet suction nozzle wear on the nozzle ID was observed. Due to the sharp corner at the impeller ID on 3013, vortices were formed and the corner was severely chewed up. This chewing wear carried back into the blades also.

13) Concentric Collector

In order to move the cutwater to an extreme radius, so as to reduce throat velocities, a concentric type collector, with a cutwater radius to impeller radius ratio of 1.70 was tested. The sketch for this configuration is shown in Figure 26. The performance versus a MKII volute is shown in Figure B18. It is obvious that the volute collector has a higher efficiency, despite its being run with the hydraulically inferior SST 3 4 vane impeller. Testing the volute with a 5 vane impeller

would increase the efficiency superiority. Figures B19 and B20 show the concentric collector (SST 3012) after about 13 hours. Only slight wear can be observed. Also to be observed from Figure B20, is the concave shape to the wide angle cutwater which results from the intersection of the oval shaped diffuser throat with the collector diameter.

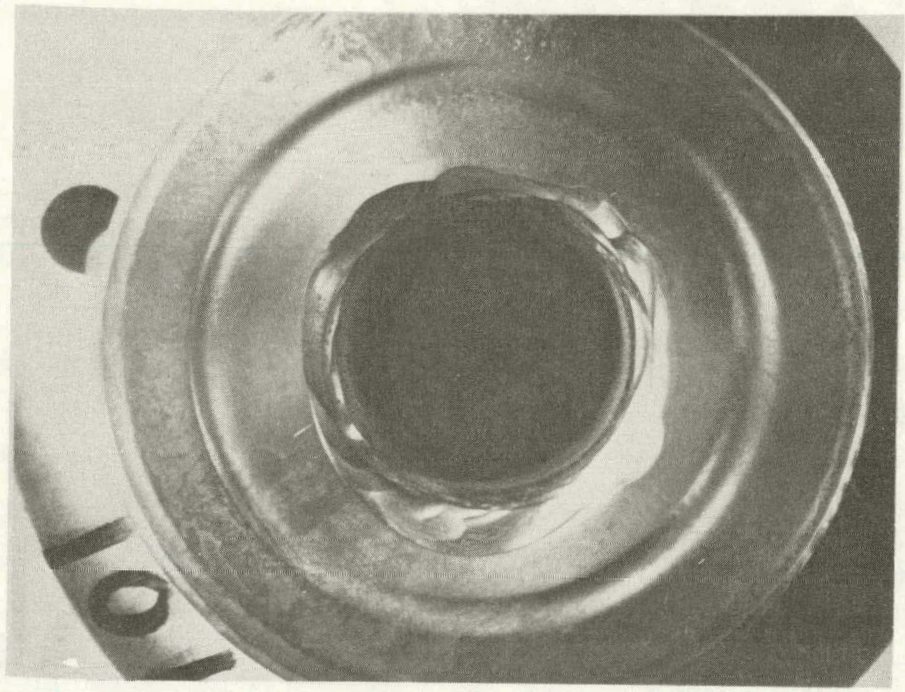

- INLET SUCTION NOZZLE, FLOW TOWARD THE VIEWER
- NOTE WEAR DUE TO LEAKAGE FLOW (PIECE WAS ORIGINALLY FLAT)
- WEAR OF CORNER DUE TO INTERACTION OF LEAKAGE FLOW WITH INCOMING MAIN FLOW

FIGURE B1: INLET SUCTION NOZZLE (SST 3002)

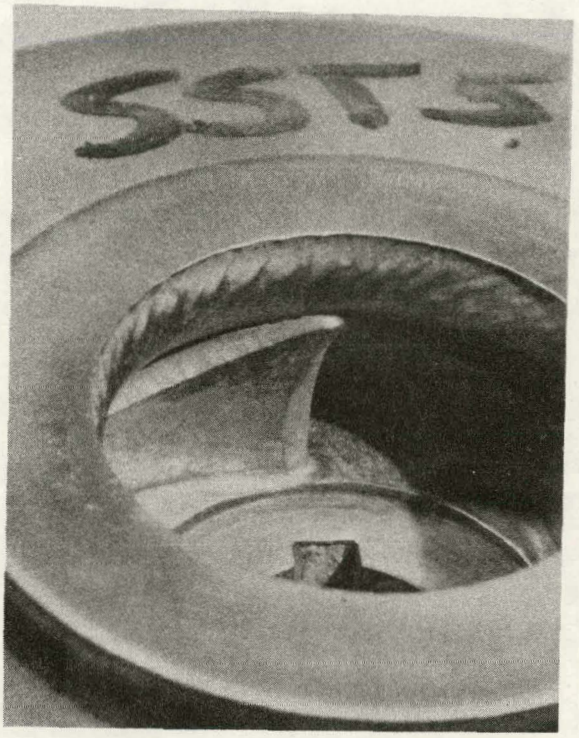

- SHARPENING OF BLADE L.E.
- HORSESHOE VORTEX FORMATION AT HUB
- BLADE WAS ORIGINALLY AXIAL; MORE WEARBACK OF THE BLADE NEAR THE HUB
- AXES OF VORTICES ALONG ID OF IMPELLER INLET IN THE DIRECTION OF THE RELATIVE FLOW

FIGURE B2: MK I IMPELLER ID (SST 5004)

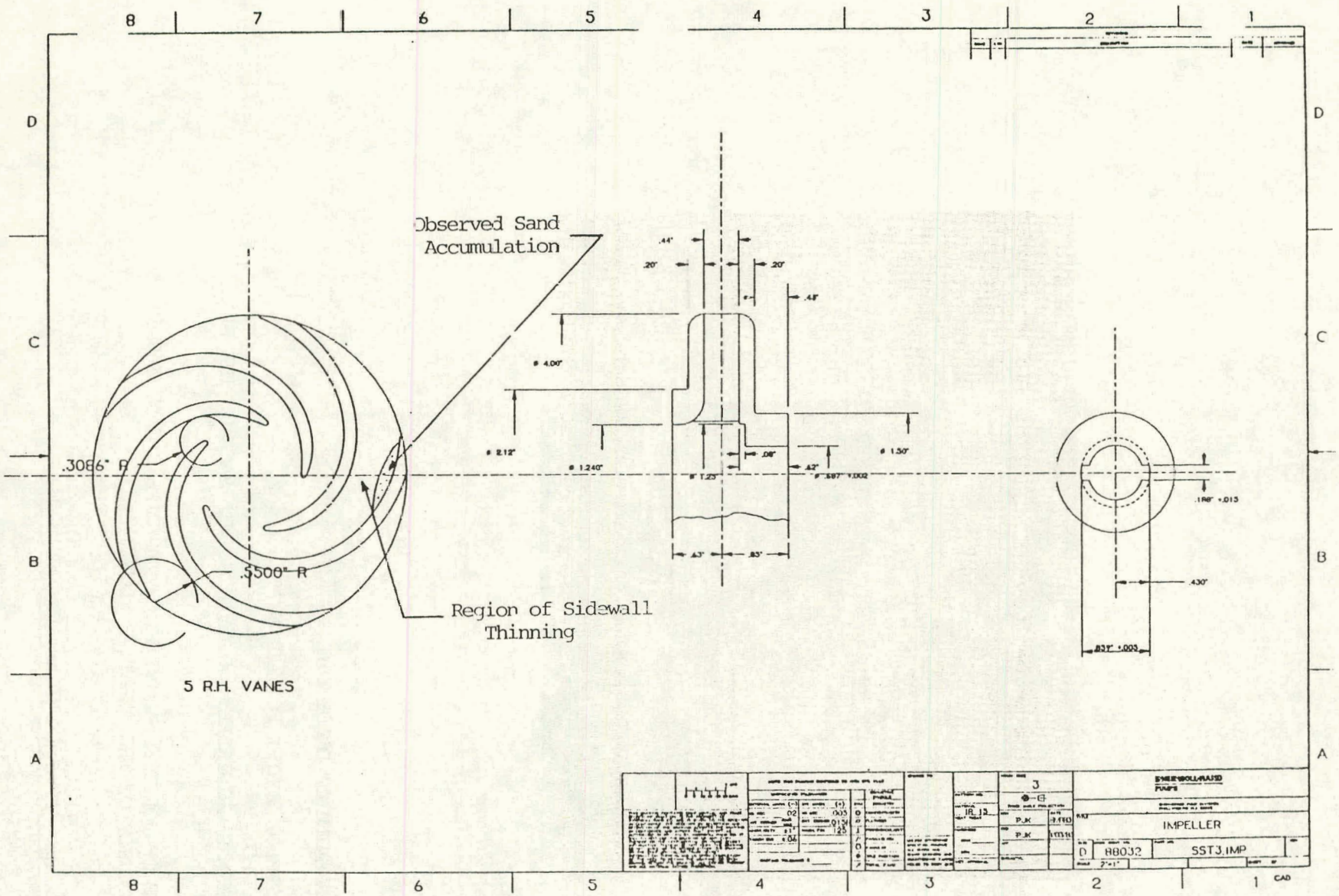

Figure B3: SST 3 Impeller with Sidewall Thinning

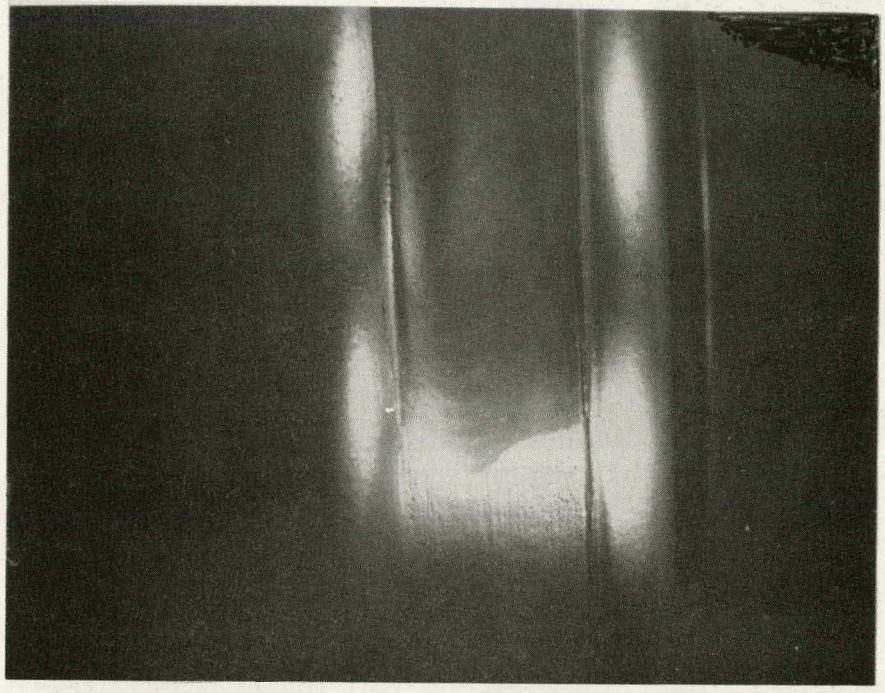

SST5 IMPELLER, PRESSURE SIDE BLADE

NOTE: GROOVING ALONG BLADE, ENDING AT IMPELLER OD. LAND.

FIGURE B4: SST5 IMPELLER (SST5004)

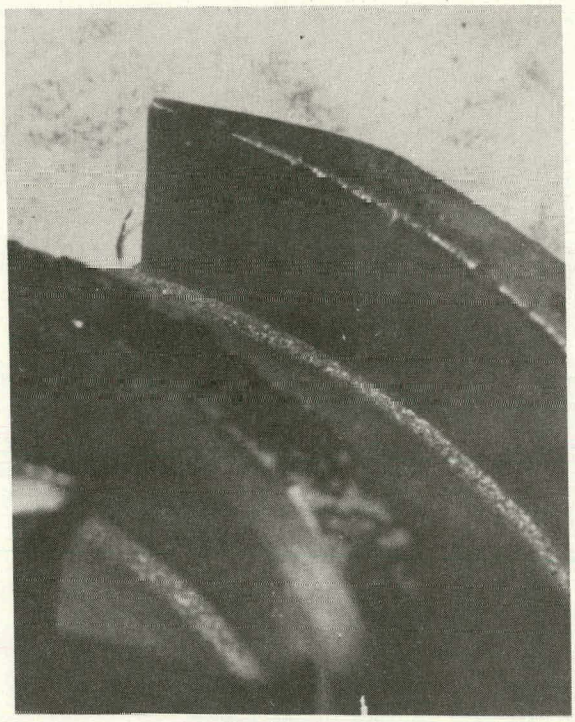

FIGURE B5
SST3 5 Vane Impeller,
(SST 3002)

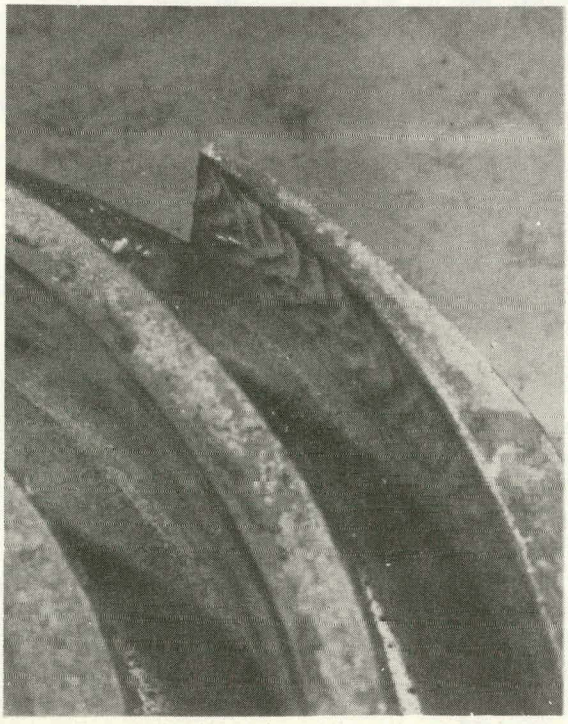

FIGURE B6:
SST 5 IMPELLER,
(SST 5003)

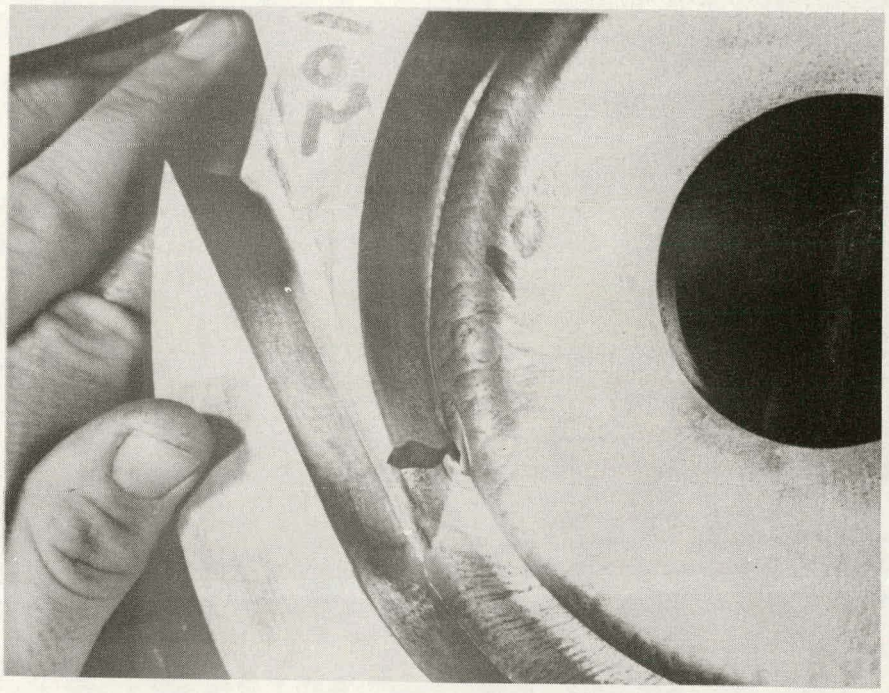

NOTE: UNDERCUTTING SHARPENING, THINNING AND
RIPPLE TYPE WEAR

FIGURE B7: SST5 MKI VOLUTE CUTWATER (SST 5003)

NOTE: WEAR MORE SEVERE THAN SEEN ON SST5 CUTWATER
IN FIGURE B7

FIGURE B8: SST3 MKI VOLUTE CUTWATER (SST 3002)

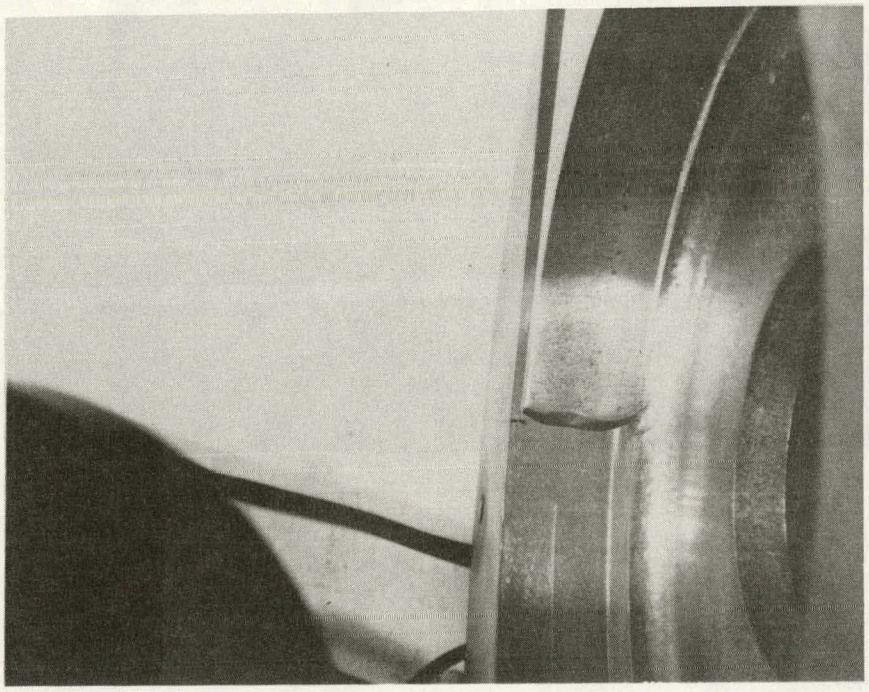

FIGURE B9: SST3 MKI VOLUTE RUN IN 2% SCMC/WATER BASED SLURRY
(SST 3005)

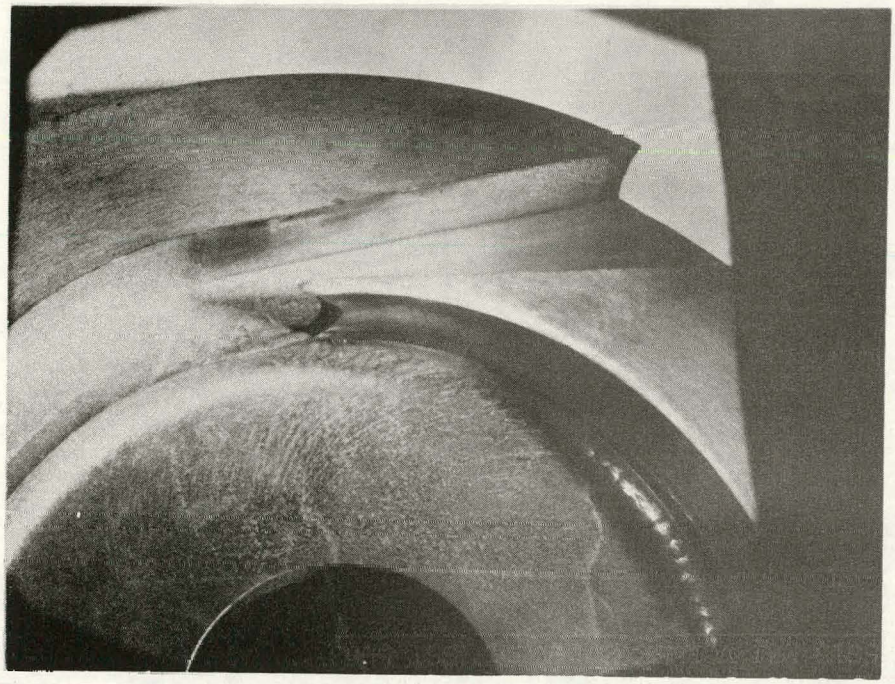

Note: 4 Hr.

FIGURE B10: SST 5 MKI VOLUTE WITH CONCAVE TRIM (SST 5004)

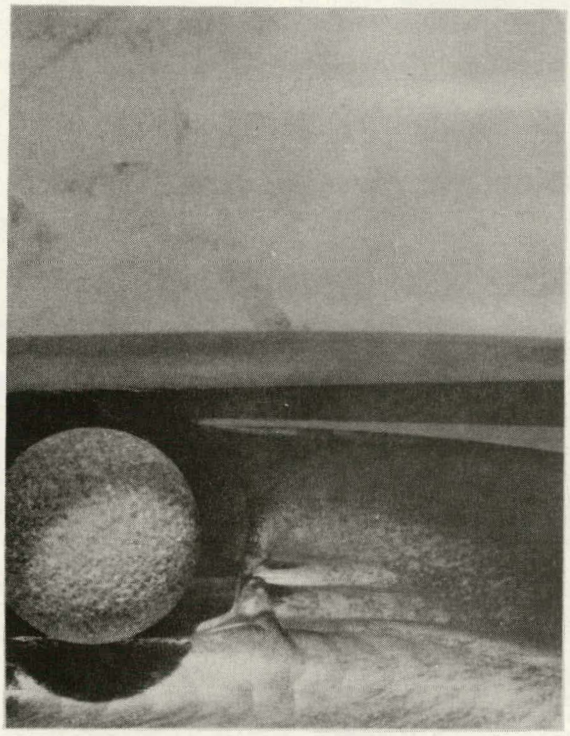

NOTE: 8 Hr.

FIGURE B11: SST5 MkI VOLUTE WITH CONCAVE CUTWATER TRIM
(SST 5004)

SST 3008

5 vane (12 hr)

SST 3009 4 vane (12 hr)

Note wear on suction side at trailing edge

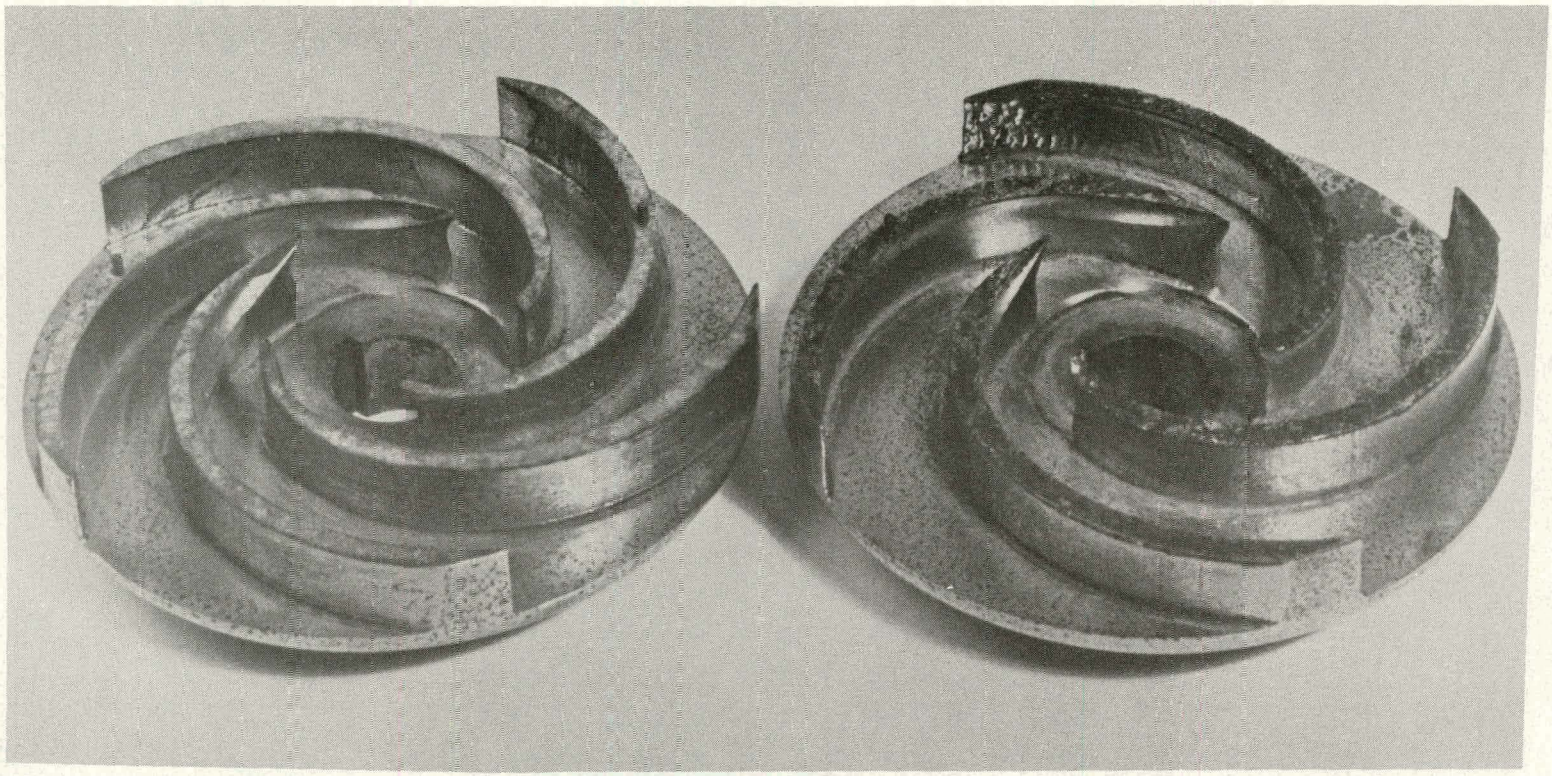

FIGURE B-2: COMPARISON OF SUCTION SIDE BLADE WEAR (SST 3008, 3009)

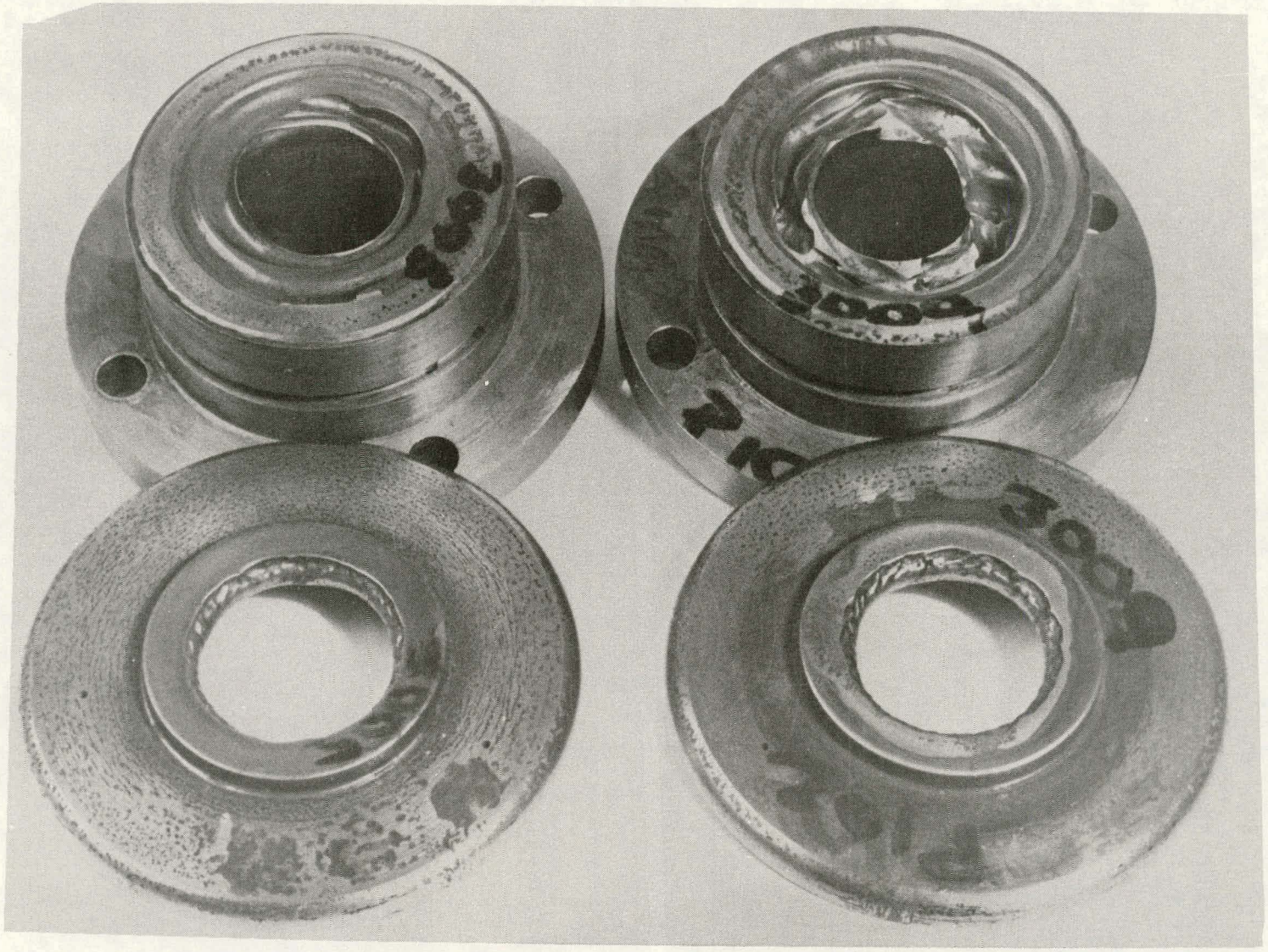

SST 3008 SST 3009

FIGURE B13: COMPARISON OF LEAKAGE PATH, WITH AND WITHOUT DIRECTED LEAKAGE LIP

(SST 3008, 3009)

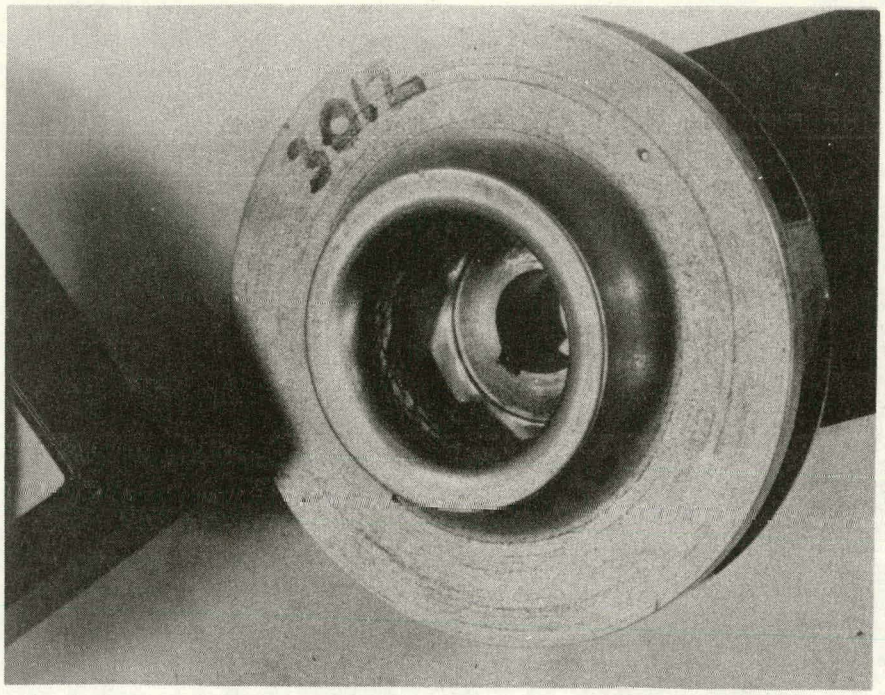

FIGURE B14: IMPELLER WITH 15° FROM AXIAL LEAKAGE PATH

(SST 3012)

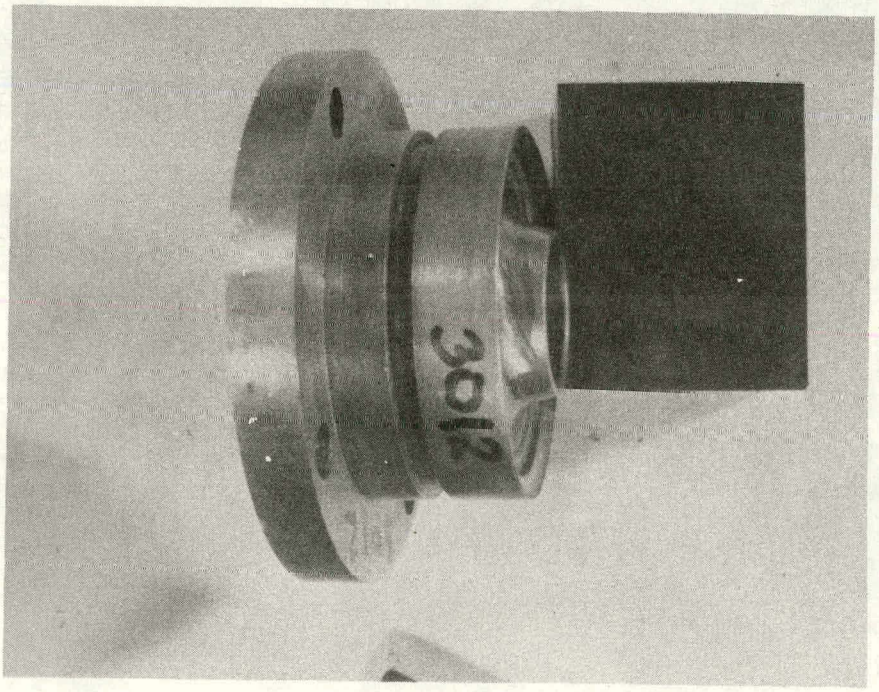

FIGURE B15: SUCTION NOZZLE FOR 15° AXIAL LEAKAGE PATH (SST 3012)

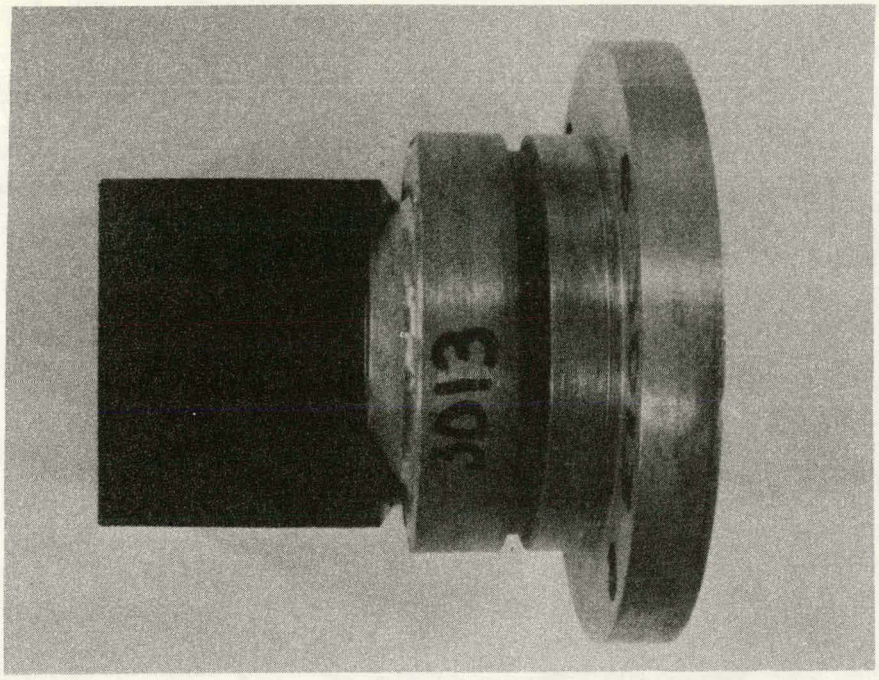

FIGURE B16: SUCTION NOZZLE FOR 30° FROM RADIAL LEAK PATH (SST 3013)

FIGURE 17: SST 3 IMPELLER WITH 30° FROM RADIAL LEAK PATH (SST 3013)

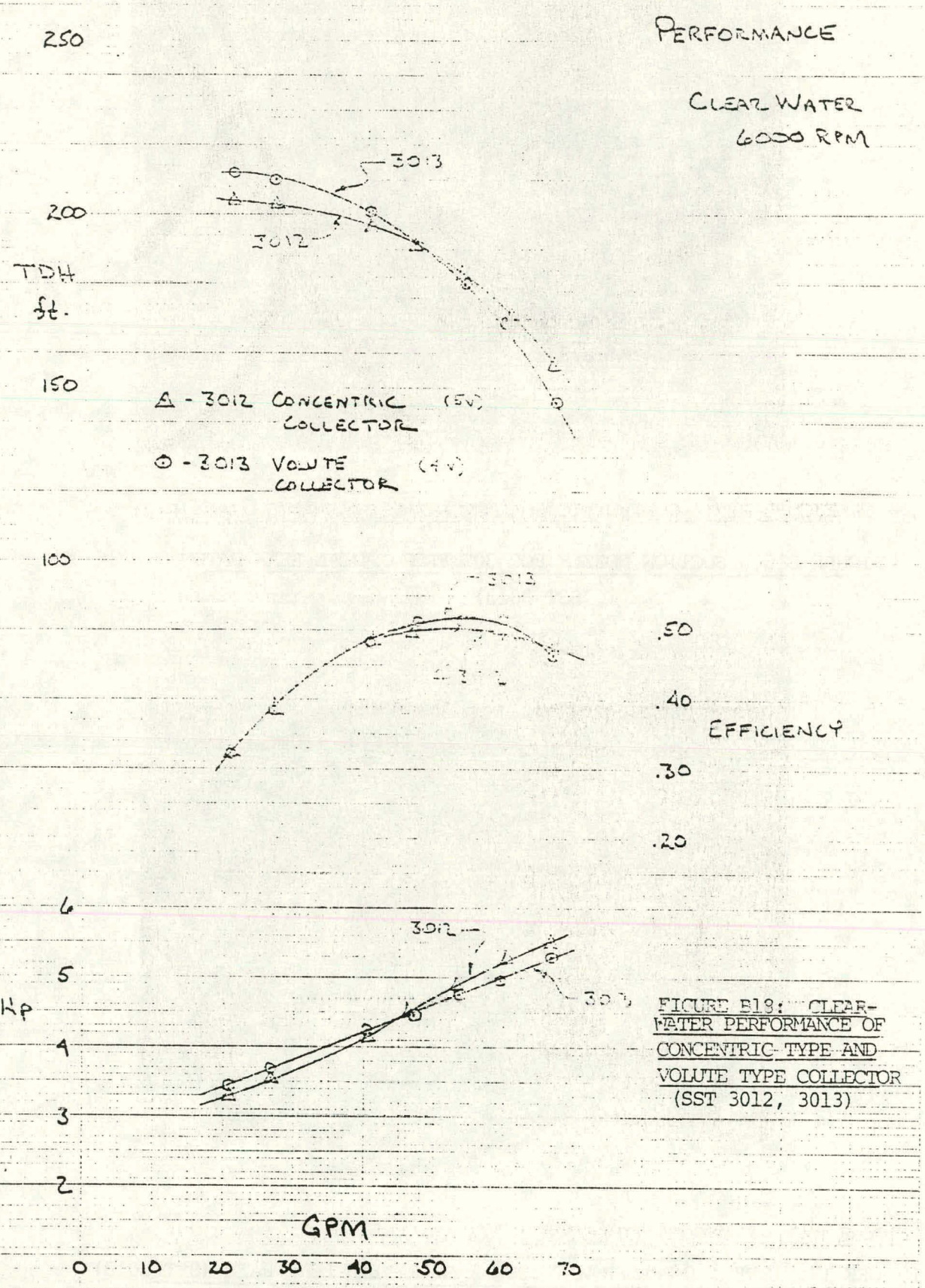

FIGURE B13: CLEAR-WATER PERFORMANCE OF CONCENTRIC TYPE AND VOLUTE TYPE COLLECTOR (SST 3012, 3013)

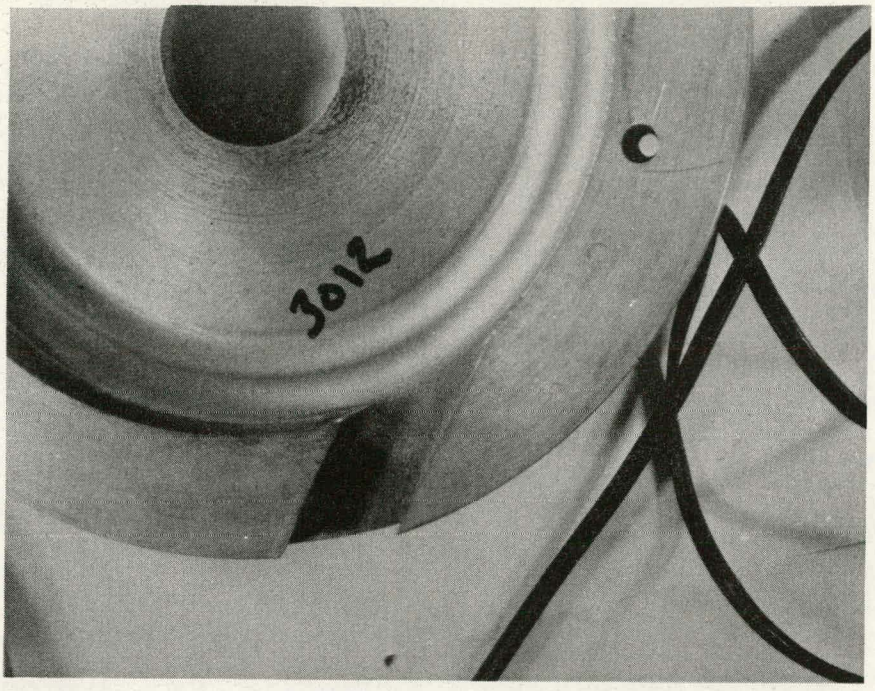

FIGURE B19: CONCENTRIC COLLECTOR AND DISCHARGE (SST 3012)

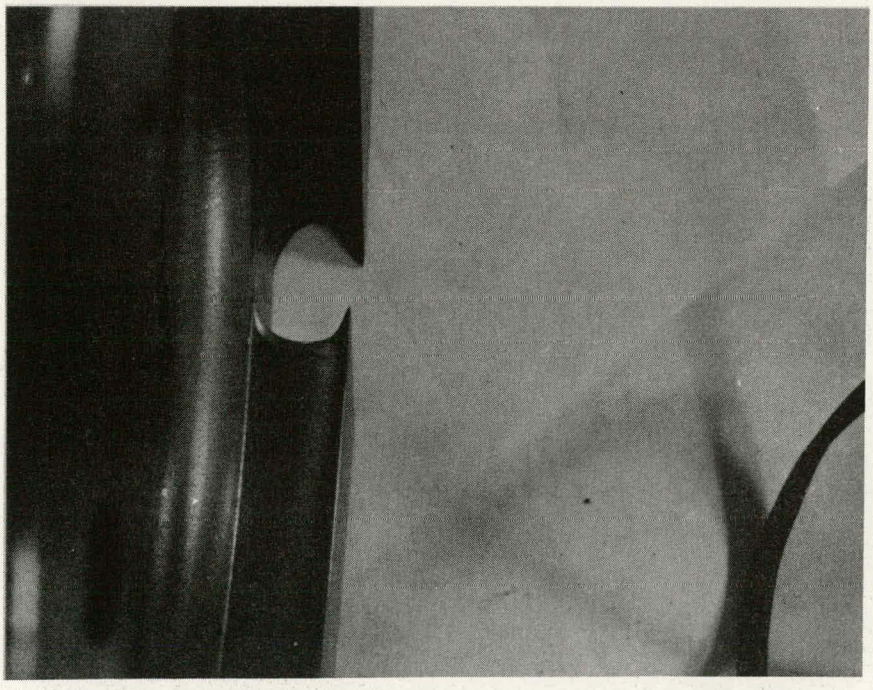

FIGURE B20: CUTWATER (IMPELLER SIDE) OF CONCENTRIC COLLECTOR

TEST REPORTS

TEST REPORT

TEST IDENTIFICATION: SST 3001

TEST PURPOSE: Loop shakedown, measure overall performance of SST 3

TEST NUMBERS: 004, 006, 007

TEST HARDWARE: SST 3 impeller and SST 3 Volute, all MkI type hardware (mkI type suction nozzle)

TOTAL HOURS IN SLURRY: 4 hrs.

TEST CONDITIONS:

RPM	-	5940-6020
FLOW	-	59-44 GPM
SAND TYPE	-	45-100 mesh
CONCENTRATION	-	.1-.37

TEST RESULTS:

CUTWATER LENGTH REDUCTION	-	.100"
IMPELLER FRONT RING LOSS	-	
IMP EYE DIA INCREASE	-	.035

TEST OBSERVATIONS:

1. Significant undercutting @ vol cutwater
2. Start of horseshoe vortex on discharge side of cutwater
3. Sharpening of cutwater. Biased toward inside of cutwater
4. Ripple type wear on volute sidewalls, endwalls and volute wall
5. Ripple type wear on impeller eye I.D. ripple axis 30° from axial direction
6. Sharpening and undercutting of leakage path corner at impeller I.D.

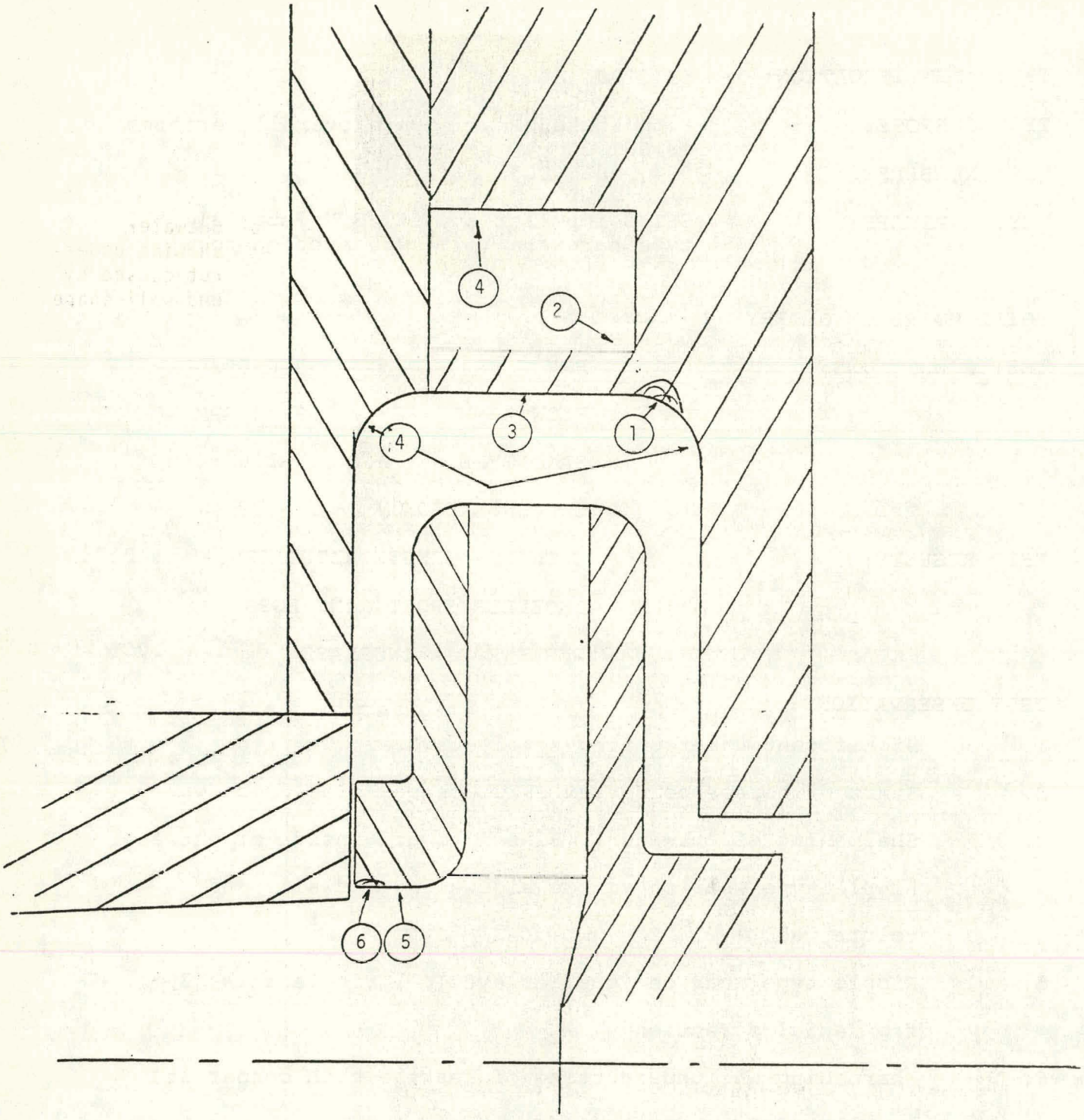

SST 3001 Wear

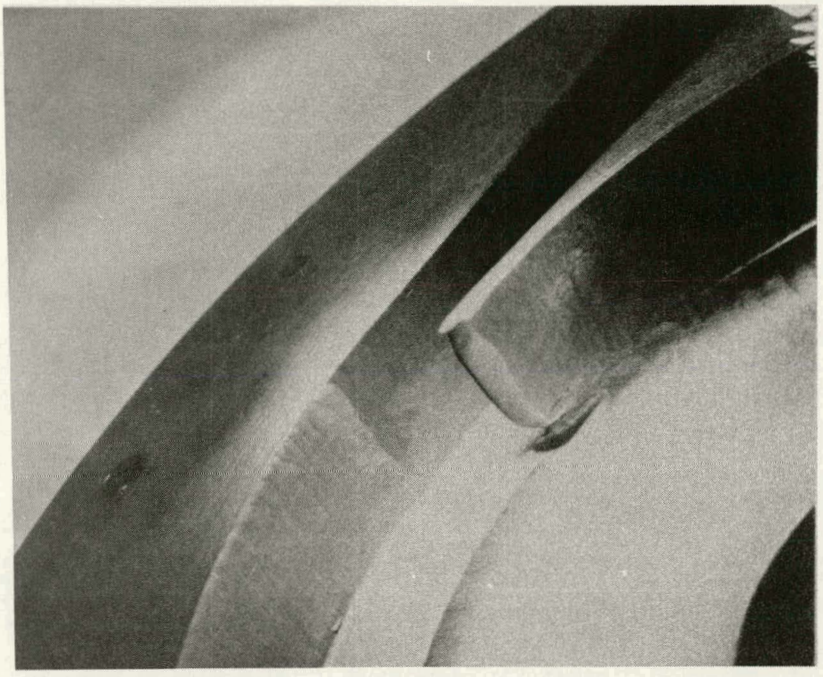

a) Cutwater, showing undercut caused by end-wall shape

SST 3001 Wear Patterns (Pump parts after four hours at 6000 rpm in 45-mesh sand-water slurry at concentration from 10 to 35% by weight)

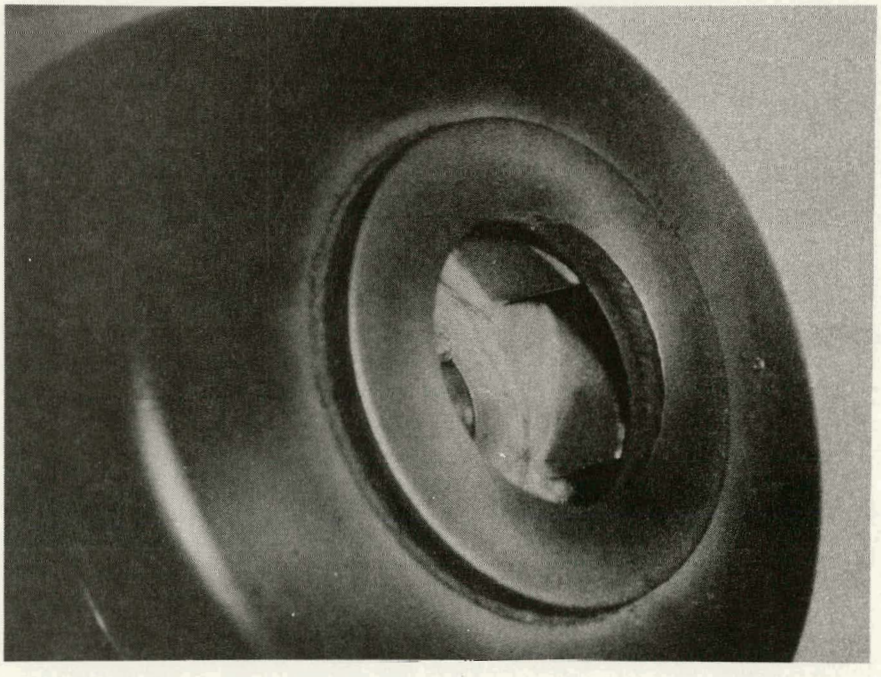

b) Impeller,

TEST REPORT

TEST IDENTIFICATION: SST 3002

TEST PURPOSE: Side by side comparison test of SST3 hardware with SST 5 hardware

TEST NUMBERS: 010, 017, 018, 026, 027, 028

TEST HARDWARE: SST 3 impeller & SST 3 volute, all MkI hardware (MkI suction nozzle)

TOTAL HOURS IN SLURRY: 10 hrs

TEST CONDITIONS:

RPM	-	5985-6030
FLOW	-	40-50 gpm
SAND TYPE	-	100 mesh
CONCENTRATION	-	.25

TEST RESULTS:

CUTWATER LENGTH REDUCTION	- .197"
IMPELLER FRONT RING LOSS	- .017
IMP EYE DIA INCREASE	- .100"

TEST OBSERVATIONS:

1. Severe undercutting at cutwater
2. Definite horseshoe vortex at volute cut on discharge side
3. Sharpening and wearing back of cutwater, plus g[illegible] and thinning on impeller side of cutwater
4. Severe ripple type wear on endwalls, volute sidewalls and volute
5. Severe wear on suction nozzle at I.D., region next to front impeller wear ring
6. Severe ripple wear, with much metal removal on impeller eye I.D., ripple axis ~ 30° from axial direction
7. Sharpening of impeller blade L.E., with more blade shortening on hub side

7	Circumferential groove forming on impeller wear ring
9	Groove forming on hub side IMP wall, suction side of passage
10	Very slight groove forming on pressure side of blade at exit of impeller
11	Sand accumulation on suction side of blade, @ 2/3 of blade length from inlet - blockage cuts relative flow passage area in half, resulting in sidewall wear.
12	Impeller sidewall wear, inside, just downstream of impeller trailing edge
14	Circumferential wear on suction nozzle next to impeller wear surface

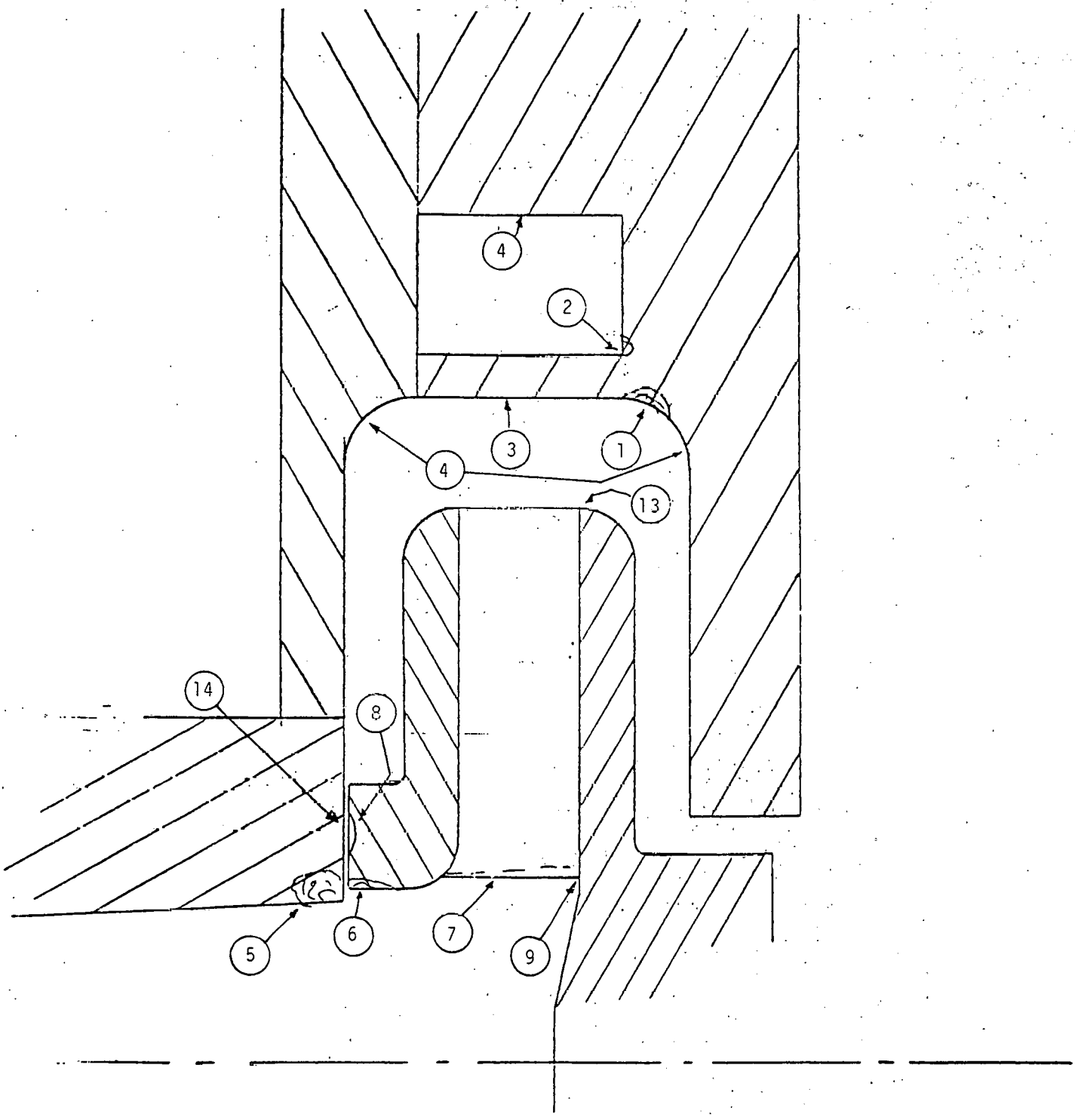

SST 3002 Wear

TEST REPORT

TEST IDENTIFICATION: SST 5003

TEST PURPOSE: Side by side comparison test of SST 5 hardware with SST 3 Hardware (3002)

TEST NUMBERS: 010, 017, 018, 021, 026, 027, 028

TEST HARDWARE: SST 5 impeller & SST 5 volute (MkI suction nozzle) all mkI hardware

TOTAL HOURS IN SLURRY: 10 hrs.

TEST CONDITIONS:

RPM - 5985-6030

FLOW - 40-50 gpm

SAND TYPE - 100 mesh

CONCENTRATION - .25

TEST RESULTS:

CUTWATER LENGTH REDUCTION - .118

IMPELLER FRONT RING LOSS - .015

IMP EYE DIA INCREASE - .052

TEST OBSERVATIONS:

1. Undercutting at volute cutwater; not as severe as 3002
2. Horseshoe vortex on discharge side of cutwater
3. Sharpening and wearing back of cutwater plus slight thinning of cutwater from impeller side
4. Ripple type wear on endwalls, volute sidewalls, and volute, not as severe as 3002
5. Sharpening of corner of suction nozzle
6. Circumferential wear on suction nozzle next to impeller wear surface
7. Sharpening of corner at impeller inlet eye I.D.
8. Slight circumferential croove forming on impeller front wear ring

9. Horseshoe wortex forming at impeller blade L.E., suction & pressure side.

10. Sharpening of impeller blad L.E. with uneven axial wearback

11. Ripple type wear on suction side of blade over last 3/4 of blade length, also suction side grooving on either side of ripple wear

12. Endwall grooving of impeller, both endwalls, over last 2/3 of passage.

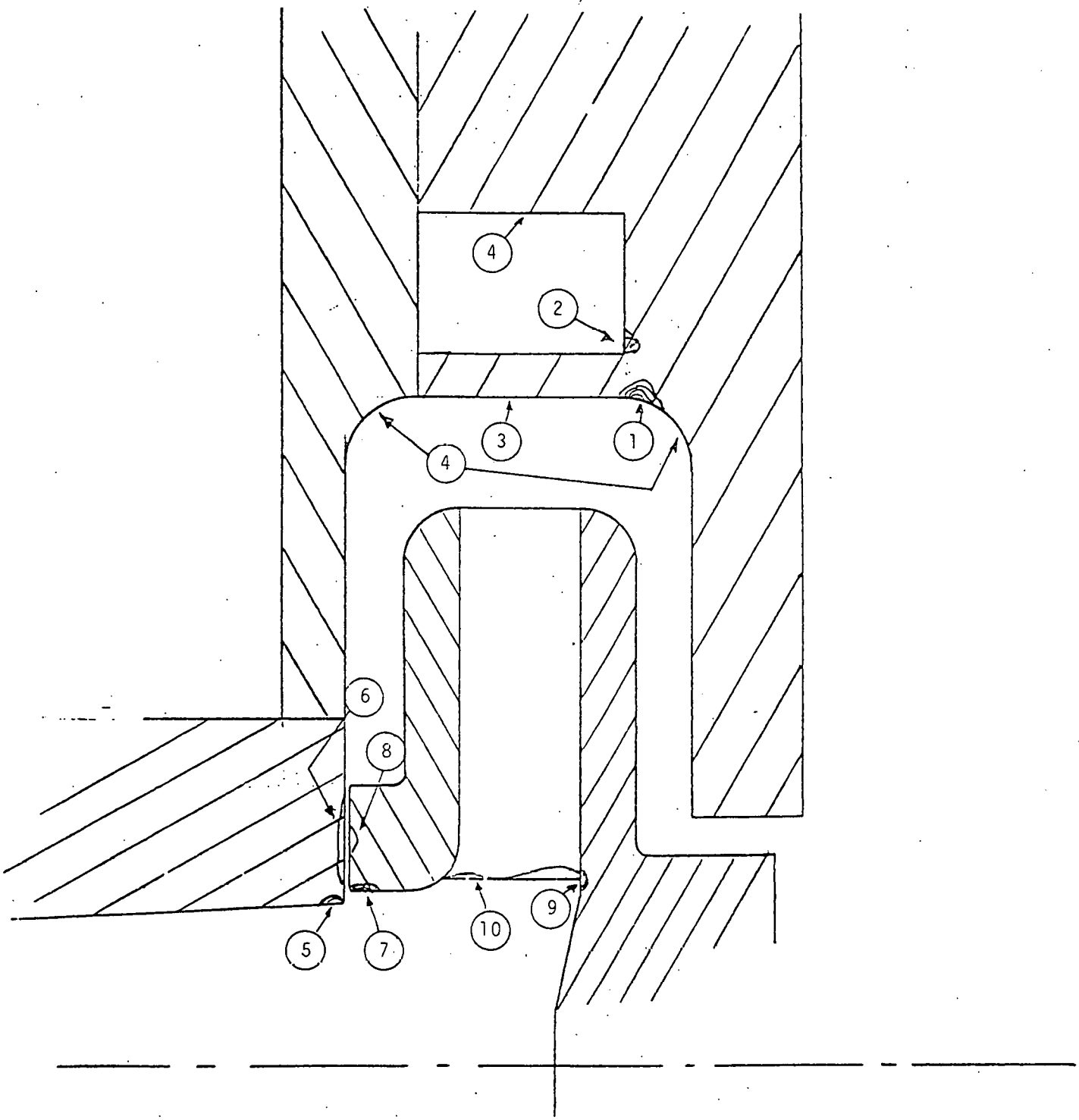

SST 5003 Wear

TEST REPORT

TEST IDENTIFICATION: SST 5004

TEST PURPOSE: Observe wear on concave cutwater modification

TEST NUMBERS: 015, 016, 022, 023, 029, 030

TEST HARDWARE: SST 5 Impeller & SST 5 Volute with concave trim on cutwater (R=.375) - MkI suction nozzle (all hardware MkI)

TOTAL HOURS IN SLURRY: 12 hrs.

TEST CONDITIONS:

RPM	-	5977-6028
FLOW	-	49-41 gpm
SAND TYPE	-	100 mesh
CONCENTRATION	-	.25

TEST RESULTS:

CUTWATER LENGTH REDUCTION	-	.350"
IMPELLER FRONT RING LOSS	-	
IMP EYE DIA INCREASE	-	.082

TEST OBSERVATIONS:

1. No horseshoe vortex on discharge side of volute cutwater
2. Some undercutting of cutwater from impeller side plus some grooving
3. Considerable wearback of cutwater leading edge with a reshaping from a circular cutback to eliptical
4. Ripple wear on endwalls, volute sidewalls and volute itself.
5. Sharpening of the cutwater's concave leading edge, biased toward impeller side
6. Very severe suction nozzle wear at ID, adjacent to impeller inlet
7. Suction nozzle wear on wearing surface opposite impeller wear surface

8 Ripple wear on impeller inlet ID-w~~h~~ vorices axis 30° from axial direction

9. Sharpening of corner at impeller leakage path ID.

10. Horseshoe vortex on impeller walls at leading edge of blades

11. Ripple type wear on suction side of impeller blade

12. Definite grooving of pressure side of impeller blade - with deepest portion shifted to hub side.

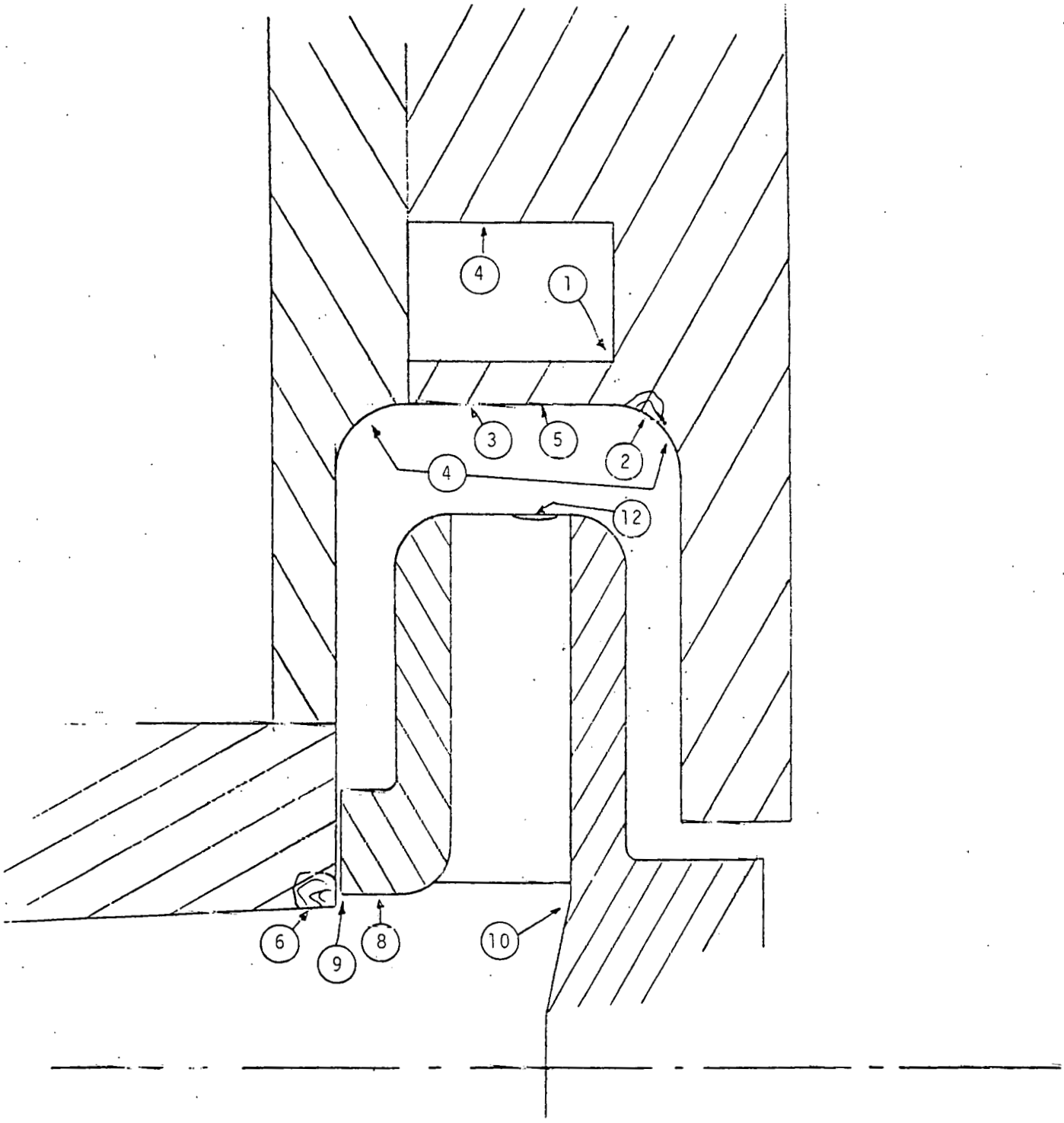

SST 5004 Wear

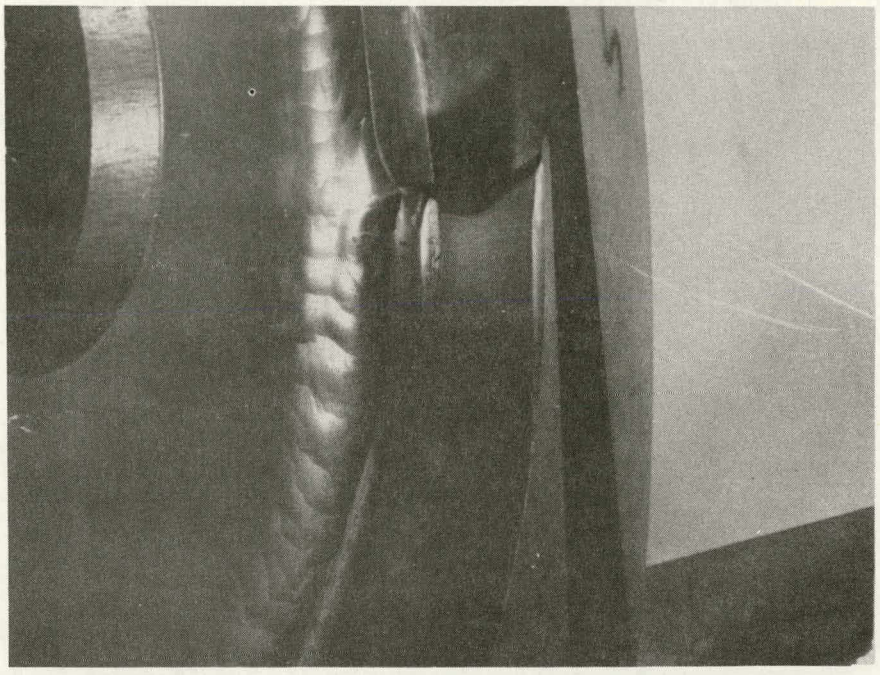

SST 5004, 12 HOURS
CONCAVE CUTWATER
MODIFICATION

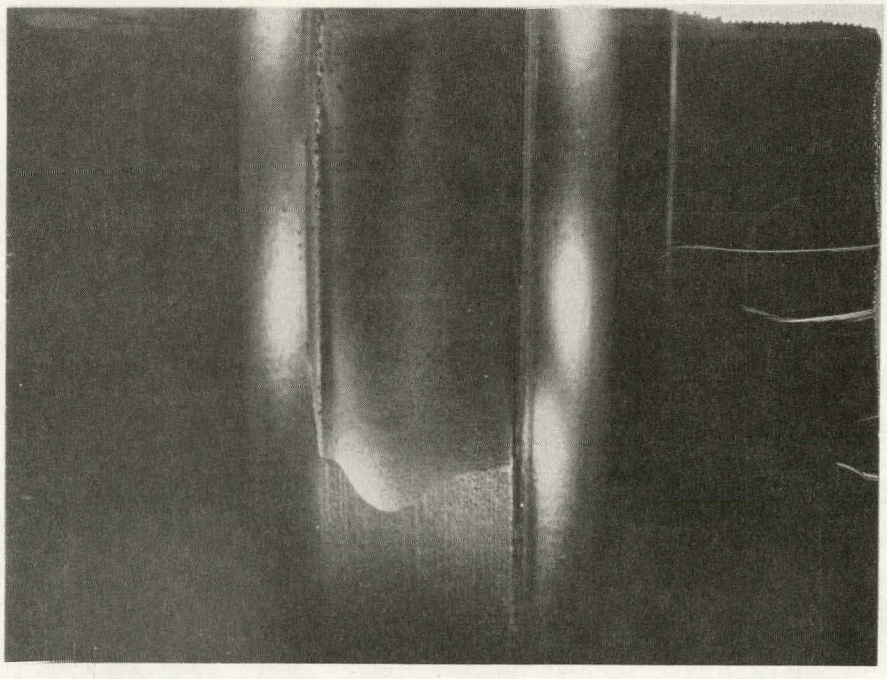

SST 5004, 12 HOUR
GROOVE ON PRESSURE
SIDE OF IMPELLER

TEST REPORT

TEST IDENTIFICATION: SST 3005

TEST PURPOSE: Loop shakedown with viscosity additive SCMC, also performance check of SST3

TEST NUMBERS: 031, 032, 033

TEST HARDWARE: SST 3 Impeller & SST 3 volute, MkI suction nozzle (all MkI hardware).

TOTAL HOURS IN SLURRY: 12 hrs.

TEST CONDITIONS:

RPM - 6021-5980

FLOW - 21-46 gpm

SAND TYPE - 100 mesh

CONCENTRATION - .10-.27 w/viscosity additive first 8hrs 2% added; last 4 hrs 1% added

TEST RESULTS:

CUTWATER LENGTH REDUCTION - .118

IMPELLER FRONT RING LOSS - .016

IMP EYE DIA INCREASE - .062

TEST OBSERVATIONS:

1. Very severe undercutting and horseshoe vortex at volute cutwater
2. No ripple wear for first 8 hours; some ripple wear from last 4 hours on end walls, volute sidewalls and volute itself
3. Sharpening of cutwater leading edge, biased toward impeller side with some thinning.
4. Some suction nozzle wear at corner
5. Circumferential wear on suction nozzle at wear surface across from impeller wear surface
6. Well defined horseshoe vortex forming at impeller leading edge (hub side)
7. Ripple type wear on impeller eye ID with sharpening of corner

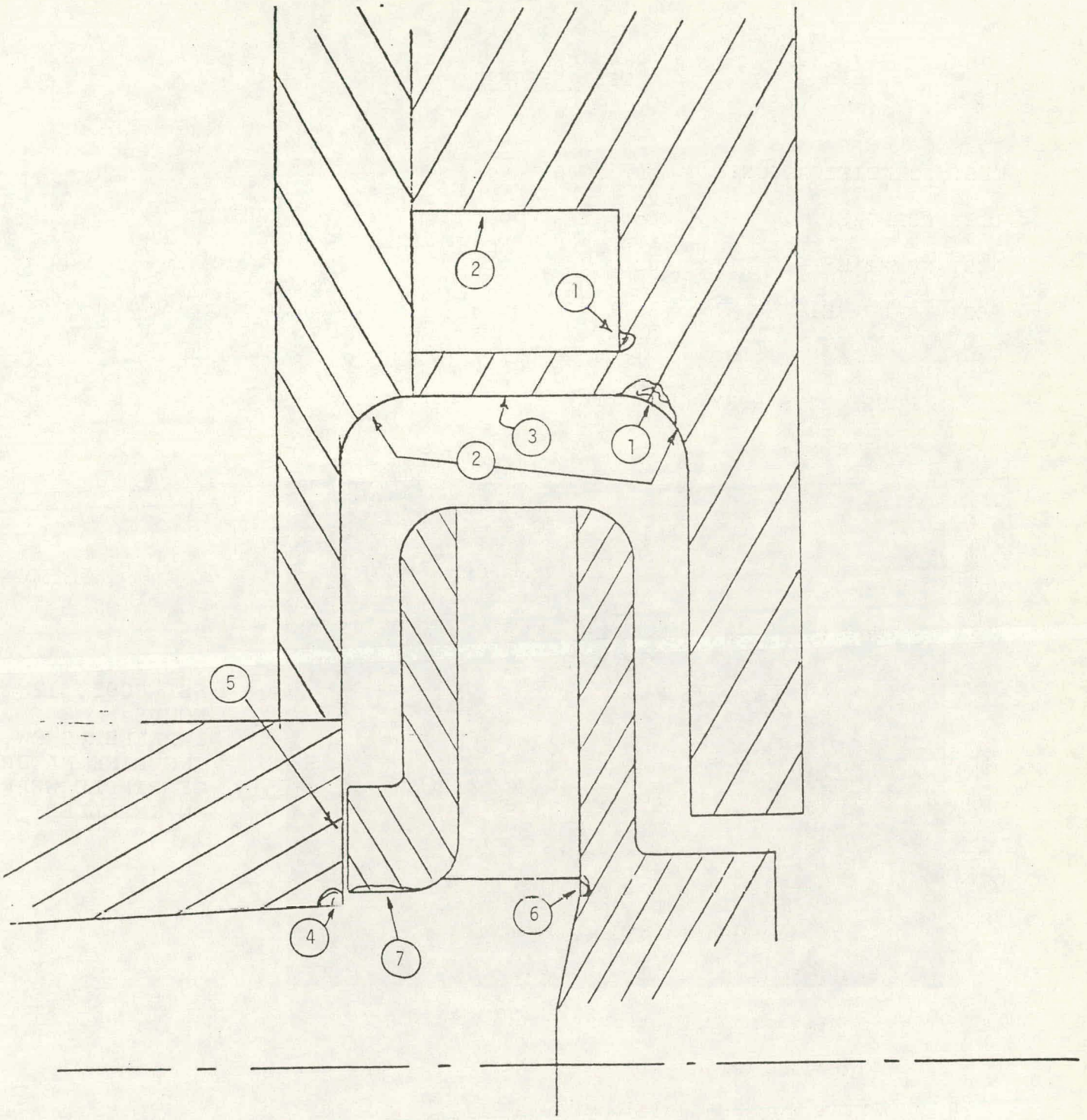

SST 3005 Wear Locations

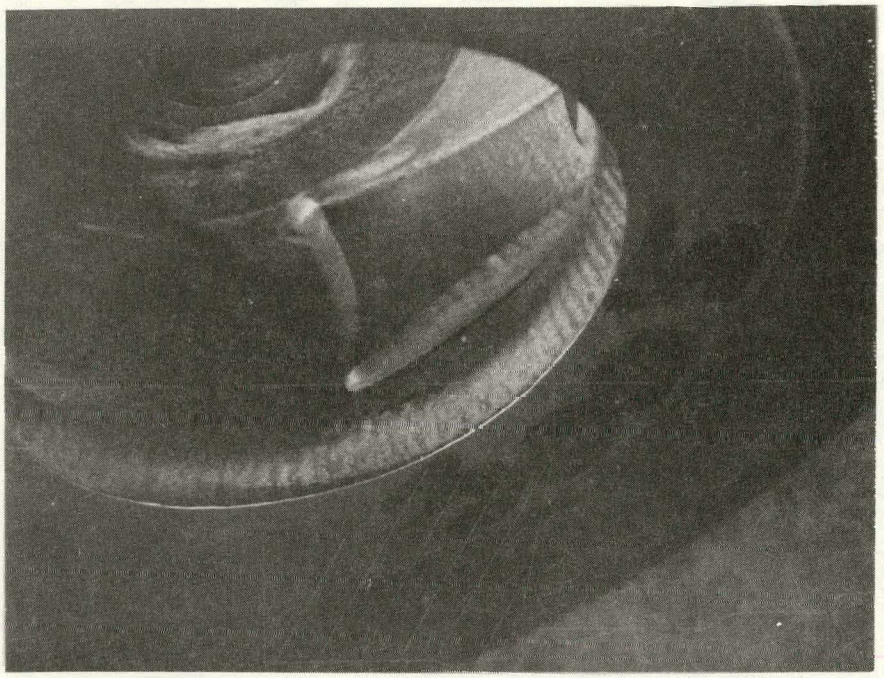

SST 3005, 12 HOURS IMPELLER SHOWING FINE NATURE OF RIPPLE WEAR ON IMPELLER I.D.

TEST REPORT

TEST IDENTIFICATION: SST 5006

TEST PURPOSE: Compare with 5007; Check wear with and without pump-out vanes; Evaluate Mk II inlet nozzles and sidewalls; and also, Compare concave CW with straight CW

TEST NUMBERS: 036, 037

TEST HARDWARE: SST5 with pump-out vanes - All Mk II hardware CW L.E. has concave trim

TOTAL HOURS IN SLURRY: 6.3 HOURS

TEST CONDITIONS:

RPM - 5990-6052

FLOW - 48.9-55.2 gpm

SAND TYPE - 100 Mesh

CONCENTRATION - .25 CW

TEST RESULTS:

CUTWATER LENGTH REDUCTION -

IMPELLER FRONT RING LOSS -

IMP EYE DIA INCREASE -

TEST OBSERVATIONS:

1. Definite wear on suction nozzle wear face opposite impeller wear face.
2. Sharpening of leakage direction lip over 70° of inlet diameter, will eventually disappear.
3. 1/8" radius on impeller at leakage path all gone--ripple wear evident at impeller I.D.
4. Classic horseshoe vortex at impeller blade L.E. (hub side).
5. Sharpening of impeller L.E. with wear back, cupping of blade noticeable with most of wear 1/8" from shroud location of blade L.E.
6. Slight ripple-type wear evident on suction side of blade towards T.E.
7. Some ripple wear on collector endwalls and volute scroll itself.
8. Concave CW eliminates groove just ahead of CW leading edge.
9. Deep groove on endwall parallel to CW on impeller side of CW. Slight groove on diffuser side.
10. Some sharpening of CW leading edge.

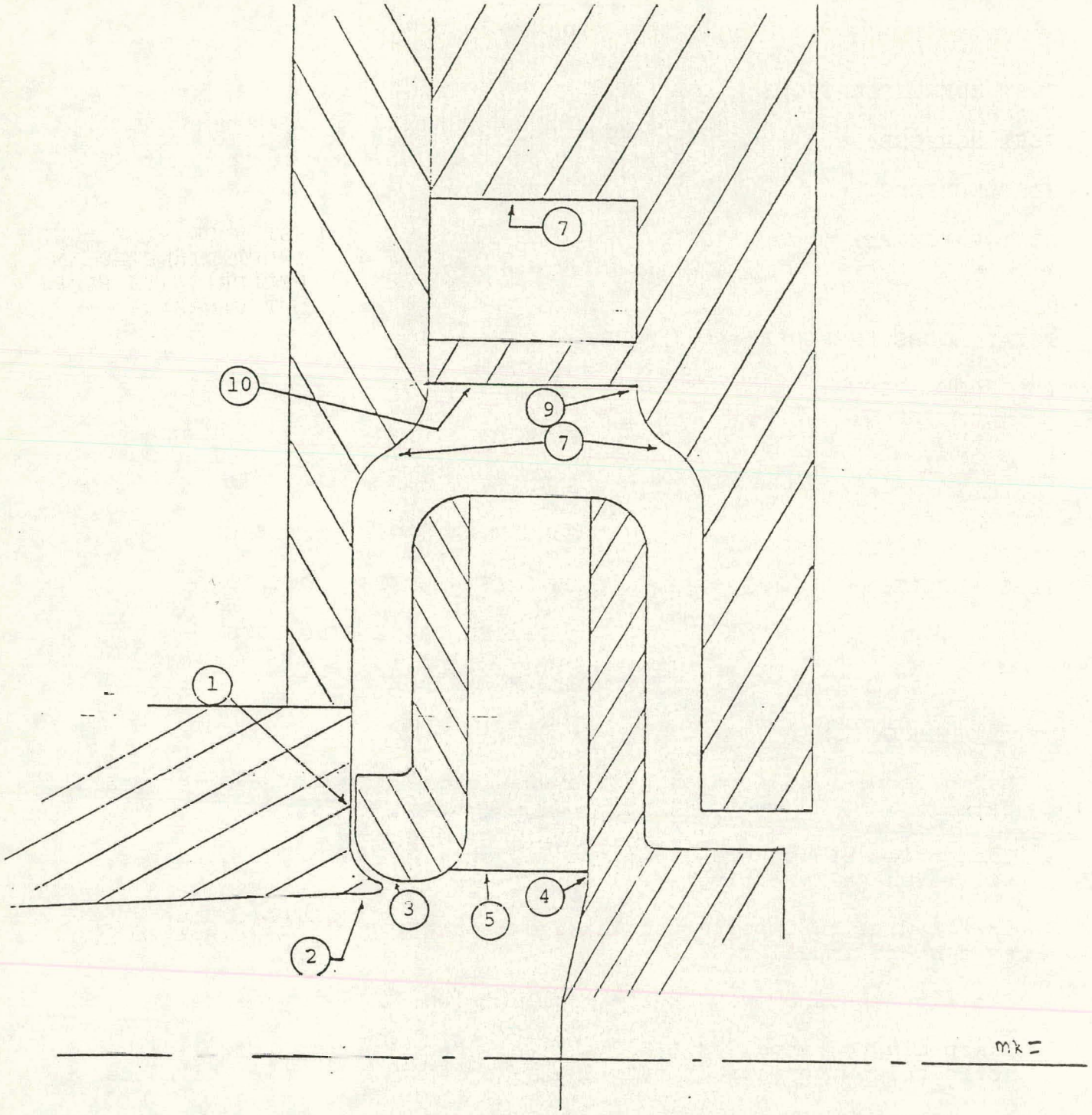

SST 5006
WEAR LOCATIONS

CIRCLED NUMBERS REFER TO TEST OBSERVATIONS ON TEST REPORT

SST 5006 - 12 HOURS
INLET DIAMETER IM-
PELLER (WITH PUMP-
OUT VANES)

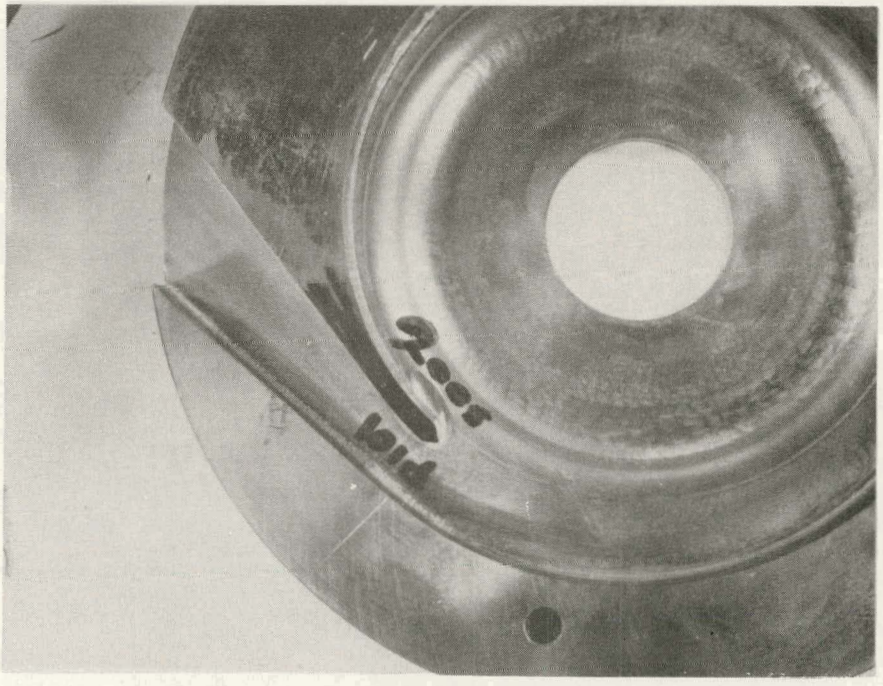

SST 5006 - 12 HOURS
STRAIGHT CUTWATER
AND HORSESHOE VOR-
TEX

TEST REPORT

TEST IDENTIFICATION: SST 5007

TEST PURPOSE: Compare with 5006; Check wear with and without pump-out vanes; and Evaluate Mk II nozzles and sidewalls--concave CW is straight

TEST NUMBERS: 036, 037

TEST HARDWARE: SST5 - No pump-out vanes - All Mk II hardware

TOTAL HOURS IN SLURRY: 6.3 Hours

TEST CONDITIONS:

RPM - 5990-6052

FLOW - 48.9-55.2 gpm

SAND TYPE - 100 mesh

CONCENTRATION - .25 CW

TEST RESULTS:

CUTWATER LENGTH REDUCTION -

IMPELLER FRONT RING LOSS -

IMP EYE DIA INCREASE -

TEST OBSERVATIONS:

1. Some wear on suction nozzle, leakage face at joint with front wall.
2. Leakage direction lip in good shape.
3. Some wear on inside impeller walls at blade T.E.
4. Scalloping of rear impeller wall at tip of pump-out vanes.
5. Some wear grooves evident on front of pump-out vane at location of front wall, suction nozzle joint.
6. Some ripple-type wear between pump-out vanes on front outside impeller wall.
7. Slight scalloping on front wall of impeller at pump-out vane tip.
8. Herringbone-type ripple pattern on impeller radius (shroud).
9. Impeller blade L.E. sharpening with some wear back--most wear back at mid-blade or biased to shroud side.
10. Slight ripple-type wear on suction side of blade at exit end.
11. Scallops on impeller hub (back side of impeller) between pump-out vanes.

12. Front impeller leakage ring not shined but more porous in texture.

13. Ripple wear on collector endwalls and volute scroll itself.

14. Formation of horseshoe vortex at cutwater--both sides of cutwater (i.e. impeller side of cutwater and diffuser side).

15. Classic sharpening of cutwater with bias towards impeller side.

16. Some horseshoe vortex-type wear on hub side wall of impeller at L.E.

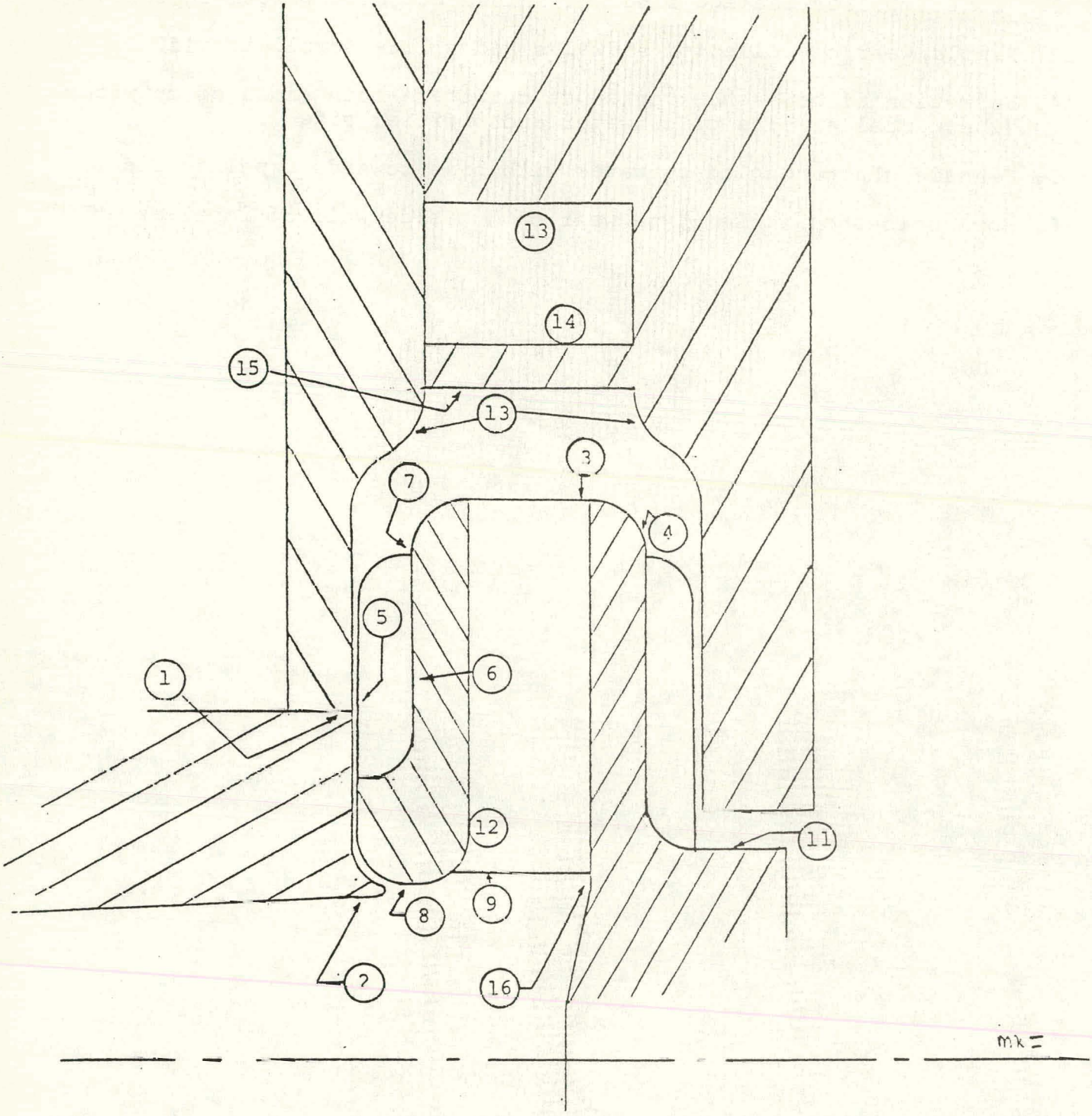

SST 5007
WEAR LOCATIONS

CIRCLED NUMBERS
REFER TO TEST
OBSERVATIONS ON
TEST REPORT

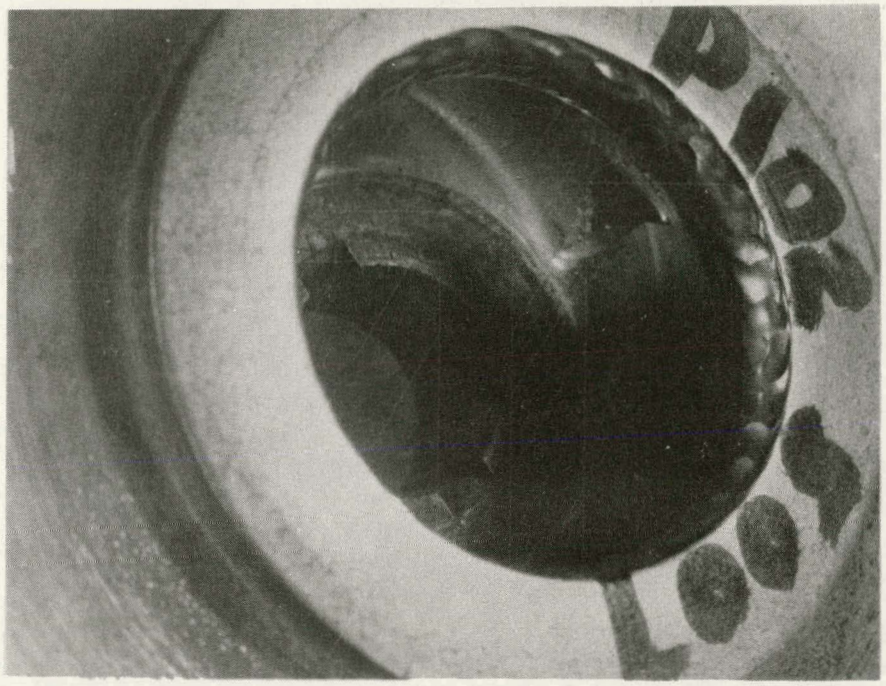

SST 5007 - 12 HOURS
INLET DIAMETER IM-
PELLER (WITHOUT
PUMP-OUT VANES)

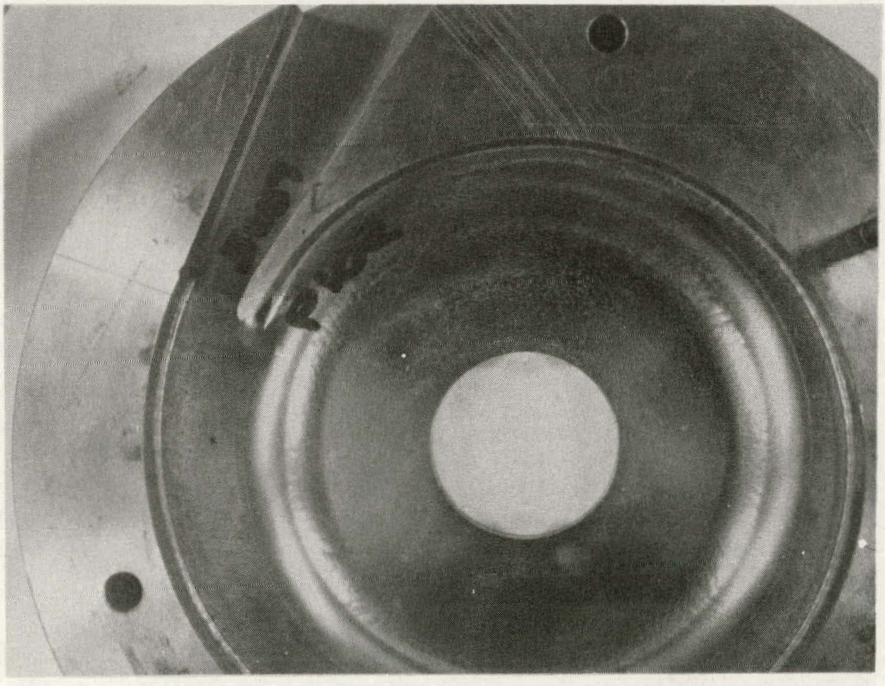

SST 5007 - 12 HOURS
CONCAVE CUTWATER
MODIFICATION

TEST REPORT

TEST IDENTIFICATION: 3008

TEST PURPOSE: Compare with 3009, Evaluate 4 vs. 5 Blade Impeller, Radical C_w Modification & Leak Direction Lip vs. Straight Leak Path

TEST NUMBERS: 046

TEST HARDWARE: SST 3 Mk II, 5 blade, no P/O Vane - Mk II volute with radically cutback cutwater (with concave Cw) Mk II suction nozzle with direction lip.

TOTAL HOURS IN SLURRY: 12 hr. (See earlier 6 hr. report)

TEST CONDITIONS:

RPM -

FLOW -

SAND TYPE -

CONCENTRATION -

TEST RESULTS:

CUTWATER LENGTH REDUCTION -

IMPELLER FRONT RING LOSS -

IMP EYE DIA INCREASE -

TEST OBSERVATIONS:

1. Directed leakage lip remains over 60° of Dia., where lip has worn away. Wear is occurring at corner where lip has disappeared.
2. Circumerencial groove formed on flat portion of suction nozzle wear surface.
3. Some rippling on sidewalls of collector and volute scroll.
4. Wide angle cutwater shows little wear, slight grooving on impeller side; no horseshoe vortex evident.

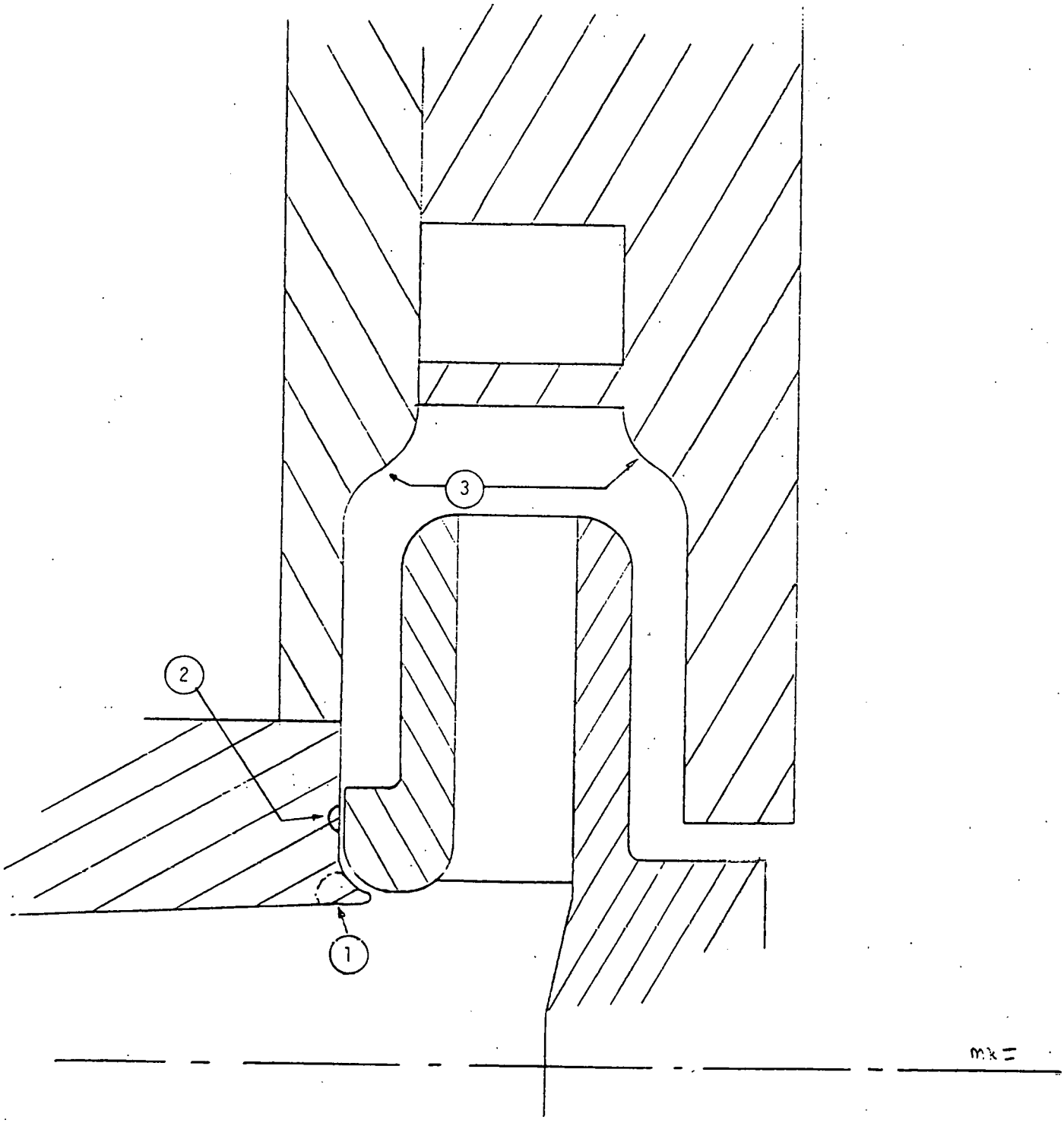

SST 3008 Wear Locations

TEST REPORT

TEST IDENTIFICATION: 3009

TEST PURPOSE: Compare with 3008 - Evaluate 4 vs. 5 Vane Impeller; Radical Cw Mod. ; and Leakage Direction Lip vs. Straight Leak Path

TEST NUMBERS: 046

TEST HARDWARE: SST 3 Mk II - 4 Vane, no PO Vanes - Mk II Volute with concave C_w - Straight Cut Suction Nozzle - No Direction Lip.

TOTAL HOURS IN SLURRY: 12 hr. (See earlier 6 hr. report)

TEST CONDITIONS:

RPM -

FLOW -

SAND TYPE -

CONCENTRATION -

TEST RESULTS:

CUTWATER LENGTH REDUCTION -

IMPELLER FRONT RING LOSS -

IMP EYE DIA INCREASE -

TEST OBSERVATIONS:

1. Continued deep erosion of suction nozzle - No flat wear surface remains.
2. Some ripple wear on collector sidewalls and volute scroll.
3. Continued sharpening of volute concave cutwater, biased toward impeller side.
4. Grooving on endwall at Cw, more along impeller side than on the Diffuser side. No evidence of grooving upstream of Cw, indicative of horseshoe vortex.
5. Pitting on suction side of Impeller, near trailing edge.

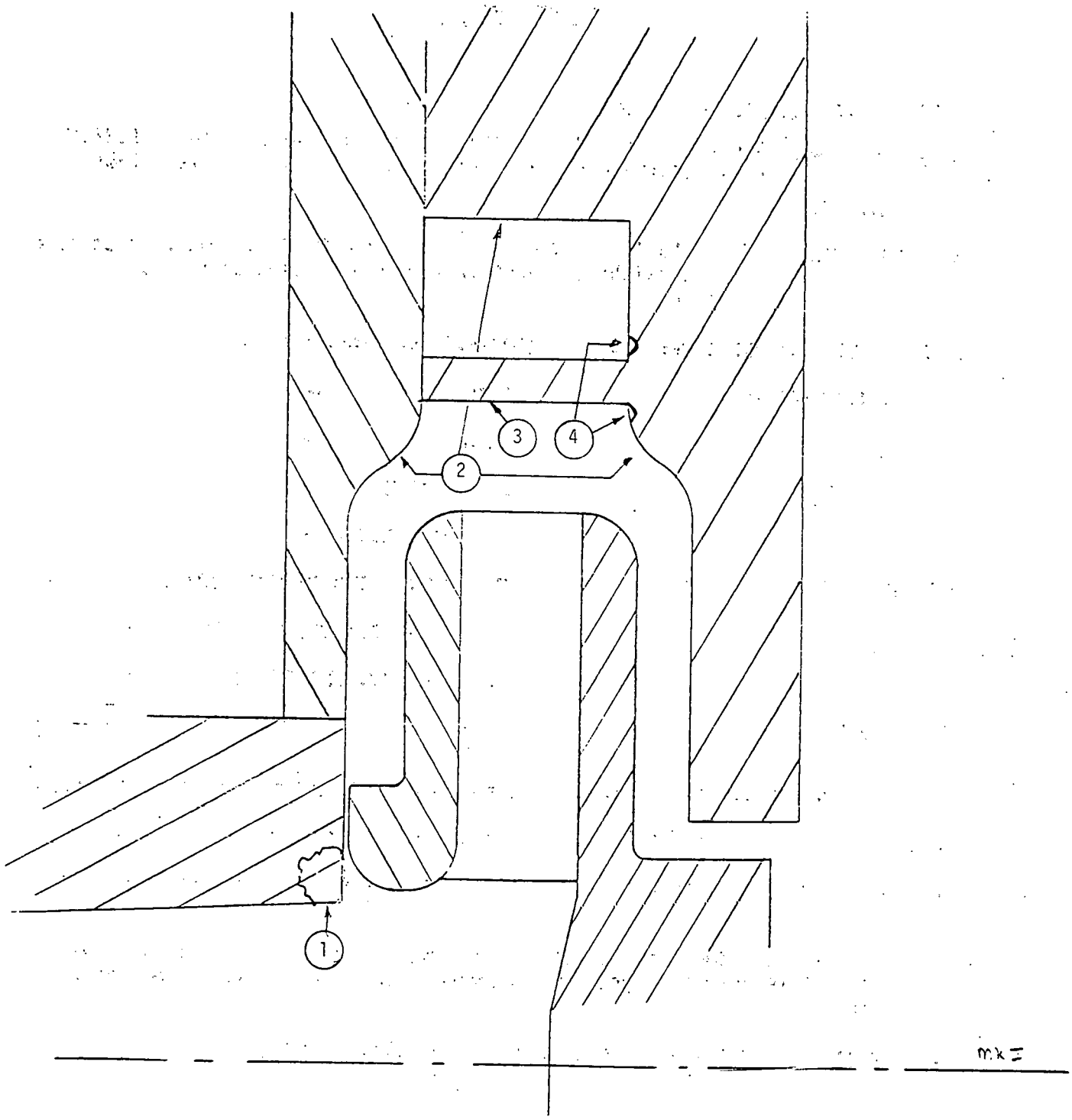

SST 3009 Wear Locations

TEST REPORT

TEST IDENTIFICATION: 5010

TEST PURPOSE: Compare with 3011, Evaluate SST 3 vs. SST 5 Impeller in ½% SCM based slurry

TEST NUMBERS: 042, 043, 044, 048

TEST HARDWARE: SST 5 Mk II - No PO Vanes - Mk II Volute with concave - LE. Trim. All Mk II suction nozzle.

TOTAL HOURS IN SLURRY: 14 hr.

TEST CONDITIONS:

RPM - 6022-5996

FLOW - 53.7 - 42.9

SAND TYPE -

CONCENTRATION - 25 % C_w

TEST RESULTS:

CUTWATER LENGTH REDUCTION -

IMPELLER FRONT RING LOSS -

IMP EYE DIA INCREASE -

TEST OBSERVATIONS:

1. Directed leakage lip worn away over ½ of inlet dia.
2. Deep grooving of wear surface on suction nozzle with some circumferential hole development.
3. Large dimple wear marks on Impeller intlet wear ring radius.
4. Wearback and sharpening of Blade LE with only slight wear back near shroud.
5. Horseshoe vortex type formation on Impeller hub wall at blade LE.
6. No grooving of pressure side of blade trailing edge or land.
7. Slight ripple wear (fine nature) along collector side walls.
8. Slight ripple type wear around volute wall.
9. Cutwater sharpening, biased towards Impeller side.
10. Grooving along Impeller side of cutwater, not in Diffuser passage.
11. No classic horseshow vortex formation on volute ring side of cutwater.

12. Horseshoe vortex type formation on front wall (Note: 90^0 mating joint with cutwater) with a trailing vortex from Impeller side of cutwater.

13. Slight ripple type wear on suction side of Impeller at the exit of blade.

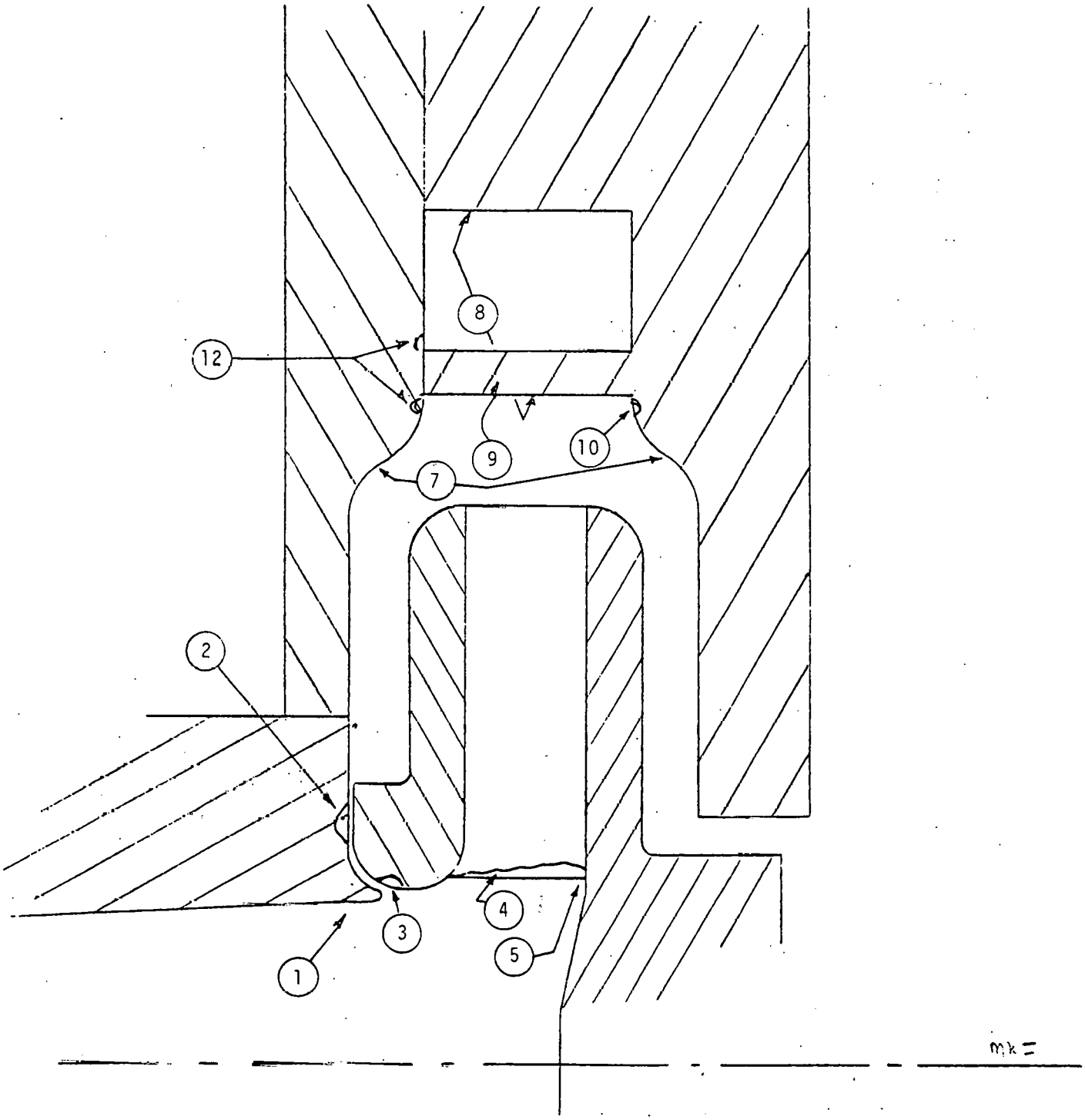

SST 5010 Wear Locations

TEST REPORT

TEST IDENTIFICATION: 3011

TEST PURPOSE: Compare with 5010 - Evaluate SST 3 vs. SST 5 Impeller in ½% SCMC slurry.

TEST NUMBERS: 042, 043, 044,045, 048

TEST HARDWARE: SST 3 Mk II 5 Vane, No PO Vanes - Mk II Volute with concave LE Trim, All Mk II suction nozzle

TOTAL HOURS IN SLURRY: 14 hr.

TEST CONDITIONS:

RPM - 6022 - 5996

FLOW - 53.7 - 42.9 GPM

SAND TYPE - 100 Mesh

CONCENTRATION - 25 % C_w

TEST RESULTS:

CUTWATER LENGTH REDUCTION -

IMPELLER FRONT RING LOSS -

IMP EYE DIA INCREASE -

TEST OBSERVATIONS:

1. Directed leakage lip worn away over 40% of inlet dia.
2. Deep grooving of wear surface on nozzle with some indication of circumferential worm hole development - wear not as severe as 5010.
3. Large dimple marks on impeller inlet ring radius similar to SST 5010.
4. Wearback & sharpening of Impeller Blade LE with almost no wear @ shroud. Note: Wearback not as severe as on 5010.
5. Only slight evidence of horseshoe vortex formation on hub side of impeller wall at blade LE - 5010 is worse.
6. Slight ripple wear (fine) along collector sidewalls.
7. Slight ripple wear around volute wall.
8. Cutwater sharpening, biased toward impeller side.
9. Grooving along Impeller side of cutwater, only very slight groove on Diffuser side.
10. No classic horseshoe vortex type formation on volute ring side of cutwater.
11. Horseshoe vortex type formation on front wall (Note 90° mating joint with cutwater) with a trailing groove from Impeller side of cutwater.
12. No wear on suction side of Impeller at exit.

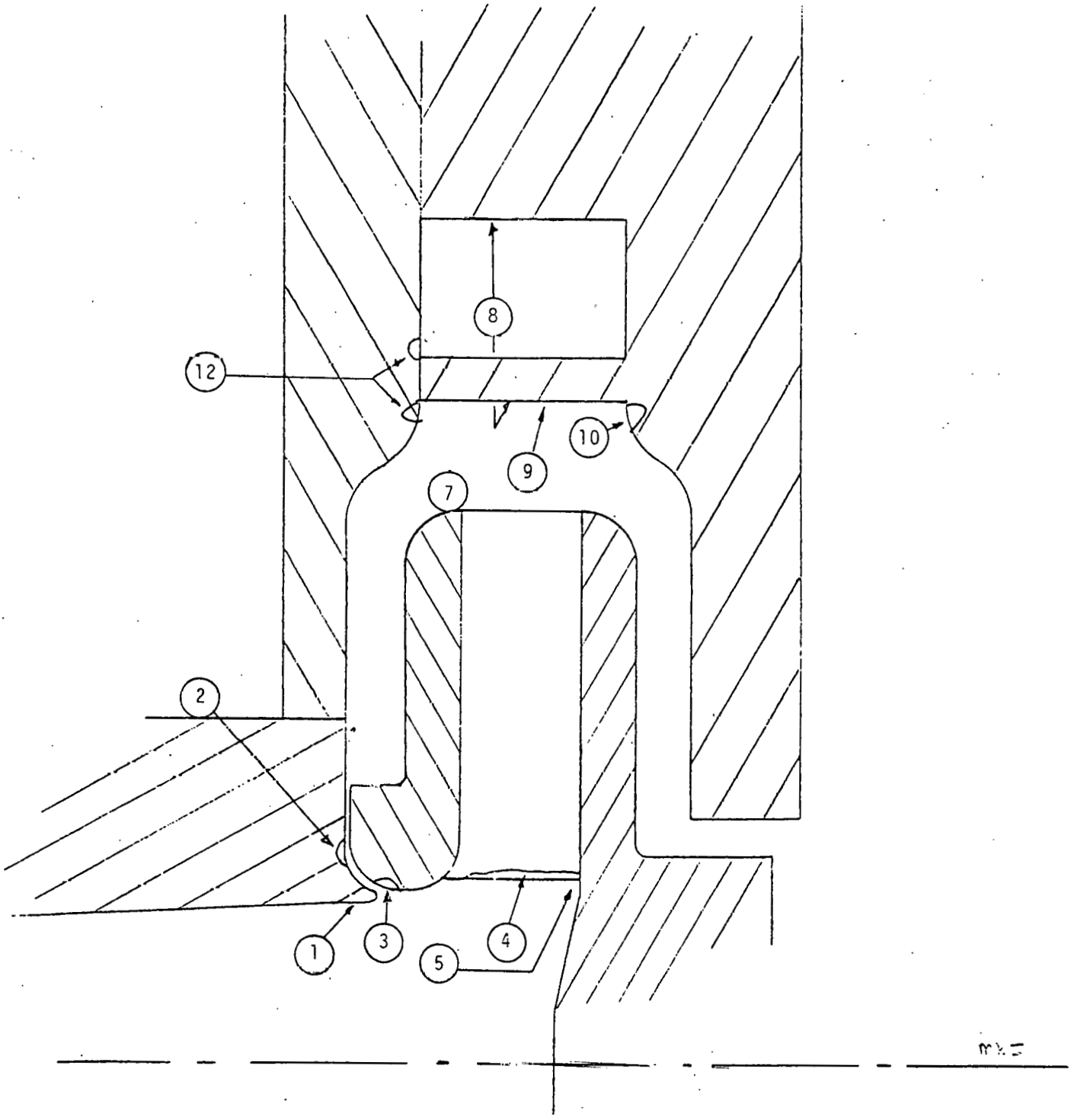

SST 3011 Wear Locations

TEST REPORT

TEST IDENTIFICATION: SST 3012

TEST PURPOSE: Compare to SST 3013 - Evaluate different impeller leakage path configurations. Different collector design. Square shroud vs. round shroud at impeller O.D. - in ½ percent SCMC slurry.

TEST NUMBERS: 051, 052, 053, and 054

TEST HARDWARE: SST 3 Mk II impeller, no PO vanes with 5 blades. One square shroud, the other is round. A nearly axial (15^{o} from axis) wear ring surface. Concentric collector with oval throat diffuser. Mk II type sidewalls.

TOTAL HOURS IN SLURRY: 12.8

TEST CONDITIONS:

RPM - 5990 - 6010

FLOW - 63.2 - 50.3

SAND TYPE - 100 mesh

CONCENTRATION - CW = .25 with ½ percent SCMC

TEST RESULTS:

CUTWATER LENGTH REDUCTION -

IMPELLER FRONT RING LOSS -

IMP EYE DIA INCREASE -

TEST OBSERVATIONS:

(1) No observable wear due to shape of shrouds.

(2) Very slight groove noticeable on pressure side of blade at exit.

(3) No suction side damage on blade.

(4) Wear on I.D. of impeller inlet at exit of leak flow nozzle, major axis of scallops of wear in the direction of rotation, about 30^{o} from the tangential.

(5) Sharpening and wear back of blade L.E.

(6) Wear on suction side of blade extending about 2" from L.E. on shroud side (probably due to separation around inlet corner).

(7) Wear on suction nozzle at entrance to leakage path.

(8) Wear on suction nozzle directing lip. Only over 60^{o} of surface, the wear marks indicate a mainly tangential component and occur in a location indicating that a majority of the leakage flow was influenced by the nonuniform, circumferential pressure gradient around the impeller imposed by the circular-type collector.

(9) No observable ripple wear on sidewalls.

(10) Some loss of material along cutwater but no horseshoe vortex.

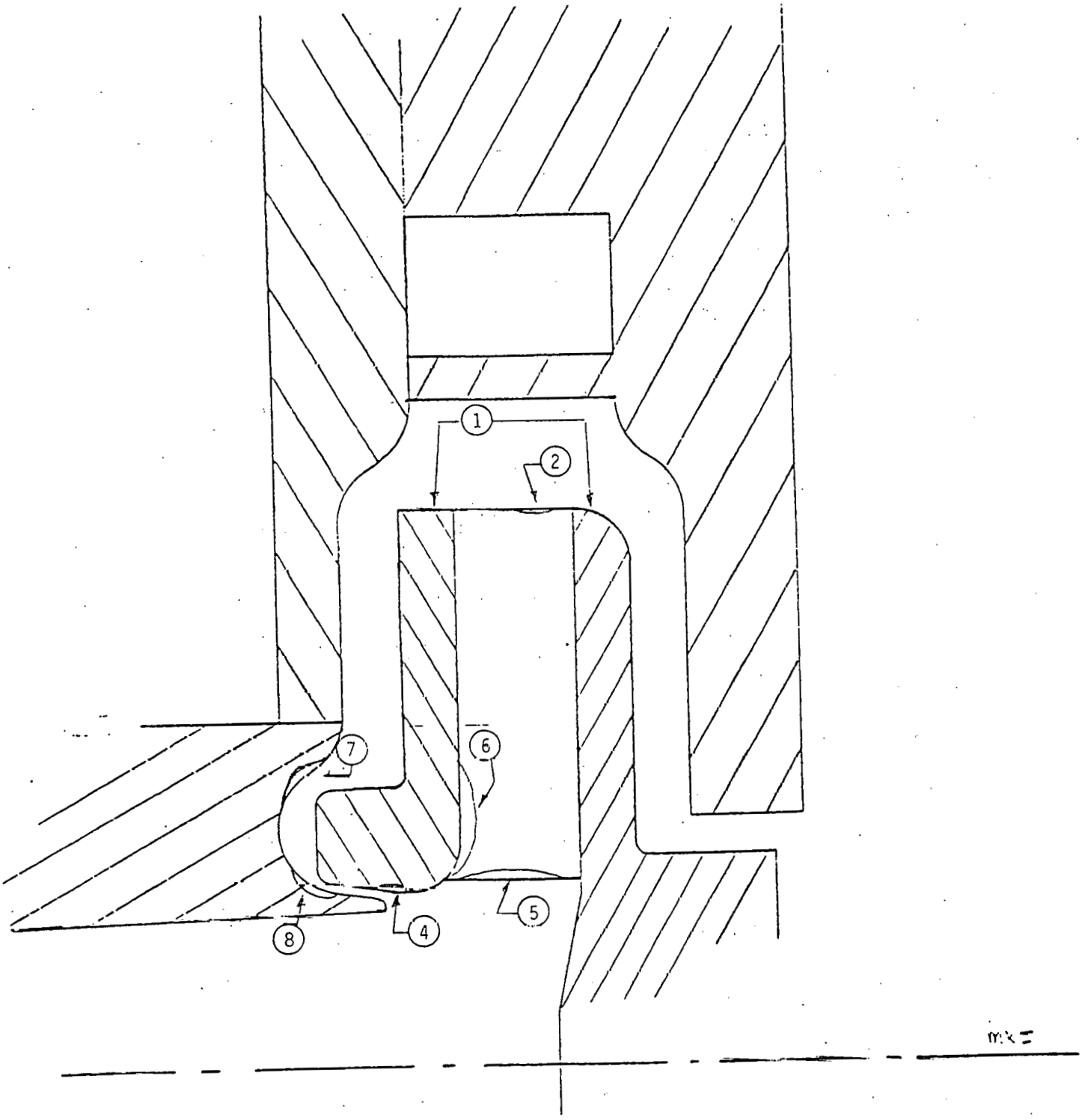

SST 3012 WEAR LOCATIONS

TEST REPORT

TEST IDENTIFICATION: SST 3013

TEST PURPOSE: Compare to SST 3012 - Evaluate collector design and front impeller leakage path designs

TEST NUMBERS: 051, 052, 053, and 054

TEST HARDWARE: SST 3 Mk II impeller, no PO vanes, with 4 vanes. A 30° from radial front leakage ring path. Typical volute with (Mk II) concave cutwater, L.E. trim

TOTAL HOURS IN SLURRY: 12.8

TEST CONDITIONS:

RPM - 5990 - 6010

FLOW - 63.2 - 50.3

SAND TYPE - 100 mesh

CONCENTRATION - CW = .25 with ½ percent SCMC

TEST RESULTS:

CUTWATER LENGTH REDUCTION -

IMPELLER FRONT RING LOSS -

IMP EYE DIA INCREASE -

TEST OBSERVATIONS:

(1) Suction side blade wear along most of the blade.

(2) Much blade L.E. sharpening and wear back.

(3) Circumferential groove forming on impeller wear ring surface.

(4) Chewing-type wear at I.D. of impeller wear ring surface which extends into eye of impeller and tip portions of the blade. Axis of wear marks typically 30° from tangential.

(5) Suction side, shroud side wear on impeller blade (probably due to separation around inlet radius).

(6) Some hub side wear.

(7) Suction nozzle wear at entrance to leakage path.

(8) Some ripple wear on sidewalls.

(9) Typical grooving on both sides of cutwater on end walls - no upstream groove typically horseshoe vortex.

(10) Sharpening of cutwater and cutwater L.E. wear back.

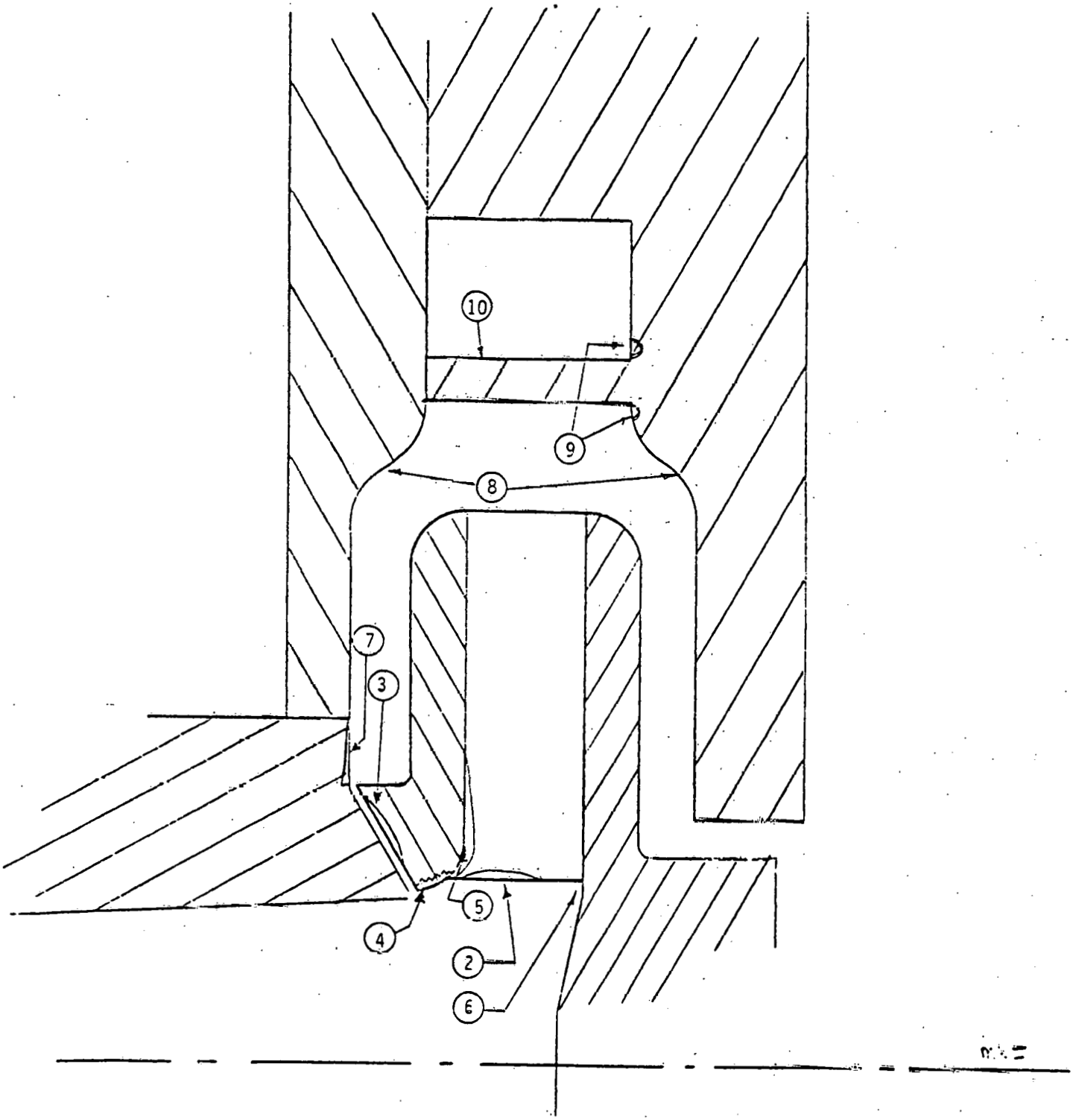

SST 3013 WEAR LOCATIONS

APPENDIX C

SLURRY VISCOSITY MEASUREMENT

In an effort to provide a more viscous carrier for the sand slurry, and evaluate its effect on wear, an additive known as sodium carboxy methyl cellulose (SCMC) was mixed with water. The resultant fluid is subject to considerable shear thinning. The need to understand more about the behavior of this fluid brought about the tests which produced the results shown in Figure C1. It is desireable to use a mixture of SCMC, sand and water during the prototype pump evaluation in an effort to approach the conditions faced by the pump in a synfuel application.

The test method consisted of timing a measured quantity of slurry flowing through a 0.490" diameter, about 10 feet long tube, and recording the pressure drop at several flow rates. Each flow rate can be related to an "average" shear rate and the viscosity may be calculated by choosing an appropriate friction factor. For the highly viscous slurry (2% SCMC mixture), a laminar friction factor is assumed. The curve on the top of Figure C1 appears insensitive to sand concentration, perhaps due to the laminar nature of the flow. For the less viscous slurry (1/2% SCMC mixture), a turbulent fraction factor is used in calculating viscosity. Here, a definite sensitivity to sand concentration exists perhaps as a result of the motion of the particles in the turbulent flow field.

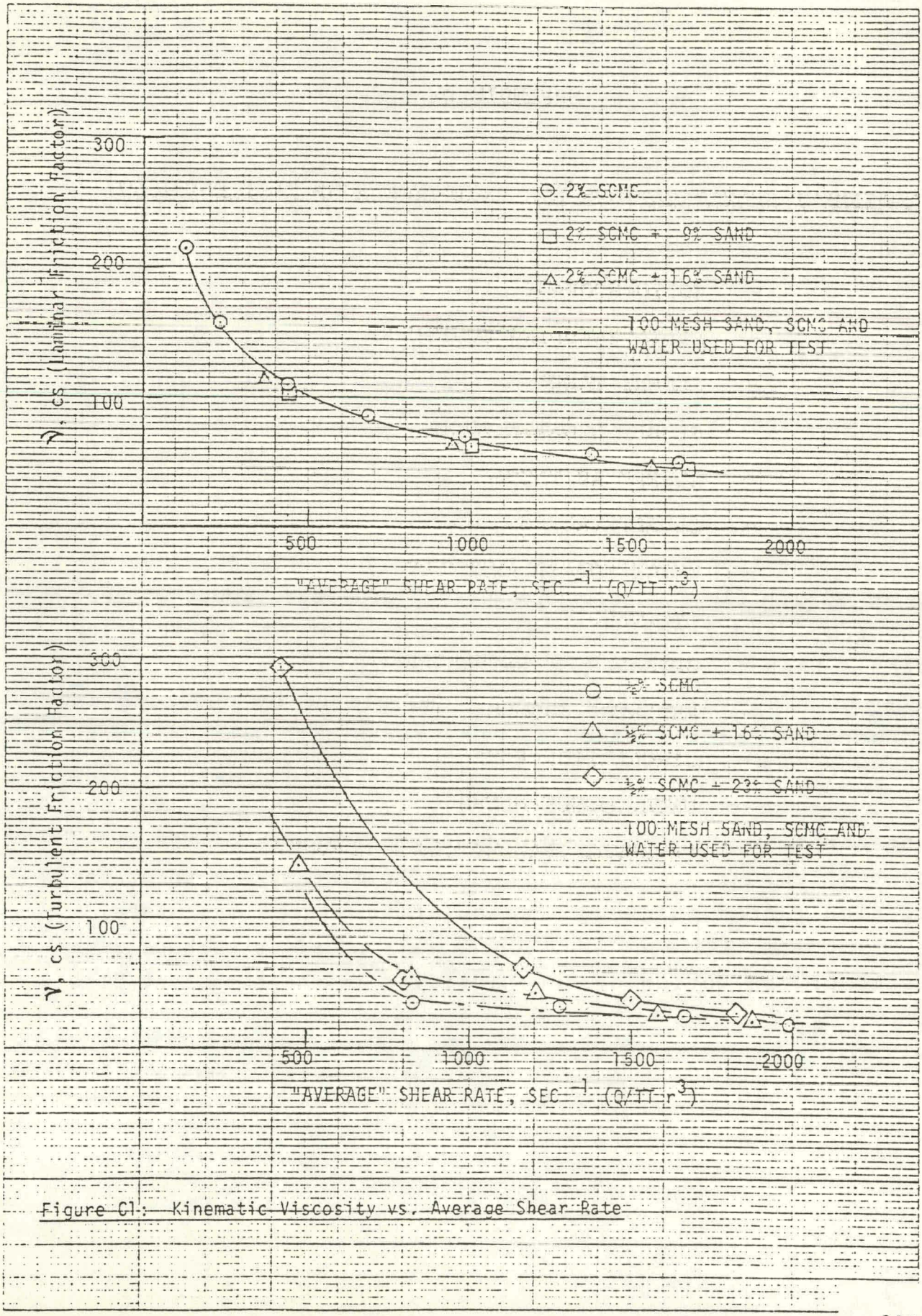

Figure C1: Kinematic Viscosity vs. Average Shear Rate

APPENDIX D

EQUIPMENT SPECIFICATIONS FOR PROTOTYPE PUMP TEST FACILITY

- SOLID STORAGE SILO
- SOLID HANDLING EQUIPMENT
- SLURRY TANK
- SLURRY BOOSTER PUMP
- SLURRY AGITATOR
- SLURRY VALVES
- WEIGH HOPPER ASSEMBLY
- CYCLONE
- SPIRAL HEAT EXCHANGER
- RADIATOR COOLER
- CIRCULATION PUMP
- DATA LOGGER-ALARM
- PRESSURE TRANSMITTER & READOUT

SOLID STORAGE SILO

* Manufacturer: Schuld Manufacturing, Mosinee, Wisconsin

* Application: Dry Sand Storage

* Features: Capacity - 25 Tons

  8 Ft Dia., 9 Ft Straight Sides, 60 Deg Cone, 19 Ft 6 In. High.

  10 In. Dia., Flanged Opening with 4 Ft Clearance Above Grade

  Ave Height - 19 Ft 6 In.

  20 In. Dia. Combination Manway P/V Relief Valve in Deck

  24 In. Dia. Flanged Hillside Opening for Dust Collector in Deck

  2 In. Sch 40 Flanged Opening for Continuoos Level Sensor in Deck

  OSHA Ladder, Cage and Perimeter Guard with Toeboard

  Full Skirted Bottom with Hinged Door

  4 In. Dia Sch 80 Internal Fill Line W/Quick Disconnect Coupling

SOLID HANDLING EQUIPMENT

* Manufacturer: Duplex Mill & Manufacturing Co., Springfield, OH (513) 325-5555
* Application: Dry Sand Feed from Silo to Slurry Tank
* Model K-64-9 Kelly Duplex Bucket Elevator
* Features:

  Feeding Capacity - 10 Ton/Hr

  Discharge Height - 25 Ft

  Gear Reducer Drive W/1.5 HP TEFC Motor 230/460 V

  Lower Hinged Inspection Door

  Service Platform

  10 Ft Ladder on Side

* Model 6" U-Through Kelly Duplex Screw Conveyor
* Features:

  Feeding Capacity - 10 Ton/Hr

  Gear Motor 3 HP TEFC 230/460 V

  Inlet - 14 Inch Diameter

  Top Shroud

* References: Drawing No. DM1467 Kelly Duplex

SLURRY TANK

* Manufacturer: Tampa Tank, Tampa, Florida
  (813) 623-2675

* Application: Sand-Water Slurry Mixing Tank

* Features:

  Capacity - 1500 Gallons Brim Full

  7 Ft Dia., 5 Ft Straight Side, 15 Deg Conical Bottom

  Four Baffles, 8" Wide, 2" Standoff, Spaced 90 Deg. Apart

  Reinforced Cover with Openings & Hinged Man-Way

  Structural Leg Supports

  Overall Height - 8 Ft 10 In

  Bottom Discharge Pipes - One 5 In. Sch 80, One 2 In. Sch 80

  Mounting Support Structure for Weigh Hopper, Agitator and Cyclone

* References: Drawing No. 740-2 Coleman Equipment

SLURRY BOOSTER PUMP

* Manufacturer: Warman International., Inc.
  Madison, WI (608) 221-2261
* Model 4/3 CAH Heavy Duty Slurry Pump
* Application: Sand/Water Slurry (50% Sand by Wt.)
* Features:

  Impeller - Molded Elastomer with Pump Out Vanes

  Liner - Rubber Bolted to Outer Casing

  Gland Seal (Requires 5 GPM Water)

  Motor - 30 HP, Overhead Mounted, V-Belt Drive

* Performance Specifications:

  Flowrate - 500 GPM Sand/Water (50% Sand by Wt.)

  Head - 80 Ft TDH

  Specific Gravity - 1.45

  Efficiency - 57%

  BHP - 26 HP

  Pump RPM - 1600

  NPSH Req. - 11 Ft

* References: Performance Curve WPA 43A01AU March, 1979

AGITATOR

* Manufacturer: Philadelphia Mixer
  Div. of Philadelphia Gear Corp.
  Palmyra, PA 17078 (717) 838-1341

* Model: MT-02-PTO

  Total Gear Ratio: 17.1 : 1

  Output Speed: 100 RPM

  Motor: 5 Hp 1800 rpm 3/60/230-460 Volt TEFC

  Shaft: 2" Diameter 62" Long

  Impeller: 30" Diameter Four 45 Degree Blades

  Wetter Part Material: Carbon Steel

  Reference: S/N 83BAF1035

SLURRY VALVES

* Manufacturer: Clarkson Company, Palo Alto, CA 94303
  (415) 494-1010

* Model: KGA-4-AC-X-M1-R1
  KGA-3-AC-X-M1-R1

* Description: Knifesate Valve for On/Off Application

  Air Cylinder Actuator

  316 Stainless Steel Sate

  Retainer Flanges

  Limit Switch

  Gum Rubber Sleeve

* Model* B3-PM36A-M1
  B2-PM34A-M1

* Description: Pinch Valve for On/Off and Throttling Application

  Positioning Pneumatic Actuator

  Gum Rubber Sleeve

  Limit Switch

* Model: C3-U1-X

* Description: Concentric Sleeve Constriction for Throttling Application

  Unitized Pneumatic Actuator and Positioner

  Gum Rubber Sleeve

WEIGH HOPPER ASSEMBLY

* Manufacturer: Tampa Tank, Tampa, Florida
  (813) 623-2675

* Features:

  Capacity - 200 Gal. Brim Full

  42 In. Dia 24 In. Straight Side, 90 Deg Cone

  14 In. Dia Bottom Opening

  Top Centerline Hook for Load Cell

* Manufacturer: Kistler-Morse Corp., Bellevue, Wash.
  (206) 641-4200

* Model Load Link 300 Series Rating 5000 Lb Transducer

* Model 926 Digital Indicator

* Features:

  Load Capacity - 5000 Lb

  Load Link Accuracy - 0.25 Percent

  Indicator - Solid State Electronics

  Sensor Excitation Voltage - 24 V

  Separate Span and Zero Controls

  Wall Mounted JIC Enclosure

* References: Drawing No. T1-0078 Kistler Morse Load Link

CYCLONE

* Manufacturer: Krebs Engineers, Menlo Park, CA
  (415) 325-0751

* Model D10B-840

* Application* Desanding Water
  (40% Sand by Weight Max.)

* Features: Involuted Feed Nozzle

  Replaceable Gum Rubber Liner

  Replaceable Nihard Vortex Finder

  Fixed Ceramic Apex Assembly No. 368

* Specified Flowrates: Feed- 200 GPM

  Overflow - 118.5 GPM

  Underflow - 81.7 GPM

* Pressure Drop - 25 psi

* References: Drawing No. 840

  Parts List PL-116

  Capacity Curve D10B-840-467

SPIRAL HEAT EXCHANGER

* Manufacturer: Alfa-Laval, Inc. Ft. Lee, NJ
  (201) 592-7800

* Model: AHRCO Spiral Exchanger, Type 1HH

* Application: Sand-Water Slurry Cooling
  (15% Sand by Weight Max.)

* Features: 60 Sq. Ft. Area

  0.1875 Inch Thick Carbon Steel

  Removable End Covers

  Slurry Channel Open for Clean-Out

  Ethylene Glycol Channel Welded Closed

  Channel Spacing - 0.5 Inch Slurry Side
  0.313 Inch E. Glycol Side

  Diameter - 18 Inches

  Width - 24 Inches

* Performance Specifications:

  Heat Exchanged - 5.825 BTU/MIN

  Slurry Temperature - 125-130 Deg. F

  E. Glycol Temperataure 90-93.6 Deg. F

  LMTD - 35.7 Deg. F

  Slurry Velocity 3.2 Ft/Sec

  E. Glycol Velocity 9.4 Ft/Sec

  Allowable Pressure Drop - 15 psi Max

  Working Pressure - 50 psig

  Design Temperature - 250 Deg F.

* References: Drawing No. 1HN8004-1

RADIATOR COOLER

* Manufacturer: O & M Manufacturing Co., Houston, TX
  (713) 675-3511

* Model VS-17.5-7.5 Vertical Remote Radiator

* Application: 50/50 Water/Ethylene Glycol Solution Cooling

* Features:

  Motor - Direct Drive, 7.5 Hp, 1150 RPM
  230/460 Volt, 3 PH, 60 CY, 254-T TEFC
  Frame

  Fan - 48 Inch Diaa Western 16 Deg Pitch

  Radiator Core Assembly Type 995

  Frame Mounted

  Fan and Core Guards

  Filler and Pressure Cap

* Performance Specifications:

  Heat Rejection - 5.726 BTU/MIN

  Fluid Flowrate - 220 GPM

  Fan Air Delivery - 28.00 SCFM

  Fluid Temperature - 90-94 Deg F

* References: Drawing No. 8536

CIRCUCLATION PUMP

* Manufacturer: Ingersoll-Rand Co., Allentown, PA.
* Model 3 x 5 SMP - 3 HP 3000 Series
* Application: 50/50 Water/Ethylene Glycol Circulation
* Features:
  - Single-Stage, End Suction
  - Closed Impeller Design
  - Close Coupled Motor Driver - 3 HP
  - Maximum Temperature - 212 Deg F.
  - Maximum Pressure - 100 Psig
* Performance Specifications:
  - Flowrate - 220 GPM
  - Head - 45 Ft TDH
  - Efficiency - 76%
  - Pump RPM - 3450
  - NPSH Req - 8 Ft.
* References: Performance Curve SMP-3000-1 8-2-82

DATA LOGGER-ALARM

* Manufacturer: Yokogawa Electric Works, Shenandoah, GA
  (404) 253-7000

* Model 4088

* Application: Record Unattended Operation and provide Automatic Shutdown with Alarm Circuit

* Features:

  30 Channels Individually Programmable for Range

  Voltage Input - 0 MV to 50 Volts

  Thermocouple Input - Type R,K,E,J and T with Built-In Compensation

  Scans 30 Channels in 8 Seconds

  Channel Identification Numbering

  Chart Speed - Selectable from 1-999 MM/HR

  Program List Printout

  Battery-Backup Memory

  Program and Panel Lock-Out Capability

  30 Alarm Relays - 120 V, 5A, SPST

  Wire-Dot Printer, 6 Color Ribbon

  Basic Accuracy: 0.25 Percent of Span

  Z-Fold Chart Paper

PRESSURE TRANSMITTER-READOUT

* Transmitter Manufacturer: Rosemount, Inc.
  Hasbrouck Heights, NJ
  (201) 288-1101
* Differential Pressure Transmitter QTY-2
  - Basic Transmitter - Model 1151DP-7-E-12-S2-B2
  - Remote Seal - Model 1199RTW-21-A-11-E-13
  - Capillary Tubing - Model 119CAP-11-A-10-A-11
  - Fluid Fill - Model C10485-0007
* Gage Pressure Transmitter QTY-2
  - Basic Transmitter - Model 1151GP-6-E-12-S1-B2
  - Remote Seal - Model 1199RTW-21-A-11-E-13
  - Capillary Tubing - Modoel 1199CAP-11-A-10-A-11
  - Fluid Fill - Model C10485-0007
* Application: Pump Inlet and Differential Pressure for Sand/Water Slurry
* Features:
  - Pressure Range - Differential Model 0-300 Psig
    Gage Model 0-100 Psig
  - Output - 4-20 Milliamp
  - External Span and Zero Adjustments
  - Accuracy - 0.25 Percent of Span
  - Required Power Supply - 12 to 45 VDC
  - Solid State, Plug-In Printed Circuit Boards
  - Compatible with any 2-Wire System
* Readout Manufacturer: International Microtronics, Tucson, AZ (602) 748-7900
* Model 357 Process Monitor
* Features:
  - Input - 4 to 20 Miliamp DC
  - Output - 0 to 100 Psi QTY-2
    0 to 300 Psi QTY-2
  - Analog Output - 0 to 1.000 Volt for Input Range
  - Power Supply Required - 115/230 VAC
  - Zero and Gain Adjustable
  - Sampling Rage - 3/Sec.

☆U.S. GOVERNMENT PRINTING OFFICE:1984 -746 -081/ 2640 REGION NO. 4